Forschungszentrum Karlsruhe
Technik und Umwelt

Wissenschaftliche Berichte
FZKA 5785
INDC(GER)-41

Integral Data Tests of the FENDL-1 Nuclear Data Library for Fusion Applications

Summary Report of the International Working Group on „Experimental and Calculational Benchmarks on Fusion Neutronics for FENDL Validation"

U. Fischer (Ed.)

Institut für Neutronenphysik und Reaktortechnik
Projekt Kernfusion

August 1996

Forschungszentrum Karlsruhe

Technik und Umwelt
Wissenschaftliche Berichte
FZKA 5785
INDC(GER)-41

Integral Data Tests of the FENDL-1 Nuclear Data Library for Fusion Applications

Summary Report of the International Working Group on „Experimental and Calculational Benchmarks on Fusion Neutronics for FENDL Validation"

U. Fischer (Ed.)

Institut für Neutronenphysik und Reaktortechnik

Projekt Kernfusion

Forschungszentrum Karlsruhe GmbH, Karlsruhe

1996

Abstract

A co-ordinated international benchmark task has been conducted to validate the Fusion Evaluated Nuclear Data Library FENDL-1 through data tests against integral 14-MeV neutron experiments. The main objective was to qualify the FENDL-1 working libraries for fusion applications and to elaborate recommendations for further data improvements .

Several laboratories and institutions from the European Union, Japan, the Russian Federation and the United States have contributed to the benchmark task. A large variety of existing integral 14 MeV benchmark experiments was analysed with the FENDL-1 working libraries covering the majority of fusion-relevant materials. The contributed benchmark experiments and analyses are presented and discussed in the report. A comprehensive documentation of the numerical data tests results is included in graphical and tabulated form.

With regard to the data quality, it is summarised that fusion nuclear data have reached a high confidence level with the available FENDL-1 data library. With few exceptions this holds for the materials of highest importance for fusion reactor applications. Some still existing deficiencies and discrepancies have been identified and are recommended to be removed in the forthcoming FENDL-2 data file.

Integrale Datentests der Kerndatenbibliothek FENDL-1 für Fusionsanwendungen

Zusammenfassung

Zur Überprüfung der Fusionskerndatenbibliothek FENDL-1 („Fusion Evaluated Nuclear Data Library") wurde eine koordiniertes internationales Benchmarkprogramm durchgeführt. Übergeordnetes Ziel war es, die FENDL-1 - Arbeitsbibliotheken anhand von Benchmarkanalysen integraler 14-MeV-Neutronenexperimente für Fusionsanwendungen zu qualifizieren und auf dieser Grundlage Empfehlungen für weiterführende Datenverbesserungen zu erarbeiten.

Mehrere Laboratorien und Institutionen der Europäischen Union, Japans, der Russischen Föderation und den USA beteiligten sich an dem Benchmarkprogramm. Es wurde eine Vielzahl existierender integraler 14-MeV-Benchmarkexperimente mit den FENDL-1 Arbeitsbibliotheken analysiert, wobei die wichtigsten fusionsrelevanten Materialien berücksichtigt werden konnten. Die beigetragenen Benchmarkexperimente und -analysen werden im Bericht dargestellt und diskutiert. Die numerischen Ergebnisse der Datentests sind in graphischer und tabellarischer Form umfassend dokumentiert.

In bezug auf die Datenqualität läßt sich zusammenfassen, daß mit der FENDL-1 - Datenbibliothek ein hohes Qualtitätsniveau erreicht worden ist. Mit wenigen Ausnahmen gilt dies für die bei Fusionstechnologieanwendungen wichtigsten Materialien. Noch vorhandene Unzulänglichkeiten und Diskrepanzen wurden identifiziert und sollten in der nächsten Version FENDL-2 behoben werden.

Table of contents

I. INTRODUCTION

The Fusion Evaluated Nuclear Data Library (FENDL) is a compilation of fusion-oriented data evaluations selected from the nuclear data files ENDF/B-VI (USA), BROND (Russian Federation), JENDL (Japan) and EFF (European Union) in an international effort initiated and co-ordinated by the IAEA Nuclear Data Section. The FENDL data file will serve as reference library for design calculations in the Engineering Design Activity (EDA) phase of the International Thermonuclear Experimental Reactor (ITER) Project.

A first version of the file, FENDL-1, has been compiled and released /Muir 91, Ganesan 94/. Working libraries in processed form for use both in Monte Carlo (MCNP-code) and discrete ordinates (e. g. ONEDANT/TWODANT, ANISN/DOT) transport calculations have been derived by R .E. MacFarlane, Los Alamos National Laboratory, /Garching 94/ using the NJOY code system.

Prior to their use in design calculations there is a need to validate the FENDL-1 working libraries through integral data tests. At the IAEA Advisory Group Meeting on „Improved Evaluations and Integral Data Testing for FENDL", Garching, Germany, September 12 - 16, 1994 it was agreed to organise an international FENDL benchmark task for that purpose. It was assumed that data tests are being performed on a short term time scale to attest the quality and completeness of the FENDL-1 working libraries for fusion applications. In addition to that, it was anticipated that the results of the data testing will contribute to the further improvement of FENDL data and give guidance to the development of the FENDL-2 data file.

Several laboratories and institutions from the European Union, Japan, the Russian Federation and the United States have contributed to this benchmark task by analysing a large variety of existing integral 14 MeV benchmark experiments with the FENDL-1 working libraries, i. e. the FENDL/MC-1.0 (Monte Carlo) and the FENDL/MG-1.0 (multigroup) data library. Results of the FENDL-1 data testing have been collected and are summarised and evaluated in this report.

II. FENDL-1 Data Libraries

II.1 General Purpose Evaluation Data File FENDL/E-1.0

Following the recommendations of several IAEA Consultants Meetings, a FENDL-1 general purpose evaluation data file, designated as FENDL/E-1.0, has been compiled including the following neutron interaction and photon production cross section data from the BROND-2, ENDF/B-VI, and JENDL-3 data files /Ganesan 94/:

Nuclide	Source	Nuclide	Source	Nuclide	Source
H-1	ENDF/B-VI	H-2	BROND-2	H-3	ENDF/B-VI
Li-6	ENDF/B-VI	Li-7	ENDF/B-VI	Be-9	ENDF/B-VI
B-10	ENDF/B-VI	B-11	ENDF/B-VI	C-nat	ENDF/B-VI
N-14	BROND-2	N-15	BROND-2	O-16	ENDF/B-VI
F-19	ENDF/B-VI	Na-23	JENDL-3	Mg-nat	JENDL-3
Al-27	JENDL-3	Si-nat	BROND-2	P-31	ENDF/B-VI
S-nat	ENDF/B-VI	Cl-nat	ENDF/B-VI	K-nat	ENDF/B-VI
Ca-nat	JENDL-3	Ti-nat	JENDL-3	V-nat	ENDF/B-VI
Cr-50	ENDF/B-VI	Cr-52	ENDF/B-VI	Cr-53	ENDF/B-VI
Cr-54	ENDF/B-VI	Mn-55	ENDF/B-VI	Fe-54	ENDF/B-VI
Fe-56	ENDF/B-VI	Fe-57	ENDF/B-VI	Fe-58	ENDF/B-VI
Co-59	ENDF/B-VI	Ni-58	ENDF/B-VI	Ni-60	ENDF/B-VI
Ni-61	ENDF/B-VI	Ni-62	ENDF/B-VI	Ni-64	ENDF/B-VI
Cu-63	ENDF/B-VI	Cu-65	ENDF/B-VI	Zr-90	BROND-2
Zr-91	BROND-2	Zr-92	BROND-2	Zr-94	BROND-2
Zr-96	BROND-2	NB-93	BROND-2	Mo-nat	JENDL-3
Sn-nat	BROND-2	Ba-134	ENDF/B-VI	Ba-135	ENDF/B-VI
Ba-136	ENDF/B-VI	Ba-137	ENDF/B-VI	Ba-138	ENDF/B-VI
Ta-181	JENDL-3	W-182	ENDF/B-VI	W-183	ENDF/B-VI
W-184	ENDF/B-VI	W-186	ENDF/B-VI	Pb-206	ENDF/B-VI
Pb-207	ENDF/B-VI	Pb-208	ENDF/B-VI	Bi-209	JENDL-3

Table II.1 List of FENDL/E-1.0 data evaluations

The FENDL/E-1.0 photon-atom interaction data are taken from the ENDF/B-VI photon-interaction library /Lemmel 90/.

Data for the following materials are included:

Al, B, Ba, Be, Bi, C, Ca, Cl, Co, Cr, Cu, F, Fe, H, K, Li, Mg, Mn, Mo, N, Na, Nb, Ni, O, P, Pb, S, Si, Sn, Ta, Ti, V, W, Zr.

The FENDL/E-1.0 data files are freely available at the IAEA Nuclear Data section. They can be retrieved via on-line access through international computer networks /Ganesan 94/.

II.2 Processed Data Files: FENDL/MC-1.0 and FENDL/MG-1.0

The FENDL/E-1.0 data evaluations follow the ENDF-6 format rules and can be processed by the NJOY-code system. Working libraries for use in ITER-EDA design calculations have been derived by the author of NJOY-code, R. E. MacFarlane of LANL, in the framework of an ITER-task.

For use in discrete ordinates calculations a FENDL-1 multigroup library, denoted as FENDL/MG-1.0, has been created applying the VITAMIN-J 175 neutron and 42 photon group structure and the related VITAMIN-J weighting spectrum /MacFarlane 94/.

For use in continuous-energy Monte Carlo calculations with the MCNP-code, a FENDL-ACE data library was derived, denoted as FENDL/MC-1.0 /MacFarlane 94/.

FENDL/MG-1.0 and FENDL/MC-1.0 are designed as reference working libraries for ITER-EDA design calculations. For the purpose of the FENDL validation it was mandatory to use these working libraries for the analyses of appropriate 14 MeV neutron benchmark experiments. The application of other data sources e. g. processed libraries derived from BROND-2, EFF-2, ENDF/B-VI and JENDL-3, was recommended for comparison and cross-checking purposes /Ganesan 94a/.

III. Integral Fusion Neutronics Experiments and FENDL Data Testing

The IAEA Advisory Group Meeting on „Review of Uncertainty Files and Improved Multigroup Cross Section Files for FENDL" held at Tokai-mura, November 8 -12, 1993, has pointed out the urgent need to validate the FENDL-1 data base by performing data testing through available benchmark experiments. A first selection of appropriate fusion neutronics benchmark experiments has been performed at that meeting /Ganesan 94a/. A series of existing integral benchmark experiments, relevant for fusion reactor blanket and shield design, was identified. It was recommended to make available the measured data and the information needed to analyse the experiments to interested individuals who are validating FENDL data.

In a subsequent IAEA Consultants' Meeting held at IAEA Headquarters Vienna, Austria, December 13 -16, 1993, a compilation of experimental benchmark data has been assembled in electronic format /Ganesan 94b/. It includes contributions from JAERI (FNG-facility), the Universities of Osaka and Kyoto (OKTAVIAN-facility), ENEA Frascati, TU Dresden, IPPE Obninsk, KIAE Moscow and BARC Bombay. This compilation is available on-line from IAEA/NDS. It represents a unique data source for use in integral data validation analyses for fusion applications and formed one of the main experimental data sources for the international FENDL data testing analyses, the results of which are presented in this report.

IV. The FENDL Benchmark Task

At the IAEA Advisory Group Meeting on „Improved Evaluations and Integral Data Testing for FENDL" held at Garching, Germany, September 12 - 16, 1994 an international FENDL benchmark task was launched with the objective of performing integral data tests that could provide confidence in using the FENDL-1 working libraries for fusion applications at the time they are released.

Several laboratories and institutions from the European Union, Japan, the Russian Federation and the United States have contributed to this benchmark task by analysing a variety of existing integral 14 MeV neutron benchmark experiments. The majority of them are included in the compilation of fusion neutronics benchmark experiments /Ganesan 94b/ which is freely available at IAEA/NDS.

The following contributions were submitted to the task organiser U. Fischer, Forschungszentrum Karlsruhe, for inclusion in the joint report on the international FENDL-1 benchmark validation.

IV.1 Japanese Contributions

The Japanese contributions comprise benchmark analyses of FNS (Fusion Neutron Source of JAERI), OKTAVIAN (14-MeV neutron facility of the University of Osaka) and IPPE Obninsk integral experiments that mainly have been performed with the MCNP-code and the FENDL/MC-1.0 data library. Selected integral experiments have been analysed by discrete ordinates calculations using the FENDL/MG -1.0 data library. In addition, comparisons with the JENDL-3 data were included.

In detail, the following experiments have been analysed:

- **FNS time-of-flight measurements of angular neutron spectra from cylindrical slabs from 50 keV to 15 MeV neutron energy.**

  Experiments have been performed at FNS for the materials

  Li_2O, Be, C, O, N, Fe and Pb.

A comprehensive documentation of the FNS TOF-experiments is included in the Japanese collection of experimental data for fusion neutronics benchmarks /JAERI 94/. The FENDL benchmark analyses have been performed by Y. Oyama and M. Wada of JAERI using the MCNP code and the FENDL/MC-1.0 data library.

- **FNS in-system measurements for cylindrical slabs**

  In this type of experiment the neutron spectrum, various reaction rates, the gamma ray spectrum and heating rate has been measured in a central channel inside cylindrical slabs. Data for the following materials were provided /JAERI 94/:

  Li_2O, Be, C, Fe, Cu and W.

The FENDL benchmark analyses have been performed by F. Maekawa, Y. Oyama and M. Wada of JAERI using the MCNP code and the FENDL/MC-1.0 data library. In addition, the experiments on **Li_2O, Be and C** were analysed by K. Hayashi of Hitachi Eng. Co. using the DOT3.5 code and the FENDL/MG-1.0 data library. Note that the JENDL-3 dosimetry file was used for calculating the activation reaction rates.

- **OKTAVIAN spherical shell measurements of neutron leakage spectra**

  Spectral measurements of neutrons leaking spherical shell assemblies have been performed at the University of Osaka for the materials

  Be, Li, LiF, CF_2, Al, Si, Ti, Cr, Mn, Co, Ni, Cu, Zr, Nb, Mo and W.

The documentation of these experiments is also included in the Japanese collection of experimental fusion benchmark data /JAERI 94/. The FENDL benchmark analyses have been performed by C. Ichihara of the Kyoto University and A. Takahashi of the Osaka University using the MCNP code and the FENDL/MC-1.0 data library. For the experiments on beryllium and nickel, calculations with the NITRAN-code and appropriately processed FENDL and JENDL data were included.

- **OKTAVIAN spherical shell measurements of gamma ray leakage spectra**

  Gamma ray spectrum measurements have been also performed for spherical shell configurations at the University of Osaka. The benchmark analyses comprise the following materials:

  LiF, CF_2, Al, Si, Ti, Cr, Mn, Co, Cu, Nb, Mo, W and Pb.

The experimental results again are documented in /JAERI 94/. The FENDL benchmark analyses have been performed by F. Maekawa and Y. Oyama of JAERI using the MCNP code and the FENDL/MC-1.0 data library.

- **FNS bulk shield experiment on large SS-316 assemblies**

  Two bulk shield experiments on large SS-316 assemblies were performed at JAERI /Konno 94, 95 and Maekawa 94,95/: one with and one without a source can. The function of the source can was to produce a more prototypical incident neutron source by including back scattered neutrons in addition to the virgin 14 MeV neutrons, and to reduce the room-return effect at the back of the SS-316 assembly.

  The neutron spectrum, various activation and fission rates and the gamma-ray heating rate has been measured along the central axis of the 111.76 cm thick SS-316 steel cylinder.

  On Japanese side, the FNS SS-316 experiments were analysed by F. Maekawa of JAERI using the MCNP-code with FENDL/MC-1.0 and JENDL-3 data.

- **Analysis of IPPE Obninsk iron spherical shell experiment**

The IPPE iron experiment was analysed on Japanese side by K. Ueki of the Ship Research Institute using FENDL-1 and JENDL-3 data. For a more detailed description of the IPPE spherical shell experiments see section IV.4 below.

IV.2 U. S. Contributions

The U. S. contributions comprise analyses of bulk shield experiments performed at FNS and ORNL. Calculations have been performed with the two-dimensional discrete ordinates code DORT using the FENDL multigroup library FENDL/MG-1.0. In addition, comparisons with ENDF/B-VI based calculations were included.

Results of computational analyses have been submitted for the following experiments:

- **FNS bulk shield experiment on large SS-316 assemblies**

On the US side, the FNS bulk shield experiments on large SS-316 assemblies (see section IV.1 above) were analysed with FENDL/MG-1.0 data using the discrete ordinates code DORT. The FENDL-1 multigroup data were collapsed to 80 neutron and 24 gamma groups for use in the two-dimensional DORT-calculations.

Comparisons were performed with ENDF/B-VI based multigroup calculations. In addition, the multigroup calculations were performed with and without resonance shielded cross-section data, both for FENDL-1 and ENDF/B-VI data.

For calculating the activation reaction rates, the ENDF/B-VI dosimetry file was applied, complemented by JENDL-3 activation cross-section for the missing reactions.

The analysis has been performed by M. Youssef of UCLA for which the experimental data were provided by C. Konno, F. Maekawa and H. Maekawa of JAERI. The U. S. analysis of these experiments are extensively documented in /Youssef 94/.

- **Analysis of ORNL fusion shielding benchmark experiments**

Two experiments included in the RSIC/ORNL compilation of shielding benchmark experiments SINBAD /Hunter 94/ were analysed: a bulk shield experiment with stainless steel with and without a polyethylene shield, and an iron duct experiment for both a plugged and unplugged configuration. For each experiment neutron and gamma ray spectra have been measured.

The experiments were analysed by two-dimensional DORT calculations using the FENDL/MG-1.0 multigroup library with 175 neutrons and 42 gamma groups. Comparisons with ENDF/B-VI data were performed using the VITAMIN-B6 data set with 199 neutron and 42 gamma groups.

The benchmark analyses were performed by H. Hunter and C. Slater of ORNL.

IV.3 European Contributions

The European contributions comprise analyses of spherical shell experiments performed at OKTAVIAN, IPPE Obninsk, FZK Karlsruhe and TUD Dresden, analyses of the bulk shield and heating experiments at FNG (Frascati Neutron Generator of ENEA) and the TUD iron slab experiment. Calculations were performed with MCNP and FENDL/MC-1.0 as well as one-dimensional discrete ordinate codes (ONETRAN, ONEDANT) and the FENDL/MG-1.0 data. Comparisons were performed with EFF-1 and EFF-2 data.

The following contributions were submitted:

- **Analyses of FNG experiments - ENEA Frascati**

Two types of SS-316 experiments were performed at FNG and analysed with FENDL-1 data:

(i) SS-316 bulk shield experiment

In this experiment, reaction rates were measured as a function of the penetration depth inside a SS-316 block with a total thickness of 70 cm. Both fission chambers and activation foils were used for the measurements. This experiment is included in the compilation of fusion neutronics benchmark experiments /Ganesan 94b/ and is comprehensively documented in /Batistoni 94, Batistoni 95/.

(ii) SS-316 nuclear heating experiment

This type of experiment consists of a 60 cm thick shielding block made of alternate plates of SS-316 (5 cm thickness) and perspex (2 cm thickness, for simulating water layers). The SS-316/perspex configuration is backed by a 30 cm thick block of alternate SS-316 and copper layers simulating a toroidal field coil.

In this experiment, the heating rate distribution has been measured inside the shielding block using TLD-300 thermo-luminescent dosimeters. The FNG nuclear heating experiment is documented in /Rado 95/.

FENDL benchmark analyses were performed for both FNG experiments by P. Batistoni, V. Rado and L. Petrizzi of ENEA Frascati using the MCNP-code and the FENDL/MC-1.0 data library /Rado 95/. Comparisons are included with MCNP-calculations using both EFF-1 and EFF-2 data. Activation cross-section data were taken from the IRDF-90 dosimetry file.

- **TUD iron slab experiment - TU Dresden analysis**

Neutron and photon spectra leaking from a 30 cm thick iron slab with and without a straight gap were measured at the Technical University Dresden. Photon spectra were recorded in the energy range 0.2 to 8 MeV and neutron spectra between 0.03 and 15 MeV. In addition to the pulse height spectra, the neutron time-of-arrival spectra were measured simultaneously in this experiment. This allows a direct comparison with calculated time-of-arrival spectra without the need for applying corrections to the measured data. The experiment is documented in the IAEA compilation of fusion neutronics benchmark experiments /Ganesan 94b/. A more comprehensive description is given in /Freiesleben 95/ including detailed calculational results obtained with EFF-1 data.

The benchmark analyses were performed by K. Seidel of TUD using the MCNP code and the FENDL/MC-1.0 data library. Neutron and photon spectra leaking from the iron slab were calculated both for an ideal (point neutron source, iron slab and point detector) and a real (including in addition: collimator, air, rack, etc.) geometrical set-up of the experiment.

Comparisons are included with MCNP-calculations using both EFF-1 and EFF-2 data.

- **Benchmark analyses of Forschungszentrum Karlsruhe**

Calculations of neutron leakage spectra from spherical shell assemblies were performed with the ONEDANT-code and FENDL/MG-1.0 data for the following neutron transmission experiments:

(1) Be, Be-Li, Al, Cu, Si and Zr spherical shells (OKTAVIAN-facility)

The documentation of these experiments is included in the JAERI collection of experimental fusion benchmark experiments /JAERI 94/.

(2) Be, Al, Fe, Pb and Pb-17Li spherical shells (IPPE Obninsk)

These experiments are documented in the IAEA compilation of fusion neutronics benchmark experiments /Ganesan 94b/.

(3) Pb spherical shell (TU Dresden)

This experiment is documented in /Elfruth 87/ and is also included in the the IAEA compilation /Ganesan 94b/.

Comparisons are included with EFF-1 and -2 calculations performed with the discrete ordinate codes ONEDANT, ANTRA1 and the Monte Carlo code MCNP. FENDL/MC-1.0 calculations with MCNP were performed for selected spherical shell experiments applying the one-dimensional geometrical model of the discrete ordinates calculations. In addition, secondary neutron emission cross-section spectra derived from the FENDL/MG-1.0 data library were compared to measured neutron emission spectra.

Analyses were performed by U. Fischer, E. Stein, H. Tsige-Tamirat and E. Wiegner of FZK.

Three-dimensional calculations with the MCNP-code and the FENDL/MC-1.0 data library were performed for the following benchmark experiments:

(3) Karlsruhe neutron transmission experiment (KANT) on beryllium spherical shells

Measurements of the neutron leakage spectra between 15 MeV and thermal energy were performed at Forschungszentrum Karlsruhe for beryllium spherical shells with varying shell thicknesses /Möllendorff 94/. In addition, the total leakage neutron multiplications were measured using a Bonner sphere system.

Analyses were performed by U. Fischer, F. Kappler and E. Stein of FZK using FENDL/MC-1.0 and both EFF-1 and EFF-2 data. Analyses of the KANT-experiment were also performed by R. Tayama, T. Tsukiyama, K. Hayashi of Hitachi Eng. Co. Ltd. and H. Giese, F. Kappler, U. v. Moellendorff of FZK applying three-dimensional MCNP-calculations with ENDF/B-VI, EFF-1, JENDL-3.2 and JENDL-Fusion-File data.

(4) TUD iron slab transmission experiment

Neutron spectra leaking from the 30 cm thick iron slab with no gap included were calculated in the ideal geometrical set-up of this experiment (see description above).

Analyses were performed by U. Fischer and E. Stein of FZK using the MCNP-code with FENDL/MC-1.0 and EFF-2 data.

- **Integral data testing of Fe-56 cross-sections - CEA Cadarache**

Calculations of neutron leakage spectra from spherical iron shell assemblies (IPPE Obninsk, OKTAVIAN and Gulf General Atomic experiments) were performed with the two-dimensional discrete ordinates code BISTRO using the FENDL/MG-1.0 iron data.

Comparisons with EFF-1 and EFF-2 multigroup data and sensitivity/uncertainty analyses were included for the mentioned spherical shell experiments.

Analyses were performed by L. Benmansour and A. Santamarina of CEA Cadarache.

IV.4 Russian Contributions

Contributions from the Russian Federation comprise analyses of spherical shell experiments performed at IPPE Obninsk, OKTAVIAN and KIAE Moscow, and analyses of FNS TOF slab experiments and the MEPhI-KIAE iron mock-up experiment. Calculations were performed using both the MCNP-code with FENDL/MC-1.0 and ONEDANT-calculations with the FENDL/MG-1.0 data library. In addition, calculations were performed with the ANISN discrete ordinate code using BROND-2, ENDF/B-VI, JENDL-3 and FENDL-1 data processed with the Russian GRUCON/EXPERT system from the corresponding evaluated data files.

The following contributions were submitted:

- **Analyses of spherical shell transmission experiments - IPPE Obninsk**

Calculations of neutron leakage spectra were performed by A. Blokhin, S. P. Simakov and V. Sinitsa of IPPE Obninsk for the following transmission experiments:

(1) Be and Fe spherical shells (IPPE Obninsk experiments)

These experiments are partially included in the IAEA compilation of fusion neutronics benchmark experiments /Ganesan 94b/. In addition, new experimental results on neutron leakage spectra from iron spherical shells with wall thicknesses between 2.5 and 28 cm were contributed and analysed with FENDL-1 multigroup data /Simakov 95/. Experimental details for this set of measurements are briefly documented in /Devkin 94/ and in more detail in /Devkin 95/.

(2) Nb, Si and Zr spherical shells (OKTAVIAN experiments)

The documentation of these experiments again is included in the JAERI collection of experimental fusion benchmark experiments /JAERI 94/, see section IV.1 above.

Calculations for the spherical shell experiments were performed with one-dimensional discrete ordinates codes (ONEDANT, ANISN) and FENDL/MG-1.0, ENDF/B-VI and BROND-2 data.

- **Benchmark analyses of Kurchatov Institute Moscow**

FENDL-1 benchmark analyses were performed for both spherical shell experiments and slab experiments using the MCNP4A-code and the FENDL/MC-1.0 data library. Comparisons were performed with Monte Carlo calculations using the BLANK-code and data processed from the ENDF/B-VI -data file. The calculations were performed by V. Markovskij of KIAE Moscow. The following types of experiments were analysed /Markovskij 95/:

(1) Beryllium integral benchmark experiments

The FNS TOF experiment on beryllium slabs with thicknesses of 50 and 152 mm (see section IV.1 above) was analysed and the spherical shell experiments of OKTAVIAN (see again section IV.1), IPPE Obninsk (see above) as well as the total multiplication experiment of KIAE on 5 and 8 cm thick spherical shells applying the total absorption measuring technique („boron tank method") /Zagryadskij 88/.

(2) Iron integral benchmark experiments

The FNS TOF experiment on iron slabs with thicknesses of 5 and 40 cm (see section IV.1 above) was analysed and the spherical shell experiments of OKTAVIAN (thickness of 50.32 cm) and IPPE Obninsk (see above). In addition, an iron shield mock-up experiment, performed at MEPhI-KIAE Moscow, was analysed with FENDL-1 data for configurations with and without a straight gap.

Table IV.1 shows an overview of the benchmark experiments analysed and contributed to the FENDL benchmark validation task by the various laboratories.

Type of integral experiment	Material configuration	Material	Experiment	Benchmark analysis
TOF-measurements of angular leakage spectra	Cylindrical slabs	Li_2O, Be, C, O, N, Fe, Pb	FNS/JAERI	FNS/JAERI
In-system measurements of neutron spectra & reaction rates	Cylindrical slabs	Li_2O, Be, C, Fe, Cu, W	FNS/JAERI	FNS/JAERI, Hitachi Ltd., KIAE Moscow
TOF-measurements of neutron leakage spectra	Spherical shells	Be, Be-Li, Li, Li_2O, LiF, C, CF_2, Al, Si, Ti, Cr, Mn, Co, Ni, Cu, Zr, Nb, Mo, W	Universities of Osaka & Kyoto	Universities of Osaka & Kyoto, FZK Karlsruhe, IPPE Obninsk, KIAE Moscow
TOF-measurements of gamma ray leakage spectra	Spherical shells	LiF, CF_2, Al, Si, Ti, Cr, Mn, Co, Cu, Nb, Mo, W, Pb	Universities of Osaka & Kyoto	FNS/JAERI
Bulk shield experiment	Cylindrical block	SS-316	FNS/JAERI	FNS/JAERI, UCLA
Bulk shield and streaming experiment	Rectangular block, with and without duct	SS-316	ORNL	RSIC/ORNL
Bulk shield and nuclear heating experiment	Rectangular block	SS-316, SS-316 and perspex	ENEA Frascati	ENEA Frascati
TOF-measurements of neutron leakage spectra	Spherical shells	Be, Al, Fe, Pb-17Li	IPPE Obninsk	IPPE Obninsk, KIAE Moscow, FZK Karlsruhe, CEA Cadarache
TOF-measurements of neutron leakage spectra	Spherical shells	Be	FZK Karlsruhe	FZK Karlsruhe, Hitachi Ltd.
Neutron and photon leakage spectra measurements	Rectangular slab, with and without straight gap	Fe	TUD Dresden	TUD Dresden, FZK Karlsruhe
Multiplication experiment	Spherical shells	Be	KIAE Moscow	KIAE Moscow
Mock-up shield experiment	Rectangular slab, with and without straight gap	Fe	MePhI-KIAE Moscow	KIAE Moscow

Table IV.I: Integral experiments and analyses contributed to the FENDL-1 benchmark validation task

V. Main Results of FENDL-1 Data Test Analyses

In this chapter are summarised and evaluated the main results of the internationally performed integral data tests that were contributed to this report. Selected figures, comparing calculated and measured quantities (mainly neutron or photon spectra), are presented where appropriate and available. C/E tables are given to a larger extent to provide better information on the data quality when applied in neutronics design calculations, to facilitate subsequent uncertainty analyses and aid in improving the forthcoming FENDL-2 data base.

In view of their different use and importance for fusion reactor applications, the results of the benchmark experiments are categorised into the following three material groups:

(1) Multiplying and breeding materials

Neutron multipliers:	**Be, Pb**
Breeding material:	**Li**
Breeding material constituents:	**Al, Si, Zr**

(2) Shielding and/or structural materials

Fe, Cr, Mn, Ni, Cu, W

(3) Other materials

C, O, N, F, Co, Nb, Mo, Ti

In the following the focus is on the comparison of measured and calculated neutron spectra, as the neutron spectrum is the primary quantity of interest in neutron transport calculations. This includes analyses of direct neutron spectrum measurements and of activation and fission rate measurements, which are sensitive to different parts of the neutron spectrum.

The analyses of the gamma-ray spectra and heating rate experiments are presented subsequently, comprising all materials for which results are available.

V.1 Multiplying and breeding materials

(1) Beryllium

Beryllium is the most favoured neutron multiplier candidate for solid breeder blankets of fusion power reactors. Its neutron multiplication power has been assessed in several transmission experiments on spherical beryllium shells, see e. g. /Möllendorff 94/ and references given there. The measured total neutron multiplication factor, which accounts for the total number of neutron leakages, can be reproduced fairly well by calculations with beryllium cross-sections from the different data files, e. g. FENDL-1, EFF-1, -2 and ENDF/B-VI /Fischer 94/. In general the deviation is within the experimental uncertainty band of 3 to 7 %, see e. g. tables 1-7.

The spectral breakdown of the neutron leakage spectra shows, however, that this agreement is caused by compensating over- and underestimations in the lower and upper part of the spectra, see e. g. tables 6, 7. In particular, the spectrum is underestimated with FENDL-1 data by 10 to 20% in the evaporation region around 1 MeV (see e. g. tables 6,7 and figure 11). Much better agreement is obtained with the measured leakage spectra when using the Young & Stewart beryllium data evaluation /Young 79/ which is contained e. g. in the EFF-1 data file (figure 11). An inconsistent trend was detected in the OKTAVIAN integral beryllium experiment, when comparing the integrated neutron leakages which were measured for the different shell configurations /Markovskij 95/.

In the FNS TOF-experiments an overall good agreement is obtained for the angular spectra of the 5.08 cm and 15.24 cm thick slabs (tables 9, 10, figures 1 - 3). This is different from the observations found in the spherical shell experiments. It may be due to the fact that in the latter experiments all scattering angles (including backward directions) contribute to the measured leakage spectra, whereas in the TOF slab experiments the leakage spectra are measured in forward directions between 0 and 66.8° with no significant contributions from backward scattering events. This is confirmed by comparisons of secondary energy and angle distributions with measured single and double-differential data where a strong underestimation of the neutron emission spectrum is observed for FENDL-1 (ENDF/B-VI) data at backward angles /Fischer 94/.

The analyses of the FNS slab in-system experiments show large overestimations (20 to 50%) of the reaction rates that are sensitive to low energy neutrons (^{235}U(n,f), ^{6}Li(n,α) , ^{197}Au (n,γ)), whereas there is better agreement for fast responses, see fig. 5 - 10. The agreement obtained for the ^{115}In(n,n') reaction rates - being sensitive to the energy range 1 to 5 MeV - is consistent with the results of the TOF experiments. The neutron spectra measured with small NE-213 spectrometers are overestimated systematically by the calculations in the energy range 1 to 10 MeV, while the spectrum above 10 MeV is in good agreement. The neutron spectra measured by PRC detectors in the energy range between 2 keV and 0.5 MeV inside the beryllium slab are well reproduced by the FENDL-1 calculations.

In conclusion, a revision is needed for the secondary energy and angle distributions of the FENDL-1 Be data evaluation.

(2) Lead

Lead is considered as neutron multiplier in liquid metal breeder blankets applying the eutectic alloy Pb-17Li as breeding and/or cooling material. Neutron multiplication factors have been measured in several spherical shell experiments, see e. g. /Elfruth 87/, where there have been observed systematic underestimations of the measured

values independent on the used nuclear data evaluations /Fischer 88/ . Actually, this disagreement was mainly caused by experimental errors apparent in the large spread of measured neutron multiplication factors.

The currently most accurately measured neutron multiplication factor has been obtained by the total absorption measurement (using the „boron tank method") performed at KIAE Moscow for the TUD lead spherical shell of 22.5 cm wall thickness. This shell configuration has been used previously at TU Dresden /Elfruth 87/ for TOF-measurements of the neutron leakage spectrum. It can be reproduced fairly well with FENDL-1 data (fig. 15), although there is a slight underestimation of the evaporation region around 1 MeV. The total neutron multiplication factor obtained in the KIAE boron tank experiment amounts to M=1.856±0.077 /Bessonov 89/, while a MCNP4A-calculation with FENDL/MC-1.0 data gives M=1.79. Thus there is agreement within the experimental error, although the calculated value is still at the lower end of the experimental uncertainty band.

For the IPPE Obninsk experiment on a 7.5 cm thick spherical shell a similar trend is observed as for the TUD experiment when calculated and measured neutron leakage spectra are compared (fig. 15). In addition, the Pb(n,xn)-SED agrees well with measured neutron emission cross-section data (fig. 15).

For the FNS TOF experiments very good agreement is obtained between calculated and measured angular spectra, both for thin (5.08 cm) and thick (20.3, 40.6 cm) lead slab configurations (fig. 12 - 14 and table 14).

It is concluded that no major revisions or improvements are needed for the FENDL-1 lead data evaluation.

(3) Lithium

There are available the following integral experiments involving the breeding material lithium: the FNS experiments on Li_2O slabs with both TOF and in-system measurements, the OKTAVIAN experiments on Lithium metal and LiF spherical shells as well as on combined Be/Li shell configurations, and the IPPE Obninsk experiment on a spherical Pb-17Li shell. All of them were analysed with FENDL-1 data.

Good agreement was obtained for the angular spectra measured in the TOF-experiments for thin (4.8 cm) and thick (20 and 40 cm) **Li_2O** slabs (figs. 17-19, table 16) although the forward neutron transmission above 14 MeV tends to be overestimated with increasing thickness. This would become serious for fusion reactor design applications, if thick Li_2O breeding zones were used in the blanket. Further investigations are required, however, to trace back the source of this discrepancy to one of the Li_2O-constituents, i. e. lithium or oxygen.

For the in-system measurement of the neutron spectrum there is a systematic overestimation in the energy range 1 to 10 MeV (fig. 20), which analogously was observed in the beryllium in-system measurements (fig. 4). This is due to common experimental errors involved in the spectrum unfolding method in this energy region. Measured and calculated reaction rates agree in general well within the experimental uncertainty. There are few exceptions, e. g. the ^{7}Li(n,n'α)t-rate measured by the NE213 indirect method, which is overestimated throughout by about 15% (fig. 21). This, however, is only caused by the use of the JENDL-3PR1 dosimetry file for the ^{7}Li(n,n'α)t reaction.

An overall good agreement for the neutron leakage spectrum is also observed in the OKTAVIAN experiment on a lithium metal spherical shell (fig. 16). There is, however, a significant underestimation of the high energy spectrum at 5-10 MeV which is not seen in the FNS slab experiments. Although this discrepancy is not too serious with regard to fusion applications, investigations are required to address and remove the

related deficiencies in the underlying cross-section data. It is indicated to check again the the secondary energy and angle distributions of the ^{6,7}Li FENDL-1 data evaluations

In case of the LiF OKTAVIAN experiment serious discrepancies are observed in the neutron leakage spectra (fig. 97). Based on the good agreement obtained for the Li sphere experiment, it may be deduced that the observed disagreement should be caused by deficiencies in the involved F cross-section data.

For the IPPE Obninsk experiment on a 14.0 cm thick **Pb-17Li** spherical shell an overall good reproduction of the measured leakage spectrum is observed with a similar trend as for the IPPE lead spherical shell (fig. 15). No conclusion on the quality of the involved Li data can be deduced from this experiment.

The shape of the leakage spectra measured for the combined **beryllium/lithium** spherical shell assemblies at OKTAVIAN can be reproduced quite satisfactorily in general (fig. 11, table 5). Note, however, that the quantitative agreement throughout is unsatisfactory both for FENDL-1 and EFF-1 data. This disagreement is most likely the result of systematic errors involved in the experiment, as may be deduced e. g. from the shift in the transmitted neutron source neutron peak.

(4) Breeding material constituents : Al, Si, Zr

Results are available for the measured neutron leakage spectra of spherical shell experiments performed at OKTAVIAN (Al, Si, and Zr) and IPPE Obninsk (Al). For these materials the agreement between experiment and FENDL-1 calculations in general is very unsatisfactory.

In the OKTAVIAN experiment for **aluminium** there is an overestimation of the low energy part of the spectrum (E< 1 MeV) by about 25 %, but a significant underestimation by about 40 % of the high energy region 5 - 10 MeV (tab. 18-20 and figs. 26, 27). The latter underestimation is also observed in the Al (n,xn)-SED when compared to measured neutron emission cross-section data (fig. 26). In the IPPE experiment, on the other hand, a systematic underestimation by about 10 to 20% is observed, whereas the spectrum above 10 MeV is reproduced satisfactorily. Note that JENDL-3.2 and EFF-2 data give similar results as FENDL-1, with a better reproduction of the high energy range.

For the OKTAVIAN experiments on **silicon** there is a similar behaviour as for aluminium: there is a strong overestimation of the low energy part of the spectrum (E< MeV) by as much as 50 - 100 %, but a systematic underestimation by about 30 % of the high energy region 1 - 10 MeV (tables 21-23 and figs. 28, 29). Again the latter underestimation is observed in the (n,xn)-SED when compared to measured Si neutron emission cross-section data (fig. 28). Note that both the more recent JENDL-FF (Fusion File) and EFF-2 data give a better reproduction of the leakage spectrum in the energy range below 1 MeV. The shifting of the peak at .15 MeV with regard to the calculated spectra may be due to errors in the experimental determination of the neutron energies.

The leakage spectrum of **zirconium** measured in the OKTAVIAN experiment can be reproduced more satisfactorily with FENDL-1 data. There is, however, a systematic overestimation by about 20% of the high energy part between 1 and 10 MeV (figs. 30, 31) which does not correspond to the good agreement of the Zr(n,xn)-SED when compared to measured neutron emission cross-section data (fig. 30). There is a need to check the SED/SAD of the individual isotopes forming the natural zirconium.

V.2 Structural and/or shielding materials

In case of the structural materials, at first we present the benchmark results for individual elements and subsequently the results obtained for the combined materials, i. e. SS-316 that is used in the FNS and FNG shielding experiments.

(1) Iron

For the IPPE Obninsk experiment on a 7.5 cm thick iron spherical shell there is an underestimation of the measured total neutron leakages by about 10% which is mainly caused by the underestimated low energy part (E<1.5 MeV) (tables 26-28, fig. 43). Note that this holds for all data files including FENDL-1 and EFF-1, and EFF-2. There is, in addition, an underestimation of the transmitted neutron source peak by about 10%.

A similar trend is observed in the TUD iron slab experiment (thickness: 30 cm), where the low energy part (E<1.0 MeV) is underestimated by about 15% and the total measured neutron flux by 10% (tables 32, 33, and figs 40, 42). In the high energy range (2 -10 MeV) good improvement over the outdated EFF-1 data is obtained with both the FENDL-1 and EFF-2 data (fig. 42). This is due to a good description of the correlated energy-angle distributions of the neutrons emitted in the (n,xn')-reactions.

For the TUD iron slab experiment it has been shown only recently that there is no longer an underestimation of the leakage spectrum when using EFF-3 iron data that take into account the fine structure („fluctuations") of the partial iron reaction cross-sections up to about 7 MeV /Hogenbirk 95/. In the EFF-3 iron evaluation this fluctuation fine structure is taken into account on the basis of experimental data obtained in high resolution measurements at CBNM Geel. In view of the perfect agreement obtained by Hogenbirk for the TUD experiment with this approach, there is a clear need to apply this scheme also for FENDL-2.

In the FNS TOF-experiments the angular leakage spectra for 5, 20, 40 and 60 cm thick slabs have been measured. The overall trend with regard to FENDL-1 calculations is as follows. Except for the 60 cm thick slab, an underestimation of the low energy spectra (E< 0.1 MeV) is observed for almost all angles (fig. 32, table 34). It amounts to about 10 t0 20 % for the thin slabs and up to 50% for the 40 cm thick slab. For the 60 cm thick slab, there is, on the other hand, an overestimation of the low energy spectra by about 20%. At some angles, e. g. 12.2 and 24.9°, there is an overestimation of the spectra in the energy range 5 - 10 MeV (figs. 33, 34) which cannot be seen in the integrated leakage spectra of the spherical shell experiments and the TUD slab experiment. In addition, the high energy spectrum above 10 MeV is overestimated by as much as 20 to 30 % at some angles (tables 34, 35 and figs. 33, 34).

In the FNS in-system slab experiment, on the other hand, very good agreement is obtained for the neutron spectrum over the energy range 1 MeV down to 1 eV, see figs. 35, 36. This holds both for shallow and deep detector positions inside the iron block, ranging from 31 to 81 cm. For the measured reaction rates sensitive to fast neutrons (E>10 MeV) a systematic underestimation by 10 t0 20% is observed which may be caused by some systematic error of the experiment (figs. 36 - 39).

(2) Nickel

There is one OKTAVIAN experiment on a nickel spherical shell. However, there appears to be a normalisation problem in this experiment as the transmitted neutron source peak is overestimated by about a factor 2.5. Apart from this, it can be

deduced that the qualitative shape of the leakage spectrum can be reproduced by the FENDL-1 calculations.

(3) Chromium

For chromium there is an OKTAVIAN experiment on a 9.8 cm thick spherical shell. There is quite good agreement with the measured neutron leakage spectrum over the energy range 15 to about 2 MeV with only a slight overestimation by about 10 % (fig. 48). Below 1 MeV neutron energy, there is an overestimation by as much as 50%. As for iron, this discrepancy may be resolved by the inclusion of the fluctuation fine structure of the chromium cross-section data which in Europe is underway for the development of the EFF-3 file.

(4) Copper

For the OKTAVIAN copper experiment on a 27.5 cm thick spherical shell there is good agreement with the measured neutron leakage spectrum below 5 MeV. The spectrum in the energy range 5 to 10 MeV is overestimated by about 36 %. (fig. 60, table 38). Better agreement is obtained with JENDL-data (fig. 60).

For the FNS in-system slab experiment, a similar trend is observed for the neutron spectrum above 1 MeV (fig. 54). The low energy spectrum (10 eV<E<0.1 MeV) is overestimated while the ^{197}Au (n,γ) reaction rate, which is sensitive to very low energy neutrons, is underestimated as much as 40% (fig. 56, table 40). For fast responses there is an inconsistency: while the ^{58}Ni(n,2n) rate is underestimated by about 20%, the ^{93}Nb(n,2n) rate shows good agreement (figs. 55, 56).

(5) Manganese

For manganese there is an OKTAVIAN experiment on a 27.5 cm thick spherical shell. As for chromium there is rather good agreement with the measured neutron leakage current over the energy range 15 to about 0.5 MeV with a slight overestimation in the order of 10% (table 41, fig. 49).

(6) Tungsten

For the OKTAVIAN experiment on a 9.8 cm thick tungsten spherical shell there is an underestimation of the measured neutron leakage spectrum by about 10% on the average (table 42, fig. 50). For the high energy range 5 - 10 MeV the underestimation amounts up to 30%. This holds likewise for JENDL-3 tungsten data.

In the FNS in-system slab experiment a similar trend is observed. The neutron spectrum is underestimated in the energy range 1 to about 12 MeV at most locations in the tungsten slab (fig. 51) The high energy spectrum part (E>12 MeV), however, is considerably overestimated. This is consistent with the overestimation of the fast responses, e. g. the ^{92}Nb(n,2n)-reaction, by 10 to 20% (fig. 52). The low energy part of the spectrum is underestimated and this holds likewise for the reaction rates which are sensitive to the low energy neutrons. For the ^{197}Au(n,γ) - reaction rate the underestimation amounts to 20% (fig. 53).

(7) SS-316

For the SS-316 bulk shield experiments (FNG and FNS) a unique trend was observed in underestimating the high energy tail (E>10 MeV) of the neutron spectrum. This is also consistent with the results observed in the integral experiments on iron, which is the main constituent of SS-316. Inconsistent results were obtained for the low energy (E<0.1 MeV) tail of the neutron spectrum as for the energy range between 1 and 10 MeV. Some consistency has been also found for that energy range in underestimating the corresponding reaction rates both at FNG and FNS.

In the two FNS experiments the underestimation of the high energy neutron flux (E>10 MeV) amounts to 25 to 35% at deep locations when using discrete ordinate calculations with multigroup data and to about 10% when using Monte Carlo calculations, see fig. 70. Reactions that are sensitive to this component are also underestimated at these deep locations by as much as ~20%, see e. g. fig. 68 for the ^{93}Nb-(n,2n)^{92m}Nb, or fig. 67 for the ^{27}Al(n,α)^{24}Na reaction rate. In the FNG-experiment, the underestimation of the fast responses which are sensitive to this energy range, e. g. the ^{27}Al(n,α)-reaction, amounts to 10 to 20% at maximum, cf. fig 67. Self-shielding the cross-section has no impact on the calculated values of these high-energy reactions.

For the neutron spectrum in the energy range 2 to 10 MeV an overestimation is observed at the front locations of the FNS steel block. With increasing depth this overestimation turns into an underestimation of ~10%, both with Monte Carlo and discrete ordinates calculations, see fig. 71. This is consistent with the observations found in iron spherical shell experiments (tables 29,30 and figs. 44-46). The results for the reaction rates sensitive to that reaction rates show the same trend. One notices that for the Monte Carlo calculations, the deviations from the measured values are in general much smaller and there is a tendency to agree with the measurements within the experimental error. In the FNG experiment, there is a trend for underestimating the reaction rates sensitive to the neutrons in the energy range 1-10 MeV, e. g. the ^{115}In (n,n') reaction by about 10 to 20% (fig. 63) and the ^{237}Np fission rate by up to 25% (fig. 69). In the FNS experiment, the ^{115}In (n,n') reaction rate is also underestimated (fig. 63), and so is the ^{238}U fission rate (fig. 64).

In the energy range 0.1 to 1.0 MeV, there is again an underestimation observed in the neutron spectra of the FNS SS-316 experiments that amounts up to 40 % both with Monte Carlo and discrete ordinates calculations, see fig. 71. Note that these observations are similar in the two FNS test assemblies. Below 0.1 MeV there is an underestimation at deep locations inside the block, but again an overestimation at the front part (fig. 75). For the Monte Carlo calculations this trend is not so clear than it is for the discrete ordinates calculations. Again the Monte Carlo calculations tend to agree with the measurements within the experimental error.

In the FNG-experiment, the ^{235}U fission (fig. 62) and the ^{55}Mn(n,γ) rate (fig. 69) are satisfactorily predicted with FENDL-1 data while the ^{197}Au(n,γ) - rate is underestimated by about 10%, see fig. 61 . In the FNS experiment, on the other hand, the ^{235}U fission rate is underestimated (fig. 62) whereas the ^{197}Au(n,γ) - rate is well predicted by Monte Carlo calculations with a tendency to overestimations for the locations deep inside the steel block (fig. 61). For the discrete ordinates calculations, however, there is a different trend: underestimations at the front locations, overestimations in the middle part of the block and strong underestimations at the back positions for the ^{197}Au(n,γ) - rate, fig. 61. In addition, a strong impact of resonance shielding and data processing can be detected in this case (self-shielded data gives better agreement with measurements).

In summary, there is a trend of underestimating the integrated spectrum in the energy ranges En>10 MeV and 2<En<10 MeV at deep locations which is also reflected on high-threshold reactions at these locations. No unique trend can be deduced from the analyses of the SS-316 experiments for the neutron energy below 0.1 MeV. It can be stated, however, that, except for locations that are deep inside the SS-316 assembly, the agreement with the experimental results is not too bad taking into account the experimental errors as well as the uncertainties in the dosimetry cross-section data. In particular this holds for Monte Carlo calculations that agree much better with the measurements than do the discrete ordinates calculations with multigroup data.

V.3 Other materials: C, O, N, F, Co, Nb, Mo, Ti

(1) Graphite

In the FNS TOF-experiments an underestimation of the low energy leakage spectra by 10 to 20% is observed (figs 78 -80, table 74). A too soft neutron emission spectrum is indicated for FENDL-1 data. JENDL-3 data agree better with the measured spectra. For the high energy spectra the agreement with FENDL-1 data is in general satisfactory.

In the FNS in-system experiment there is a trend for overestimating the measured neutron spectra in the range 1 to about 10 MeV (fig. 81). Likewise, the ^{235}U fission rate is overestimated by about 10% on average, see fig. 83. There is, however, a nonuniform trend (under- and overestimations) for the fast responses, although the deviations are not significantly outside the band of experimental uncertainties, except for $^{93}Nb(n,2n)$, see fig. 82.

(2) Oxygen

The analyses of the FNS TOF-experiments show a systematic underestimation of the measured leakage spectrum, except for the forward direction. The underestimation amounts to about 20% for the low energy part (E<1MeV) and up to 40% for the high energy parts of the spectrum (table 46 and figs. 88, 89). Better agreement is obtained with JENDL-3 data.

(3) Nitrogen

As for oxygen, the analyses of the FNS TOF-experiments show a clear trend of underestimating the measured leakage spectra with FENDL-1 data. The underestimation in general is as much as 40% . JENDL-3 data can better reproduce the measured spectra, see figs. 90, 91.

(4) Fluorine

There are two OKTAVIAN experiments involving fluorine: one on a LiF and one on a CF_2 spherical shell assembly. Both experiments show serious deficiencies that may be addressed to the FENDL-1 data for fluorine: there is an underestimation of the leakage spectra by as much as 40% over the whole measured energy range in case of the CF_2 spherical shell and a strong underestimation of the energy range .3 to 1 MeV in case of the LiF sphere (tables 47, 48 and fig. 97).

(5) Cobalt

There is a strong underestimation (about 40%) of the leakage current below 10 MeV measured in the OKTAVIAN experiment on a 9.8 cm thick cobalt spherical shell (table 49 and fig. 92). The high energy part of the spectrum (E>10 MeV) is well predicted.

(6) Niobium

For Niobium an overestimation is observed (20 to 30%) of the leakage current below 10 MeV. It has been measured in an OKTAVIAN experiment for a 11.2 cm thick spherical shell. The high energy part of the spectrum (E>10 MeV) again is well reproduced (table 50 and figs. 95, 96).

(5) Molybdenum

The leakage spectrum for a 27.5 cm thick molybdenum spherical shell again has been measured in an OKTAVIAN experiment. The agreement for the calculated FENDL-1 leakage spectrum is rather satisfactory, although there is an underestimation of the spectrum in the energy range 5 to 10 MeV by as much as 30 % (table 94 and fig. 94). There is an overall better agreement forJENDL-3.2 data.

(6) Titanium

As for cobalt, there is a large discrepancy for titanium in the leakage spectrum measured in an OKTAVIAN experiment for a 9.8 cm thick spherical shell. There is a significant overestimation by about 40 % in the spectrum below 5 MeV (table 51 and fig. 93). The high energy part of the spectrum (E>10 MeV) is overestimated by 20%.

V.4 Gamma-ray spectra and heating rates

Gamma-ray spectra have been measured in OKTAVIAN experiments for the materials:

LiF, CF_2, Al, Si, Ti, Cr, Mn, Co, Cu, Nb, Mo, W and Pb.

There is an overall good agreement between measured and calculated gamma-spectra in the energy range 0.5 to about 5 - 6 MeV for most of the analysed materials, e. g. LiF, CF_2, Al, Si, Cu, Mo, W and Pb, see figs. 98 -102. Significant discrepancies are observed in this part of the spectrum for the structural materials Cr, Mn, Nb, Co and Ti. This results in underestimations of the integrated spectra by about 20% (table 53, fig. 98) for Mn and Nb, and an overestimation by abot 30% for Cr. Systematic discrepancies - in general underestimations - are observed for the high energy part (E>5 MeV) of the gamma-spectra. In particular this holds for titanium, manganese, cobalt, niobium, tungsten, and lead (figs. 99 - 102). With regard to FENDL-1 data, this is serious for lead, for which JENDL-3.2 data give much better agreement. When comparing C/E-data for the integrated gamma spectra and energy release rates it is observed that there is much more disagreement for the latter ones, cf. 98. For Co, e. g. , FENDL-1 gives the correct total gamma flux but an underestimation of the related heating rate by about 20%.

Gamma-ray spectra and heating rates have been measured in the FNS in-system experiments for **iron, copper and tungsten.** Good agreement was found in comparing measured and calculated gamma heating rates for iron (fig. 39) and copper (fig. 59), whereas a serious overestimation by 20 to 80% was obtained for tungsten (fig. 54). This, however, is inconsistent with the good agreement obtained for the gamma heating rates in the OKTAVIAN-experiment. In addition, the tungsten gamma ray spectra of both the FNS in-system and the OKTAVIAN-experiment are rather well reproduced by FENDL-1-calculations.

Contrary to the FNS in-system experiment, an underestimation of the measured photon spectra (0.2 to 8.0 MeV) by about 20% is observed in the TUD iron slab experiment (table 32, fig. 41). This is consistent with the underestimation of the neutron leakage spectra in the same experiment.

In the FNG nuclear heating experiment the nuclear heating rate has been measured for **SS-316** inside the layered shielding block up to 70 cm depth. An underestimation by about 10% has been found for MCNP-calculations with FENDL/MC-1.0 data, both at shallow and deep positions inside the block (fig. 73). This underestimation, hoewever, is within the experimental error. As the nuclear heating in SS-316 is mainly due to gamma ray interactions, this underestimation has to be addressed to the gamma heating of the SS-316 constituents which is mainly iron.

In the FNS bulk shielding experiment on large **SS-316** assemblies the gamma heating rate has been measured along a central channel up to 91 cm depth. A similar trend of underestimating the nuclear heating in SS-316 has been obtained as in the FNG-experiment, although the results of the MCNP-calculations with FENDL-1 data largely lie within the band of experimental uncertainties (fig. 72). The underestimation is stronger at the front positions and at deep locations in the steel block. When analysing the FNS-experiment with discrete ordinates calculations and FENDL/MG-1.0 data (a collapsed set of 80 neutron and 24 gamma groups was used in the calculations) even larger underestimations are obtained that amount up to 30% at deeper positions with the self-shielded data and up to 60% underestimation with the unshielded data (fig. 72).

VI. Conclusions and recommendations

Comprehensive data test analyses have been performed for the FENDL-1 data file in an international co-ordinated effort. Benchmark calculations have been performed with the working libraries FENDL/MG-1.0 for discrete ordinates calculations and FENDL/MC-1.0 for Monte Carlo calculations with the MCNP-code. A variety of available integral fusion benchmark experiments has been analysed for that purpose. The obtained results allow to qualify the FENDL-1 working libraries for fusion applications.

In addition to that, Monte Carlo calculations with FENDL/MC-1.0 data and discrete ordinates calculations with FENDL/MG-1.0 multigroup data have been performed for the same benchmark experiments to allow a direct comparison of the two different computational approaches and data libraries. In general, the two approaches give the same results as has been shown both for analyses of spherical shell and slab experiments. There are, however, two exceptions to this rule encountered in the course of the benchmark analyses:

(1) Transport problems involving neutron thermalisation cannot be properly accounted for in discrete ordinates calculations with multigroup data in the VITAMIN-J group structure. This is due to missing up-sacttering capabilities while splitting the thermal energy range into two groups, see e. g. the results of thermal responses in the FNS beryllium (figs. 9, 10) and graphite slab (figs. 85,86) in-system experiments.

(2) Deep penetration problems can be better described by Monte Carlo calculations with continuously represented cross-section data than by discrete ordinates calculations with multigroup data. This observation is based on the use of a collapsed set of multigroup data (80 energy groups vs. 175 in FENDL/MG-1.0) in analysing the FNS SS-316 experiment and is affected by the applied group structure, the spatially varying weighting functions, the resonance shielding and the associated multigroup data processing. In addition to this, deficiencies are introduced by the discrete ordinate technique itself in describing the strongly forward peaked neutron transport in a deep penetration problem.

In summarising these items, it may be stated as an outcome of the performed benchmark analyses that the Monte Carlo technique with continuously represented cross-section data allows to handle all the encountered fusion neutronics problems with confidence while discrete ordinates calculations do not necessarily. Consequently, care has to be taken in applying the FENDL/MG-1.0 library to fusion neutronics problem where it may not be appropriate.

With regard to the data quality, it can be stated that fusion nuclear data have reached a high confidence level with the available FENDL-1 data library. With few exceptions this holds for the materials of highest importance for fusion reactor applications. As a result of the performed benchmark analyses, some existing deficiencies and discrepancies have been identified that may be removed in the forthcoming FENDL-2 data file.

It is to be stated that while the results of the many benchmarks described in this report and summarised below is very useful in guiding data evaluators to improve the existing data bases, it can also give guidance to blanket/shield designers of fusion reactors (e.g. ITER) to reasonable estimates of design margins/safety factors to be implemented in the design process. These design margins are based on the observed discrepancies between calculations and measurements. This is articularily useful from the benchmarking results on test assemblies composed of several materials (e.g. SS-316 assembly).

In the following, results are summarised for the three material categories. In addition, an evaluation table is given including the major findings of the benchmark analyses as well as recommendations for improvements.

(1) Multiplying and breeding materials

The neutron multiplication power can be well predicted for both neutron multiplier candidates, **beryllium** and **lead.** In addition, the neutron spectra in lead assemblies can be calculated very satisfactorily. This does not hold for beryllium: there is a need for a revision of the secondary energy-angle distributions and, possibly, the (n,2n) cross-section which should be accomplished in FENDL-2.

The data quality of the breeding material **lithium** look rather satisfactory. The measured angular neutron spectra for Li_2O. e. g. can be well reproduced.

For the breeding material constituent **aluminium, silicon and zirconium** there is a clear need for an improvement of the neutron emission cross-section data: the measured leakage spectra cannot be reproduced satisfactorily with FENDL-1 data. In addition, obvious deficiencies are detected in the secondary energy distributions of the (n,xn)-reactions. Thus there is a strong need for an updating of the **Al, Si** and **Zr** evaluations for FENDL-2.

Neutron multiplication and breeding materials

Element	Data quality	Comments
Be	further improvements needed	SED/SAD to be improved; neutron multiplication well predicted; discrepant integral experiments need to be clarified
Pb	satisfactory	
Li	satisfactory	
Al, Si, Zr	further improvements needed	SED to be improved; γ-production to be improved for Si

Table VI.1: FENDL-1 evaluation table: Major findings for neutron multiplication and breeding materials

(2) Structural and/or shielding materials

For the most important structural material **iron** there is an underestimation of the measured neutron spectra below ≅ 1.5 MeV which especially affects the calculations of the shielding efficiency. As shown by Hogenbirk for the TUD iron slab experiment, this discrepancy may be resolved with the inclusion of the fine resonance structure in the total and partial iron cross-section data above 0.8 MeV, as it is accounted for e. g. in the current EFF-3 iron evaluation. This task can be accomplished within the FENDL-2 development.

No evidence for urgent data improvements can be deduced from the available benchmark results for **manganese,** whereas the results for **copper** suggest a revision of the emission cross-section data both in the high (5-10 MeV) and low energy (E< 0.1 MeV) range. This holds also for **chromium** below 1 MeV. Again this should be accounted for in FENDL-2. For **nickel** the is a need for better experimental integral data.

The results from the available benchmark experiments for the shielding material **tungsten** also indicate the need for a data revision for FENDL-2.

With regard to required data revisions for FENDL-2, there is one unique trend that can be deduced from the analysis of the **SS-316** bulk shield experiments: there is an increasing trend of underestimating the high energy tail (E > 10 MeV) of the neutron spectrum at deep locations both by Monte Carlo calculations with FENDL/MC-1.0 data and discrete ordinates calculations with FENDL/MG-1.0

multigroup data. This may lead to underestimations in calculating radiation damages to the superconducting coils in fusion devices like ITER. In addition, there are indications that low energy spectra (E<0.1 MeV) are likewise underestimated in the **SS-316** experiments. For the fast energy range (1 to 10 MeV) there is a trend of underestimating the neutron spectrum at deep locations. In any case sensitivity and uncertainty analyses are required to assign observed discrepancies to individual materials and their cross-section data.

No integral experimental data are available for the low-activation structural material **vanadium.** In view of its increasing importance for future fusion reactors with enhanced safety features, integral benchmark experiments are required to check the nuclear performance of vanadium for such applications.

Structural and/or shielding materials

Element	Data quality	Comments
Fe	further improvements needed	fluctuation factors to be included in partial neutron cross-sections; need for including anisotropic γ-emission data indicated
Cr	further improvements needed	need for additional integral experiments; γ-production to be improved
Cu	further improvements needed	SED in 5-10 MeV range and below 1 MeV to be improved
Mn	satisfactory	need for additional integral experiments
Ni	unclear	urgent need for new integral experiment
W	further improvements needed	improvements for SED and γ-production needed
SS-316	further improvements needed	disagreement for high and intermediate energy range of neutron spectrum
V	unclear	urgent need for integral experiment; currently no data available

Table VI.2: FENDL-1 evaluation table: Major findings for structural and/or shielding materials

(3) Other materials

For most of these materials the results from the available benchmark experiments indicate the need for further improvements of their cross-section data for FENDL-2. Especially this holds for **titanium, cobalt, fluorine, oxygen, nitrogen,** and **graphite.** For **niobium** and **molybdenum** the deviations between measured and calculated neutron spectra are less serious.

Other materials

Element	Data quality	Comments
C	further improvements needed	SED needs improvement
N	further improvements needed	SED/SAD needs improvement
O	further improvements needed	SED/SAD needs improvement
F	further improvements needed	large discrepancies observed in integral data tests; SED possibly to be improved although differential data in agreement with experimental data
Ti	further improvements needed	SED needs improvement
Co	further improvements needed	SED needs improvement; need for more integral experiments
Nb	further improvements needed	SED needs improvement; γ-production to be improved
Mo	satisfactory	minor discrepancy in neutron spectrum

Table VI.3: FENDL-1 evaluation table: Major findings for other materials

(4) Gamma-ray spectra and heating rates

There is an overall good agreement between the OKTAVIAN experiments and the FENDL-1 calculations for the materials **LiF, CF_2, Al, Si, Ti, Cu, Mo, W, and Pb** for the gamma heating rates. The agreement for Cr, Mn, Co and Nb is not satisfactory. This holds likewise for the gamma-ray spectra. In addition, a serious underestimation of the high energy gamma spectrum (E>5 MeV) is observed for lead.

The measured gamma heating rates for **iron** and **copper** can be reproduced satisfactorily. This is also holds for **SS-316,** although there is a trend for underestimating the measured gamma heating rates in the analysed steel assemblies.

VII. References

/Muir 91/ D. W. Muir, S. Ganesan and A. B. Pashchenko: FENDL - A reference nuclear data library for fusion applications, Int. Conference on Nuclear Data for Science and Technology, May 13 -17, 1991, Juelich, Germany.

/Ganesan 94/ S. Ganesan, P. K. McLaughlin: FENDL/E - Evaluated nuclear data library of neutron interaction cross-sections and photon production cross-sections and photon-atom interaction cross-sections for fusion applications, Version 1.0 of May 1994, IAEA-NDS-128, May 1994

/Garching 94/ IAEA Advisory Group Meeting on „Improved Evaluations and Integral Data Testing for FENDL", September 12 -16, 1994, Garching, Germany

/MacFarlane 94/ R. E. MacFarlane: Status of processing for FENDL-1, presented at IAEA Advisory Group Meeting on „Improved Evaluations and Integral Data Testing for FENDL", September 12 -16, 1994, Garching, Germany

/Ganesan 94a/ S. Ganesan: Summary Report on the IAEA Advisory Group Meeting on „Review of Uncertainty Files and Improved Multigroup Cross Section Files for FENDL", November 8 -12, 1993, Tokai-mura, Japan, Report INDC(NDS)-297, January 1994

/Ganesan 94b/ S. Ganesan: Preparation of Fusion Benchmarks in Electronic Format for Nuclear Data Validation Studies, Summary Report of the IAEA Consultants' Meeting at IAEA Headquarters Vienna, Austria, December 13 -16, 1993, Report INDC(NDS)-298, March 1994

/Vienna 90/ A. B. Pashchenko and D. W. Muir: Summary Report of the IAEA Consultants Meeting on „First Results of FENDL-1 Testing and Start of FENDL-2", June 25 -28, 1990, Vienna, Austria; Report INDC(NDS)-241, November 1990.

/Lemmel 90/ H. D. Lemmel: „ENDF/B-VI Photon Atomic Interaction Data", Report NDS-58, Rev. 2, September 1990.

/Bessonov 89/ S. I. Bessonov et al.: Measurement of a total flux of neutrons from a lead sphere using the total absorption method, in: Proc. XIX. Int. Symp. on Nuclear Physics, Gaussig, Germany, Nov. 6 -10 1989, Report ZfK-733, Dec. 1989.

/Smith 93/ J. R. Smith: Neutron Multiplication in Beryllium, Fusion Technology 21, 2117 (1992)

/Fischer 94/ U. Fischer, E. Wiegner: Benchmark analyses of the ENDF/B-VI, EFF-1 and EFF-2 beryllium data evaluations for neutron transport calculations, 3. Int. Symp. on Fusion Nuclear Technology, Los Angeles, USA, June 27 - July 1, 1994.

/Fischer 88/ U. Fischer, A. Schwenk-Ferrero, E. Wiegner: Neutron multiplication in lead: A comparative study based on a new calculational procedure and new nuclear data, 1. Int. Symp. on Fusion Nuclear Technology, Tokyo, Japan, April 10 - 19, 1988.

/Fischer 94a/ U. Fischer, E. Wiegner: FENDL data testing for beryllium, lead, iron and copper, 3. Int. Symp. on Fusion Nuclear Technology, Los Angeles, USA, June 27 - July 1, 1994.

/Hunter 94/ H. T. Hunter, D. T. Ingersoll, R. W. Roussin, E. Sartori and C. O. Slater: SINBAD - A shielding integral benchmark archive and database for PC's, 8. Int. Conf. on Radiation Shielding, Arlington, USA, April 1994.

/Möllendorff 94/ U. v. Möllendorff et al.: Measurements of 14-MeV neutron multiplication in spherical beryllium shells, 3. Int. Symp. on Fusion Nuclear Technology, Los Angeles, USA, June 27 - July 1, 1994.

/Zagryadskij 88/ V. A. Zagryadskij et al.: Calculated neutron transport verifications by integral 14 MeV neutron source experiments with multiplying assemblies, Proc. 1. Int. Symp. on Fusion Nuclear Technology, Tokyo, Japan, April 10 - 19, 1988, Part B, pp. 353-358.

/Elfruth 87/ T. Elfruth et al.: The neutron multiplication of lead at 14 MeV neutron incidence energy, Atomkernenergie - Kerntechnik 49(1987), 121.

/Young 79/ P. G. Young, L. Stewart: Evaluated data for n + ^{9}Be reactions, Report LA-7932-MS, July 1979.

/Batistoni 94/ P. Batistoni, M. Angelone, M. Martone, M. Pillon, V. Rado: The benchmark experiment on stainless steel bulk shielding at the Frascati Neutron Generator, ENEA Report RT/ERG/FUS/94/15, 1994

/Batistoni 95/ P. Batistoni, M. Angelone, M. Martone, et al.: The bulk shield benchmark experiment at the Frascati Neutron Generator, Fus. Eng. Design 28 (1995), 504 - 514.

/Rado 95/ V. Rado, L. Petrizzi, P. Batistoni: Validation of the FENDL library using the FNG integral experiments, report presented at IAEA consultants' meeting on „Benchmark Validation of FENDL-1", Karlsruhe, Germany, October 17 -19, 1995.

/Markovskij 95/ D. Markovskij: Contribution to FENDL-1 integral data test, report presented to IAEA consultants' meeting on „Benchmark Validation of FENDL-1", Karlsruhe, Germany, October 17 -19, 1995.

/Devkin 94/ D. B. Devkin, M. G. Kobozev, S. P. Simakov, V. V. Sinitsa, V. A. Talalev, U. Fischer, U. von Möllendorff, E. Wiegner: Neutron leakage spectra from iron spheres, Proc. 18. Symp. on Fusion Technology, Karlsruhe, Germany, 22-26 August 1994, 1357-1360.

/Devkin 95/ B. V. Devkin, H. Giese, M. G. Kobozev, S. P. Simakov, V. A. Talalaev, U. v. Möllendorff: Neutron leakage spectra from spherical iron shells, unpublished report, Forschungszentrum Karlsruhe 1995

/Simakov 95/ S. P. Simakov: New results of IPPE experiments on spherical iron shells, presented to IAEA consultants' meeting on „Benchmark Validation of FENDL-1", Karlsruhe, Germany, October 17 -19, 1995.

/Youssef 94/ M. Z. Youssef, A. Kumar, M. A. Abdou, C. Konno, F. Maekawa, H. Maekawa: Benchmarking FENDL library through analysis of existing benchmark experiments - Part (I): Analysis of bulk shielding experiments on large SS-316 assemblies bombarded by d-t neutrons, Report UCLA-FNT-90, ITER/US/95/IV-BL-14A, University of California, Los Angeles, December 1994

/JAERI 94/ Sub working group of fusion reactor physics subcommittee (ed.): Collection of experimental data for fusion neutronics benchmarks, Report JAERI-M 94-014, February 1994.

/Konno 94/ C. Konno, F. Maekawa, Y. Oyama, Y. Ikeda, K. Kosako and H. Maekawa: Bulk shielding experiments on large SS-316 assemblies bombarded by d-t neutrons, Volume I: Experiment, JAERI-Research 94-043, December 1994

/F. Maekawa 94/ F. Maekawa, C. Konno, K. Kosako, Y. Oyama, Y. Ikeda, and H. Maekawa: Bulk shielding experiments on large SS-316 assemblies bombarded by d-t neutrons, Volume II: Analysis, JAERI-Research 94-044, December 1994

/Konno 95/ C. Konno, F. Maekawa, Y. Oyama, Y. Ikeda, K. Kosako and H. Maekawa: Bulk shielding experiments on large SS-316/water assembly bombarded by d-t neutrons, Volume I: Experiment, JAERI-Research 95-017, January 1995

/F. Maekawa 95/ F. Maekawa, C. Konno, K. Kosako, Y. Oyama, Y. Ikeda, and H. Maekawa: Bulk shielding experiments on large SS-316/water assembly bombarded by d-t neutrons, Volume II: Analysis, JAERI-Research 95-018, January 1995

/Hogenbirk 95/ A. Hogenbirk, A. J. Koning and H. Gruppelaar: Validation of the EFF-3.0 evaluation for 56Fe, ECN Petten, Report ECN-R--95-019/EFF-DOC-382, July 1995

/Hayashi 95/ K. Hayashi, Y. Oyama: Test of FENDL/MG-1.0 and JSSTDL3.2 by Analysis of FNS Benchmark Experiment, Report presented to IAEA consultants' meeting on Benchmark Validation of FENDL-1, Karlsruhe, Germany, October 17-19, 1995.

/Tayama 95/ R. Tayama, T. Tsukiyama, K. Hayashi, H. Giese, F. Kappler and U. v. Möllendorff: Test of Various Evaluated Beryllium Nuclear Data against the Karlsruhe Neutron Transmission Experiment, Report presented to IAEA consultants' meeting on Benchmark Validation of FENDL-1, Karlsruhe, Germany, October 17-19, 1995.

/Freiesleben 95/ H. Freiesleben, W. Hansen, H. Klein, T. Novotny, D. Richter, R. Schwierz, K. Seidel, M. Tichy and S. Unholzer: Experimental Results of an Iron Slab Benchmark, Report TUD-PHY-94/2, TU Dresden, 1995.

/Oyama 95/ Y. Oyama: JAERI-contributions to the FENDL benchmark validation task, Report presented to IAEA consultants' meeting on Benchmark Validation of FENDL-1, Karlsruhe, Germany, October 17-19, 1995.

/Ichihara 95/ C. Ichihara: Contributions of the Kyoto and Osaka Universities to the FENDL benchmark validation task, Report presented to IAEA consultants' meeting on Benchmark Validation of FENDL-1, Karlsruhe, Germany, October 17-19, 1995

/Youssef 95/ M. Z. Youssef: UCLA-contribution to the FENDL benchmark validation task, Report presented to IAEA consultants' meeting on Benchmark Validation of FENDL-1, Karlsruhe, Germany, October 17-19, 1995

/Simakov 95/ S. P. Simakov: New results of IPPE experiments on spherical iron shells, presented to IAEA consultants' meeting on „Benchmark Validation of FENDL-1", Karlsruhe, Germany, October 17 -19, 1995.

VIII. Tables

- List of tables -

Table 1: MCNP-calculations with FENDL-1, JENDL-FF and JENDL-3.2 data for OKTAVIAN Be spherical shells
- Y. Makita, A. Takahashi - University of Osaka

Beryllium shell #1: Inner radius =5.7 cm, outer radius = 17.35 cm, wall thickness = 11.65 cm

	FENDL-1		JENDL-FF		JENDL-3.2	
Energy range [MeV]	C/E	error	C/E	error	C/E	error
16.40 - 10.00	1.37	.01	1.39	.01	1.37	.01
10.00 - 5.00	.86	.01	.90	.01	.9	.01
5.00 - 1.00	.81	.00	.84	.00	.95	.01
1.00 - .10	.86	.01	.86	.01	.97	.01
Total [0.1 - 16.4]	.99	.01	1.02	.01	1.08	.01

Beryllium shell #2: Inner radius =6.9 cm, outer radius = 17.35 cm, wall thickness = 10.45 cm

	FENDL-1		JENDL-FF		JENDL-3.2	
Energy range [MeV]	C/E	error	C/E	error	C/E	error
16.40 - 10.00	1.44	.01	1.47	.01	1.45	.01
10.00 - 5.00	.79	.01	.83	.01	.84	.01
5.00 - 1.00	.76	.00	.79	.00	.89	.00
1.00 - .10	.83	.00	.83	.00	.93	.01
Total [0.1 - 16.4]	.98	.01	1.00	.01	1.06	.01

Beryllium shell #3: Inner radius =9.7 cm, outer radius = 17.35 cm, wall thickness = 7.65 cm

	FENDL-1		JENDL-FF		JENDL-3.2	
Energy range [MeV]	C/E	error	C/E	error	C/E	error
16.40 - 10.00	1.79	.12	1.82	.12	1.80	.12
10.00 - 5.00	.66	.01	.70	.01	.71	.01
5.00 - 1.00	.64	.00	.66	.00	.75	.00
1.00 - .10	.72	.00	.71	.00	.79	.00
Total [0.1 - 16.4]	.98	.02	.99	.02	1.04	.02

Beryllium shell #4: Inner radius =12.8 cm, outer radius = 17.35 cm, wall thickness = 4.55 cm

	FENDL-1		JENDL-FF		JENDL-3.2	
Energy range [MeV]	C/E	error	C/E	error	C/E	error
16.40 - 10.00	1.09	.00	1.10	.00	1.10	.00
10.00 - 5.00	.89	.01	.93	.01	.94	.01
5.00 - 1.00	.87	.01	.90	.01	1.01	.01
1.00 - .10	.88	.01	.85	.01	.91	.01
Total [0.1 - 16.4]	1.00	.00	1.01	.00	1.04	.01

Table 2: MCNP-calculations with FENDL/MC-1.0 data for OKTAVIAN Be spherical shells with 17.3 cm outer radius - D. Markovskij - RRC "KI", Moscow

Inner radius, cm	5.7 (11.65)		6.9 (10.45)		9.7 (7.65)		12.8 (4.55)	
Energy range,	E	C/E	E	C/E	E	C/E	E	C/E
0.1- 0.2	0.0615	0.949	0.0620	0.908	0.0620	0.872	0.0340	1.217
0.2- 0.4	0.1050	0.771	0.1060	0.777	0.1078	0.721	0.0646	0.978
0.4- 0.8	0.1060	0.876	0.1068	0.876	0.1176	0.785	0.0754	1.151
0.8- 1.4	0.1135	0.792	0.1192	0.756	0.1236	0.708	0.0788	1.051
1.4- 2.5	0.1455	0.744	0.1450	0.741	0.1589	0.650	0.0854	1.037
2.5- 4.0	0.0605	0.807	0.0672	0.725	0.0768	0.642	0.0476	0.977
4.0- 6.5	0.0802	0.877	0.0948	0.745	0.1012	0.672	0.0620	0.942
6.5-10.5	0.1038	0.838	0.1112	0.772	0.1248	0.664	0.0779	0.904
10.5-16.4	0.3120	1.083	0.3228	1.151	0.3128	1.470	0.6440	0.900
0.1-16.4	1.096	0.889	1.135	0.886	1.186	0.906	1.170	0.924

Table 3: MCNP- and BLANK-calculations with FENDL/MC-1.0 and ENDF/B-VI beryllium data for RRC-KI Be spherical shells - D. Markovskij - RRC "KI", Moscow

Total neutron leakages

Thickness, cm	Expt.	BLANK ENDF/B4	C/E	BLANK ENDF/B6	C/E	MCNP/4A FENDL-1	C/E
5 (6-11)	1.36+0.04	1.39	1.022	1.328	0.976	1.332	0.979
8 (3-11)	1.53+0.05	1.60	1.046	1.506	0.984	1.513	0.989

Leakage spectrum for RRC-KI 5 cm thick beryllium shell

E, MeV	Expt.	BLANK ENDF/B4	C/E	BLANK ENDF/B6	C/E	MCNP/4A FENDL-1	C/E
0.35-0.7	0.096+0.005	0.075	0.78	0.0689	0.717	0.0659	0.686
0.7 -3	0.20+0.01	0.16	0.81	0.160	0.8	0.179	0.885
3 -10	0.19+0.01	0.20	1.005	0.183	0.963	0.161	0.847
10 -15	0.69+0.03	0.69	0.99	0.680	0.985	0.725	1.05
0.35-10	0.49+0.02	0.43	0.88	0.412	0.841	0.406	0.828

Table 4: MCNP- and ONEDANT-calculations with FENDL-1 data for OKTAVIAN Be spherical shell (inner radius = 5.7 cm, outer radius = 17.35 cm) - U. Fischer, E. Wiegner, FZK

		ONEDANT/FENDL/MG-1.0		MCNP4A/FENDL/MC-1.0	
	Experiment	C	C/E	C	C/E
0.20000E+06 - 0.40000E+06	0.10485E+00	0.83439E-01	0.79579E+00	0.82739E-01	0.78912E+00
0.40000E+06 - 0.80000E+06	0.10903E+00	0.95614E-01	0.87695E+00	0.95171E-01	0.87289E+00
0.80000E+06 - 0.14000E+07	0.11280E+00	0.94743E-01	0.83992E+00	0.93763E-01	0.83124E+00
0.14000E+07 - 0.25000E+07	0.14336E+00	0.11458E+00	0.79925E+00	0.11475E+00	0.80040E+00
0.25000E+07 - 0.40000E+07	0.61662E-01	0.55965E-01	0.90761E+00	0.53503E-01	0.86767E+00
0.40000E+07 - 0.65000E+07	0.87455E-01	0.76692E-01	0.87693E+00	0.76225E-01	0.87160E+00
0.65000E+07 - 0.10500E+08	0.10371E+00	0.10208E+00	0.98428E+00	0.96876E-01	0.93410E+00
0.10500E+08 - 0.20000E+08	0.31350E+00	0.38287E+00	0.12213E+01	0.36959E+00	0.11789E+01
0.10000E+06 - 0.20000E+08	0.12573E+01	0.12606E+01	0.10026E+01	0.16401E+01	0.13045E+01

Table 5: MCNP- and ONEDANT-calculations with FENDL-1 data on OKTAVIAN BeLi spherical shell (inner Be radius = 12.8 cm, outer Be radius = 17.35 cm, inner Li radius = 17.35 cm, outer Li radius = 57.35 cm) - U. Fischer, E. Wiegner, FZK

		ONEDANT/FENDL/MG-1.0		MCNP4A/FENDL/MC-1.0	
	Experiment	C	C/E	C	C/E
0.20000E+06 - 0.40000E+06	0.69087E-01	0.37563E-01	0.54371E+00	0.37477E-01	0.54246E+00
0.40000E+06 - 0.80000E+06	0.16667E+00	0.13324E+00	0.79942E+00	0.13335E+00	0.80010E+00
0.80000E+06 - 0.14000E+07	0.10327E+00	0.83544E-01	0.80899E+00	0.83624E-01	0.80976E+00
0.14000E+07 - 0.25000E+07	0.92687E-01	0.73993E-01	0.79831E+00	0.74434E-01	0.80307E+00
0.25000E+07 - 0.40000E+07	0.49216E-01	0.37614E-01	0.76426E+00	0.37792E-01	0.76788E+00
0.40000E+07 - 0.65000E+07	0.51746E-01	0.34557E-01	0.66782E+00	0.34891E-01	0.67427E+00
0.65000E+07 - 0.10500E+08	0.70862E-01	0.63985E-01	0.90295E+00	0.64350E-01	0.90811E+00
0.10500E+08 - 0.20000E+08	0.17101E+00	0.19845E+00	0.11605E+01	0.20484E+00	0.11978E+01
0.10000E+06 - 0.20000E+08	0.10708E+01	0.10301E+01	0.96199E+00	0.10600E+01	0.98994E+00

Table 6: MCNP- and ONEDANT-calculations with FENDL-1 data on IPPE Obninsk Be spherical shell (inner radius = 6.0 cm, outer radius = 11.0 cm) - U. Fischer, E. Wiegner, FZK

		ONEDANT/FENDL/MG-1.0		MCNP4A/FENDL/MC-1.0	
	Experiment	C	C/E	C	C/E
0.40000E+06 - 0.80000E+06	0.48498E-01	0.67713E-01	0.13962E+01	0.70402E-01	0.14516E+01
0.80000E+06 - 0.14000E+07	0.83882E-01	0.65460E-01	0.78038E+00	0.67236E-01	0.80155E+00
0.14000E+07 - 0.25000E+07	0.85739E-01	0.79904E-01	0.93194E+00	0.83230E-01	0.97073E+00
0.25000E+07 - 0.40000E+07	0.45211E-01	0.47908E-01	0.10597E+01	0.48241E-01	0.10670E+01
0.40000E+07 - 0.65000E+07	0.61215E-01	0.63004E-01	0.10292E+01	0.63963E-01	0.10449E+01
0.65000E+07 - 0.10500E+08	0.10806E+00	0.95571E-01	0.88443E+00	0.95168E-01	0.88069E+00
0.10500E+08 - 0.20000E+08	0.67967E+00	0.68058E+00	0.10013E+01	0.66893E+00	0.98420E+00
0.10000E+06 - 0.20000E+08	0.11123E+01	0.11002E+01	0.98912E+01	0.10972E+01	0.98640E+00

Table 7: 3d-MCNP4A-calculation with FENDL/MC-1.0 data for KANT Be spherical shell experiment (inner radius = 5.0 cm, outer radius = 22.0 cm) - U. Fischer, F. Kappler, FZK

	Experiment	FENDL/MC	C/E
0.10000E-02 - 0.10000E+02	0.433	0.4188	0.967
0.10000E+02 - 0.10000E+06	0.373	0.4243	0.879
0.10000E+06 - 0.50000E+06	0.162	0.1588	0.98
0.50000E+06 - 0.32000E+07	0.307	0.2592	0.840
0.32000E+07 - 0.15000E+08	0.386	0.40195	1.04
0.10000E-02 - 0.15000E+08	1.661	1.672	1.007

FNS slab TOF-experiment

Table 8: MCNP-calculations with FENDL-1 and JENDL-3.1 data for FNS cylindrical slabs - Y. Oyama, M. Wada -FNS/JAERI

Be slab thickness: 50.8 mm

Angle [degree]	Expt.	JENDL-3.1	C/E	FENDL-1.0	C/E
>10 MeV					
0.0000	3.9237	4.0976	1.0443	4.1620	1.0607
12.200					
24.900	0.25730	0.26648	1.0357	0.27411	1.0653
41.800	0.10240	0.10077	0.98410	0.10592	1.0344
66.800	0.046623	0.034223	0.73404	0.033224	0.71261
2-10 MeV					
0.0000	0.12646	0.12404	0.98086	0.12523	0.99027
12.200					
24.900	0.060269	0.064480	1.0699	0.064690	1.0734
41.800	0.055711	0.061630	1.1062	0.060402	1.0842
66.800	0.052344	0.055930	1.0685	0.052171	0.99669
0.5-2 MeV					
0.0000	0.091218	0.095849	1.0508	0.089182	0.97768
12.200					
24.900	0.052268	0.060839	1.1640	0.053302	1.0198
41.800	0.051627	0.058982	1.1425	0.051191	0.99155
66.800	0.048394	0.049985	1.0329	0.043833	0.90575
0.1-0.5 MeV					
0.0000	0.037633	0.035516	0.94375	0.042862	1.1389
12.200					
24.900	0.036902	0.031874	0.86375	0.038301	1.0379
41.800	0.034073	0.030921	0.90750	0.036219	1.0630
66.800	0.030698	0.025382	0.82683	0.029075	0.94713

Be slab thickness: 152 mm

Angle [degree]	Expt.	JENDL-3.1	C/E	FENDL-1.0	C/E
>10 MeV					
0.0000	0.77370	0.83305	1.0767	0.85603	1.1064
12.200	0.23382	0.20797	0.88944	0.21452	0.91747
24.900	0.10482	0.11283	1.0764	0.11805	1.1262
41.800	0.048073	0.041294	0.85899	0.043313	0.90098
66.800	0.013860	0.011555	0.83369	0.011506	0.83016
2-10 MeV					
0.0000	0.055637	0.059066	1.0616	0.059530	1.0700
12.200	0.047807	0.055127	1.1531	0.055619	1.1634
24.900	0.044247	0.051038	1.1535	0.051061	1.1540
41.800	0.038230	0.043156	1.1289	0.042407	1.1093
66.800	0.025545	0.028356	1.1100	0.026498	1.0373
0.5-2 MeV					
0.0000	0.052382	0.059414	1.1342	0.051159	0.97665
12.200	0.047168	0.058781	1.2462	0.050047	1.0610
24.900	0.044885	0.055655	1.2400	0.047160	1.0507
41.800	0.041152	0.048912	1.1886	0.041350	1.0048
66.800	0.030190	0.034589	1.1457	0.028900	0.95727
0.1-0.5 MeV					
0.0000	0.040696	0.038527	0.94670	0.038358	0.94255
12.200	0.035622	0.039566	1.1107	0.039226	1.1012
24.900	0.034456	0.037720	1.0947	0.037134	1.0777
41.800	0.030839	0.033588	1.0891	0.032868	1.0658
66.800	0.023463	0.024091	1.0268	0.023203	0.98892

Table 9: MCNP4A- and BLANK- calculations with FENDL/MC-1.0 and ENDF/B-VI beryllium data for FNS cylindrical slabs - D. Markovskij, RRC "KI"

Be slab thickness: 5.08 cm

		MCNP 4/A		BLANK	
Angle	Expt.	FENDL 1.0	C/E	ENDF/B-VI	C/E
>10 MeV					
0.0	3.92370	3.7590	0.958	4.0300	1.027
24.9	0.25730	0.2488	0.966	0.2515	0.977
41.8	0.10240	0.09648	0.942	0.0990	0.967
66.8	0.046623	0.03039	0.649	0.0288	0.617
2-10 MeV					
0.0	0.12646	0.1151	0.909	0.1299	1.027
24.9	0.060269	0.05862	0.972	0.06193	1.027
41.8	0.055711	0.05481	0.983	0.05786	1.038
66.8	0.052344	0.04814	0.920	0.05157	0.985
0.5-2 MeV					
0.0	0.091218	0.07038	0.870	0.09053	0.992
24.9	0.052268	0.04766	0.912	0.05141	0.983
41.8	0.051627	0.04561	0.883	0.05099	0.987
66.8	0.048394	0.03938	0.813	0.04313	0.891
0.1-0.5 MeV					
0.0	0.037633	0.03917	1.041	0.03917	1.040
24.9	0.036902	0.03497	0.947	0.03516	0.952
41.8	0.034073	0.03292	0.966	0.03405	0.999
66.8	0.030698	0.02637	0.859	0.02829	0.921

Be slab thickness: 15.2 cm

		MCNP 4/A		BLANK	
Angle	Expt.	FENDL 1.0	C/E	ENDF/B-VI	C/E
>10 MeV					
0.0	0.77370	0.7455	0.963	0.8122	1.049
12.2	0.23382	0.1876	0.802	0.1866	0.798
24.9	0.10482	0.1035	0.987	0.1041	0.993
41.8	0.048073	0.03820	0.794	0.0380	0.790
66.8	0.013860	0.01034	0.746	0.01019	0.735
2-10 MeV					
0.0	0.055637	0.05251	0.943	0.05614	1.009
12.2	0.047807	0.04893	1.023	0.04960	1.037
24.9	0.044247	0.04513	1.020	0.04596	1.038
41.8	0.038230	0.03738	0.977	0.03889	1.017
66.8	0.025545	0.02397	0.938	0.02542	0.995
0.5-2 MeV					
0.0	0.052382	0.04448	0.848	0.04699	0.897
12.2	0.047168	0.04359	0.924	0.04366	0.925
24.9	0.044885	0.04174	0.921	0.04202	0.936
41.8	0.041152	0.03632	0.883	0.03764	0.914
66.8	0.030190	0.02567	0.850	0.02748	0.910
0.1-0.5 MeV					
0.0	0.040696	0.03378	0.830	0.03447	0.847
12.2	0.035622	0.03455	0.970	0.03404	0.956
24.9	0.034456	0.03284	0.953	0.03292	0.952
41.8	0.030839	0.02913	0.945	0.03007	0.975
66.8	0.023463	0.02055	0.876	0.02265	0.965

Table 10: MCNP-calculations with FENDL-1 and JENDL-3.2 data for reaction rates inside FNS cylindrical slabs - F. Maekawa, M. Wada, Y. Oyama -FNS/JAERI

ReactionPosition [mm]	Expt.	error	JENDL-3.2 C/E	error	FENDL-1 C/E	error
6Li(n,a)T						
1	3.5830e-26	0.0307	0.9545	0.0200	0.9811	0.0187
52	2.0650e-25	0.0319	1.2106	0.0161	1.1923	0.0142
102	2.9830e-25	0.0306	1.3233	0.0139	1.3377	0.0132
128	3.2260e-25	0.0235	1.3416	0.0129	1.3432	0.0128
204	3.2540e-25	0.0235	1.3640	0.0124	1.3399	0.0119
279	2.3390e-25	0.0292	1.4545	0.0116	1.3952	0.0113
305	2.0070e-25	0.0292	1.4862	0.0126	1.4070	0.0118
406	7.8630e-26	0.0271	1.3274	0.0158	1.3111	0.0167
431	5.0500e-26	0.0301	1.2163	0.0159	1.1678	0.0152
27Al(n,a)24Na						
0	2.5880e-29	0.0270	0.9471	0.0044	0.9333	0.0041
48	1.3820e-29	0.0290	0.9840	0.0073	0.9600	0.0067
149	3.7500e-30	0.0300	1.0318	0.0149	1.0001	0.0141
251	1.0390e-30	0.0320	1.0745	0.0249	1.0280	0.0238
352	2.8530e-31	0.0370	1.0546	0.0373	1.0940	0.0420
456	7.5590e-32	0.0320	1.0343	0.0575	1.1376	0.0590
56Fe(n,p)						
0	2.2400e-29	0.0270	1.0273	0.0046	1.0132	0.0044
48	1.2210e-29	0.0270	1.0468	0.0075	1.0218	0.0069
149	3.3650e-30	0.0280	1.0809	0.0150	1.0513	0.0144
251	9.8860e-31	0.0300	1.0650	0.0239	1.0201	0.0229
352	2.7460e-31	0.0320	1.0425	0.0357	1.0685	0.0397
456	7.4120e-32	0.0370	0.9880	0.0529	1.0872	0.0547
58Ni(n,2n)57Ni						
0	9.4160e-30	0.0290	0.9040	0.0038	0.9032	0.0037
48	3.6750e-30	0.0270	0.9425	0.0061	0.9500	0.0060
149	6.8810e-31	0.0360	0.9734	0.0138	0.9960	0.0137
251	1.3380e-31	0.0430	1.0076	0.0272	1.0422	0.0273
352	3.2710e-32	0.0450	0.8509	0.0408	0.9431	0.0429
456	7.5430e-33	0.0900	0.7562	0.0644	0.8829	0.0701
58Ni(n,p)58Co						
0	7.6320e-29	0.0270	1.0212	0.0070	0.9719	0.0062
48	6.1620e-29	0.0270	1.0717	0.0110	0.9779	0.0092
149	2.2920e-29	0.0280	1.0849	0.0175	1.0052	0.0164
251	7.6280e-30	0.0340	1.1189	0.0241	1.0285	0.0231
352	2.3040e-30	0.0310	1.1781	0.0419	1.0939	0.0422
456	6.0010e-31	0.0410	1.0547	0.0471	1.0611	0.0475
90Zr(n,2n)89Zr						
0	1.7720e-28	0.0270	0.9825	0.0041	0.9817	0.0040
48	7.6270e-29	0.0270	0.9745	0.0062	0.9839	0.0062
149	1.4650e-29	0.0270	1.0572	0.0146	1.0870	0.0147
251	3.3160e-30	0.0340	1.0100	0.0261	1.0504	0.0263
352	7.5080e-31	0.0410	0.9762	0.0436	1.0966	0.0466
456	1.6820e-31	0.0340	0.9698	0.0741	1.1413	0.0814
93Nb(n,2n)92mNb						
0	9.9330e-29	0.0270	1.0107	0.0043	1.0056	0.0042
48	4.9610e-29	0.0270	1.0174	0.0068	1.0099	0.0067
149	1.3050e-29	0.0290	0.9962	0.0136	0.9846	0.0136
251	3.3260e-30	0.0310	1.0380	0.0251	1.0280	0.0246
352	9.0150e-31	0.0310	0.9734	0.0362	1.0451	0.0390
456	2.2950e-31	0.0330	0.9836	0.0607	1.1238	0.0639

Table 10: (cont'd) MCNP-calculations with FENDL-1 and JENDL-3.2 data for reaction rates inside FNS cylindrical slabs - F. Maekawa, M. Wada, Y. Oyama -FNS/JAERI

ReactionPosition [mm]		Expt.	error	JENDL-3.2 C/E	error	FENDL-1 C/E	error
115In(n,n')115mIn							
0	3.3880e-29		0.0290	0.9740	0.0096	0.8808	0.0088
48	3.9120e-29		0.0290	1.0892	0.0123	0.9448	0.0106
149	1.7190e-29		0.0290	1.1453	0.0181	1.0093	0.0169
251	6.0060e-30		0.0320	1.2089	0.0232	1.0651	0.0220
352	1.9250e-30		0.0340	1.2790	0.0430	1.1261	0.0420
456	4.6030e-31		0.0520	1.0914	0.0434	0.9563	0.0397
197Au(n,g)198Au							
0	8.6280e-27		0.0300	0.9282	0.0981	0.8567	0.0688
48	4.8060e-26		0.0270	1.2061	0.0759	1.2232	0.0536
149	7.2720e-26		0.0300	1.1272	0.0419	1.2363	0.0659
251	4.9570e-26		0.0290	1.2831	0.0449	1.1911	0.0264
352	2.3300e-26		0.0290	1.2666	0.0320	1.2707	0.0410
456	2.1510e-27		0.0300	0.9311	0.0602	0.8300	0.0403
U-235(n,f)							
41	9.2670e-26		0.0381	1.4162	0.0193	1.4266	0.0190
67	1.3070e-25		0.0380	1.4081	0.0173	1.4158	0.0170
92	1.5790e-25		0.0380	1.4034	0.0152	1.4506	0.0154
117	1.7940e-25		0.0380	1.4107	0.0140	1.4307	0.0142
143	1.9060e-25		0.0380	1.4359	0.0142	1.4225	0.0135
219	1.7710e-25		0.0380	1.4507	0.0115	1.4260	0.0111
270	1.4320e-25		0.0380	1.5089	0.0122	1.4380	0.0114
321	1.0730e-25		0.0380	1.5068	0.0136	1.4333	0.0126
371	7.0710e-26		0.0380	1.4488	0.0161	1.3878	0.0150
422	3.3680e-26		0.0381	1.4039	0.0173	1.3572	0.0157

Table 11: MCNP- and ONEDANT-calculations with FENDL-1 data for TUD Pb spherical shell experiment (inner radius = 2.5 cm, outer radius = 25.0 cm) - U. Fischer, E. Wiegner, FZK Karlsruhe

		ONEDANT/FENDL/MG-1.0		MCNP4A/FENDL/MC-1.0	
	Experiment	C	C/E	C	C/E
0.10000E+06 - 0.20000E+06	0.16184E+00	0.13358E+00	0.82538E+00	0.10683E+00	0.66007E+00
0.20000E+06 - 0.40000E+06	0.25760E+00	0.21770E+00	0.84511E+00	0.24059E+00	0.93395E+00
0.40000E+06 - 0.80000E+06	0.51263E+00	0.45545E+00	0.88846E+00	0.50810E+00	0.99115E+00
0.80000E+06 - 0.14000E+07	0.46411E+00	0.39551E+00	0.85219E+00	0.41999E+00	0.90493E+00
0.14000E+07 - 0.25000E+07	0.31287E+00	0.30356E+00	0.97024E+00	0.29377E+00	0.93895E+00
0.25000E+07 - 0.40000E+07	0.72624E-01	0.74681E-01	0.10283E+01	0.55818E-01	0.76859E+00
0.40000E+07 - 0.65000E+07	0.18544E-01	0.18578E-01	0.10018E+01	0.11239E-01	0.60607E+00
0.65000E+07 - 0.10500E+08	0.14381E-01	0.14219E-01	0.98874E+00	0.98855E-02	0.68740E+00
0.10500E+08 - 0.20000E+08	0.61726E-01	0.71568E-01	0.11594E+01	0.72047E-01	0.11672E+01
0.10000E+06 - 0.20000E+08	0.18763E+01	0.16848E+01	0.89794E+00	0.17902E+01	0.95412E+00

Table 12: ONEDANT-calculations with FENDL-1 data for IPPE Obninsk spherical shell experiment (inner radius = 4.5 cm, outer radius = 12.0 cm) - U. Fischer, E. Wiegner, FZK Karlsruhe

		ONEDANT/FENDL/MG-1.0	
	Experiment	C	C/E
0.40000E+06 - 0.80000E+06	0.17351E+00	0.14831E+00	0.11699E+01
0.80000E+06 - 0.14000E+07	0.21208E+00	0.27364E+00	0.77503E+00
0.14000E+07 - 0.25000E+07	0.23135E+00	0.27070E+00	0.85464E+00
0.25000E+07 - 0.40000E+07	0.10003E+00	0.98787E-01	0.10126E+01
0.40000E+07 - 0.65000E+07	0.35854E-01	0.39523E-01	0.90717E+00
0.65000E+07 - 0.10500E+08	0.38466E-01	0.47261E-01	0.81391E+00
0.10500E+08 - 0.20000E+08	0.48897E+00	0.42157E+00	0.11599E+01
0.10000E+06 - 0.20000E+08	0.12802E+01	0.12998E+01	0.10153E+01

Table 13: MCNP- and ONEDANT-calculations with FENDL-1 data for IPPE Obninsk LiPb spherical shell experiment (inner radius = 6.0 cm, outer radius = 20.0 cm) - U. Fischer, E. Wiegner, FZK Karlsruhe

		ONEDANT/FENDL/MG-1.0		MCNP4A/FENDL/MC-1.0	
	Experiment	C	C/E	C	C/E
0.10000E+06 - 0.20000E+06	0.72553E-01	0.70494E-01	0.97162E+00	0.70363E-01	0.96982E+00
0.20000E+06 - 0.40000E+06	0.15803E+00	0.10332E+00	0.65380E+00	0.15735E+00	0.99570E+00
0.40000E+06 - 0.80000E+06	0.38276E+00	0.27579E+00	0.72053E+00	0.36266E+00	0.94749E+00
0.80000E+06 - 0.14000E+07	0.40761E+00	0.28705E+00	0.70423E+00	0.36356E+00	0.89194E+00
0.14000E+07 - 0.25000E+07	0.32139E+00	0.26968E+00	0.83911E+00	0.31776E+00	0.98872E+00
0.25000E+07 - 0.40000E+07	0.92916E-01	0.95850E-01	0.10316E+01	0.90277E-01	0.97160E+00
0.40000E+07 - 0.65000E+07	0.32100E-01	0.31782E-01	0.99009E+00	0.23367E-01	0.72795E+00
0.65000E+07 - 0.10500E+08	0.39707E-01	0.33423E-01	0.84174E+00	0.24214E-01	0.60981E+00
0.10500E+08 - 0.20000E+08	0.27416E+00	0.31911E+00	0.11640E+01	0.19348E+00	0.70573E+00
0.10000E+06 - 0.20000E+08	0.17812E+01	0.14865E+01	0.83455E+00	0.16408E+01	0.92116E+00

Table 14: MCNP-calculations with FENDL-1 and JENDL-3.2 data for FNS cylindrical slabs - Y. Oyama, M. Wada -FNS/JAERI

Pb slab thickness: 5 cm

	Angle	Expt.	JENDL-3.2	C/E	FENDL-1.0	C/E
>10 MeV						
	0.0000	4.6297	4.5919	0.99185	4.6467	1.0037
	24.900	0.092092	0.10039	1.0901	0.13193	1.4326
	41.800	0.052042	0.041212	0.79191	0.061719	1.1859
	66.800	0.022230	0.013894	0.62502	0.022044	0.99166
1-10 MeV						
	0.0000	0.29878	0.30454	1.0193	0.29597	0.99060
	24.900	0.10373	0.10908	1.0515	0.10553	1.0173
	41.800	0.10986	0.10526	0.95816	0.10422	0.94871
	66.800	0.11937	0.10905	0.91353	0.11024	0.92357
0.1-1 MeV						
	0.0000	0.13459	0.16195	1.2033	0.14571	1.0826
	24.900	0.049010	0.076534	1.5616	0.054896	1.1201
	41.800	0.053161	0.079039	1.4868	0.057949	1.0901
	66.800	0.060643	0.081073	1.3369	0.062113	1.0242

Pb slab thickness: 20 cm

	Angle	Expt.	JENDL-3.2	C/E	FENDL-1.0	C/E
>10 MeV						
	0.0000	0.50574	0.46321	0.91591	0.48424	0.95750
	12.200	0.12476	0.088803	0.71181	0.10960	0.87854
	24.900	0.029566	0.019761	0.66835	0.030197	1.0213
	41.800	0.012904	0.0066575	0.51591	0.012720	0.98573
	66.800	0.0035436	0.0015943	0.44991	0.0032990	0.93097
1-10 MeV						
	0.0000	0.10741	0.089511	0.83332	0.10214	0.95093
	12.200	0.091455	0.080509	0.88031	0.093362	1.0209
	24.900	0.087363	0.072849	0.83387	0.086820	0.99379
	41.800	0.078939	0.059256	0.75066	0.073678	0.93336
	66.800	0.052991	0.036369	0.68633	0.047340	0.89335
0.1-1 MeV						
	0.0000	0.093559	0.11842	1.2657	0.098052	1.0480
	12.200	0.083855	0.11541	1.3763	0.093217	1.1116
	24.900	0.081723	0.10950	1.3399	0.088788	1.0865
	41.800	0.077998	0.096331	1.2351	0.078859	1.0110
	66.800	0.056173	0.065167	1.1601	0.054283	0.96636

Table 14: (cont'd) MCNP-calculations with FENDL-1 and JENDL-3.2 data for FNS cylindrical slabs - Y. Oyama, M. Wada -FNS/JAERI

Pb slab thickness: 40 cm

	Angle	Expt.	JENDL-3.2	C/E	FENDL-1.0	C/E
>10 MeV						
	0.0000	0.024964	0.018949	0.75904	0.021044	0.84299
	12.200	0.0087390	0.0040282	0.46094	0.0068501	0.78386
	24.900	0.0031150	0.0012995	0.41718	0.0027340	0.87770
	41.800	0.0011323	0.00043758	0.38647	0.0010724	0.94716
	66.800	0.0011891	7.6204e-05	0.064083	0.00034782	0.29250
1-10 MEV						
	0.0000	0.025183	0.015598	0.61937	0.023076	0.91635
	12.200	0.022008	0.015227	0.69188	0.022777	1.0349
	24.900	0.021062	0.013070	0.62055	0.020045	0.95171
	41.800	0.016125	0.0097350	0.60372	0.0152980	.94872
	66.800	0.010955	0.0052264	0.47707	0.0087331	0.79718
0.1-1 MeV						
	0.0000	0.043930	0.047148	1.0733	0.043262	0.98479
	12.200	0.041278	0.047595	1.1530	0.043505	1.0540
	24.900	0.042652	0.043634	1.0230	0.040043	0.93881
	41.800	0.035531	0.035875	1.0097	0.032873	0.92520
	66.800	0.021069	0.022839	1.0840	0.020742	0.98447

OKTAVIAN spherical shell experiment

Table 15: MCNP-calculations with FENDL-1, JENDL-FF and JENDL-3.2 data for OKTAVIAN Li spherical shell experiment (40 cm diameter, wall thickness = 9.8 cm),
- C. Ichihara, University of Kyoto

Energy [MeV]	Experiment	FENDL-1		JENDL-3.2		JENDL-FF	
10<En<20	7.728×10-1	7.481×10-1	(0.968)	7.426×10-1	(0.960)	7.426×10-1	(0.961)
5<En<10	9.396×10-2	6.345×10-2	(0.675)	7.061×10-2	(0.771)	7.064×10-2	(0.752)
1<En<5	1.311×10-1	1.286×10-1	(0.981)	1.278×10-1	(0.963)	1.276×10-1	(0.973)
0.1<En<1	7.834×10-2	7.612×10-2	(0.972)	7.930×10-2	(1.017)	7.938×10-2	(1.013)
Total leakages	1.076	1.017	(0.945)	1.020	(0.948)	1.020	(0.948)

FNS Li_2O slab TOF-experiment

Table 16: MCNP-calculations with FENDL-1 and JENDL-3.2 data for FNS cylindrical slabs
- Y. Oyama, M. Wada -FNS/JAERI

				Li2O slab thickness: 48 mm	
	Angle	Expt.	JENDL-3.2	C/E	FENDL-1.0	C/E
>11 MeV						
	0.0000	5.1188	5.1005	0.99642	5.1447	1.0051
	24.900	0.18194	0.20352	1.1186	0.20635	1.1341
	41.800	0.077240	0.072244	0.93532	0.072301	0.93606
	66.800	0.027778	0.028855	1.0388	0.028109	1.0119
1-11 MeV						
	0.0000	0.19056	0.19801	1.0391	0.19777	1.0378
	24.900	0.045563	0.050810	1.1152	0.046913	1.0296
	41.800	0.048649	0.048619	0.99938	0.044430	0.91328
	66.800	0.049517	0.048078	0.97094	0.044910	0.90696
0.1-1 MeV						
	0.0000	0.063130	0.057267	0.90713	0.058576	0.92786
	24.900	0.011504	0.012668	1.1011	0.011060	0.96140
	41.800	0.013280	0.013376	1.0072	0.011750	0.88479
	66.800	0.011444	0.013983	1.2219	0.012426	1.0858

Table 16: (cont'd) MCNP-calculations with FENDL-1 and JENDL-3.2 data for FNS cylindrical slabs - Y. Oyama, M. Wada -FNS/JAERI

Li2O slab thickness: 200 mm

	Angle	Expt.	JENDL-3.2	C/E	FENDL-1.0	C/E
>11 MeV						
	0.0000	0.75158	0.81395	1.0830	0.84597	1.1256
	24.900	0.072925	0.070653	0.96884	0.073237	1.0043
	66.800	0.0084406	0.0072440	0.85823	0.0071750	0.85006
1-11 MeV						
	0.0000	0.061901	0.062909	1.0163	0.059468	0.96070
	24.900	0.044790	0.046206	1.0316	0.042370	0.94597
	66.800	0.026035	0.024378	0.93635	0.022740	0.87344
0.1-1 MeV						
	0.0000	0.029788	0.029083	0.97633	0.028024	0.94078
	24.900	0.025094	0.025783	1.0275	0.024237	0.96585
	66.800	0.017522	0.016132	0.92067	0.015336	0.87524

Li2O slab thickness: 400 mm

	Angle	Expt.	JENDL-3.2	C/E	FENDL-1.0	C/E
>11 MeV						
	0.0000	0.063606	0.070909	1.1148	0.077040	1.2112
	12.200	0.019672	0.019641	0.99842	0.021916	1.1141
	24.900	0.010045	0.0092850	0.92434	0.010421	1.0374
	66.800	0.0011855	0.00093460	0.78836	0.0010420	0.87895
1-11 MeV						
	0.0000	0.013824	0.014121	1.0215	0.013098	0.94748
	12.200	0.012293	0.013425	1.0921	0.012334	1.0033
	24.900	0.011470	0.011533	1.0055	0.010581	0.92249
	66.800	0.0052590	0.0048907	0.92997	0.0044845	0.85273
0.1-1 MeV						
	0.0000	0.010843	0.010982	1.0129	0.010383	0.95758
	12.200	0.0095573	0.011042	1.1553	0.010462	1.0947
	24.900	0.010060	0.010116	1.0056	0.0096880	0.96302
	66.800	0.0057444	0.0053624	0.93350	0.0051111	0.88975

FNS Li_2O slab in-system measurements

Table 17: MCNP-calculations with FENDL-1 and JENDL-3.2 data for reaction rates inside FNS Li2O cylindrical slabs - F. Maekawa, M. Wada, Y. Oyama -FNS/JAERI

Reaction	Position [mm]	Expt.	error	JENDL-3.2 C/E	error	FENDL-1 C/E	error
6Li(n,a)T							
	-1	7.6600e-29	0.0480	0.8992	0.0078	0.8671	0.0084
Li2O Pellet							
	24	8.9300e-29	0.0450	1.0337	0.0106	1.0132	0.0120
	49	9.4400e-29	0.0450	1.0309	0.0119	1.0039	0.0121
	75	9.2300e-29	0.0450	1.0573	0.0106	1.0492	0.0229
	100	9.1500e-29	0.0450	1.0498	0.0112	1.0156	0.0121
	151	8.1800e-29	0.0470	1.0511	0.0133	1.0102	0.0132
	202	7.0100e-29	0.0490	1.0114	0.0129	1.0070	0.0133
	253	5.7100e-29	0.0530	1.0298	0.0114	0.9959	0.0118
	303	4.5500e-29	0.0580	1.0587	0.0132	1.0106	0.0153
	354	3.4800e-29	0.0650	1.0368	0.0143	1.0122	0.0172
	405	2.7600e-29	0.0730	0.9902	0.0145	0.9500	0.0156
	456	2.0300e-29	0.0870	0.9652	0.0128	0.9373	0.0144
	507	1.4600e-29	0.1050	0.9297	0.0165	0.9130	0.0199
	557	8.3600e-30	0.1570	0.9748	0.0189	0.9607	0.0226
7Li(n,n'a)T							
	-1	6.3200e-29	0.0420	0.9338	0.0028	0.9362	0.0031
Li2O Pellet							
	24	4.6000e-29	0.0490	1.0558	0.0045	1.0468	0.0047
	49	3.8500e-29	0.0560	0.9780	0.0051	0.9764	0.0056
	75	2.6700e-29	0.0640	1.0800	0.0064	1.0784	0.0069
	100	2.0800e-29	0.0760	1.0653	0.0072	1.0671	0.0080
	151	1.2600e-29	0.1070	1.0368	0.0092	1.0351	0.0099
	202	4.5700e-30	0.2380	1.7444	0.0194	1.7870	0.0222
	253	3.9200e-30	0.2810	1.2557	0.0153	1.2515	0.0165
7Li(n,n'a)T							
	16	4.6100e-29	0.0391	1.1344	0.0044	1.1359	0.0050
NE213	115	1.6600e-29	0.0288	1.1507	0.0086	1.1392	0.0092
	216	6.2300e-30	0.0288	1.1330	0.0120	1.1377	0.0133
	317	2.4000e-30	0.0347	1.1236	0.0181	1.1493	0.0199
	418	9.0400e-31	0.0400	1.0981	0.0228	1.0790	0.0229
	520	3.4600e-31	0.0475	1.0928	0.0315	1.1298	0.0321
	621	1.2500e-31	0.0427	1.1158	0.0452	1.1771	0.0534
27Al(n,a)24Na							
	0	2.1200e-29	0.0320	1.0109	0.0027	1.0117	0.0029
	24	1.5700e-29	0.0310	1.0568	0.0039	1.0530	0.0041
	50	1.1800e-29	0.0310	1.0475	0.0046	1.0485	0.0051
	75	8.6100e-30	0.0330	1.0640	0.0055	1.0741	0.0061
	101	6.3100e-30	0.0330	1.0895	0.0065	1.1082	0.0076
	151	3.6000e-30	0.0330	1.0779	0.0086	1.0885	0.0094
	202	2.1200e-30	0.0350	1.0594	0.0111	1.0974	0.0129
	253	1.2800e-30	0.0350	1.0455	0.0128	1.0583	0.0138
	303	7.6200e-31	0.0350	1.0547	0.0148	1.1083	0.0174
	355	4.4900e-31	0.0310	1.0846	0.0204	1.1232	0.0215
	406	2.8400e-31	0.0380	0.9882	0.0218	1.0422	0.0268
	456	1.6700e-31	0.0380	1.0298	0.0234	1.1014	0.0332
	507	9.8700e-32	0.0370	1.0263	0.0265	1.0889	0.0339
	558	6.1100e-32	0.0360	1.0086	0.0341	1.1121	0.0403

Table 17: (cont'd) MCNP-calculations with FENDL-1 and JENDL-3.2 data for reaction rates inside FNS Li2O cylindrical slabs - F. Maekawa, M. Wada, Y. Oyama -FNS/JAERI

ReactionPosition [mm]	Expt.	error	JENDL-3.2 C/E	error	FENDL-1 C/E	error
58Ni(n,2n)57Ni						
-1	8.0000e-30	0.0310	0.9060	0.0024	0.9073	0.0026
23	5.1900e-30	0.0280	0.9526	0.0030	0.9551	0.0033
49	3.6100e-30	0.0320	0.9318	0.0035	0.9364	0.0039
74	2.3400e-30	0.0450	0.9766	0.0044	0.9898	0.0049
100	1.6200e-30	0.0530	0.9882	0.0053	1.0026	0.0059
150	8.8400e-31	0.0530	0.8947	0.0067	0.9150	0.0075
201	4.1000e-31	0.0660	0.9925	0.0102	1.0120	0.0115
252	2.3500e-31	0.0670	0.9102	0.0115	0.9333	0.0129
303	1.2300e-31	0.0710	0.9410	0.0145	0.9973	0.0170
354	6.1300e-32	0.0280	1.0306	0.0200	1.0844	0.0229
405	3.2200e-32	0.0950	1.0150	0.0262	1.0918	0.0298
455	2.0100e-32	0.0960	0.9044	0.0274	0.9573	0.0309
506	1.1600e-32	0.1030	0.8608	0.0313	0.9241	0.0357
557	6.1200e-33	0.0890	0.9149	0.0399	1.0427	0.0480
115In(n,n')115mIn						
100	2.0100e-29	0.0380	1.1064	0.0098	1.0395	0.0097
201	9.1200e-30	0.0410	1.1112	0.0128	1.0917	0.0138
303	3.7700e-30	0.0460	1.1746	0.0155	1.1287	0.0173
405	1.6200e-30	0.0720	1.1613	0.0217	1.0919	0.0217
506	6.5800e-31	0.0950	1.1409	0.0307	1.0753	0.0279
115In(n,g)116In						
100	3.3800e-29	0.0560	1.2624	0.0168	1.2068	0.0211
201	2.6500e-29	0.0490	1.3231	0.0220	1.3066	0.0260
303	1.7900e-29	0.0430	1.3825	0.0253	1.3183	0.0258
405	1.1300e-29	0.0470	1.2827	0.0249	1.2468	0.0324
506	4.9200e-30	0.0450	1.5225	0.0344	1.4612	0.0373
Th232(n,f)						
39	5.7400e-29	0.0470	1.0138	0.0038	1.0119	0.0042
64	4.2900e-29	0.0470	1.0474	0.0047	1.0401	0.0051
90	3.2900e-29	0.0470	0.9357	0.0051	0.9255	0.0056
115	2.4500e-29	0.0470	1.0775	0.0065	1.0596	0.0069
166	1.4400e-29	0.0470	1.1035	0.0086	1.0770	0.0095
217	8.7300e-30	0.0470	1.1076	0.0095	1.0995	0.0104
267	5.4000e-30	0.0470	1.0836	0.0107	1.0746	0.0119
318	3.2900e-30	0.0480	1.1179	0.0135	1.1215	0.0151
369	2.0500e-30	0.0520	1.0833	0.0164	1.0989	0.0197
471	7.8700e-31	0.0640	1.0774	0.0217	1.0842	0.0223
521	5.2200e-31	0.0560	0.9955	0.0220	1.0131	0.0238
U-235(n,f)						
39	5.0000e-28	0.0410	0.9850	0.0040	0.9759	0.0044
64	4.2500e-28	0.0420	1.0090	0.0046	0.9969	0.0055
90	3.6700e-28	0.0410	0.9566	0.0055	0.9319	0.0059
115	3.1500e-28	0.0410	1.0154	0.0065	0.9907	0.0069
166	2.4000e-28	0.0410	1.0379	0.0088	0.9908	0.0093
217	1.8300e-28	0.0410	1.0175	0.0078	0.9864	0.0081
267	1.4000e-28	0.0410	0.9795	0.0075	0.9726	0.0090
318	1.0600e-28	0.0410	0.9999	0.0099	0.9837	0.0121
369	7.9600e-29	0.0410	0.9639	0.0125	0.9431	0.0123
420	5.9000e-29	0.0410	0.9518	0.0103	0.9355	0.0124
471	4.1800e-29	0.0410	0.9373	0.0116	0.9229	0.0131
521	2.8100e-29	0.0410	0.9464	0.0151	0.9168	0.0160

Table 17: (cont'd) MCNP-calculations with FENDL-1 and JENDL-3.2 data for reaction rates inside FNS Li2O cylindrical slabs - F. Maekawa, M. Wada, Y. Oyama -FNS/JAERI

ReactionPosition [mm]		Expt.	error	JENDL-3.2	error	FENDL-1	error
				C/E		C/E	
U-238(n,f)							
39	1.8500e-28		0.0390	0.9646	0.0036	0.9612	0.0040
64	1.4100e-28		0.0390	0.9883	0.0044	0.9799	0.0048
90	1.0500e-28		0.0390	0.9229	0.0051	0.9087	0.0055
115	8.0400e-29		0.0390	1.0376	0.0062	1.0184	0.0067
166	4.8700e-29		0.0390	1.0479	0.0082	1.0167	0.0088
217	2.9700e-29		0.0390	1.0552	0.0089	1.0422	0.0097
267	1.8100e-29		0.0390	1.0592	0.0104	1.0472	0.0114
318	1.1400e-29		0.0390	1.0650	0.0127	1.0588	0.0138
369	7.0500e-30		0.0390	1.0374	0.0152	1.0548	0.0184
420	4.4200e-30		0.0400	1.0511	0.0167	1.0152	0.0170
471	2.8000e-30		0.0400	1.0152	0.0197	1.0220	0.0205
521	1.7200e-30		0.0400	1.0094	0.0213	1.0237	0.0236
Np237(n,f)							
39	4.7100e-28		0.0510	0.9231	0.0036	0.9146	0.0040
64	3.6700e-28		0.0510	0.9694	0.0046	0.9526	0.0049
90	2.9300e-28		0.0510	0.8918	0.0050	0.8678	0.0052
115	2.3800e-28		0.0510	0.9680	0.0058	0.9366	0.0062
166	1.5100e-28		0.0510	0.9987	0.0077	0.9536	0.0080
217	9.5700e-29		0.0510	1.0102	0.0076	0.9887	0.0083
267	6.3300e-29		0.0510	0.9879	0.0088	0.9596	0.0094
318	4.0500e-29		0.0510	1.0249	0.0109	0.9821	0.0115
369	2.6800e-29		0.0520	0.9467	0.0123	0.9399	0.0145
420	1.6800e-29		0.0520	0.9905	0.0132	0.9415	0.0135
471	1.1000e-29		0.0520	0.9497	0.0149	0.9385	0.0165
521	7.1300e-30		0.0530	0.9019	0.0163	0.9123	0.0183

OKTAVIAN spherical shell experiment

Table 18: MCNP-calculations with FENDL-1, JENDL-FF and JENDL-3.2 data for OKTAVIAN Al spherical shell experiment (40 cm diameter, wall thickness = 0.5 mfp,
- C. Ichihara, University of Kyoto

Energy [MeV]	Experiment	FENDL-1		JENDL-3.2		JENDL-FF	
10<En<20	6.735×10-1	7.089×10-1	(1.050)	7.147×10-1	(1.058)	7.159×10-1	(1.060)
5<En<10	4.954×10-2	3.195×10-2	(0.645)	3.925×10-2	(0.792)	4.062×10-2	(0.820)
1<En<5	1.475×10-1	1.489×10-1	(1.009)	1.316×10-1	(0.892)	1.310×10-1	(0.888)
0.1<En<1	6.924×10-2	8.429×10-2	(1.217)	8.728×10-2	(1.261)	8.619×10-2	(1.245)
total	0.942	0.974	(1.034)	0.973	(1.033)	0.973	(1.033)

Table 19: MCNP- and ONEDANT-calculations with FENDL-1 data on OKTAVIAN Al spherical shell experiment (inner radius = 20.2 cm, outer radius = 39.8 cm)
- U. Fischer, E. Wiegner, FZK Karlsruhe

		ONEDANT/FENDL/MG-1.0		MCNP4A/FENDL/MC-1.0	
	Experiment	C	C/E	C	C/E
0.10000E+06 - 0.20000E+06	0.63038E-02	0.12658E-01	0.20080E+01	0.12052E-01	0.19119E+01
0.20000E+06 - 0.40000E+06	0.15072E-01	0.32560E-01	0.21603E+01	0.32869E-01	0.21808E+01
0.40000E+06 - 0.80000E+06	0.31622E-01	0.59287E-01	0.18749E+01	0.58814E-01	0.18599E+01
0.80000E+06 - 0.14000E+07	0.44757E-01	0.72451E-01	0.16188E+01	0.73434E-01	0.16407E+01
0.14000E+07 - 0.25000E+07	0.55969E-01	0.83147E-01	0.14856E+01	0.82506E-01	0.14741E+01
0.25000E+07 - 0.40000E+07	0.43944E-01	0.55098E-01	0.12538E+01	0.54341E-01	0.12366E+01
0.40000E+07 - 0.65000E+07	0.38491E-01	0.37595E-01	0.97672E+00	0.37236E-01	0.96739E+00
0.65000E+07 - 0.10500E+08	0.35205E-01	0.22854E-01	0.64917E+00	0.22666E-01	0.64384E+00
0.10500E+08 - 0.20000E+08	0.67033E+00	0.55363E+00	0.82591E+00	0.55877E+00	0.83358E+00
0.10000E+06 - 0.20000E+08	0.94170E+00	0.92928E+00	0.98681E+00	0.93964E+00	0.99782E+00

Table 20: MCNP- and ONEDANT-calculations with FENDL-1 data for IPPE Obninsk Al spherical shell experiment (inner radius = 4.5 cm, outer radius = 12.0 cm)
- U. Fischer, E. Wiegner, FZK Karlsruhe

		ONEDANT/FENDL/MG-1.0		MCNP4A/FENDL/MC-1.0	
	Experiment	C	C/E	C	C/E
0.10000E+06 - 0.20000E+06	0.73595E-02	0.74190E-02	0.10081E+01	0.71511E-02	0.97168E+00
0.20000E+06 - 0.40000E+06	0.29144E-01	0.22328E-01	0.76613E+00	0.21715E-01	0.74510E+00
0.40000E+06 - 0.80000E+06	0.59583E-01	0.47164E-01	0.79157E+00	0.46481E-01	0.78010E+00
0.80000E+06 - 0.14000E+07	0.70325E-01	0.60450E-01	0.85958E+00	0.60796E-01	0.86450E+00
0.14000E+07 - 0.25000E+07	0.82397E-01	0.74311E-01	0.90187E+00	0.72832E-01	0.88392E+00
0.25000E+07 - 0.40000E+07	0.64631E-01	0.52810E-01	0.81710E+00	0.51618E-01	0.79866E+00
0.40000E+07 - 0.65000E+07	0.59966E-01	0.42609E-01	0.71055E+00	0.42029E-01	0.70088E+00
0.65000E+07 - 0.10500E+08	0.67140E-01	0.42948E-01	0.63968E+00	0.43288E-01	0.64475E+00
0.10500E+08 - 0.20000E+08	0.60739E+00	0.59738E+00	0.98352E+00	0.60254E+00	0.99201E+00
0.10000E+06 - 0.20000E+08	0.10479E+01	0.94741E+00	0.90410E+00	0.95175E+00	0.90824E+00

Table 21: MCNP-calculations with FENDL-1, JENDL-FF and JENDL-3.2 data for OKTAVIAN Si spherical shell experiment (40 cm diameter, wall thickness = 0.55 mfp),
- C. Ichihara, University of Kyoto

Energy [MeV]	Experiment	FENDL-1		JENDL-3.2		JENDL-FF	
10<En<20	7.599×10-1	6.522×10-1	(0.858)	7.377×10-1	(0.971)	7.091×10-1	(0.933)
5<En<10	4.512×10-2	2.956×10-2	(0.655)	3.090×10-2	(0.685)	2.926×10-2	(0.648)
1<En<5	1.341×10-1	9.927×10-2	(0.740)	1.040×10-1	(0.776)	1.149×10-1	(0.857)
0.1<En<1	5.872×10-2	1.058×10-1	(1.802)	4.983×10-2	(0.849)	6.480×10-2	(1.104)
total	1.076	0.887	(0.824)	0.923	(0.858)	0.918	(0.853)

Table 22: MCNP-calculations with FENDL-1, JENDL-FF and JENDL-3.2 data for OKTAVIAN Si spherical shell experiment (60 cm diameter, wall thickness = 1.1 mfp),
- C. Ichihara, University of Kyoto

Energy [MeV]	Experiment	FENDL-1		JENDL-3.2		JENDL-FF	
10<En<20	4.814×10-1	4.416×10-1	(0.917)	5.261×10-1	(1.093)	5.302×10-1	(1.102)
5<En<10	4.696×10-2	3.340×10-2	(0.711)	3.585×10-2	(0.763)	3.705×10-2	(0.789)
1<En<5	1.714×10-1	1.353×10-1	(0.789)	1.670×10-1	(0.974)	1.702×10-1	(0.993)
0.1<En<1	9.300×10-2	1.800×10-1	(1.935)	1.084×10-1	(1.166)	(0.974)-1	(1.094)
total	0.792	0.796	(1.005)	0.838	(1.058)	0.840	(1.061)

Table 23: ONEDANT-calculations with FENDL-1 data for OKTAVIAN Si spherical shell experiment (inner radius = 10.0 cm, outer radius = 30.0 cm)
- U. Fischer, E. Wiegner, FZK Karlsruhe

		ONEDANT/FENDL/MG-1.0	
	Experiment	C	C/E
0.10000E+06 - 0.20000E+06	0.52349E-01	0.19160E-01	0.27322E+01
0.20000E+06 - 0.40000E+06	0.26015E-01	0.17517E-01	0.14851E+01
0.40000E+06 - 0.80000E+06	0.59050E-01	0.39977E-01	0.14771E+01
0.80000E+06 - 0.14000E+07	0.46365E-01	0.55956E-01	0.82860E+00
0.14000E+07 - 0.25000E+07	0.43450E-01	0.61492E-01	0.70660E+00
0.25000E+07 - 0.40000E+07	0.32279E-01	0.52092E-01	0.61965E+00
0.40000E+07 - 0.65000E+07	0.29116E-01	0.39897E-01	0.72978E+00
0.65000E+07 - 0.10500E+08	0.20181E-01	0.30991E-01	0.65119E+00
0.10500E+08 - 0.20000E+08	0.46087E+00	0.47681E+00	0.96657E+00
0.10000E+06 - 0.20000E+08	0.76968E+00	0.79389E+00	0.96950E+00

OKTAVIAN spherical shell experiment

Table 24: MCNP-calculations with FENDL-1, JENDL-FF and JENDL-3.2 data for OKTAVIAN Zr spherical shell experiment (61 cm diameter, wall thickness = 2.0 mfp),
- C. Ichihara, University of Kyoto

Energy [MeV]	Experiment	FENDL-1		JENDL-3.2		JENDL-FF	
10<En<20	3.165×10-1	3.748×10-1	(1.184)	3.590×10-1	(1.138)	3.602×10-1	(1.138)
5<En<10	3.327×10-2	3.982×10-2	(1.197)	3.215×10-2	(0.987)	3.284×10-2	(0.987)
1<En<5	3.074×10-1	3.744×10-1	(1.218)	3.344×10-1	(1.072)	3.295×10-1	(1.072)
0.1<En<1	4.415×10-1	4.885×10-1	(1.106)	5.495×10-1	(1.245)	5.443×10-1	(1.233)
total	1.076	1.277	(1.187)	1.275	(1.185)	1.267	(1.178)

Table 25: MCNP- and ONEDANT-calculations with FENDL-1 data for OKTAVIAN Al spherical shell experiment (inner radius = 25.0 cm, outer radius = 30.0 cm)
- U. Fischer, E. Wiegner, FZK Karlsruhe

		ONEDANT/FENDL/MG-1.0		MCNP4A/FENDL/MC-1.0	
	Experiment	C	C/E	C	C/E
0.10000E+06 - 0.20000E+06	0.80703E-01	0.67054E-01	0.83087E+00	0.49424E-01	0.61242E+00
0.20000E+06 - 0.40000E+06	0.11230E+00	0.11602E+00	0.10331E+01	0.11504E+00	0.10244E+01
0.40000E+06 - 0.80000E+06	0.20095E+00	0.22234E+00	0.11064E+01	0.22141E+00	0.11018E+01
0.80000E+06 - 0.14000E+07	0.18140E+00	0.21872E+00	0.12057E+01	0.21326E+00	0.11756E+01
0.14000E+07 - 0.25000E+07	0.13447E+00	0.16942E+00	0.12599E+01	0.16778E+00	0.12477E+01
0.25000E+07 - 0.40000E+07	0.51009E-01	0.68005E-01	0.13332E+01	0.68240E-01	0.13378E+01
0.40000E+07 - 0.65000E+07	0.28823E-01	0.37264E-01	0.12929E+01	0.37233E-01	0.12918E+01
0.65000E+07 - 0.10500E+08	0.23222E-01	0.25570E-01	0.11011E+01	0.25547E-01	0.11001E+01
0.10500E+08 - 0.20000E+08	0.31308E+00	0.38591E+00	0.12326E+01	0.39739E+00	0.12693E+01
0.10000E+06 - 0.20000E+08	0.11259E+01	0.13103E+01	0.11638E+01	0.13203E+01	0.11727E+01

Table 26: MCNP-calculations with FENDL-1 and JENDL-3.2 data for IPPE Obninsk iron spherical shell experiment (inner radius = 4.5 cm, outer radius = 12.0 cm)
- K. Ueki, Ship Research Institute

Energy Range	JENDL-3.2	FENDL-1
0.2-0.4	0.96100	0.79700
0.4-0.8	0.88200	0.80800
0.8-1.4	0.91500	0.89000
1.4-2.5	1.0000	0.96100
2.5-4.0	0.87600	0.98200
4.0-6.5	0.89700	1.0710
6.5-10.5	1.0310	1.2240
10.5-15.0	0.87400	0.90700

Table 27: MCNP-calculations with FENDL-1 data for IPPE Obninsk iron spherical shell experiment (inner radius = 4.5 cm, outer radius = 12.0 cm)
- D. Markovskij, RRC "KI", Moscow

E, MeV	Expt.	MCNP/4A FENDL-1	C/E
5 - 10	0.0481 ± 0.003	0.0415	0.864
2.2 - 5	0.1051 ± 0.00	0.0967	0.921
1 - 2.2	0.2101 ± 0.010	0.177	0.842
0.12 - 1	0.4001 ± 0.020	0.336	0.840

Table 28: MCNP- and ONEDANT-calculations with FENDL-1 data for IPPE Obninsk iron spherical shell experiment (inner radius = 4.5 cm, outer radius = 12.0 cm)
- U. Fischer, E. Wiegner, FZK Karlsruhe

		ONEDANT/FENDL/MG-1.0		MCNP4A/FENDL/MC-1.0	
	Experiment	C	C/E	C	C/E
0.20000E+06 - 0.40000E+06	0.10699E+00	0.91193E-01	0.85235E+00	0.86026E-01	0.80405E+00
0.40000E+06 - 0.80000E+06	0.19230E+00	0.16406E+00	0.85315E+00	0.15973E+00	0.83061E+00
0.80000E+06 - 0.14000E+07	0.17235E+00	0.15232E+00	0.88378E+00	0.15516E+00	0.90023E+00
0.14000E+07 - 0.25000E+07	0.12658E+00	0.12218E+00	0.96524E+00	0.12152E+00	0.96005E+00
0.25000E+07 - 0.40000E+07	0.61653E-01	0.62185E-01	0.10086E+01	0.61238E-01	0.99326E+00
0.40000E+07 - 0.65000E+07	0.40266E-01	0.42382E-01	0.10526E+01	0.41818E-01	0.10385E+01
0.65000E+07 - 0.10500E+08	0.31960E-01	0.38598E-01	0.12077E+01	0.38846E-01	0.12155E+01
0.10500E+08 - 0.20000E+08	0.43327E+00	0.37387E+00	0.86290E+00	0.38548E+00	0.88971E+00
0.10000E+06 - 0.20000E+08	0.11904E+01	0.10828E+01	0.90961E+00	0.10834E+01	0.91010E+00

Table 29: MCNP-, ANISN- and ONEDANT-calculations with FENDL-1, JENDL-3, BROND and ENDF/B-VI data for IPPE Obninsk iron spherical shell experiments - S. P. Simakov, IPPE-Obninsk

Fe shell	Energy Bin MeV	C/E MCNP4A FENDL-1(3D)	MCNP4A FENDL-1(1D)	ONETRAN FENDL-1	ANISN ENDF/B6	ANISN BROND-2	ANISN JENDL-3
	0.1 - 0.2	0.93+0.08	1.11+0.08	1.17+0.09	1.25+0.10	0.96+0.08	1.55+0.12
	0.2 - 0.4	0.92+0.05	1.10+0.05	1.14+0.05	1.18+0.05	1.07+0.04	1.57+0.07
Shell #1	0.4 - 0.8	0.93+0.05	1.10+0.05	1.12+0.05	1.14+0.05	1.11+0.05	1.27+0.06
r_i=2.0 cm	0.8 - 1.4	0.93+0.05	1.09+0.05	1.14+0.05	1.14+0.05	1.13+0.05	1.22+0.05
r_o=4.5 cm	1.4 - 2.5	0.97+0.05	1.09+0.05	1.13+0.05	1.14+0.05	1.15+0.05	1.20+0.05
	2.5 - 4.0	0.98+0.05	1.12+0.05	1.13+0.05	1.15+0.05	1.11+0.05	1.17+0.05
	4.0 - 6.5	1.10+0.05	1.21+0.05	1.25+0.05	1.24+0.05	1.16+0.05	1.08+0.05
	6.5 -10.5	0.82+0.06	0.92+0.06	1.18+0.07	0.94+0.06	0.97+0.06	0.71+0.05
	> 10.50	1.02+0.07	1.02+0.07	1.08+0.08	1.02+0.07	1.03+0.07	1.01+0.07
	0.1 - 0.2	1.06+0.06	1.14+0.06	1.24+0.07	1.30+0.08	1.18+0.06	1.50+0.08
	0.2 - 0.4	1.05+0.05	1.14+0.06	1.23+0.05	1.22+0.05	1.23+0.05	1.47+0.06
Shell #2	0.4 - 0.8	1.01+0.05	1.07+0.05	1.12+0.05	1.10+0.05	1.10+0.05	1.21+0.05
r_i=4.5 cm	0.8 - 1.4	1.02+0.05	1.08+0.05	1.10+0.05	1.08+0.05	1.05+0.05	1.10+0.05
r_o=12.0 cm	1.4 - 2.5	1.03+0.05	1.08+0.05	1.13+0.05	1.07+0.05	1.06+0.05	1.13+0.05
	2.5 - 4.0	1.09+0.05	1.13+0.05	1.18+0.05	1.15+0.05	1.11+0.05	1.17+0.05
	4.0 - 6.5	1.30+0.06	1.34+0.06	1.37+0.05	1.32+0.06	1.28+0.05	1.11+0.05
	6.5 -10.5	1.08+0.07	1.10+0.07	1.26+0.08	1.09+0.07	1.17+0.07	0.76+0.05
	> 10.50	0.97+0.07	0.97+0.07	1.01+0.07	0.95+0.07	0.99+0.07	0.92+0.07
	0.1 - 0.2	1.03+0.07	1.21+0.08	1.32+0.08	1.38+0.08	1.28+0.08	1.48+0.09
	0.2 - 0.4	1.00+0.05	1.17+0.05	1.28+0.05	1.26+0.05	1.27+0.05	1.32+0.06
Shell #3	0.4 - 0.8	0.96+0.05	1.10+0.05	1.15+0.05	1.11+0.05	1.12+0.05	1.22+0.05
r_i=2.0 cm	0.8 - 1.4	0.99+0.05	1.10+0.05	1.11+0.05	1.08+0.05	1.05+0.05	1.11+0.05
r_o=12.0 cm	1.4 - 2.5	1.00+0.05	1.09+0.05	1.14+0.05	1.06+0.05	1.05+0.05	1.17+0.05
	2.5 - 4.0	1.07+0.05	1.15+0.05	1.19+0.05	1.15+0.05	1.13+0.05	1.30+0.06
	4.0 - 6.5	1.29+0.05	1.30+0.06	1.31+0.06	1.35+0.06	1.32+0.06	1.26+0.05
	6.5 -10.5	1.12+0.08	1.17+0.08	1.29+0.08	1.15+0.08	1.26+0.08	0.85+0.08
	> 10.50	0.89+0.07	0.89+0.07	0.92+0.07	0.86+0.07	0.92+0.07	0.84+0.06
	0.1 - 0.2	1.07+0.07	1.11+0.07	1.24+0.08	1.26+0.08	1.30+0.08	1.34+0.08
	0.2 - 0.4	1.11+0.05	1.16+0.05	1.31+0.05	1.22+0.05	1.21+0.05	1.40+0.06
Shell #4	0.4 - 0.8	1.05+0.05	1.08+0.05	1.08+0.05	0.98+0.04	1.03+0.05	1.15+0.05
r_i=1.9 cm	0.8 - 1.4	1.07+0.05	1.10+0.05	1.02+0.05	0.97+0.04	0.94+0.04	0.98+0.04
r_o=20.0 cm	1.4 - 2.5	1.07+0.05	1.09+0.05	1.09+0.05	1.00+0.04	0.98+0.04	1.09+0.05
	2.5 - 4.0	1.14+0.05	1.16+0.05	1.19+0.05	1.15+0.05	1.15+0.05	1.20+0.05
	4.0 - 6.5	1.39+0.06	1.43+0.06	1.44+0.06	1.39+0.06	1.42+0.06	1.11+0.05
	6.5 -10.5	1.21+0.08	1.22+0.08	1.32+0.08	1.19+0.08	1.39+0.09	0.78+0.05
	> 10.50	1.01+0.07	1.02+0.07	1.04+0.07	0.98+0.07	1.11+0.08	0.93+0.07
	0.1 - 0.2	1.06+0.07	1.10+0.08	1.21+0.08	1.17+0.08	1.28+0.08	1.26+0.08
	0.2 - 0.4	1.17+0.05	1.19+0.05	1.24+0.05	1.10+0.05	1.03+0.05	1.37+0.06
Shell #5	0.4 - 0.8	1.05+0.05	1.08+0.05	0.94+0.04	0.81+0.04	0.91+0.04	1.05+0.05
r_i=2.0 cm	0.8 - 1.4	1.03+0.05	1.05+0.05	0.85+0.05	0.79+0.05	0.76+0.05	0.82+0.04
r_o=30.0 cm	1.4 - 2.5	0.98+0.05	1.00+0.05	0.94+0.04	0.85+0.04	0.82+0.04	0.95+0.04
	2.5 - 4.0	1.04+0.05	1.06+0.05	1.09+0.05	1.03+0.05	1.08+0.05	1.10+0.05
	4.0 - 6.5	1.31+0.06	1.32+0.06	1.35+0.06	1.27+0.06	1.37+0.06	0.97+0.04
	6.5 -10.5	1.08+0.08	1.14+0.08	1.21+0.08	1.08+0.08	1.36+0.08	0.66+0.04
	> 10.50	0.90+0.07	0.90+0.07	0.92+0.07	0.85+0.07	1.03+0.07	0.80+0.07

Table 30: Comparison of MCNP4A/FENDL-1 calculations with measured data from Ref. /Simakov 92/ for IPPE Obninsk iron spherical shell #2 (inner radius = 4.5 cm, outer radius = 12.0 cm) using both a one- and a three-dimensional geometrical model.
- S. P. Simakov, IPPE-Obninsk

Energy Bins, MeV	Experiment	Calculation	C/E	Experiment	Calculation	C/E
	1D geometry			3D geometry		
0.2 - 0.4	8.66+/-0.60E-02	8.62E-02	1.00+/-0.07	8.22+/-0.60E-02	8.11E-02	0.99+/-0.07
0.4 - 0.8	1.55+/-0.09E-01	1.53E-01	0.99+/-0.06	1.45+/-0.09E-01	1.45E-01	1.00+/-0.06
0.8 - 1.4	1.39+/-0.08E-01	1.47E-01	1.06+/-0.06	1.30+/-0.08E-01	1.41E-01	1.08+/-0.07
1.4 - 2.5	1.03+/-0.06E-01	1.13E-01	1.10+/-0.07	9.75+/-0.60E-02	1.09E-01	1.12+/-0.07
2.5 - 4.0	5.00+/-0.30E-02	5.86E-02	1.17+/-0.07	4.79+/-0.30E-02	5.55E-02	1.16+/-0.08
4.0 - 6.5	3.12+/-0.20E-02	3.86E-02	1.24+/-0.08	3.03+/-0.20E-02	3.77E-02	1.24+/-0.08
6.5 - 10.5	2.72+/-0.20E-02	2.56E-02	0.94+/-0.07	2.72+/-0.20E-02	2.50E-02	0.92+/-0.07
10.5 - 20.0	3.62+/-0.30E-01	4.09E-01	1.12+/-0.08	4.04+/-0.30E-01	4.04E-01	1.00+/-0.07

Table 31: Comparison (C/E) of evaluated and measured secondary energy distribution data for neutrons emitted in the Fe(n,xn) reaction at 14 MeV neutron incidence energy.
- S. P. Simakov, IPPE-Obninsk

Energy Range MeV	Average Experim. Data	C/E			
		FENDL-1	ENDF/B-B6	BROND-2	JENDL-3
0.20 - 0.40	7.72E+01	1.19	1.28	.62	1.33
0.40 - 0.80	2.06E+02	.98	1.03	.69	.95
0.80 - 1.40	2.92E+02	.94	.89	.87	.91
1.40 - 2.50	3.66E+02	.88	.82	1.18	1.01
2.50 - 4.00	2.79E+02	.85	.79	.81	1.10
4.00 - 6.50	2.15E+02	.94	.88	.91	.84
6.50 - 10.50	1.43E+02	.97	.88	1.10	.74

Table 32: MCNP4A-calculations with FENDL/MC-1.0, EFF-1 and -2 data for TUD iron slab experiment (thickness: 30 cm) - K. Seidel, TU Dresden

Fe slab (t=30 cm), no gap, ideal geometry

Neutron fluence in energy intervals per source neutron

E / MeV	Calcul. / Experim.		
	EFF-1	EFF-2	FENDL-1
0.04 - 1.0	0.82 +- 0.09	0.82 +- 0.09	0.81 +- 0.11
1.0 - 5.0	0.76 +- 0.02	0.84 +- 0.02	0.82 +- 0.03
5.0 - 10.0	0.56 +- 0.02	0.78 +- 0.02	0.84 +- 0.02
10.0 - 15.0	0.80 +- 0.02	0.88 +- 0.02	0.84 +- 0.02

Photon fluence in the measured energy range per source neutron

E / MeV	Calcul. / Experim.		
	EFF-1	EFF-2	FENDL-1
0.2 - 8.0	0.72 +- 0.01	0.86 +- 0.01	0.80 +- 0.01

Fe slab (t = 30 cm), no gap, real geometry

Neutron fluence in energy intervals per source neutron

E / MeV	Calcul. / Experim.		
	EFF-1	EFF-2	FENDL-1
0.04 - 1.0	0.86 +- 0.10	0.89 +- 0.10	0.88 +- 0.10
1.0 - 5.0	0.90 +- 0.04	0.95 +- 0.04	0.94 +- 0.03
5.0 - 10.0	0.65 +- 0.04	0.92 +- 0.08	1.00 +- 0.07
10.0 - 15.0	0.77 +- 0.03	0.87 +- 0.03	0.87 +- 0.04

Photon fluence in the measured energy range per source neutron

E / MeV	Calcul. / Experim.		
	EFF-1	EFF-2	FENDL-1
0.2 - 8.0	0.62 +- 0.02	0.80 +- 0.02	0.76 +- 0.02

Fe slab (t = 30 cm with straight gap 5/20 cm), real geometry

Neutron fluence in energy intervals per one source neutron

E / MeV	Calcul. / Experim.		
	EFF-1	EFF-2	FENDL-1
0.04 - 1.0	0.76 +- 0.09	0.79 +- 0.09	0.78 +- 0.09
1.0 - 5.0	0.76 +- 0.03	0.82 +- 0.02	0.80 +- 0.02
5.0 - 10.0	0.69 +- 0.03	0.91 +- 0.02	0.97 +- 0.02
10.0 - 15.0	0.84 +- 0.03	0.92 +- 0.02	0.88 +- 0.02

Photon fluence in the measured energy range per one source neutron

E / MeV	Calcul. / Experim.		
	EFF-1	EFF-2	FENDL-1
0.2 - 8.0	0.73 +- 0.03	0.88 +- 0.02	0.80 +- 0.01

TUD iron slab experiment

Table 33: MCNP4A-calculations with FENDL/MC-1.0 for TUD iron slab experiment (thickness: 30 cm) with no gap, ideal geometry - U. Fischer, FZK Karlsruhe

	Experiment	FENDL/MC	C/E
0.10000E+06 - 0.20000E+06	0.59535E-07	0.31058E-07	0.522
0.20000E+06 - 0.40000E+06	0.62572E-07	0.66567E-07	1.064
0.40000E+06 - 0.80000E+06	0.61034E-07	0.69003E-07	1.130
0.80000E+06 - 0.14000E+07	0.29670E-07	0.29617E-07	0.998
0.14000E+07 - 0.25000E+07	0.15534E-07	0.10193E-07	0.656
0.25000E+07 - 0.40000E+07	0.42726E-08	0.31802E-08	0.744
0.40000E+07 - 0.65000E+07	0.22400E-08	0.18632E-08	0.830
0.65000E+07 - 0.10500E+08	0.17895E-08	0.14139E-08	0.790
0.10500E+08 - 0.20000E+08	0.14989E-07	0.11987E-07	0.800
0.10000E+06 - 0.20000E+08	0.25164E-06	0.22488E-06	0.894

FNS Fe slab TOF-experiment

Table 34: MCNP-calculations with FENDL-1 and JENDL-3.2 data for FNS cylindrical slabs - Y. Oyama, M. Wada -FNS/JAERI

				Fe slab thickness: 5 cm	
Angle	Expt.	JENDL-3.2	C/E	FENDL-1.0	C/E
>10 MeV					
0.0000	3.6865	3.6623	0.99341	3.6356	0.98617
24.900	0.11586	0.13732	1.1852	0.15022	1.2966
41.800	0.034574	0.031980	0.92497	0.034013	0.98377
66.800	0.021337	0.015225	0.71355	0.016640	0.77987
1-10 MeV					
0.0000	0.22336	0.21939	0.98223	0.21931	0.98186
24.900	0.083057	0.082624	0.99479	0.082084	0.98828
41.800	0.084378	0.078218	0.92699	0.078795	0.93383
66.800	0.081449	0.072871	0.89468	0.073944	0.90786
0.4-1 MeV					
0.0000	0.085460	0.082607	0.96662	0.079588	0.93128
24.900	0.035498	0.037552	1.0579	0.034118	0.96113
41.800	0.037544	0.039192	1.0439	0.036077	0.96092
66.800	0.043887	0.041231	0.93949	0.038733	0.88257
0.1-0.4 MeV					
0.0000	0.036076	0.036441	1.0101	0.032790	0.90891
24.900	0.015715	0.020454	1.3016	0.015883	1.0107
41.800	0.017265	0.021416	1.2404	0.016893	0.97847
66.800	0.022089	0.023063	1.0441	0.018981	0.85930
0.05-0.1 MeV					
0.0000	0.0024195	0.0020388	0.84267	0.0019182	0.79279
24.900	0.0020018	0.0018180	0.90816	0.0016802	0.83935
41.800	0.0020947	0.0018356	0.87631	0.0017022	0.81264
66.800	0.0024786	0.0018647	0.75230	0.0016927	0.68291

Table 34: (cont'd) MCNP-calculations with FENDL-1 and JENDL-3.2 data for FNS cylindrical slabs - Y. Oyama, M. Wada -FNS/JAERI

Fe slab thickness: 200 mm

	Angle	Expt.	JENDL-3.2	C/E	FENDL-1.0	C/E
>10 MeV						
	0.0000	0.23133	0.23349	1.0094	0.22848	0.98770
	12.200	0.058774	0.055061	0.93683	0.058362	0.99299
	24.900	0.015778	0.015670	0.99316	0.017967	1.1387
	41.800	0.0043323	0.0044099	1.0179	0.0053391	1.2324
	66.800	0.0013660	0.0011837	0.86654	0.0016632	1.2176
1-10 MeV						
	0.0000	0.043233	0.041204	0.95307	0.044183	1.0220
	12.200	0.036603	0.035866	0.97987	0.038216	1.0441
	24.900	0.033660	0.032350	0.96109	0.034457	1.0237
	41.800	0.027243	0.025785	0.94648	0.027549	1.0112
	66.800	0.016531	0.015001	0.90745	0.016142	0.97648
0.4-1 MeV						
	0.0000	0.053056	0.050783	0.95716	0.052228	0.98439
	12.200	0.043990	0.046395	1.0547	0.046624	1.0599
	24.900	0.042253	0.043918	1.0394	0.044361	1.0499
	41.800	0.038371	0.038849	1.0125	0.039466	1.0285
	66.800	0.026721	0.026401	0.98802	0.027167	1.0167
0.1-0.4 MeV						
	0.0000	0.042385	0.042507	1.0029	0.038447	0.90709
	12.200	0.035748	0.040636	1.1367	0.035351	0.98891
	24.900	0.034351	0.039384	1.1465	0.034372	1.0006
	41.800	0.034352	0.036044	1.0493	0.031990	0.93125
	66.800	0.025132	0.026180	1.0417	0.023943	0.95268
0.05-0.4 MeV						
	0.0000	0.0053635	0.0048052	0.89591	0.0038717	0.72186
	12.200	0.0043511	0.0049070	1.1278	0.0039434	0.90630
	24.900	0.0040891	0.0047130	1.1526	0.0037568	0.91874
	41.800	0.0046084	0.0043401	0.94178	0.0034503	0.74870
	66.800	0.0033264	0.0032903	0.98915	0.0025477	0.76590

Fe slab thickness: 400 mm

	Angle	Expt.	JENDL-3.2	C/E	FENDL-1.0	C/E
>10 MeV						
	0.0000	0.0052130	0.0055730	1.0691	0.0054603	1.0474
	12.200	0.0021169	0.0018317	0.86527	0.0019867	0.93849
	24.900	0.00069620	0.00066086	0.94924	0.00078397	1.1261
	41.800	0.00021809	0.00019241	0.88225	0.00025595	1.1736
	66.800	8.5131e-05	6.5145e-05	0.76523	5.3989e-05	0.63419
1-10 MeV						
	0.0000	0.0043863	0.0044170	1.0070	0.0050281	1.1463
	12.200	0.0038308	0.0039528	1.0318	0.0044062	1.1502
	24.900	0.0031953	0.0032307	1.0111	0.0035964	1.1255
	41.800	0.0024482	0.0020981	0.85700	0.0022895	0.93518
	66.800	0.0012860	0.00096800	0.75272	0.0010797	0.83958
0.4-1 MeV						
	0.0000	0.015683	0.014601	0.93101	0.016593	1.0580
	12.200	0.014258	0.013584	0.95273	0.015216	1.0672
	24.900	0.013237	0.011783	0.89016	0.013229	0.99943
	41.800	0.010699	0.0083752	0.78280	0.0093041	0.86962
	66.800	0.0064596	0.0043483	0.67315	0.0047925	0.74192

Table 34: (cont'd) MCNP-calculations with FENDL-1 and JENDL-3.2 data for FNS cylindrical slabs
- Y. Oyama, M. Wada -FNS/JAERI

Fe slab thickness: 400 mm

	Angle	Expt.	JENDL-3.2	C/E	FENDL-1.0	C/E
0.1-0.4 MeV						
	0.0000	0.024540	0.020936	0.85314	0.021185	0.86328
	12.200	0.021679	0.020241	0.93367	0.019961	0.92075
	24.900	0.021580	0.018018	0.83494	0.017735	0.82183
	41.800	0.019084	0.013480	0.70635	0.012933	0.67769
	66.800	0.012363	0.0073630	0.59557	0.0066495	0.53785
0.05-0.4 MeV						
	0.0000	0.0038640	0.0030760	0.79607	0.0021406	0.55399
	12.200	0.0030003	0.0030832	1.0276	0.0021826	0.72746
	24.900	0.0030540	0.0028340	0.92796	0.0019869	0.65059
	41.800	0.0029790	0.0022210	0.74555	0.0015757	0.52893
	66.800	0.0023510	0.0012858	0.54692	0.00096116	0.40883

Fe slab thickness: 600 mm

	Angle	Expt.	JENDL-3.2	C/E	FENDL-1.0	C/E
>10 MeV						
	0.0000	0.0001685	0.0001642	0.9745	0.0001268	0.7524
	12.200	0.0001068	7.425e-05	0.6953	5.694e-05	0.5332
	24.900	5.225e-05	1.924e-05	0.3683	2.760e-05	0.5281
	41.800	6.651e-06	3.965e-06	0.5962	6.398e-06	0.9620
1-10 MeV						
	0.0000	0.0005779	0.0005620	0.9724	0.0006745	1.167
	12.200	0.0004257	0.0004808	1.129	0.0005469	1.285
	24.900	0.0002962	0.0003432	1.159	0.0003813	1.287
	41.800	0.0001983	0.0001908	0.9622	0.0002111	1.065
0.4-1 MeV						
	0.0000	0.004439	0.004397	0.9905	0.005551	1.251
	12.200	0.003758	0.004051	1.078	0.005004	1.332
	24.900	0.003248	0.003287	1.012	0.003981	1.226
	41.800	0.002217	0.002161	0.9745	0.002614	1.179
0.1-0.4 MeV						
	0.0000	0.01206	0.01167	0.9678	0.01351	1.121
	12.200	0.01056	0.01122	1.062	0.01274	1.206
	24.900	0.009798	0.009717	0.9918	0.01087	1.109
	41.800	0.007061	0.007232	1.024	0.007780	1.102
0.05-0.4 MeV						
	0.0000	0.001840	0.002497	1.357	0.001589	0.8639
	12.200	0.001460	0.002502	1.714	0.001615	1.107
	24.900	0.001397	0.002264	1.621	0.001484	1.063
	41.800	0.001924	0.001776	0.9230	0.001211	0.6295

Table 35: MCNP4A-calculations with FENDL/MC-1.0 for FNS cylindrical slabs - D. Markovskij, RRC "KI"

Fe slab thickness: 5 cm

Angle	Expt.	FENDL-1.0	C/E
E >10 MeV			
0.0	3.6865	3.4478	0.935
24.9	0.11586	0.13678	1.181
41.8	0.034574	0.03056	0.883
66.8	0.021337	0.01554	0.728
1-10 MeV			
0.0	0.22336	0.2152	0.963
24.9	0.083057	0.07808	0.940
41.8	0.084378	0.07530	0.892
66.8	0.081449	0.07207	0.885
0.4-1 MeV			
0.0	0.08546	0.06628	0.775
24.9	0.035498	0.02805	0.790
41.8	0.037544	0.02941	0.783
66.8	0.043887	0.03181	0.725
0.1-0.4 MeV			
0.0	0.036076	0.02909	0.806
24.9	0.015715	0.01366	0.869
41.8	0.017265	0.01463	0.847
66.8	0.022089	0.01670	0.756
0.05-0.1 MeV			
0.0	0.002419	0.001518	0.628
24.9	0.002002	0.001361	0.680
41.8	0.002095	0.001419	0.677
66.8	0.002478	0.001537	0.620

Fe slab thickness: 40 cm

Angle	Expt.	FENDL-1.0	C/E
E >10 MeV			
0.0	0.052130	0.0050430	0.967
12.2	0.0021169	0.0019360	0.915
24.9	0.0006962	0.0006960	1.005
41.8	0.00021809	0.0001934	0.887
66.8	0.00008513	0.00003039	0.357
1-10 MeV			
0.0	0.0043863	0.005384	1.277
12.2	0.0038830	0.004832	1.244
24.9	0.0031953	0.004037	1.263
41.8	0.0024482	0.002767	1.130
66.8	0.0012860	0.001270	0.988
0.4-1 MeV			
0.0	0.015683	0.01559	0.994
12.2	0.014258	0.01460	1.024
24.9	0.013237	0.01281	0.968
41.8	0.010699	0.009932	0.928
66.8	0.0064596	0.005352	0.828
0.1-0.4 MeV			
0.0	0.024540	0.02252	0.917
12.2	0.021679	0.02161	0.997
24.9	0.021580	0.01971	0.913
41.8	0.019084	0.01594	0.835
66.8	0.012363	0.008868	0.717
0.05-0.1 MeV			
0.0	0.0038640	0.002760	0.714
12.2	0.0030003	0.002790	0.929
24.9	0.0030540	0.001618	0.530
41.8	0.0029790	0.002262	0.759
66.8	0.0023510	0.001404	0.597

Table 36: MCNP-calculations with FENDL-1 and JENDL-3.2 data for reaction rates inside FNS Fe cylindrical slabs - F. Maekawa, M. Wada, Y. Oyama -FNS/JAERI

ReactionPosition [mm]	Expt.	error	JENDL-3.2	error	FENDL-1	error
27Al(n,a)			C/E		C/E	
0	2.5070e-29	0.0275	0.9521	0.0059	0.9394	0.0140
100	3.8490e-30	0.0279	0.8966	0.0108	0.9043	0.0197
200	6.2940e-31	0.0277	0.8473	0.0125	0.9177	0.0212
300	1.2100e-31	0.0308	0.7821	0.0113	0.8391	0.0183
400	2.2020e-32	0.0351	0.7757	0.0102	0.8644	0.0163
500	3.8930e-33	0.0589	0.8251	0.0097	0.9370	0.0155
700	1.5340e-34		0.7793	0.0082	0.8984	0.0134
Ti(n,x)Sc48						
0	1.0904e-29	0.0344	0.9251	0.0056	0.9126	0.0136
100	1.6717e-30	0.0319	0.8471	0.0102	0.8500	0.0186
200	2.6222e-31	0.0325	0.8220	0.0121	0.8819	0.0206
300	4.8192e-32	0.0418	0.7802	0.0115	0.8346	0.0186
400	8.1879e-33	0.0402	0.8217	0.0109	0.9106	0.0176
500	1.8913e-33	0.2086	0.6648	0.0078	0.7473	0.0126
Fe56(n,p)						
0	2.1800e-29	0.0261	1.0277	0.0063	1.0144	0.0151
100	3.3780e-30	0.0269	0.9634	0.0116	0.9739	0.0210
200	5.4080e-31	0.0302	0.9316	0.0135	1.0120	0.0231
300	1.0570e-31	0.0302	0.8462	0.0122	0.9113	0.0196
400	1.4780e-32	0.0387	1.0926	0.0141	1.2230	0.0229
500	3.5090e-33	0.0562	0.8652	0.0100	0.9875	0.0162
700	1.8920e-34	0.2881	0.5961	0.0063	0.6909	0.0102
Ni58(n,2n)						
0	9.8220e-30	0.0283	0.8631	0.0051	0.8481	0.0127
100	1.2930e-30	0.0351	0.8346	0.0102	0.8250	0.0189
200	2.0520e-31	0.0308	0.7564	0.0118	0.7880	0.0202
300	3.5140e-32	0.0418	0.7231	0.0116	0.7616	0.0193
400	6.4400e-33	0.0671	0.6779	0.0103	0.7355	0.0165
500	1.7150e-33	0.1081	0.4590	0.0062	0.4951	0.0097
Ni58(n,p)						
0	7.5850e-29	0.0257	0.9231	0.0069	0.9159	0.0142
100	1.8130e-29	0.0269	0.8575	0.0099	0.9341	0.0175
200	3.8660e-30	0.0261	0.7585	0.0096	0.8882	0.0171
300	7.2330e-31	0.0292	0.8149	0.0106	0.9507	0.0169
400	1.4900e-31	0.0450	0.7881	0.0101	0.9308	0.0164
500	2.6850e-32	0.0662	0.8727	0.0121	1.0953	0.0195
Zn64(n,p)						
0	3.5120e-29	0.0263	1.0655	0.0076	1.0557	0.0160
100	7.3620e-30	0.0308	1.0168	0.0117	1.0971	0.0208
200	1.5990e-30	0.0269	0.8422	0.0109	0.9804	0.0195
300	3.1790e-31	0.0319	0.8243	0.0110	0.9553	0.0176
400	6.8550e-32	0.0380	0.7346	0.0097	0.8687	0.0158
500	1.3080e-32	0.0475	0.7404	0.0108	0.9337	0.0172
700	2.3990e-33	0.1384	0.1664	0.0029	0.2133	0.0042
Zr90(n,2n)						
0	1.9600e-28	0.0269	0.8893	0.0052	0.8752	0.0131
100	2.6410e-29	0.0269	0.8596	0.0104	0.8536	0.0193
200	4.1390e-30	0.0272	0.8012	0.0123	0.8394	0.0210
300	7.0210e-31	0.0287	0.7852	0.0124	0.8315	0.0204
400	1.4940e-31	0.0358	0.6424	0.0094	0.7013	0.0151
500	2.7410e-32	0.0450	0.6387	0.0083	0.6960	0.0130
700	5.5700e-33	0.0888	0.1100	0.0013	0.1196	0.0020

Table 36: (cont'd) MCNP-calculations with FENDL-1 and JENDL-3.2 data for reaction rates inside FNS Fe cylindrical slabs - F. Maekawa, M. Wada, Y. Oyama -FNS/JAERI

ReactionPosition [mm]	Expt.	error	JENDL-3.2	error	FENDL-1	error
Nb93(n,2n)			C/E		C/E	
0	1.0860e-28	0.0287	0.9210	0.0055	0.9088	0.0135
100	1.0760e-29	0.0297	1.2852	0.0157	1.2824	0.0285
200	2.5490e-30	0.0269	0.8193	0.0123	0.8711	0.0208
300	4.6280e-31	0.0319	0.7810	0.0117	0.8303	0.0190
400	8.5310e-32	0.0331	0.7544	0.0103	0.8290	0.0164
500	1.5530e-32	0.0467	0.7726	0.0093	0.8601	0.0147
700	1.0410e-33	0.3260	0.4228	0.0045	0.4705	0.0071
In115(n,n')						
0	3.2440e-29	0.0261	1.0177	0.0122	0.9942	0.0195
100	1.8260e-29	0.0263	0.9382	0.0095	1.0001	0.0152
200	5.1250e-30	0.0287	0.9105	0.0085	1.0052	0.0147
300	1.4070e-30	0.0287	0.8839	0.0091	0.9841	0.0144
400	3.8910e-31	0.0344	0.8757	0.0102	0.9584	0.0151
500	1.1360e-31	0.0562	0.8558	0.0163	0.9928	0.0237
700	2.0620e-32	0.1276	0.4974	0.0249	0.6128	0.0336
Au197(n,g)						
0	1.4070e-28	0.0344	0.3079	0.0553	0.1950	0.0125
100	6.2070e-28	0.0297	1.1078	0.1603	0.9260	0.1533
200	8.1830e-28	0.0283	0.9948	0.0605	0.9237	0.0771
300	7.4160e-28	0.0313	1.1637	0.0867	1.0566	0.1199
400	6.4950e-28	0.0325	1.0799	0.0644	0.9433	0.0651
500	5.0980e-28	0.0319	1.0957	0.0717	0.9903	0.0890
700	2.5830e-28	0.0331	1.1032	0.0639	0.9510	0.0949

Chromium

OKTAVIAN spherical shell experiment

Table 37: MCNP-calculations with FENDL-1, JENDL-FF and JENDL-3.2 data for OKTAVIAN Cr spherical shell experiment (40 cm diameter, wall thickness = 0.7 mfp)
- C. Ichihara, University of Kyoto

Energy [MeV]	Experiment	FENDL-1		JENDL-3.2		JENDL-FF	
10<En<20	5.493×10-1	5.413×10-1	(0.985)	5.449×10-1	(0.992)	5.625×10-1	(1.024)
5<En<10	4.101×10-2	4.621×10-2	(1.127)	4.092×10-2	(0.998)	4.158×10-2	(1.014)
1<En<5	2.210×10-1	2.472×10-1	(1.118)	2.388×10-1	(1.081)	2.334×10-1	(1.056)
0.1<En<1	1.489×10-1	2.251×10-1	(1.511)	2.384×10-1	(1.601)	2.238×10-1	(1.503)
total	0.960	1.060	(1.104)	1.063	(1.107)	1.061	(1.105)

Copper

OKTAVIAN spherical shell experiment

Table 38: MCNP-calculations with FENDL-1, JENDL-FF and JENDL-3.2 data for OKTAVIAN Cu spherical shell experiment (61 cm diameter, wall thickness = 4.7 mfp)
- C. Ichihara, University of Kyoto

Energy [MeV]	Experiment	FENDL-1		JENDL-3.2		JENDL-FF	
10<En<20	7.942×10-2	8.947×10-2	(1.127)	8.531×10-2	(1.074)	9.251×10-2	(1.165)
5<En<10	1.335×10-2	1.821×10-2	(1.364)	1.324×10-2	(0.992)	1.443×10-2	(1.081)
1<En<5	1.445×10-1	1.641×10-1	(1.136)	1.412×10-1	(0.977)	1.521×10-1	(1.053)
0.1<En<1	6.603×10-1	7.217×10-1	(1.093)	7.179×10-1	(1.087)	6.995×10-1	(1.059)
total	1.076	0.993	(0.923)	0.958	(0.890)	0.959	(0.891)

Table 39: MCNP- and ONEDANT-calculations with FENDL-1 data for OKTAVIAN Cu spherical shell experiment (inner radius = 2.5 cm, outer radius = 30.0 cm)
- U. Fischer, E. Wiegner, FZK Karlsruhe

		ONEDANT/FENDL/MG-1.0		MCNP4A/FENDL/MC-1.0	
	Experiment	C	C/E	C	C/E
0.10000E+06 - 0.20000E+06	0.23232E+00	0.17699E+00	0.76184E+00	0.16152E+00	0.69525E+00
0.20000E+06 - 0.40000E+06	0.20017E+00	0.20934E+00	0.10458E+01	0.22910E+00	0.11445E+01
0.40000E+06 - 0.80000E+06	0.23727E+00	0.26055E+00	0.10981E+01	0.26389E+00	0.11122E+01
0.80000E+06 - 0.14000E+07	0.12197E+00	0.12985E+00	0.10646E+01	0.13193E+00	0.10817E+01
0.14000E+07 - 0.25000E+07	0.55862E-01	0.56070E-01	0.10037E+01	0.57976E-01	0.10378E+01
0.25000E+07 - 0.40000E+07	0.20314E-01	0.19467E-01	0.95830E+00	0.20396E-01	0.10040E+01
0.40000E+07 - 0.65000E+07	0.11307E-01	0.12159E-01	0.10754E+01	0.12692E-01	0.11225E+01
0.65000E+07 - 0.10500E+08	0.88614E-02	0.11096E-01	0.12522E+01	0.11744E-01	0.13253E+01
0.10500E+08 - 0.20000E+08	0.78479E-01	0.69951E-01	0.89133E+00	0.77556E-01	0.98825E+00
0.10000E+06 - 0.20000E+08	0.96655E+00	0.94547E+00	0.97819E+00	0.96680E+00	0.10000E+01

Table 40: MCNP-calculations with FENDL-1 and JENDL-3.2 data for reaction rates inside FNS Cu cylindrical slabs - F. Maekawa, M. Wada, Y. Oyama -FNS/JAERI

ReactionPosition [mm]	Expt.	error	JENDL-3.2	error	FENDL-1	error
27Al(n,a)24Na			C/E		C/E	
-0.	2.3870e-29	0.0311	0.9975	0.0139	0.9957	0.0137
101	3.3560e-30	0.0323	0.9719	0.0178	0.9842	0.0176
204	4.8590e-31	0.0334	0.9826	0.0167	0.9892	0.0165
356	3.1420e-32	0.0423	1.0423	0.0143	1.0052	0.0139
508	2.3120e-33	0.0608	1.0525	0.0124	0.9660	0.0113
610	2.4030e-34	0.0494	1.7675	0.0223	1.5591	0.0218
Ti(n,x)47Sc						
-0.	4.5168e-30	0.0294	0.9668	0.0132	0.9656	0.0132
101	6.2227e-31	0.0292	0.9977	0.0173	1.0084	0.0168
204	8.9441e-32	0.0373	1.0270	0.0162	1.0363	0.0158
356	6.3804e-33	0.0611	0.9840	0.0128	0.9636	0.0123
508	4.2110e-34	0.1734	1.0946	0.0127	1.0305	0.0114
Ti(n,x)48Sc						
-0.	9.9948e-30	0.0311	1.0079	0.0140	1.0067	0.0139
101	1.3379e-30	0.0321	1.0009	0.0185	1.0057	0.0181
204	1.7964e-31	0.0422	1.0728	0.0183	1.0652	0.0177
356	1.2680e-32	0.0604	1.0220	0.0140	0.9681	0.0133
508	7.2752e-34	0.1415	1.3047	0.0146	1.1788	0.0132
Fe56(n,p)56Mn						
-0.	2.1730e-29	0.0291	1.0287	0.0143	1.0270	0.0142
101	2.9740e-30	0.0297	1.0343	0.0188	1.0486	0.0186
204	4.4400e-31	0.0301	1.0151	0.0172	1.0232	0.0169
356	2.9290e-32	0.0334	1.0534	0.0143	1.0184	0.0138
508	2.1782e-33	0.0495	1.0521	0.0122	0.9684	0.0111
610	1.0043e-33	0.1080	0.3970	0.0049	0.3513	0.0048
59Co(n,a)56Mn						
-0.	6.5590e-30	0.0294	1.0099	0.0140	1.0087	0.0139
101	8.6870e-31	0.0325	1.0203	0.0188	1.0278	0.0185
204	1.2330e-31	0.0345	1.0374	0.0176	1.0354	0.0171
356	8.5080e-33	0.0400	1.0147	0.0138	0.9663	0.0131
508	6.2550e-34	0.0831	1.0145	0.0114	0.9201	0.0103
610	2.4540e-34	0.3534	0.4518	0.0053	0.3939	0.0050
58Ni(n,2n)57Ni						
-0.	1.0410e-29	0.0310	0.8146	0.0115	0.8147	0.0114
101	1.2860e-30	0.0329	0.7982	0.0156	0.7853	0.0151
204	1.7160e-31	0.0392	0.8056	0.0149	0.7751	0.0139
356	9.9980e-33	0.0665	0.8597	0.0130	0.7759	0.0116
508	5.4970e-34	0.1127	1.0807	0.0126	0.9238	0.0107
Cu(n,x)64Cu						
-0.	5.7970e-29	0.0342	1.1191	0.0149	1.1182	0.0150
101	1.2970e-29	0.0343	1.2164	0.0130	1.1668	0.0159
204	5.0160e-30	0.0350	1.2357	0.0138	1.1653	0.0147
356	1.7420e-30	0.0386	1.0530	0.0335	1.0606	0.0369
508	5.4697e-31	0.0383	0.8666	0.0539	0.8932	0.0580
610	1.9412e-30	0.3910	0.0187	0.0014	0.0250	0.0033

Table 40 (cont'd): MCNP-calculations with FENDL-1 and JENDL-3.2 data for reaction rates inside FNS Cu cylindrical slabs - F. Maekawa, M. Wada, Y. Oyama -FNS/JAERI

64Zn(n,p)64Cu						
-0.	3.2120e-29	0.0330	1.1622	0.0159	1.1585	0.0158
101	6.0780e-30	0.0339	1.1453	0.0189	1.2129	0.0193
204	9.8000e-31	0.0348	1.1559	0.0192	1.2411	0.0210
356	7.4890e-32	0.0424	1.1179	0.0184	1.1756	0.0187
508	6.8520e-33	0.0485	0.9376	0.0172	0.9272	0.0139
610	5.4120e-33	0.0485	0.1868	0.0037	0.1847	0.0043
90Zr(n,2n)89Zr						
-0.	1.7390e-28	0.0310	1.0020	0.0140	1.0023	0.0140
101	2.1920e-29	0.0317	0.9807	0.0189	0.9689	0.0183
204	2.9680e-30	0.0317	0.9907	0.0178	0.9590	0.0168
356	1.8760e-31	0.0348	0.9940	0.0145	0.9030	0.0132
508	1.1190e-32	0.0437	1.1703	0.0132	1.0104	0.0113
610	2.6320e-33	0.0511	0.8696	0.0099	0.7215	0.0084
93Nb(n,2n)92mNb						
-0.	9.7970e-29	0.0305	1.0207	0.0142	1.0192	0.0142
101	1.2930e-29	0.0314	1.0119	0.0189	1.0112	0.0185
204	1.7990e-30	0.0310	1.0404	0.0180	1.0196	0.0171
356	1.1440e-31	0.0359	1.0932	0.0152	1.0203	0.0143
508	8.3850e-33	0.0518	1.0846	0.0123	0.9674	0.0110
610	3.7640e-33	0.0532	0.4246	0.0050	0.3641	0.0046
115In(n,n')115mIn						
-0.	3.3670e-29	0.0287	0.9596	0.0144	0.9442	0.0143
101	1.7030e-29	0.0291	0.9057	0.0113	0.9432	0.0117
204	3.8820e-30	0.0325	0.8838	0.0111	0.9431	0.0119
356	3.8220e-31	0.0348	0.8435	0.0139	0.9347	0.0150
508	4.1970e-32	0.0504	0.6405	0.0179	0.7566	0.0227
610	2.2700e-32	0.0356	0.1437	0.0065	0.1658	0.0066
197Au(n,g)198Au						
0	8.1880e-29	0.0470	0.4537	0.0125	0.4317	0.0121
101	1.9800e-28	0.0436	0.8024	0.0787	0.6363	0.0341
204	2.1140e-28	0.0433	0.6915	0.1050	0.5953	0.0523
356	1.3240e-28	0.0451	0.5317	0.0745	0.7413	0.1394
508	5.9810e-29	0.0451	0.5750	0.1396	0.4424	0.0869
610	2.5770e-29	0.0485	0.0858	0.0126	0.1515	0.0807

Manganese

OKTAVIAN spherical shell experiment

Table 41: MCNP-calculations with FENDL-1, JENDL-FF and JENDL-3.2 data for OKTAVIAN Mn spherical shell experiment (61 cm diameter, wall thickness = 3.4 mfp)
- C. Ichihara, University of Kyoto

Energy [MeV]	Experiment	FENDL-1		JENDL-3.2		JENDL-FF	
10<En<20	1.542×10-1	1.453×10-1	(0.942)	1.514×10-1	(0.982)	1.519×10-1	(0.985)
5<En<10	2.794×10-2	2.744×10-2	(0.982)	3.084×10-2	(1.104)	3.031×10-2	(1.085)
1<En<5	2.709×10-1	3.056×10-1	(1.127)	2.976×10-1	(1.099)	3.014×10-1	(1.113)
0.1<En<1	6.608×10-1	7.080×10-1	(1.071)	7.131×10-1	(1.079)	7.111×10-1	(1.076)
total	1.114	1.187	(1.066)	1.193	(1.071)	1.195	(1.073)

Tungsten

OKTAVIAN spherical shell experiment

Table 42: MCNP-calculations with FENDL-1, JENDL-FF and JENDL-3.2 data for OKTAVIAN W spherical shell experiment (40 cm diameter, wall thickness = 0.8 mfp)
- C. Ichihara, University of Kyoto

Energy [MeV]	Experiment	FENDL-1		JENDL-3.2		JENDL-FF	
10<En<20	7.097×10-1	6.502×10-1	(0.916)	6.404×10-1	(0.902)	6.423×10-1	(0.905)
5<En<10	4.016×10-2	2.944×10-2	(0.733)	2.471×10-2	(0.615)	2.512×10-2	(0.625)
1<En<5	2.407×10-1	2.119×10-1	(0.880)	1.899×10-1	(0.789)	1.896×10-1	(0.788)
0.1<En<1	3.597×10-1	3.030×10-1	(0.842)	3.602×10-1	(1.001)	3.563×10-1	(0.991)
Total leakages	1.350	1.194	(0.884)	1.215	(0.900)	1.213	(0.899)

Table 43: MCNP-calculations with FENDL-1 and JENDL-3.2 data for reaction rates inside FNS W cylindrical slabs - F. Maekawa, M. Wada, Y. Oyama -FNS/JAERI

Reaction	Position [mm]	Expt.	error	JENDL-3.2	error	FENDL-1	error
27Al(n,a)				C/E		C/E	
	0	2.3440e-29	0.0289	1.0166	0.0045	1.0170	0.0146
	76	4.2714e-30	0.0311	1.0021	0.0064	1.0633	0.0173
	228	1.6352e-31	0.0307	0.9307	0.0082	1.0977	0.0155
	380	6.5968e-33	0.0474	0.9138	0.0102	1.2394	0.0183
93Nb(n,2n)92mNb							
	0	1.0050e-28	0.0286	1.0001	0.0044	0.9989	0.0145
	76	1.6428e-29	0.0330	1.0653	0.0069	1.1297	0.0188
	228	5.9964e-31	0.0320	0.9996	0.0090	1.1852	0.0171
	380	2.5586e-32	0.0346	0.9025	0.0105	1.2426	0.0189
115In(n,n')115mIn							
	0	3.0365e-29	0.0287	0.9256	0.0056	1.0143	0.0142
	76	1.4673e-29	0.0297	0.9238	0.0055	1.0925	0.0120
	228	9.7686e-31	0.0391	0.7987	0.0067	1.0347	0.0119
	380	4.7099e-32	0.0718	0.7463	0.0109	1.1134	0.0244
186W(n,g)							
	76	5.2242e-29	0.0307	0.9276	0.0072	0.8023	0.0095
	228	1.5785e-29	0.0303	0.8364	0.0075	0.7038	0.0115
	380	2.5631e-30	0.0287	0.6731	0.0088	0.5262	0.0109
197Au(n,g)							
	76	1.5083e-28	0.0465	1.0322	0.0085	0.8367	0.0108
	228	4.4128e-29	0.0494	1.1376	0.0091	0.7608	0.0106
	380	8.2349e-30	0.0775	0.9385	0.0098	0.5154	0.0104

Gamma-heating rate

Reaction	Position [mm]	Expt.	error	JENDL-3.2	error	FENDL-1	error
				C/E		C/E	
g-heat	0	1.1990e-15	0.2447	0.5906	0.0093	0.6029	0.0101
	58	8.3532e-16	0.2223	1.0622	0.0119	1.0720	0.0121
	210	1.1169e-16	0.1322	1.2334	0.0123	1.1978	0.0130
	356	2.6949e-17	0.1452	1.1453	0.0169	1.0918	0.0149
	508	7.4790e-18	0.1108	0.9382	0.0232	0.9471	0.0204

Table 44: MCNP-calculations with FENDL-1 and JENDL-3.2 data for FNS cylindrical slabs - Y. Oyama, M. Wada -FNS/JAERI

C slab thickness: 5 cm

Angle [degree]	Expt.	JENDL-3.2	C/E	FENDL-1.0	C/E
>11 MeV					
0.0000	4.9440	4.8587	0.98275	4.8998	0.99106
24.900	0.12910	0.15920	1.2332	0.17350	1.3439
41.800	0.037974	0.051473	1.3555	0.056602	1.4906
66.800	0.021523	0.023020	1.0696	0.025793	1.1984
1-11 MeV					
0.0000	0.33400	0.32098	0.96102	0.31730	0.95000
24.900	0.050735	0.055440	1.0927	0.050182	0.98910
41.800	0.042117	0.049878	1.1843	0.044200	1.0495
66.800	0.041681	0.043380	1.0408	0.037480	0.89921
0.5-1 MeV					
0.0000	0.042295	0.035193	0.83208	0.034702	0.82047
24.900	0.0061039	0.0066898	1.0960	0.0055997	0.91739
41.800	0.0063499	0.0068165	1.0735	0.0057668	0.90817
66.800	0.0065321	0.006479	0.99187	0.0055087	0.84333

C slab thickness: 20 cm

Angle [degree]	Expt.	JENDL-3.2	C/E	FENDL-1.0	C/E
>11 MeV					
0.0000	0.98877	0.86653	0.87637	0.89373	0.90388
12.200	0.13101	0.12623	0.96352	0.14172	1.0817
24.900	0.054250	0.056720	1.0455	0.056312	1.1634
41.800	0.016322	0.017433	1.0680	0.020115	1.2324
66.800	0.0057410	0.0059550	1.0373	0.0066330	1.1554
1-11 MeV					
0.0000	0.099221	0.090160	0.90868	0.087960	0.88651
12.200	0.055821	0.055311	0.99086	0.054030	0.96791
24.900	0.046210	0.048133	1.0416	0.046770	1.0121
41.800	0.034760	0.036327	1.0451	0.035027	1.0077
66.800	0.022383	0.021830	0.97529	0.021050	0.94045
0.5-1 MeV					
0.0000	0.0081786	0.0081035	0.99082	0.0064023	0.78281
12.200	0.0064471	0.0075291	1.1678	0.0058939	0.91419
24.900	0.0065524	0.0071320	1.0885	0.0056062	0.85560
41.800	0.0060964	0.0062596	1.0268	0.0048931	0.80262
66.800	0.0042246	0.0043682	1.0340	0.0034363	0.81340

C slab thickness: 40 cm

Angle [degree]	Expt.	JENDL-3.2	C/E	FENDL-1.0	C/E
>11 MeV					
0.0000	0.10626	0.085800	0.80745	0.090560	0.85225
12.200	0.021899	0.018660	0.85210	0.021180	0.96718
24.900	0.0095427	0.0082016	0.85946	0.0093206	0.97673
41.800	0.0031420	0.0028385	0.90338	0.0033153	1.0551
66.800	0.00096313	0.00071657	0.74400	0.00088587	0.91978
1-11 MeV					
0.0000	0.024240	0.020920	0.86304	0.021680	0.89439
12.200	0.017701	0.016439	0.92868	0.017424	0.98436
24.900	0.014760	0.013025	0.88245	0.013942	0.94458
41.800	0.010028	0.0087563	0.87319	0.0094744	0.94479
66.800	0.0052750	0.0045950	0.87109	0.0050797	0.96298
0.5-1 MeV					
0.0000	0.0023640	0.0021733	0.91933	0.0018572	0.78562
12.200	0.0024706	0.0022402	0.90674	0.0018719	0.75766
24.900	0.0020480	0.0020594	1.0056	0.0017235	0.84155
41.800	0.0023009	0.0017942	0.77978	0.0014646	0.63651
66.800	0.0010684	0.0011696	1.0948	0.00099685	0.93305

Table 45: MCNP-calculations with FENDL-1 and JENDL-3.2 data for reaction rates inside FNS C cylindrical slabs - F. Maekawa, M. Wada, Y. Oyama -FNS/JAERI

Reaction	Position [mm]	Expt.	error	JENDL-3.2	error	FENDL-1	error
27Al(n,a)24Na				C/E		C/E	
	-1	2.3300e-29	0.0310	0.9560	0.0017	0.9567	0.0016
	99	7.4200e-30	0.0320	0.9351	0.0036	0.9918	0.0035
	202	2.6000e-30	0.0320	0.9043	0.0057	0.9945	0.0058
	303	9.6100e-31	0.0380	0.8969	0.0078	1.0207	0.0079
	405	3.6900e-31	0.0370	0.8952	0.0111	1.0279	0.0112
	507	1.4100e-31	0.0600	0.9204	0.0142	1.0802	0.0146
	609	5.0000e-32	0.0880	0.9898	0.0204	1.1314	0.0230
58Ni(n,2n)57Ni							
	-1	8.1200e-30	0.0500	0.8925	0.0014	0.8928	0.0013
	99	1.9600e-30	0.0320	0.8557	0.0028	0.8940	0.0027
	202	5.5000e-31	0.0500	0.8427	0.0051	0.9050	0.0050
	303	1.6400e-31	0.0580	0.8666	0.0078	0.9657	0.0077
	405	5.4000e-32	0.1110	0.8635	0.0119	0.9758	0.0120
	507	1.9800e-32	0.0510	0.8214	0.0151	0.9564	0.0155
58Ni(n,p)58Co							
	-1	7.9800e-29	0.0310	0.9235	0.0022	0.9307	0.0021
	99	3.7100e-29	0.0500	0.9009	0.0042	0.9587	0.0042
	202	1.5300e-29	0.0520	0.9164	0.0060	1.0075	0.0060
	303	6.7200e-30	0.0520	0.8893	0.0074	1.0187	0.0075
	405	2.9400e-30	0.0550	0.8906	0.0095	1.0165	0.0099
	507	1.2900e-30	0.0500	0.8632	0.0115	1.0147	0.0124
90Zr(n,2n)89Zr							
	-1	1.4900e-28	0.0310	1.0070	0.0016	1.0072	0.0015
	99	3.5900e-29	0.0320	1.0152	0.0032	1.0631	0.0032
	202	1.0700e-29	0.0340	0.9775	0.0059	1.0552	0.0057
	303	3.4400e-30	0.0370	0.9657	0.0084	1.0821	0.0083
	405	1.2300e-30	0.0450	0.9192	0.0122	1.0386	0.0123
	507	4.2700e-31	0.0370	0.9482	0.0166	1.1081	0.0171
93Nb(n,2n)92mNb							
	-1	8.7800e-29	0.0320	1.0321	0.0018	1.0323	0.0017
	99	2.4400e-29	0.0320	1.0486	0.0039	1.1042	0.0036
	202	8.1300e-30	0.0310	0.9942	0.0063	1.0865	0.0064
	303	2.7800e-30	0.0310	1.0098	0.0090	1.1418	0.0091
	405	1.0500e-30	0.0370	0.9790	0.0129	1.1138	0.0131
	507	3.8700e-31	0.0360	1.0027	0.0168	1.1845	0.0176
	609	1.4700e-31	0.0320	0.9900	0.0226	1.1604	0.0265
115In(n,n')115mIn							
	-1	3.1300e-29	0.0330	1.0427	0.0034	1.0252	0.0032
	99	1.9900e-29	0.0320	1.0840	0.0057	1.0659	0.0054
	202	9.8000e-30	0.0360	1.0582	0.0073	1.0834	0.0068
	303	4.5700e-30	0.0410	1.0464	0.0084	1.1251	0.0083
	405	2.1700e-30	0.0520	1.0245	0.0108	1.1057	0.0104
	507	9.2600e-31	0.0740	1.0250	0.0125	1.1777	0.0137

Table 45 (cont'd): MCNP-calculations with FENDL-1 and JENDL-3.2 data for reaction rates inside FNS C cylindrical slabs - F. Maekawa, M. Wada, Y. Oyama -FNS/JAERI

Reaction	Position [mm]	Expt.	error	JENDL-3.2	error	FENDL-1	error
U-235(n,f)				C/E		C/E	
	41	3.8800e-27	0.0410	1.0021	0.0227	1.0380	0.0223
	66	5.0400e-27	0.0410	1.0050	0.0204	1.0591	0.0217
	117	6.9300e-27	0.0410	1.0417	0.0176	1.0552	0.0174
	168	8.2300e-27	0.0410	1.0614	0.0186	1.0963	0.0186
	218	8.8200e-27	0.0410	1.0694	0.0138	1.0755	0.0124
	269	8.8400e-27	0.0410	1.0841	0.0147	1.1116	0.0137
	319	8.3000e-27	0.0410	1.0629	0.0168	1.1118	0.0152
	370	7.3900e-27	0.0410	1.0705	0.0146	1.0943	0.0137
	421	6.1800e-27	0.0410	1.0471	0.0115	1.0725	0.0107
	471	4.7900e-27	0.0410	1.0560	0.0127	1.0980	0.0121
	522	3.3000e-27	0.0410	1.0529	0.0147	1.0772	0.0142
	572	1.7400e-27	0.0410	1.0507	0.0194	1.1141	0.0198
U-238(n,f)							
	41	1.8200e-28	0.0390	0.9730	0.0024	0.9866	0.0023
	66	1.3800e-28	0.0390	0.9916	0.0029	1.0100	0.0027
	117	8.4000e-29	0.0390	0.9770	0.0037	1.0084	0.0035
	168	5.1300e-29	0.0390	0.9886	0.0048	1.0428	0.0048
	218	3.3400e-29	0.0390	0.9575	0.0050	1.0277	0.0048
	269	2.1600e-29	0.0390	0.9437	0.0057	1.0321	0.0057
	319	1.4400e-29	0.0390	0.9118	0.0064	1.0039	0.0063
	370	9.4000e-30	0.0390	0.9074	0.0077	1.0117	0.0078
	421	6.0700e-30	0.0390	0.9098	0.0079	1.0329	0.0083
	471	4.1200e-30	0.0390	0.8788	0.0086	0.9826	0.0087
	522	2.6500e-30	0.0390	0.8640	0.0098	1.0002	0.0104
	572	1.6700e-30	0.0390	0.8651	0.0124	0.9745	0.0123

Table 46: MCNP-calculations with FENDL-1 and JENDL-3.2 data for FNS liquid oxygen cylindrical slabs - Y. Oyama, M. Wada -FNS/JAERI

O2 slab thickness: 200 mm

	Angle	Expt.	JENDL-3.2	C/E	FENDL-1.0	C/E
>10 MeV						
	0.0000	2.1210	2.0669	0.97448	2.0956	0.98802
	24.900	0.073253	0.045819	0.62549	0.047440	0.64762
	41.800	0.028699	0.018299	0.63762	0.017258	0.60135
	66.800	0.013267	0.0064210	0.48398	0.0064020	0.48255
1-10 MeV						
	0.0000	0.16226	0.15834	0.97584	0.15746	0.97042
	24.900	0.040638	0.042515	1.0462	0.038263	0.94156
	41.800	0.039873	0.035247	0.88398	0.031658	0.79397
	66.800	0.026942	0.017780	0.65994	0.016311	0.60541
0.1-1 MeV						
	0.0000	0.021380	0.020505	0.95907	0.019376	0.90627
	24.900	0.011537	0.011565	1.0024	0.0097715	0.84697
	41.800	0.011540	0.010476	0.90780	0.0087100	0.75477
	66.800	0.0089793	0.0066881	0.74484	0.0060404	0.67270

Fluorine

OKTAVIAN spherical shell experiment

Table 47: MCNP-calculations with FENDL-1, JENDL-FF and JENDL-3.2 data for OKTAVIAN LiF spherical shell experiment (61 cm diameter, wall thickness = 3.5 mfp)
- C. Ichihara, University of Kyoto

Energy [MeV]	Experiment	FENDL-1		JENDL-3.2		JENDL-FF	
10<En<20	1.820×10-1	1.952×10-1	(1.073)	2.062×10-1	(1.133)	2.070×10-1	(1.137)
5<En<10	6.674×10-2	5.568×10-2	(0.834)	6.223×10-2	(0.932)	6.472×10-2	(0.970)
1<En<5	1.726×10-1	1.479×10-1	(0.857)	1.480×10-1	(0.857)	1.482×10-1	(0.859)
0.1<En<1	2.053×10-1	1.394×10-1	(0.679)	1.225×10-1	(0.597)	1.211×10-1	(0.590)
total	0.626	0.538	(0.859)	0.539	(0.861)	0.541	(0.864)

Table 48: MCNP-calculations with FENDL-1, JENDL-FF and JENDL-3.2 data for OKTAVIAN CF_2 spherical shell experiment (40 cm diameter, wall thickness = 0.7 mfp)
- C. Ichihara, University of Kyoto

Energy [MeV]	Experiment	FENDL-1		JENDL-3.2		JENDL-FF	
10<En<20	9.007×10-1	6.856×10-1	(0.761)	6.907×10-1	(0.767)	6.913×10-1	(0.768)
5<En<10	1.082×10-1	6.577×10-2	(0.606)	5.892×10-2	(0.545)	6.000×10-2	(0.555)
1<En<5	2.265×10-1	1.398×10-1	(0.617)	1.416×10-1	(0.625)	1.414×10-1	(0.624)
0.1<En<1	1.029×10-1	6.642×10-2	(0.645)	6.288×10-2	(0.888)	6.226×10-2	(0.605)
total	1.338	0.957	(0.715)	0.955	(0.714)	0.955	(0.714)

Cobalt

OKTAVIAN spherical shell experiment

Table 49: MCNP-calculations with FENDL-1, JENDL-FF and JENDL-3.2 data for OKTAVIAN Co spherical shell experiment (40 cm diameter, wall thickness = 0.5 mfp)
- C. Ichihara, University of Kyoto

Energy [MeV]	Experiment	FENDL-1		JENDL-3.2		JENDL-FF	
10<En<20	7.285×10-1	7.153×10-1	(0.981)	7.128×10-1	(0.978)	7.035×10-1	(0.966)
5<En<10	5.537×10-2	2.936×10-2	(0.530)	3.851×10-2	(0.696)	3.699×10-2	(0.668)
1<En<5	2.957×10-1	1.921×10-1	(0.650)	1.921×10-1	(0.650)	2.002×10-1	(0.667)
0.1<En<1	2.420×10-1	1.646×10-1	(0.680)	1.571×10-1	(0.677)	1.640×10-1	(0.678)
total	1.322	1.101	(0.838)	1.100	(0.832)	1.105	(0.836)

Niobium

OKTAVIAN spherical shell experiment

Table 50: MCNP-calculations with FENDL-1, JENDL-FF and JENDL-3.2 data for OKTAVIAN Nb spherical shell experiment (28 cm diameter, wall thickness = 1.1 mfp)
- C. Ichihara, University of Kyoto

28 cm diameter, wall thickness = 1.1 mfp

Energy [MeV]	Experiment	FENDL-1		JENDL-3.2		JENDL-FF	
10<En<20	5.096×10-1	5.288×10-1	(1.038)	5.298×10-1	(1.039)	5.297×10-1	(1.039)
5<En<10	3.548×10-2	3.937×10-2	(1.110)	3.301×10-2	(0.930)	3.385×10-2	(0.954)
1<En<5	2.193×10-1	2.729×10-1	(1.244)	2.269×10-1	(1.035)	2.283×10-1	(1.041)
0.1<En<1	3.350×10-1	4.168×10-1	(1.244)	4.490×10-1	(1.420)	4.523×10-1	(1.350)
total	1.099	1.258	(1.145)	1.239	(1.127)	1.244	(1.132)

Molybdenum

OKTAVIAN spherical shell experiment

Table 51: MCNP-calculations with FENDL-1, JENDL-FF and JENDL-3.2 data for OKTAVIAN Mo spherical shell experiment (61 cm diameter, wall thickness = 1.5 mfp)
- C. Ichihara, University of Kyoto

Energy [MeV]	Experiment	FENDL-1		JENDL-3.2		JENDL-FF	
10<En<20	5.242×10-1	4.682×10-1	(0.893)	4.491×10-1	(0.857)	4.499×10-1	(0.858)
5<En<10	4.262×10-2	3.022×10-2	(0.709)	3.559×10-2	(0.835)	3.643×10-2	(0.855)
1<En<5	2.871×10-1	2.853×10-1	(0.994)	2.636×10-1	(0.918)	2.647×10-1	(0.922)
0.1<En<1	5.161×10-1	4.786×10-1	(0.927)	4.831×10-1	(0.986)	4.811×10-1	(0.932)
total	1.370	1.262	(0.921)	1.231	(0.899)	1.233	(0.900)

Titanium

OKTAVIAN spherical shell experiment

Table 52: MCNP-calculations with FENDL-1, JENDL-FF and JENDL-3.2 data for OKTAVIAN Ti spherical shell experiment (40 cm diameter, wall thickness = 0.5 mfp)
- C. Ichihara, University of Kyoto

Energy [MeV]	Experiment	FENDL-1		JENDL-3.2		JENDL-FF	
10<En<20	5.980×10-1	7.048×10-1	(1.179)	7.090×10-1	(1.186)	7.097×10-1	(1.186)
5<En<10	3.838×10-2	3.725×10-2	(0.971)	3.862×10-2	(1.006)	3.928×10-2	(1.023)
1<En<5	1.515×10-1	2.086×10-1	(1.377)	1.758×10-1	(1.160)	1.748×10-1	(1.154)
0.1<En<1	8.610×10-2	1.212×10-1	(1.408)	1.343×10-1	(1.560)	1.345×10-1	(1.562)
total	0.875	1.072	(1.225)	1.058	(1.209)	1.058	(1.209)

Gamma leakage spectra

OKTAVIAN spherical shell experiments

Table 53: MCNP-calculations with FENDL-1 and JENDL-3.2 data for Integrated gamma-ray leakage spectra measured in OKTAVIAN spherical shells experiments
- F. Maekawa, Y. Oyama - FNS/JAERI

	Energy	Experiment	JENDL-3.2 Calculation	FENDL-1 Calculation	JENDL-3.2 C/E	FENDL-1 C/E
LiF	0.5 -6.5	3.9980e-01	4.1267e-01	4.0560e-01	1.0322	1.0145
CF2	0.5 -6.5	4.5959e-01	5.0901e-01	4.9837e-01	1.1075	1.0844
Al	0.5 -20.	9.9880e-01	1.0846e+00	1.0186e+00	1.0859	1.0198
Si	0.5 -20.	1.4162e+00	1.2248e+00		0.8648	
Ti	0.5 -20.	1.0819e+00	1.1082e+00	1.0512e+00	1.0243	0.9716
Cr	0.5 -20.	8.8791e-01	1.0354e+00	1.0513e+00	1.1661	1.1840
Mn	0.7 -20.	4.4030e-01	3.6623e-01	3.5023e-01	0.8318	0.7954
Co	0.5 -20.	6.5802e-01	6.1998e-01	5.2702e-01	0.9422	0.8009
Cu	0.5 -20.	1.9177e-01	1.7559e-01	1.8453e-01	0.9156	0.9622
Nb	0.7 -5.	6.0406e-01	5.1170e-01	4.5635e-01	0.8471	0.7555
Mo	0.5 -20.	6.4877e-01	7.1733e-01	7.2016e-01	1.1057	1.1100
W	0.5 -5.	3.2024e-01	3.4798e-01	3.2490e-01	1.0866	1.0146
Pb	0.5 -20.	1.6182e-01	1.3635e-01	1.5022e-01	0.8426	0.9283

IX. Figures

- List of figures -

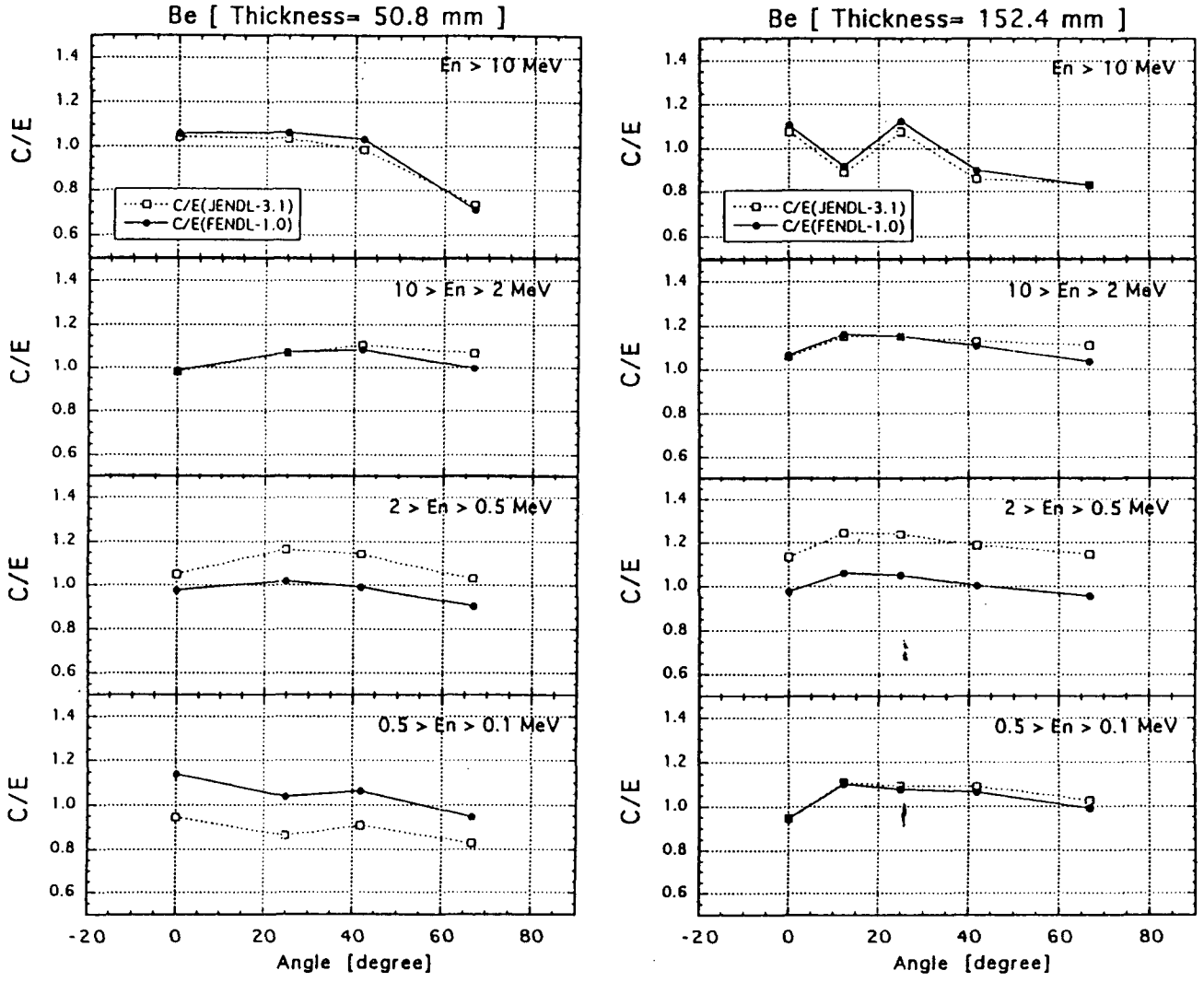

Fig. 1: MCNP-calculations with FENDL-1 and JENDL-3.1 data for FNS cylindrical slabs - Y. Oyama, M. Wada -FNS/JAERI

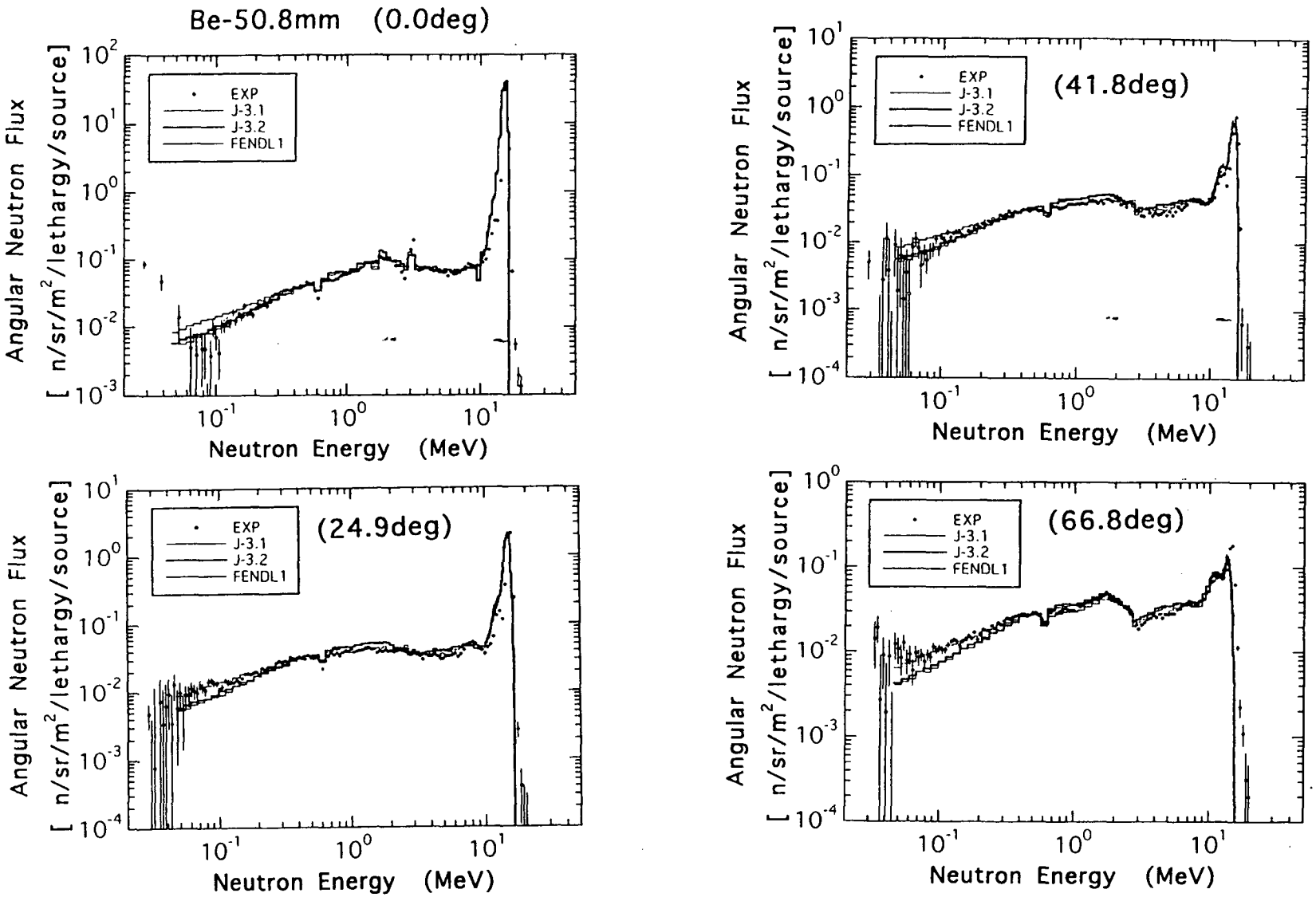

Fig. 2 : MCNP-calculations with FENDL-1 and JENDL-3.1 data for FNS cylindrical slabs - Y. Oyama, M. Wada -FNS/JAERI

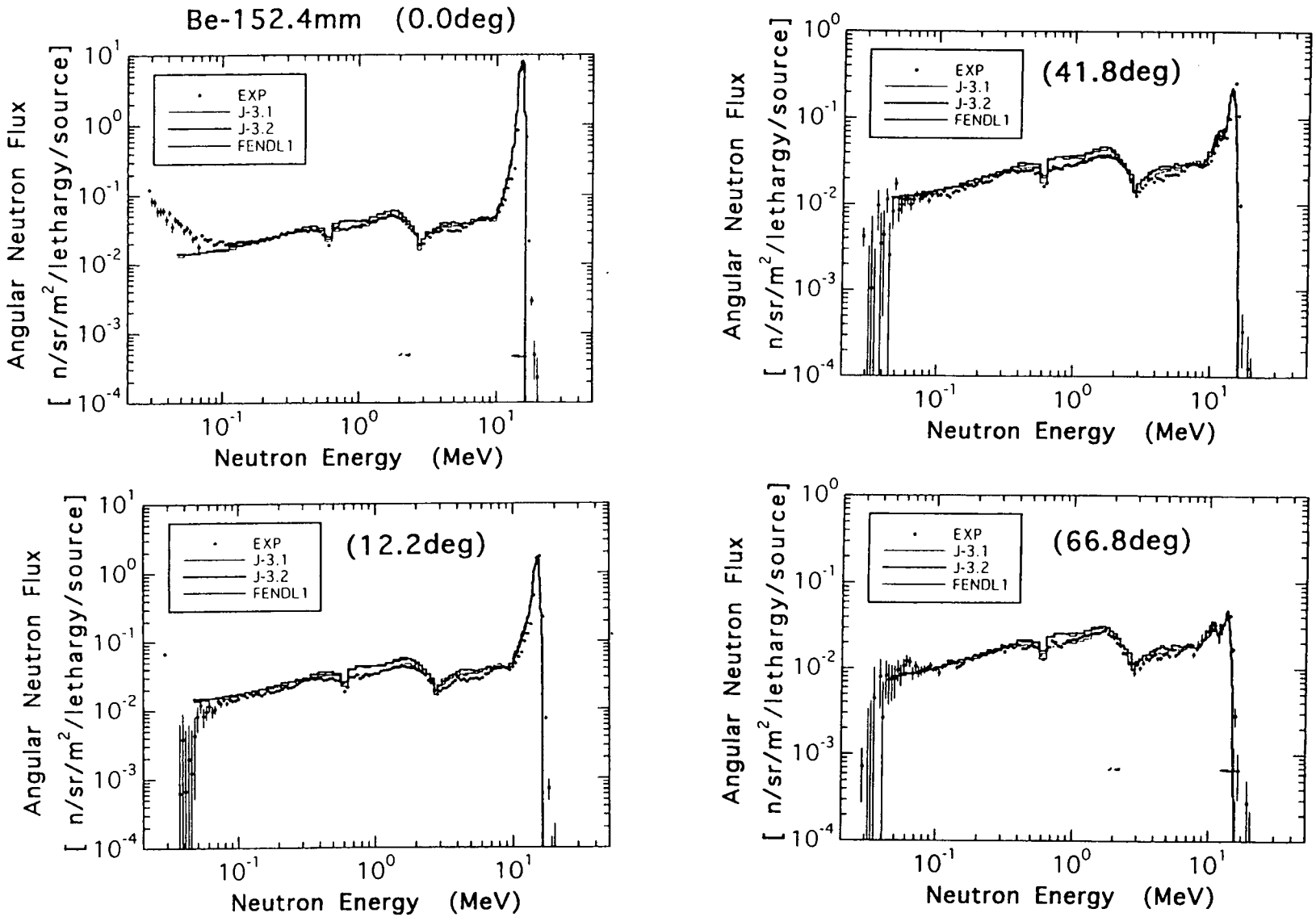

Fig. 3: MCNP-calculations with FENDL-1 and JENDL-3.1 data for FNS cylindrical slabs - Y. Oyama, M. Wada -FNS/JAERI

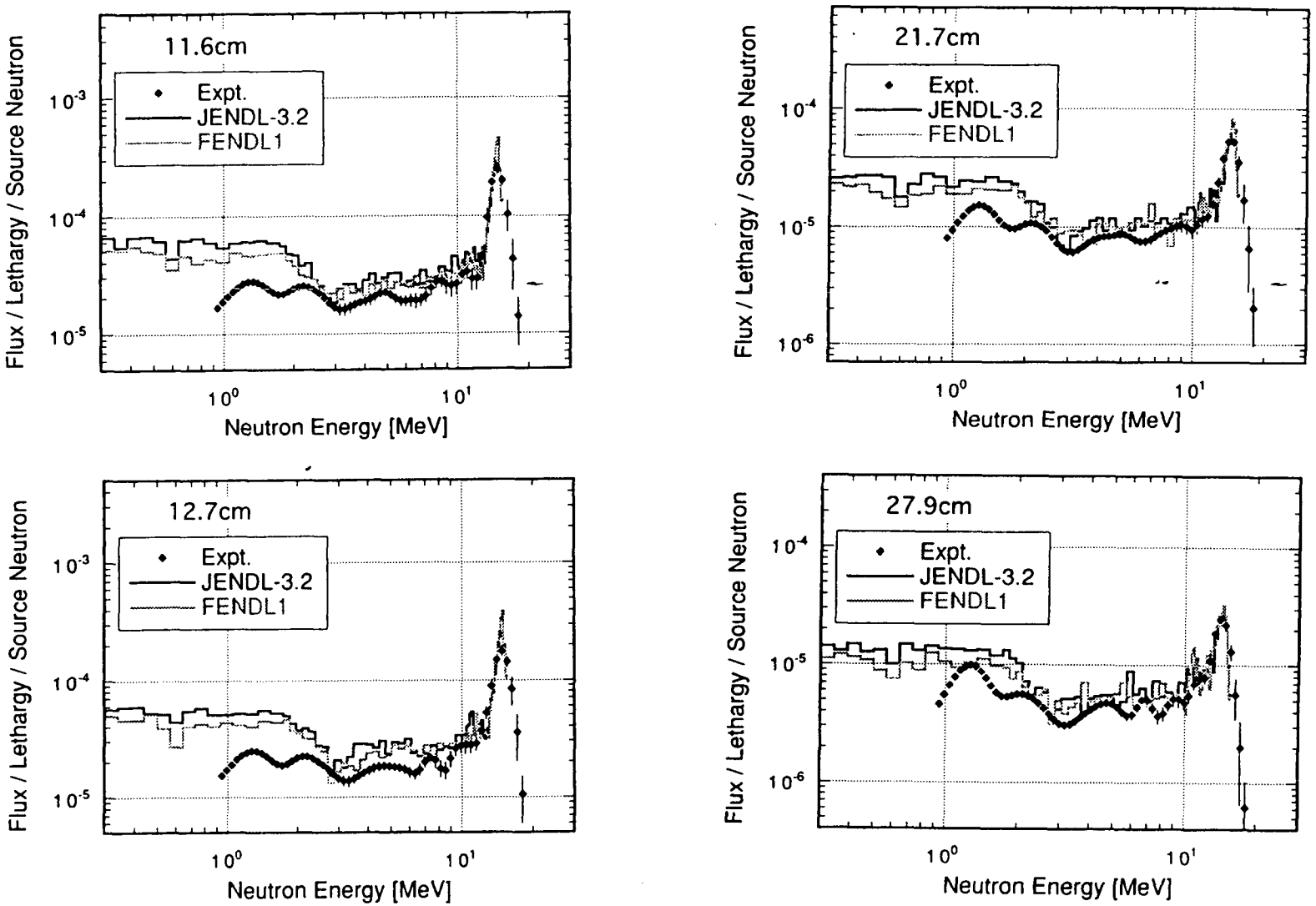

Fig. 4: MCNP-calculations with FENDL-1 and JENDL-3.2 data for reactions rates inside FNS cylindrical slabs
- F. Maekawa, M. Wada, Y. Oyama -FNS/JAERI

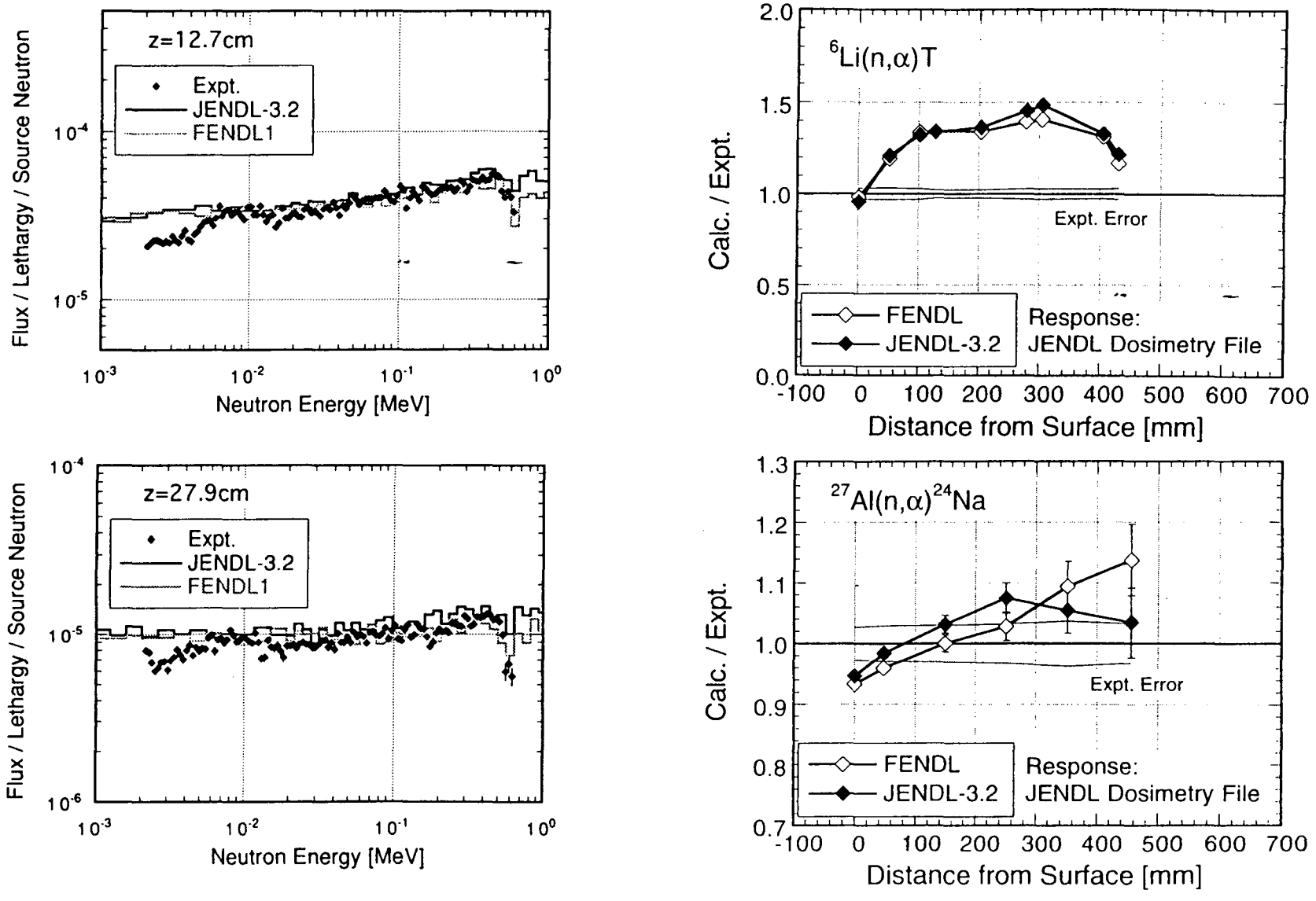

Fig. 5: MCNP-calculations with FENDL-1 and JENDL-3.2 data for reactions rates inside FNS cylindrical slabs
- F. Maekawa, M. Wada, Y. Oyama -FNS/JAERI

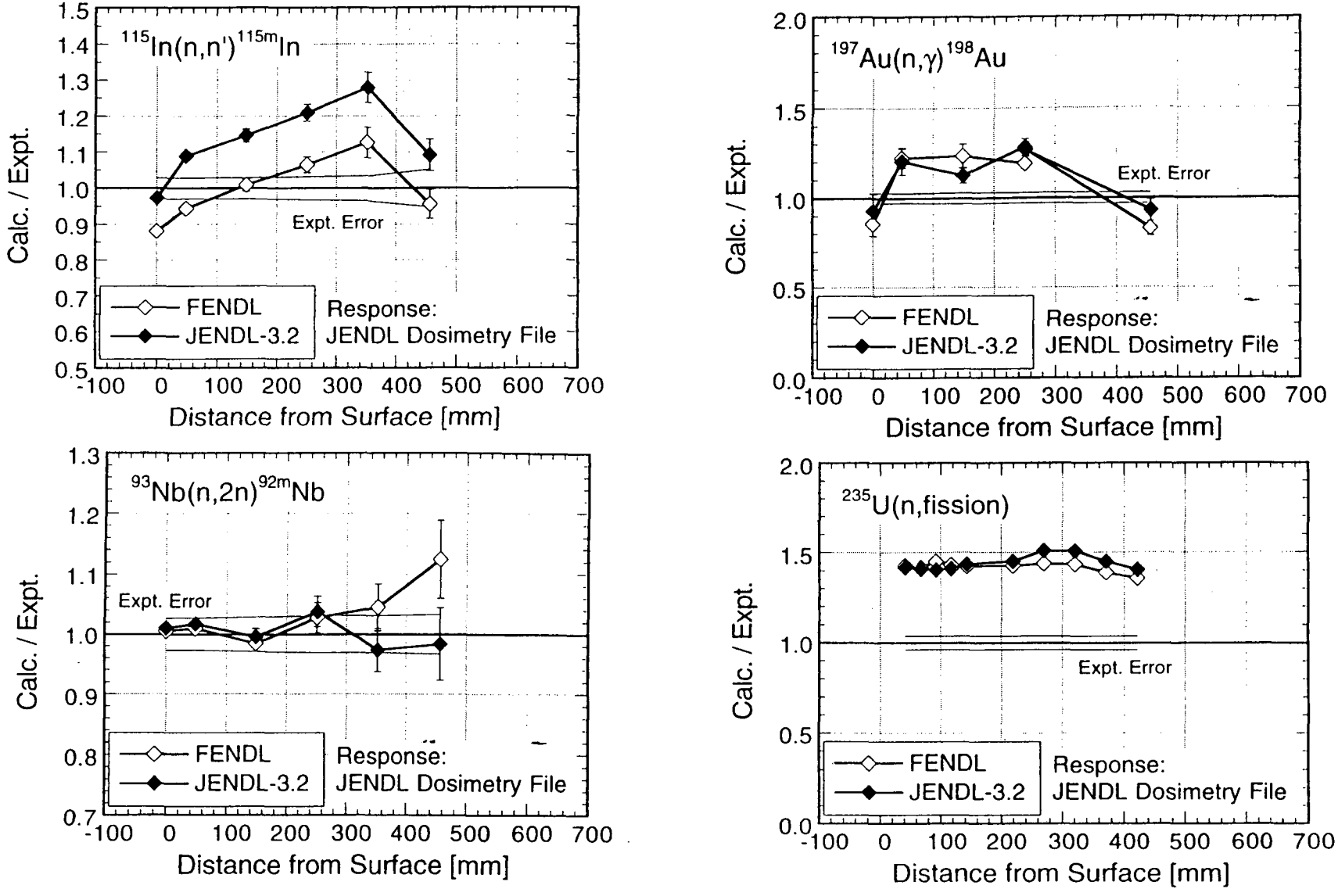

Fig. 6: MCNP-calculations with FENDL-1 and JENDL-3.2 data for reactions rates inside FNS cylindrical slabs
- F. Maekawa, M. Wada, Y. Oyama -FNS/JAERI

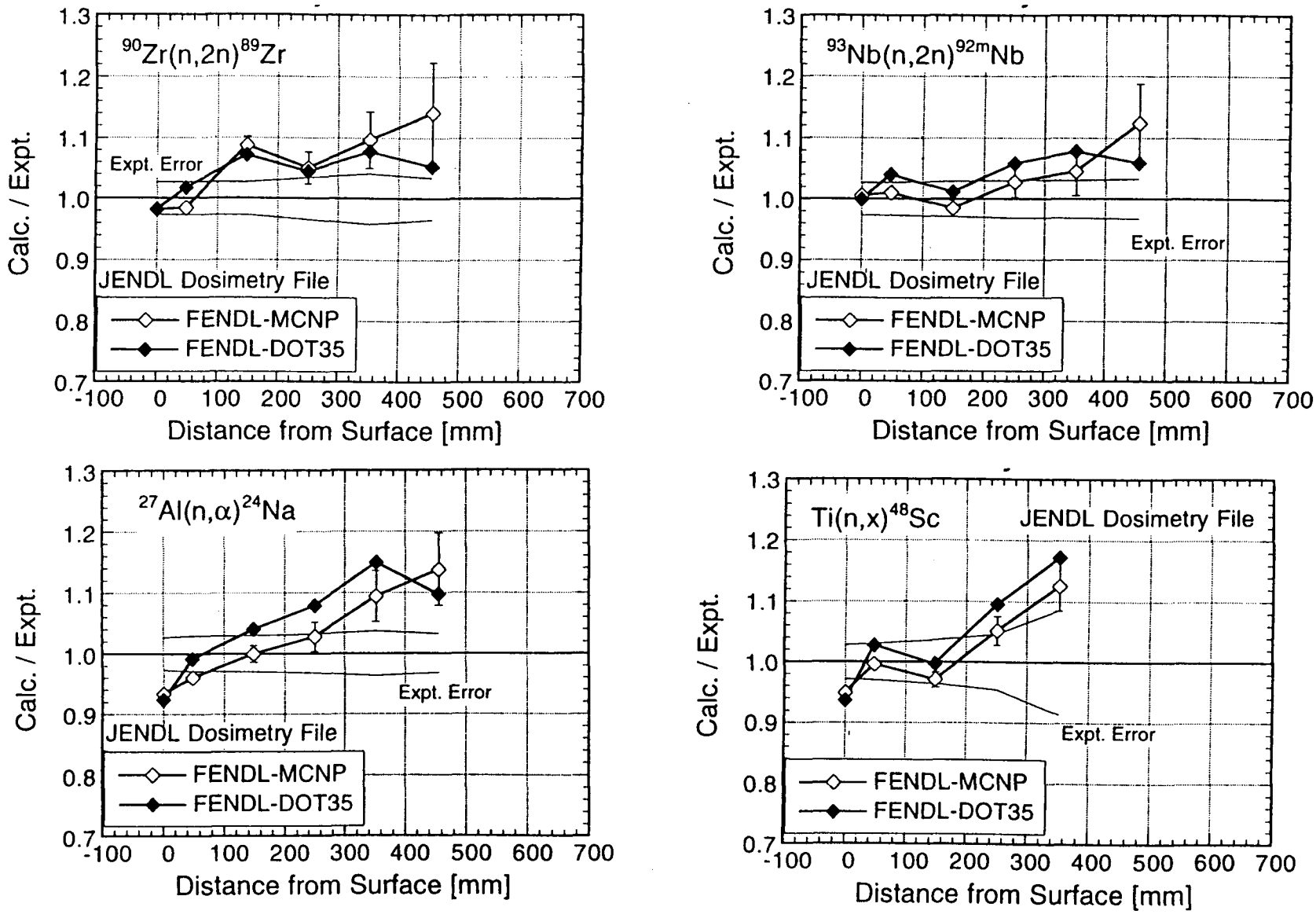

Fig. 7: MCNP- and DOT-calculations with FENDL-1 and JENDL-3.2 data for reactions rates inside FNS cylindrical slabs
- K. Hayashi - Hitachi Eng., Y. Oyama -FNS/JAERI

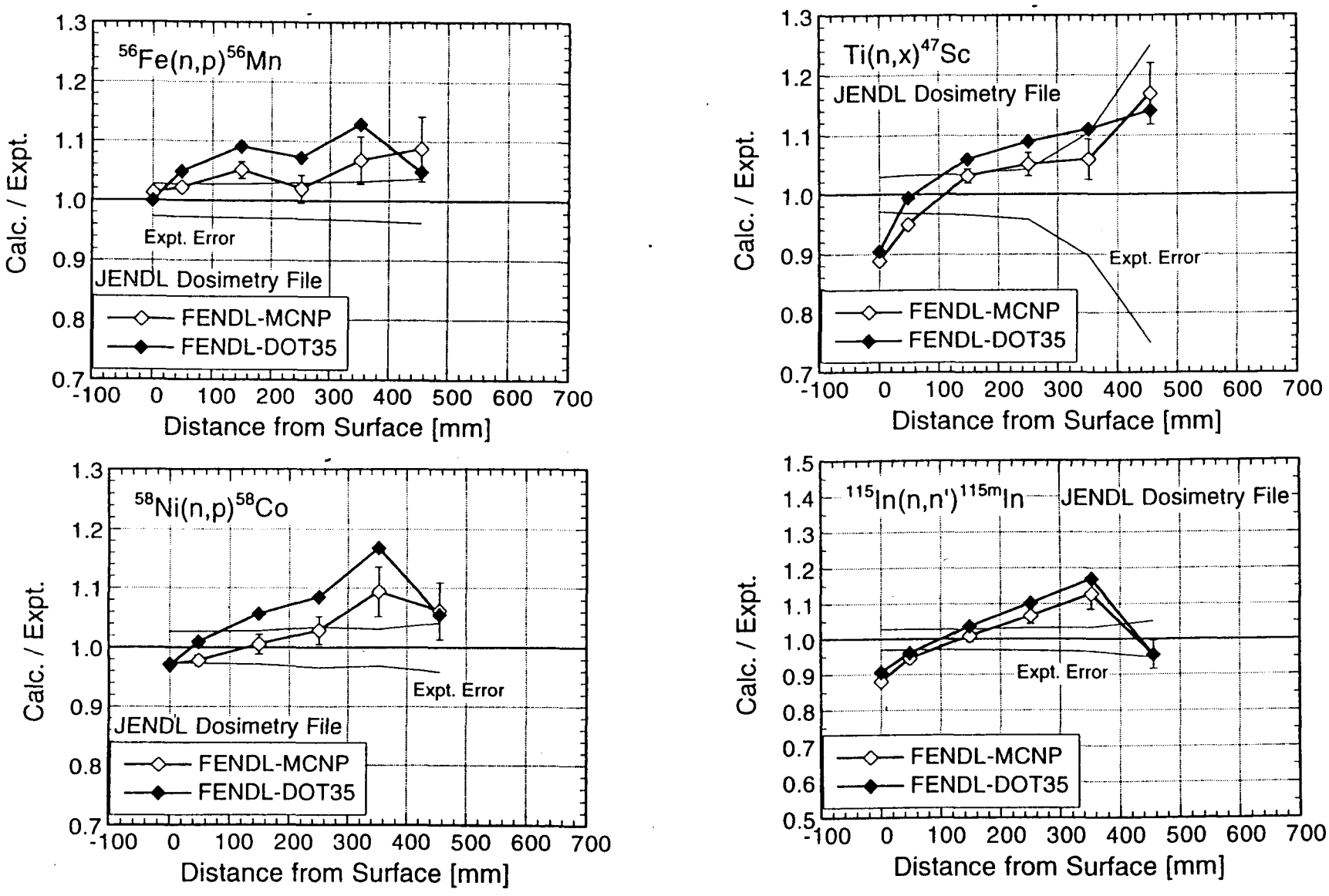

Fig. 8: MCNP- and DOT-calculations with FENDL-1 and JENDL-3.2 data for reactions rates inside FNS cylindrical slabs
- K. Hayashi - Hitachi Eng., Y. Oyama -FNS/JAERI

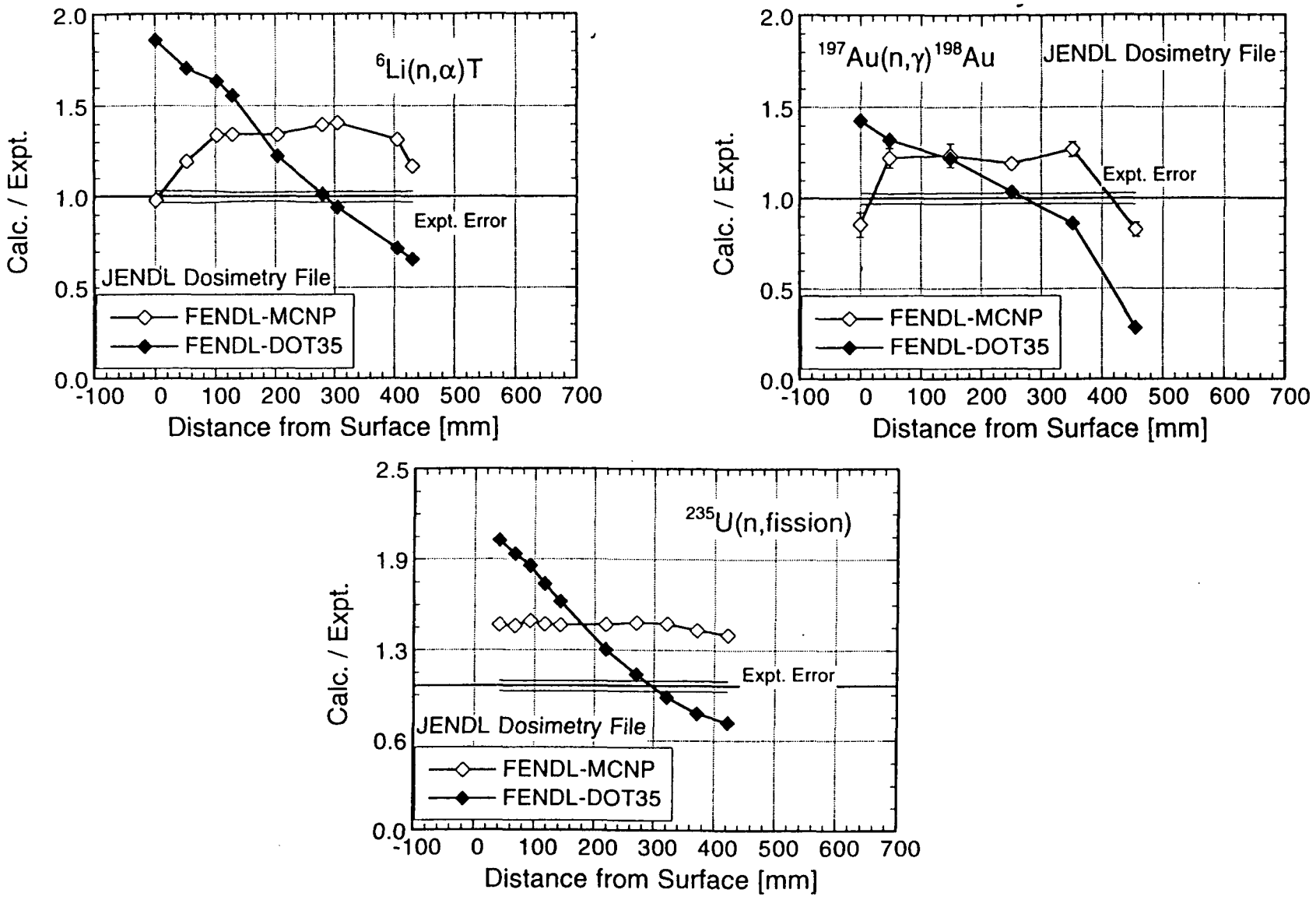

Fig. 9: MCNP- and DOT-calculations with FENDL-1 and JENDL-3.2 data for reactions rates inside FNS cylindrical slabs
- K. Hayashi - Hitachi Eng., Y. Oyama -FNS/JAERI

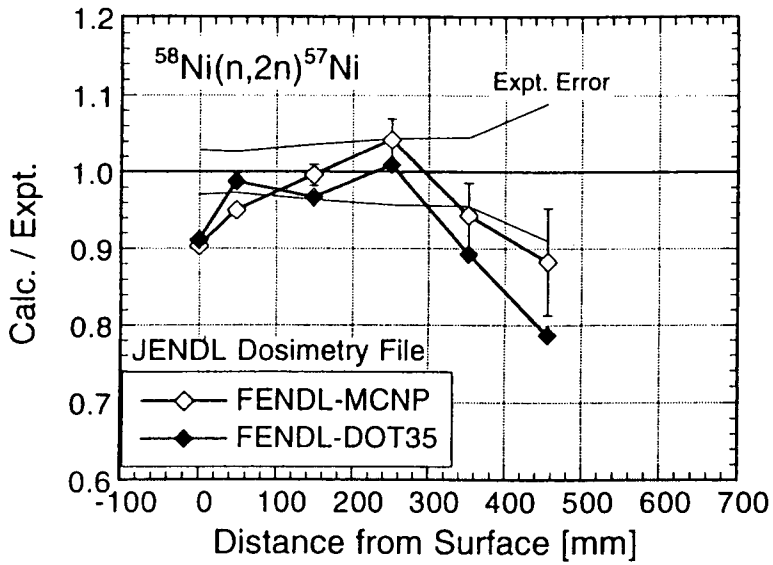

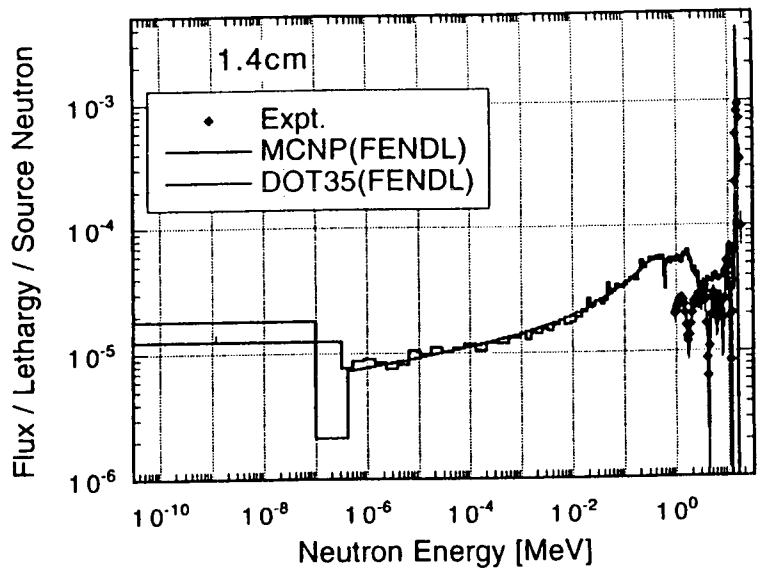

Fig. 10: MCNP- and DOT-calculations with FENDL-1 and JENDL-3.2 data for reactions rates inside FNS cylindrical slabs - K. Hayashi - Hitachi Eng., Y. Oyama -FNS/JAERI

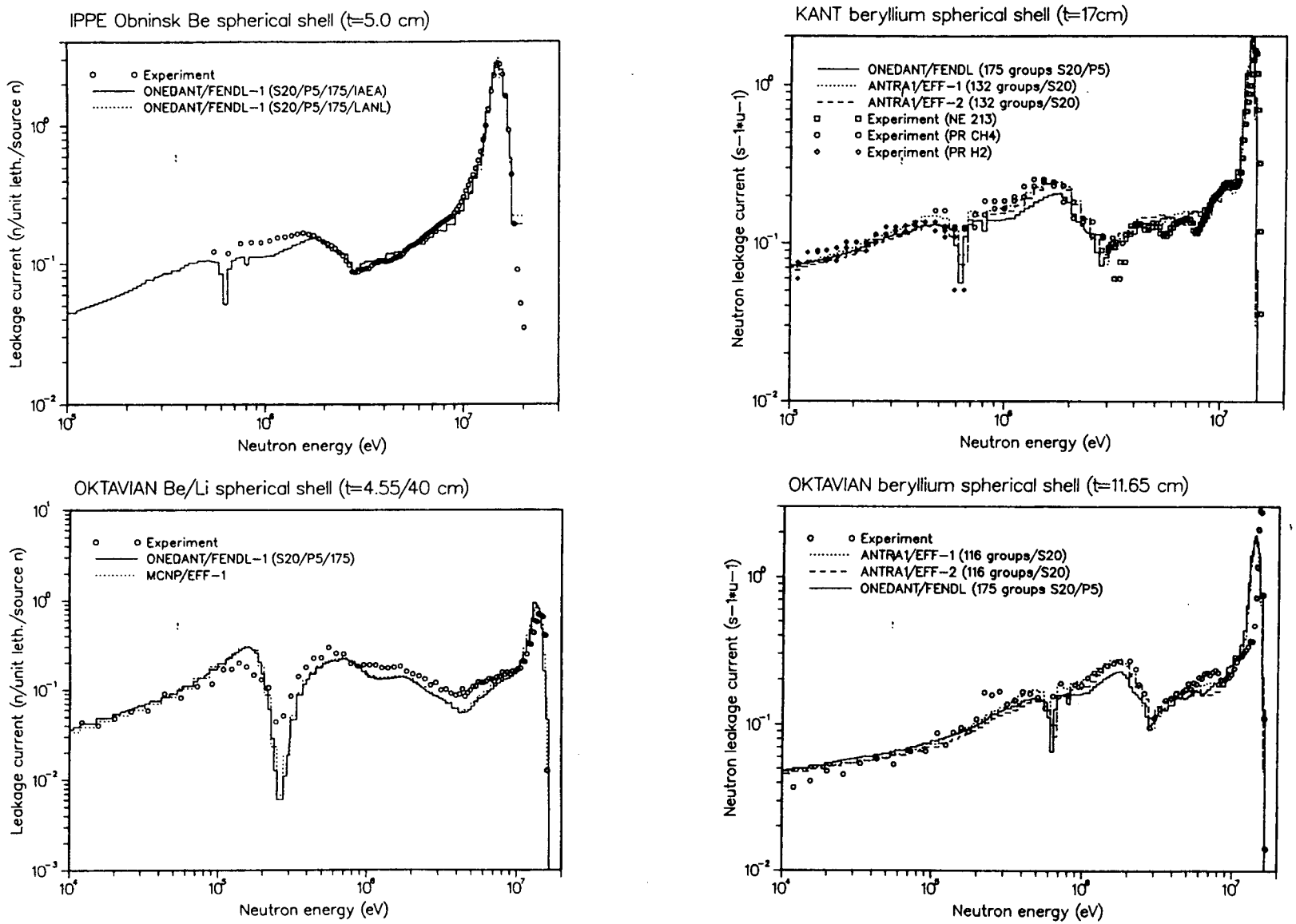

Fig. 11: ONEDANT -, ANTRA1- and MCNP- calculations with FENDL-1, EFF-1 and -2 data beryllium spherical shell experiments
- U. Fischer, E. Wiegner, F. Kappler - FZK, Karlsruhe

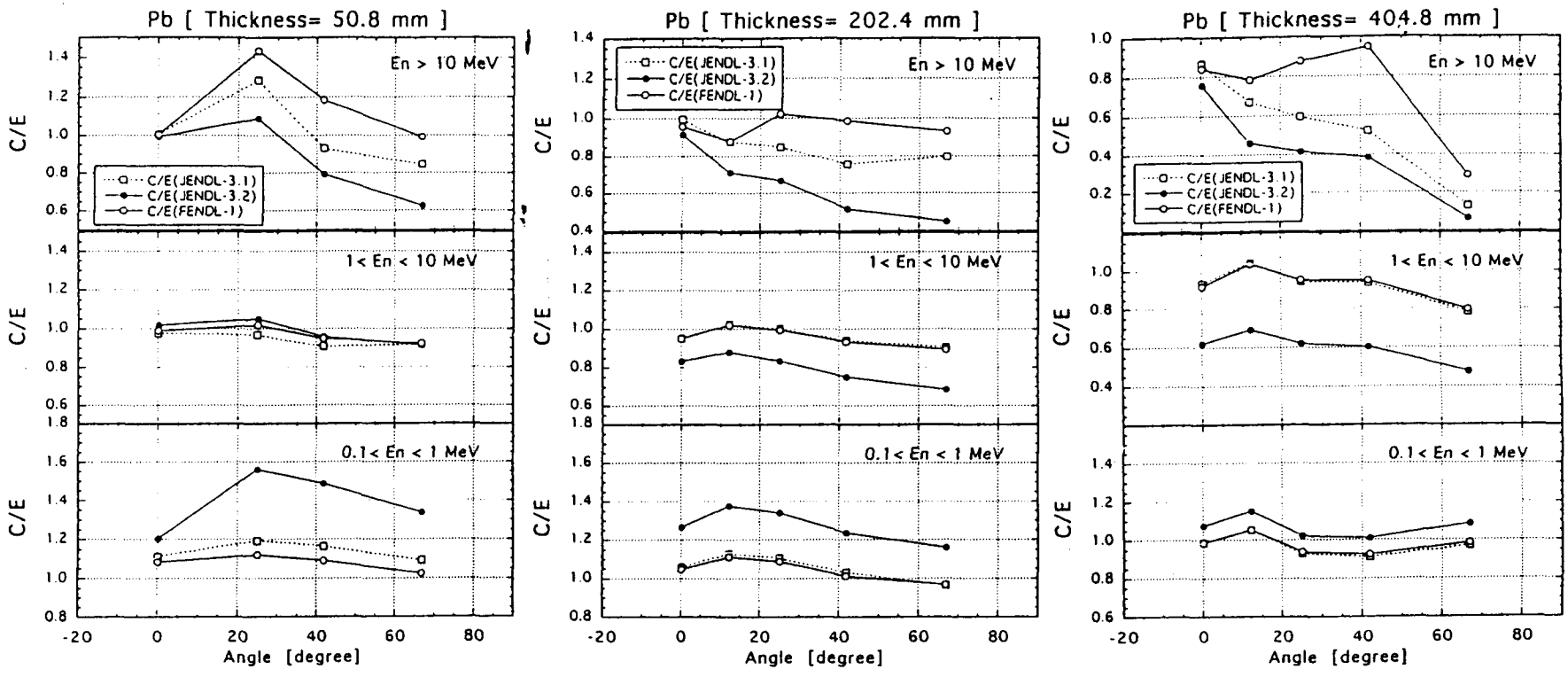

Fig. 12 : MCNP-calculations with FENDL-1 and JENDL-3 data for FNS cylindrical slabs - Y. Oyama, M. Wada -FNS/JAERI

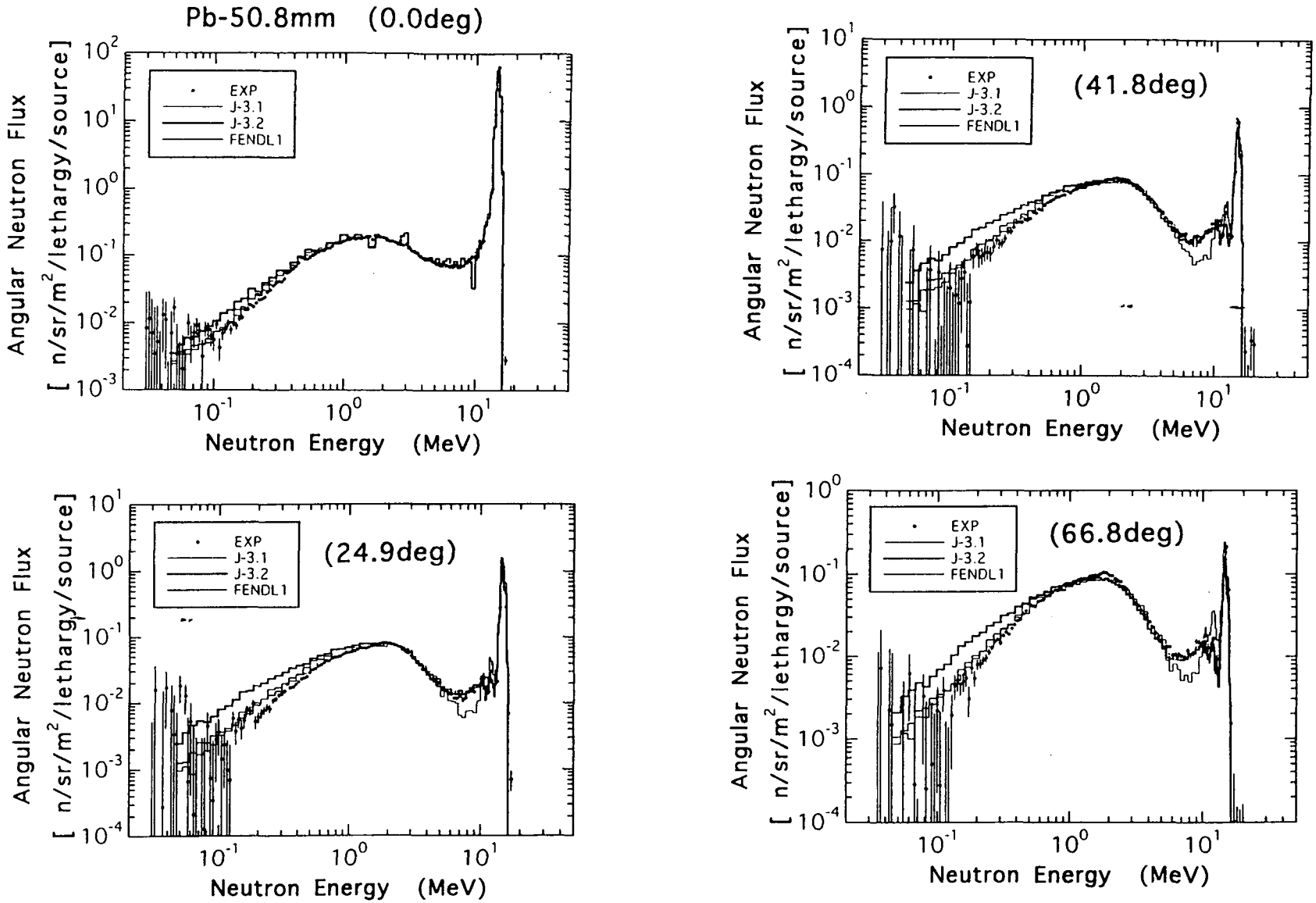

Fig. 13: MCNP-calculations with FENDL-1 and JENDL-3 data for FNS cylindrical slabs - Y. Oyama, M. Wada -FNS/JAERI

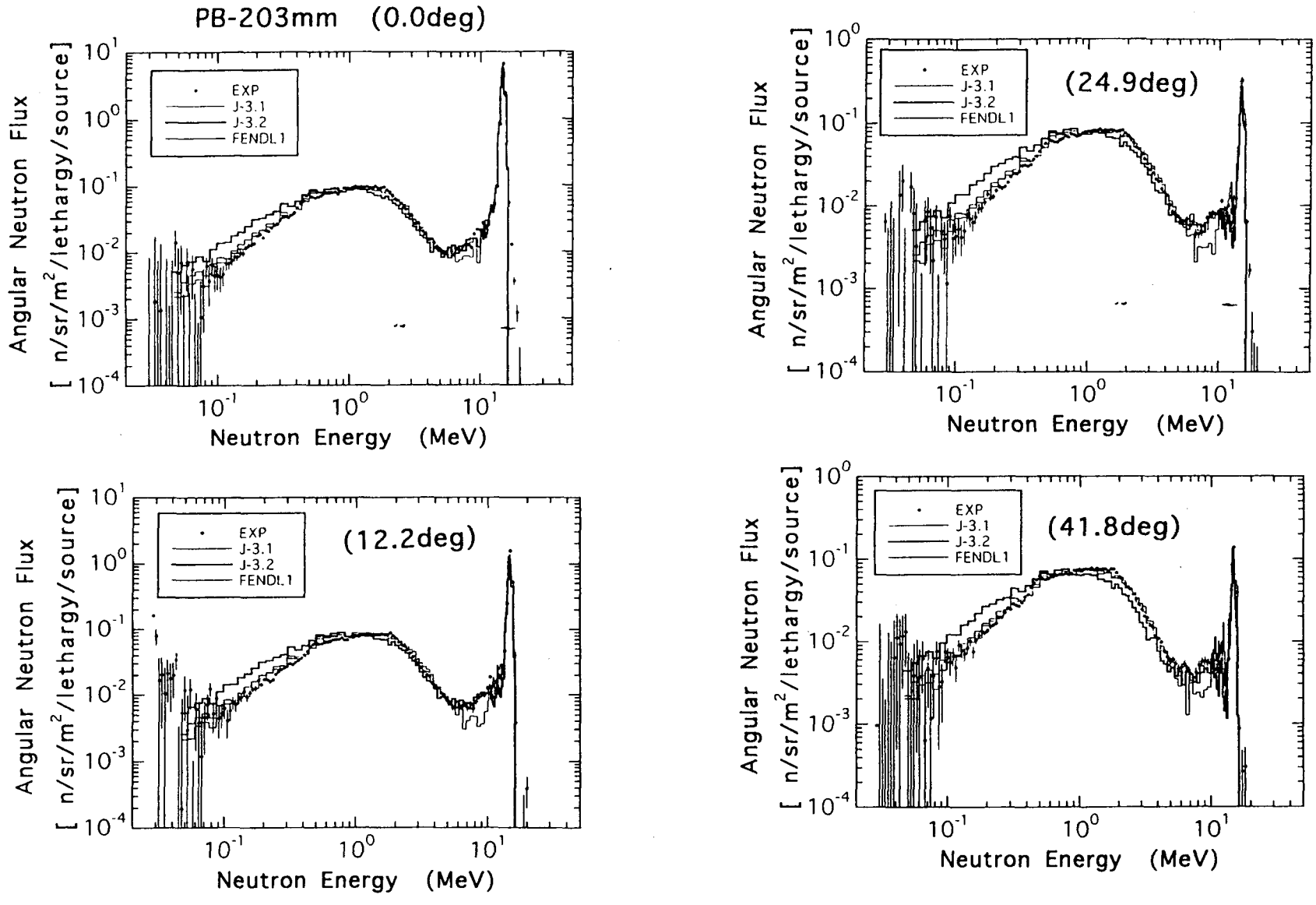

Fig. 14: MCNP-calculations with FENDL-1 and JENDL-3 data for FNS cylindrical slabs - Y. Oyama, M. Wada -FNS/JAERI

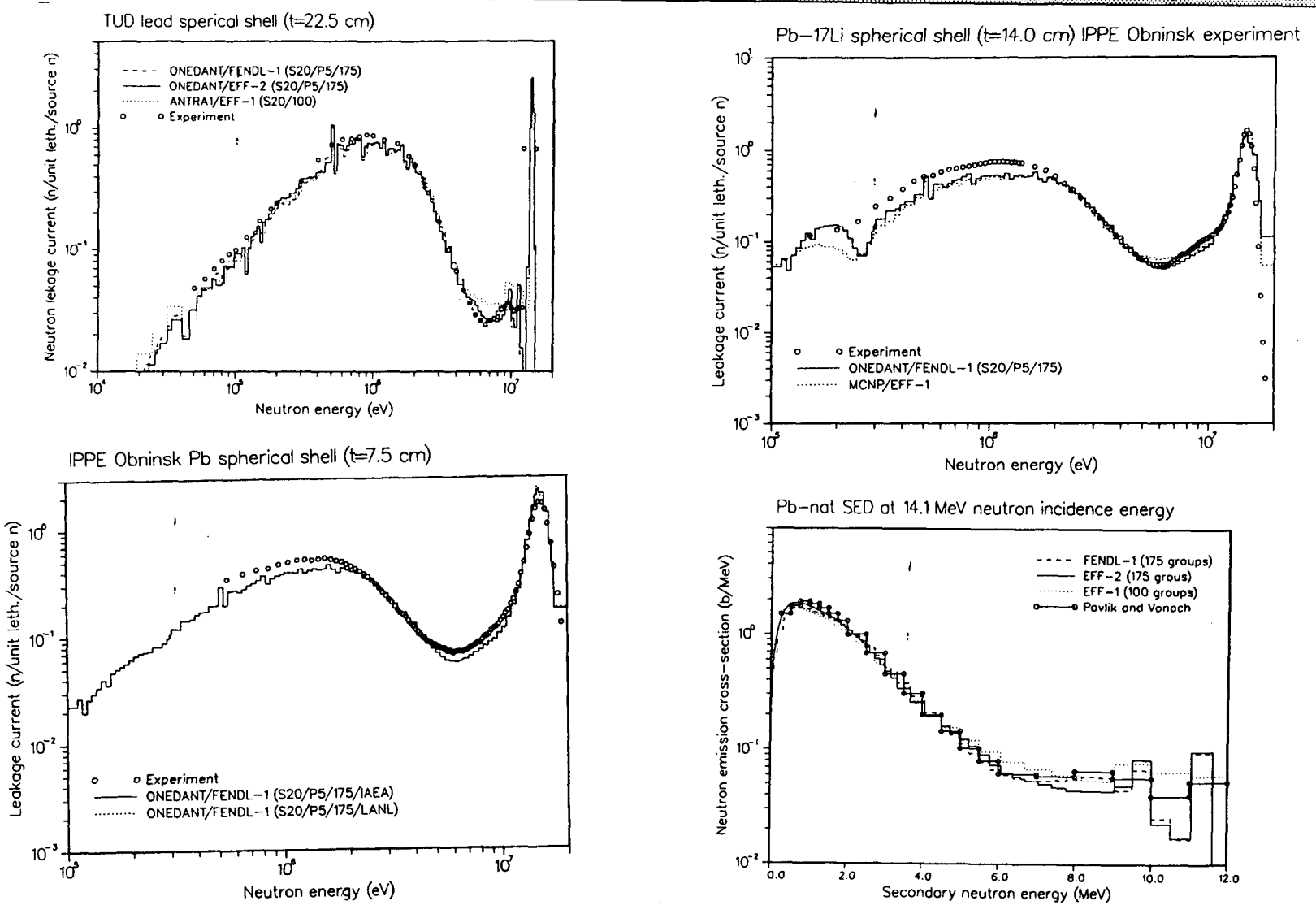

Fig. 15: ONEDANT - and ANTRA1-calculations with FENDL-1, EFF-1 and -2 data for lead spherical shell experiments and Pb(n,xn) secondary energy distribution - U. Fischer, E. Wiegner - FZK, Karlsruhe

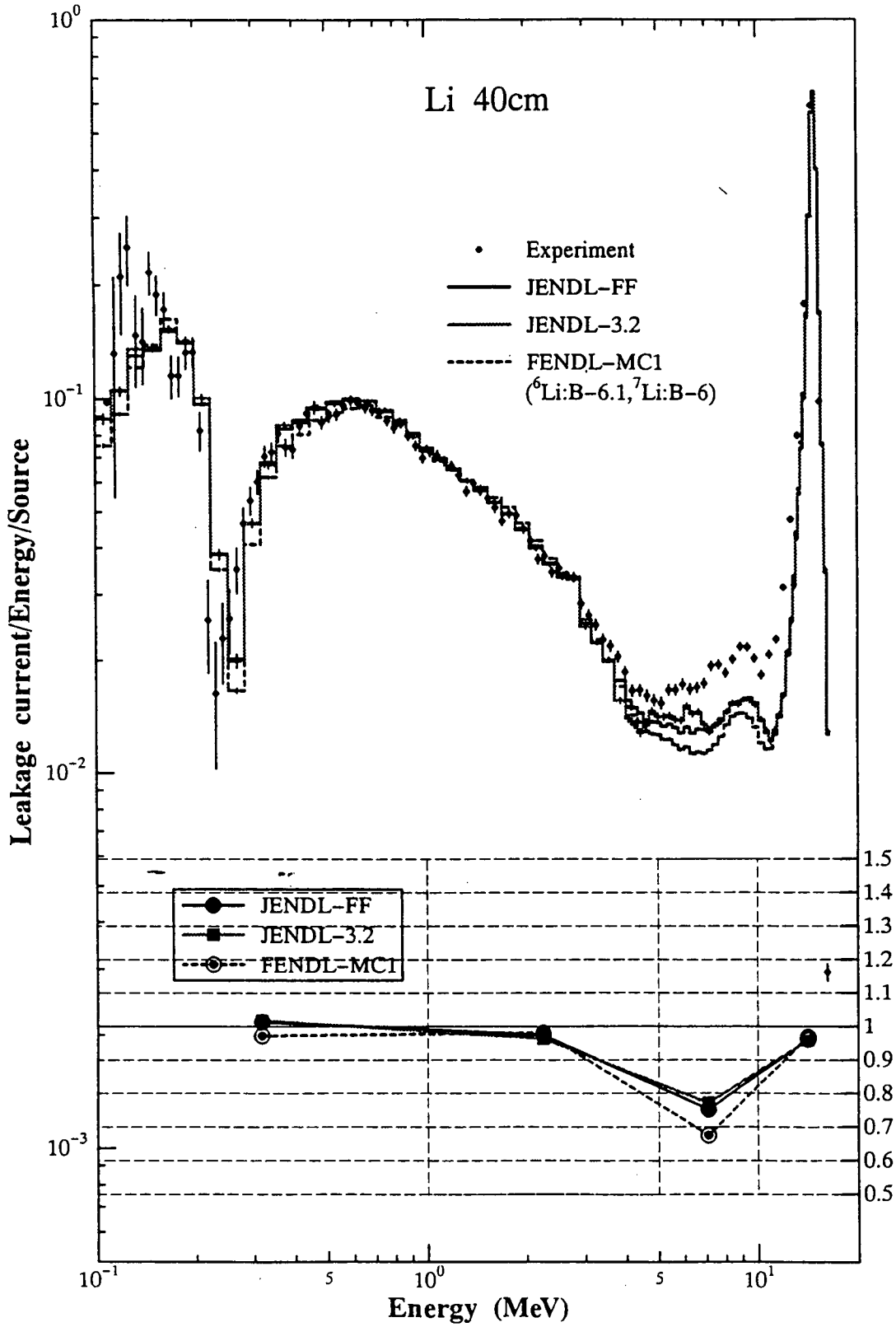

Fig. 16: MCNP -calculations with FENDL-1 and JENDL-3 data for OKTAVIAN lithium spherical shell experiment - C. Ichihara, University of Kyoto

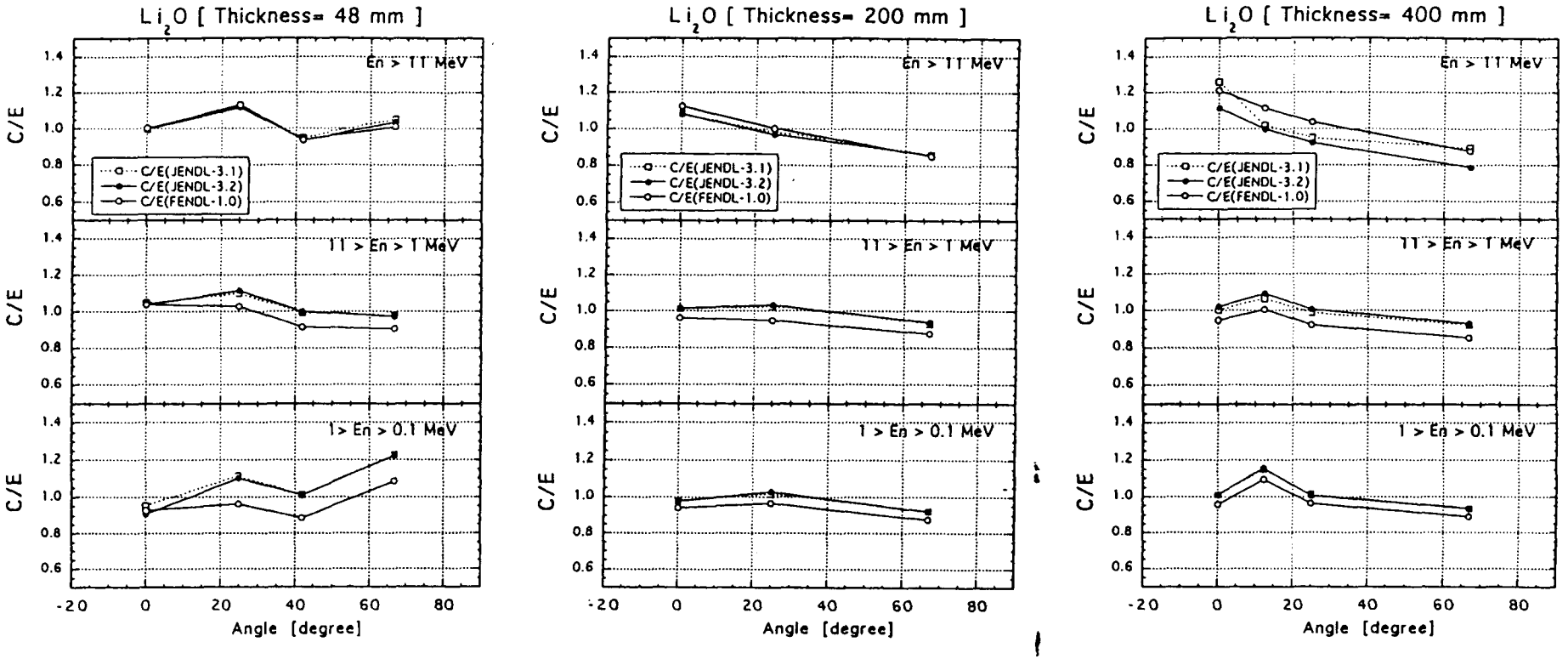

Fig. 17: MCNP-calculations with FENDL-1 and JENDL-3 data for FNS Li_2O cylindrical slabs - Y. Oyama, M. Wada -FNS/JAERI

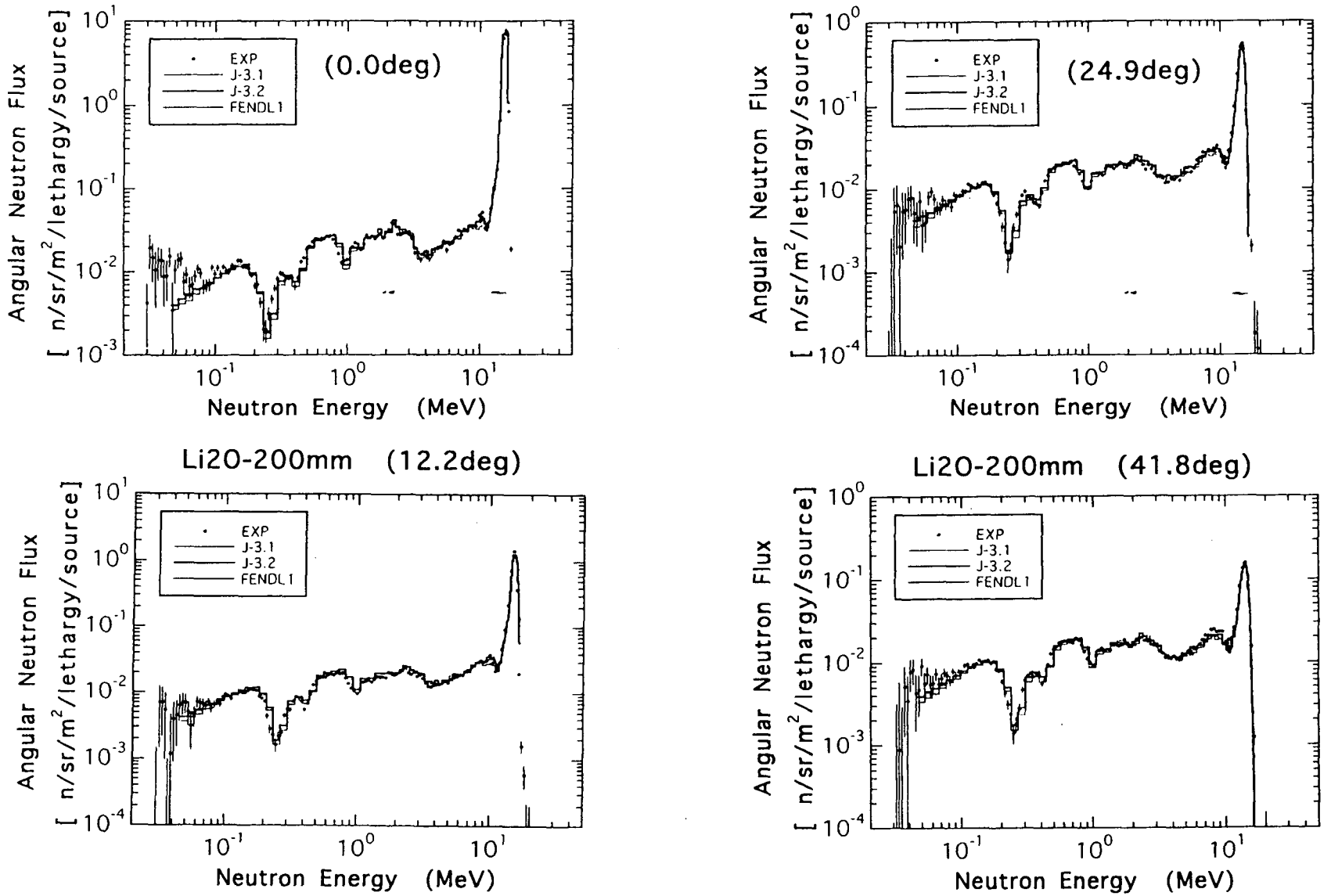

Fig. 18: MCNP-calculations with FENDL-1 and JENDL-3 data for FNS Li_2O cylindrical slabs - Y. Oyama, M. Wada -FNS/JAERI

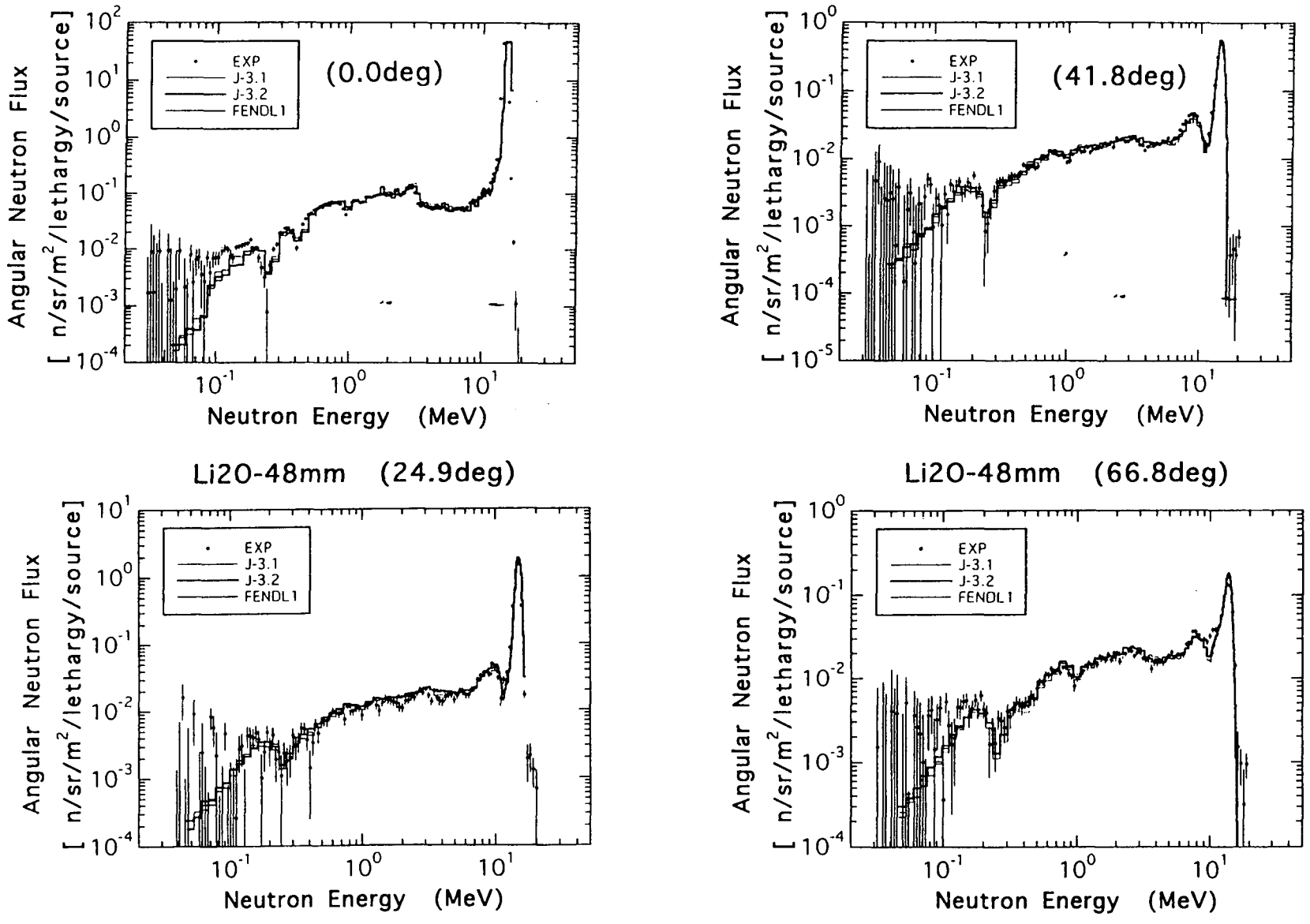

Fig. 19: MCNP-calculations with FENDL-1 and JENDL-3 data for FNS Li_2O cylindrical slabs - Y. Oyama, M. Wada -FNS/JAERI

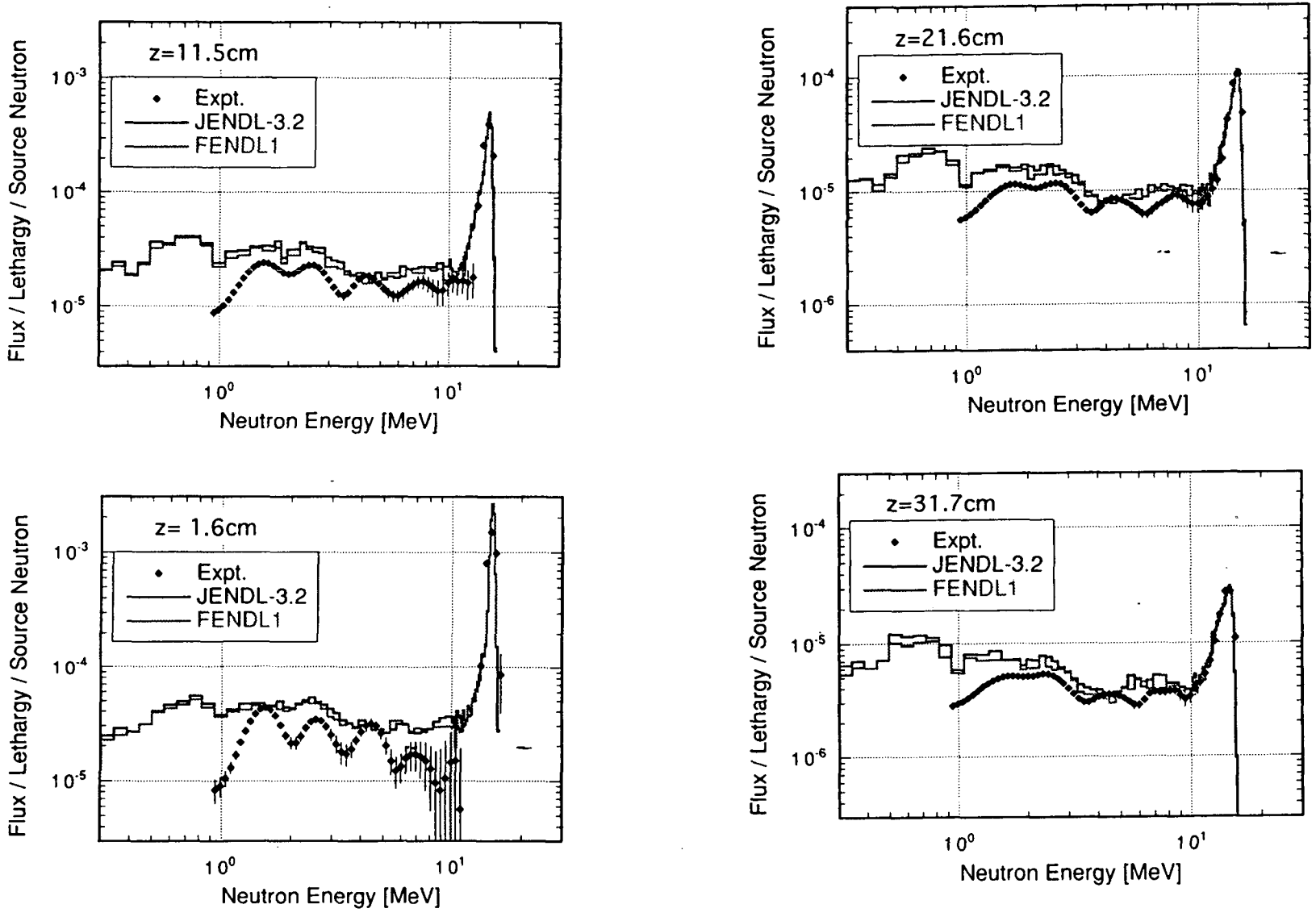

Fig. 20: MCNP-calculations with FENDL-1 and JENDL-3.2 data for neutron spectra inside Li_2O cylindrical slabs
- Y. Oyama, M. Wada -FNS/JAERI

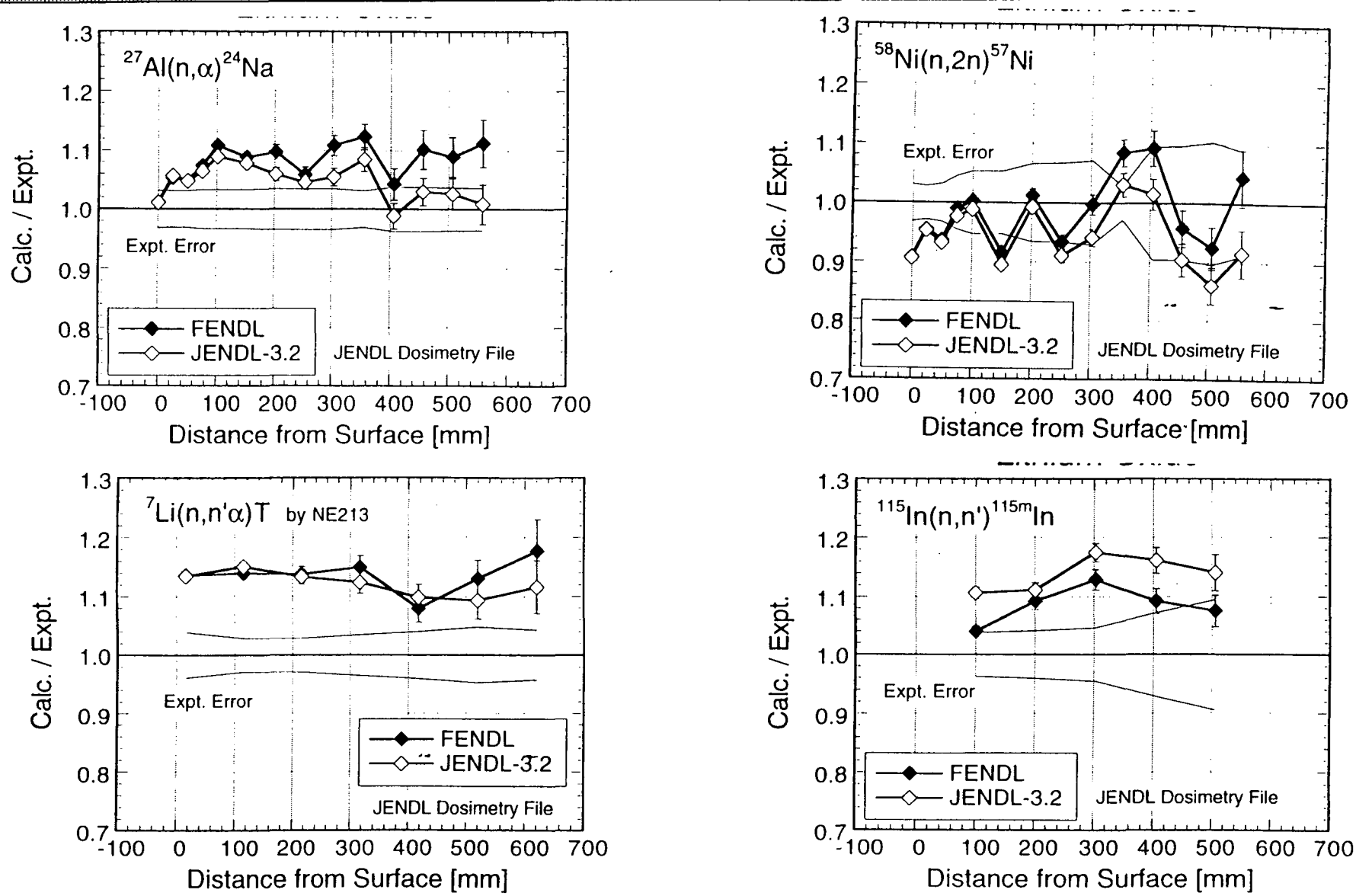

Fig. 21: MCNP-calculations with FENDL-1 and JENDL-3.2 data for reaction rates inside Li_2O cylindrical slabs
- Y. Oyama, M. Wada -FNS/JAERI

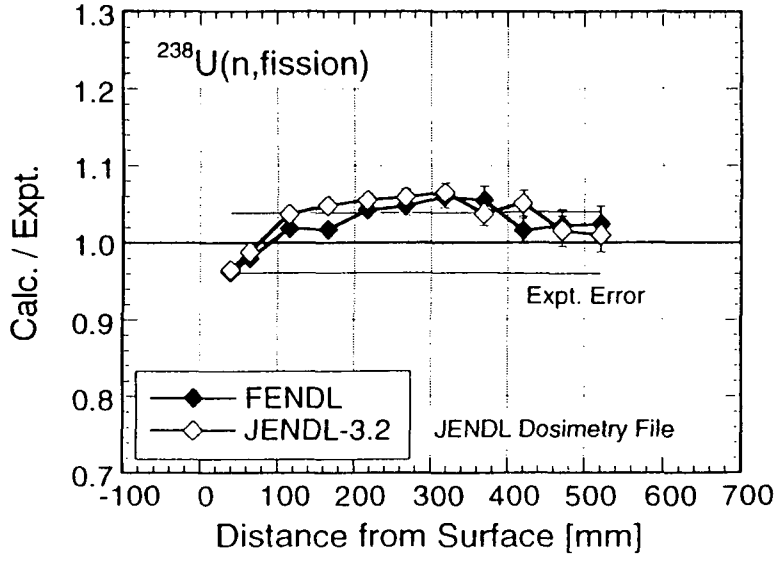

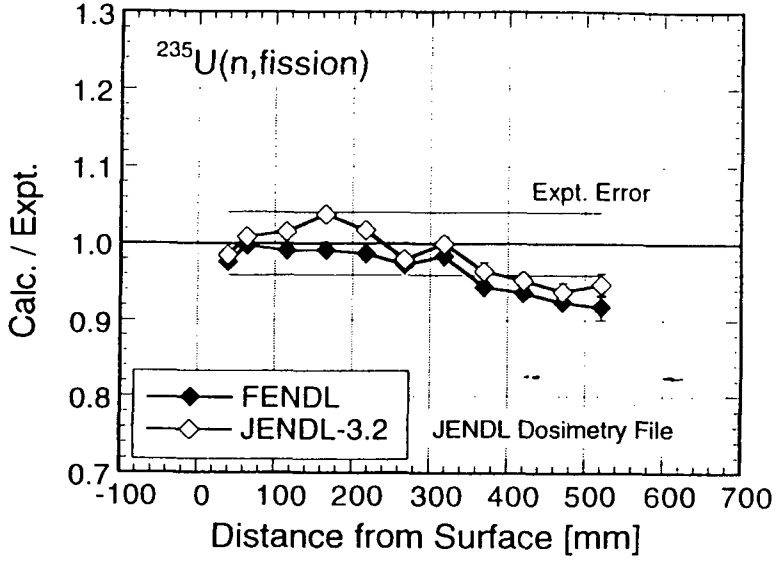

Fig. 22: MCNP-calculations with FENDL-1 and JENDL-3.2 data for reaction rates inside Li_2O cylindrical slabs
- Y. Oyama, M. Wada -FNS/JAERI

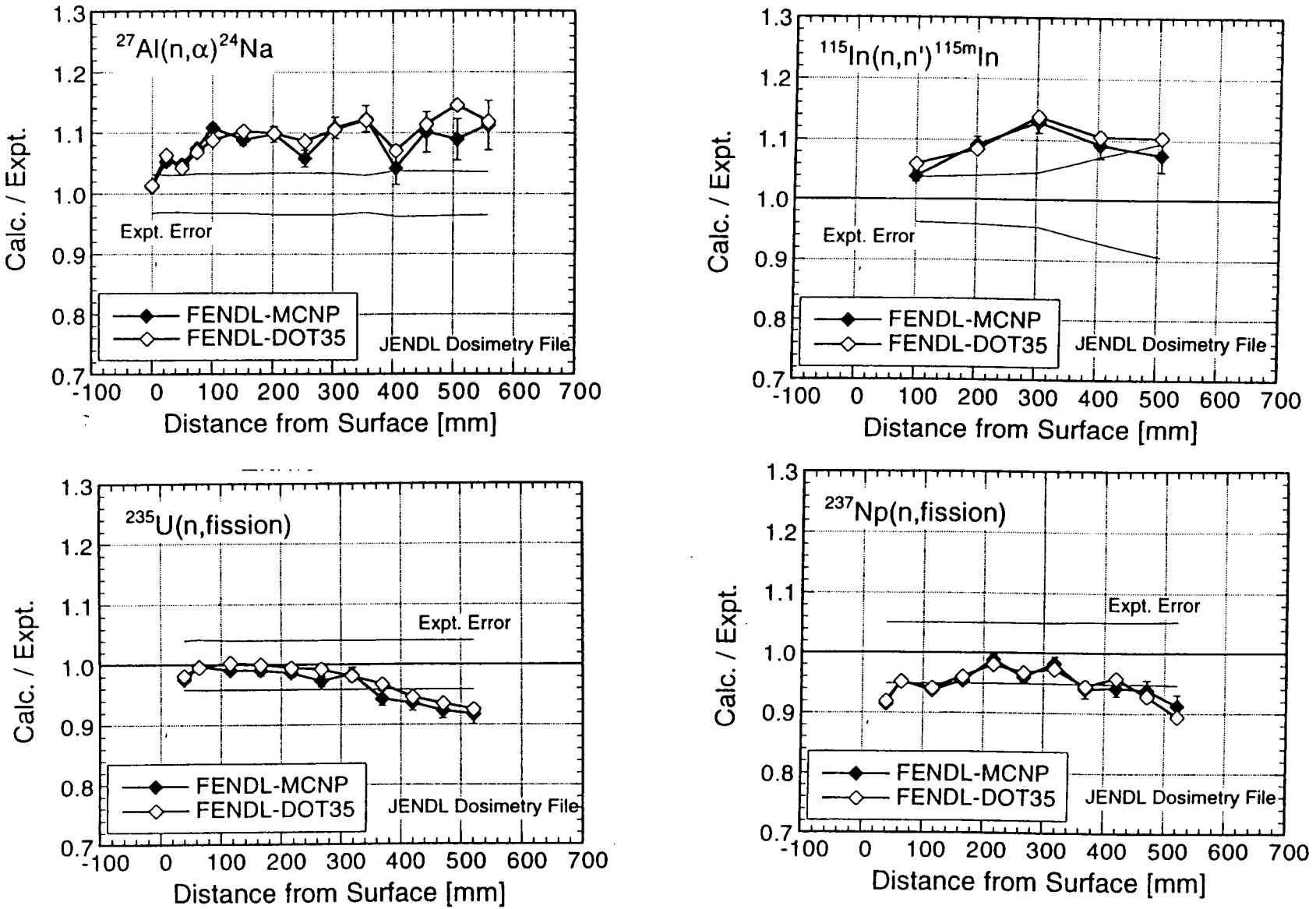

Fig. 23: MCNP- and DOT-calculations with FENDL-1 and JENDL-3.2 data for reaction rates inside Li_2O cylindrical slabs
- K. Hayashi - Hitachi Eng., Y. Oyama -FNS/JAERI

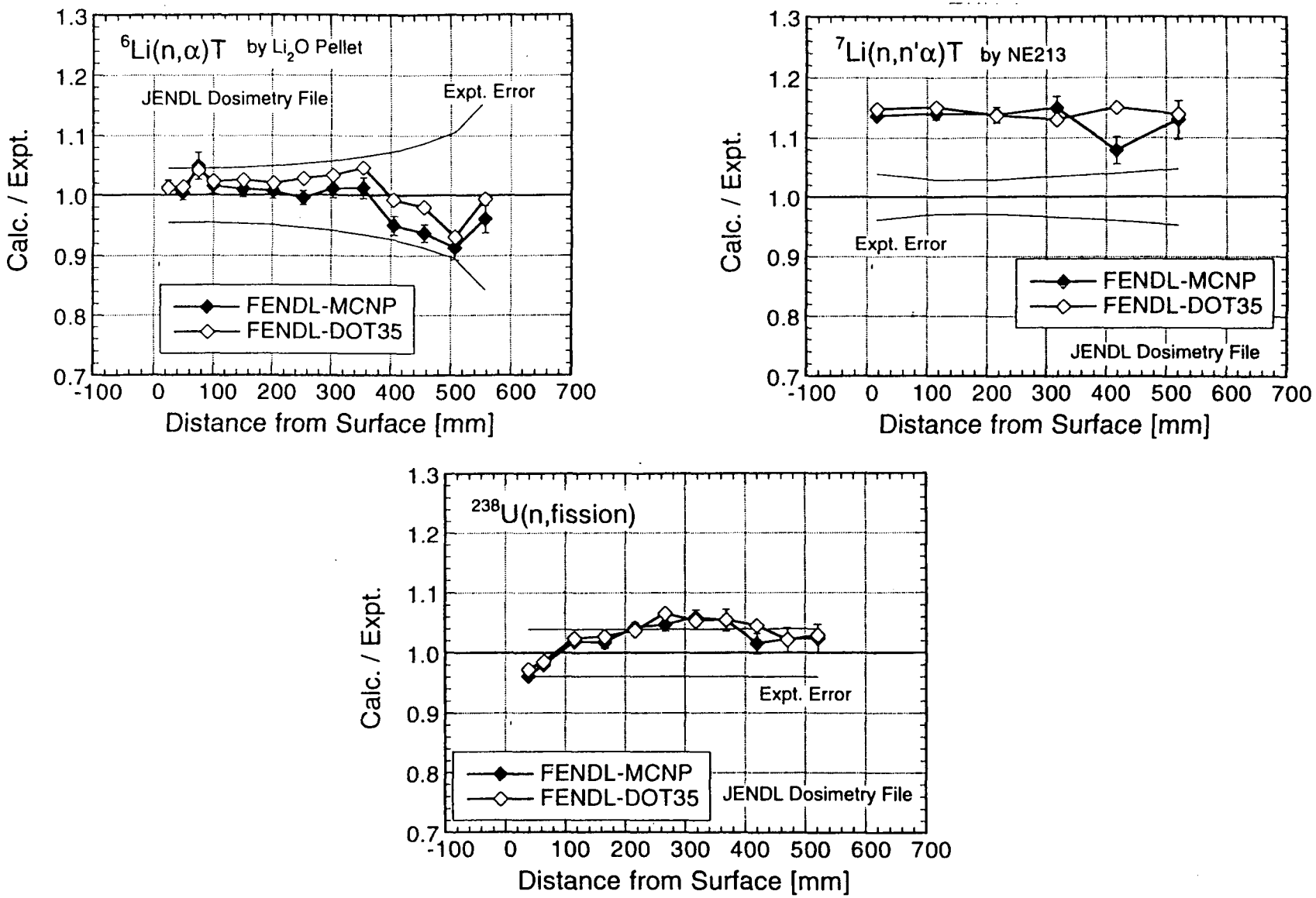

Fig. 24: MCNP- and DOT-calculations with FENDL-1 and JENDL-3.2 data for reaction rates inside Li_2O cylindrical slabs
- K. Hayashi - Hitachi Eng., Y. Oyama -FNS/JAERI

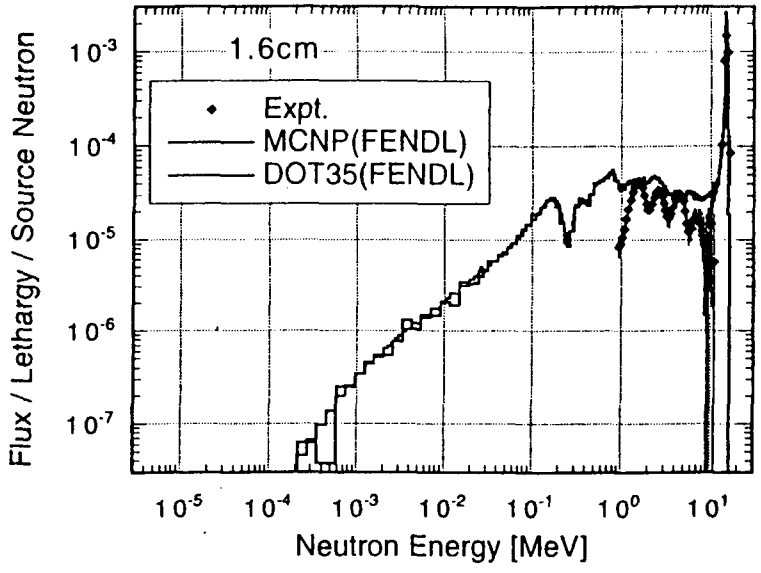

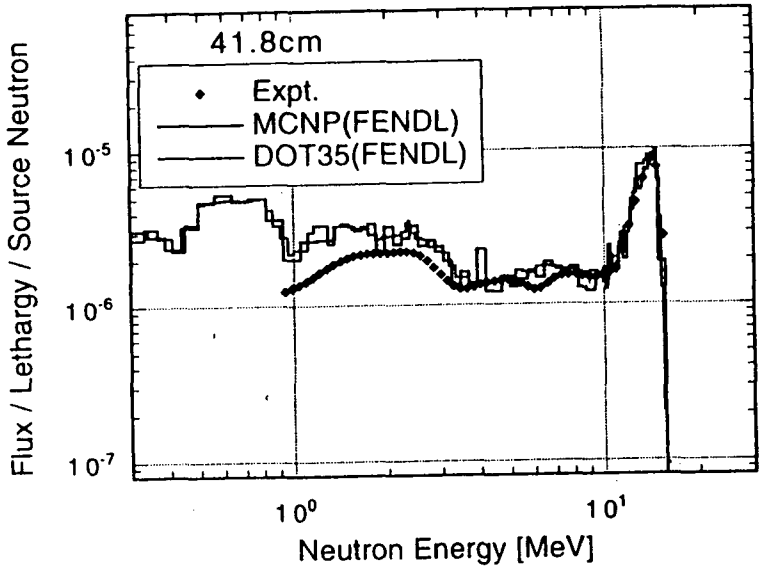

Fig. 25: MCNP- and DOT-calculations with FENDL-1 and JENDL-3.2 data for neutron spectra and reaction rates inside Li_2O cylindrical slabs - K. Hayashi, Hitachi Eng., Y. Oyama -FNS/JAERI

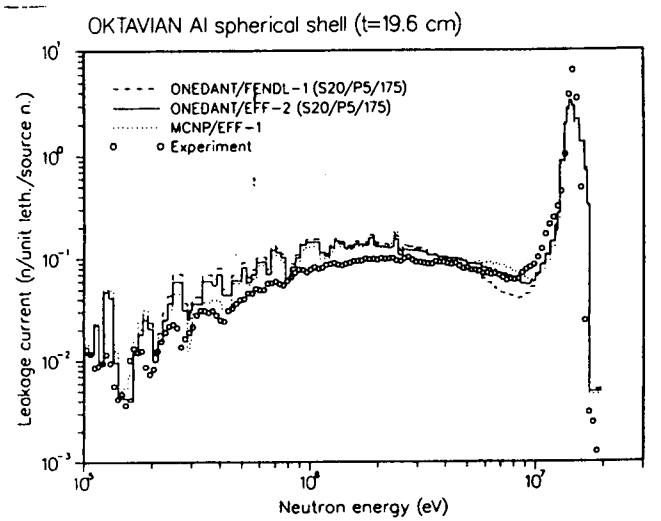

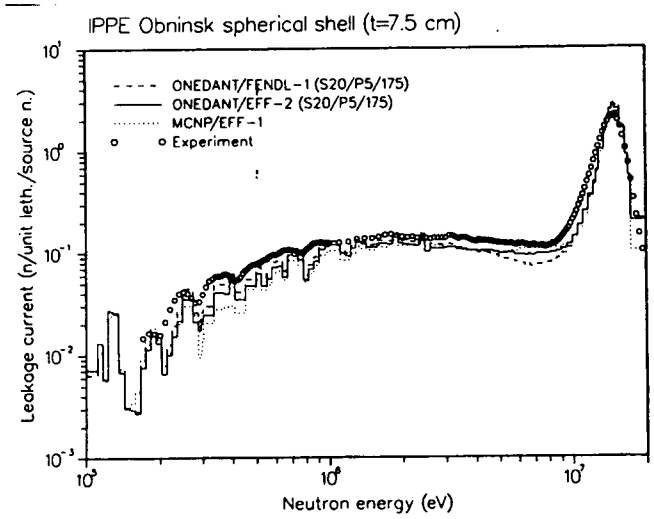

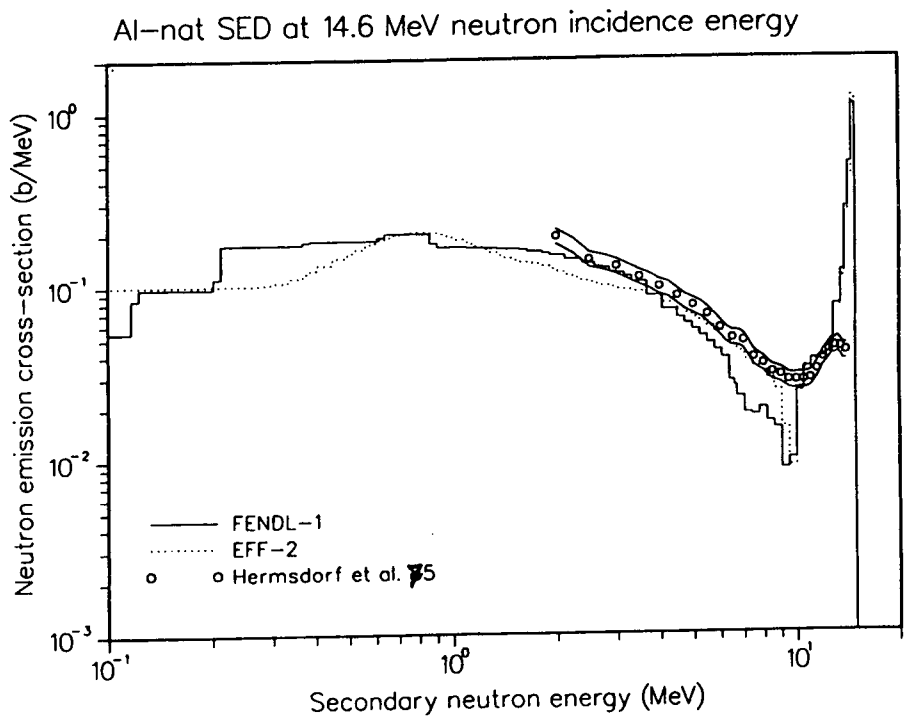

Fig. 26: MCNP- and ONEDANT-calculations with FENDL-1 and EFF-data for aluminium spherical shell experiments and secondary energy distributions - U. Fischer, E. Wiegner - FZK, Karlsruhe

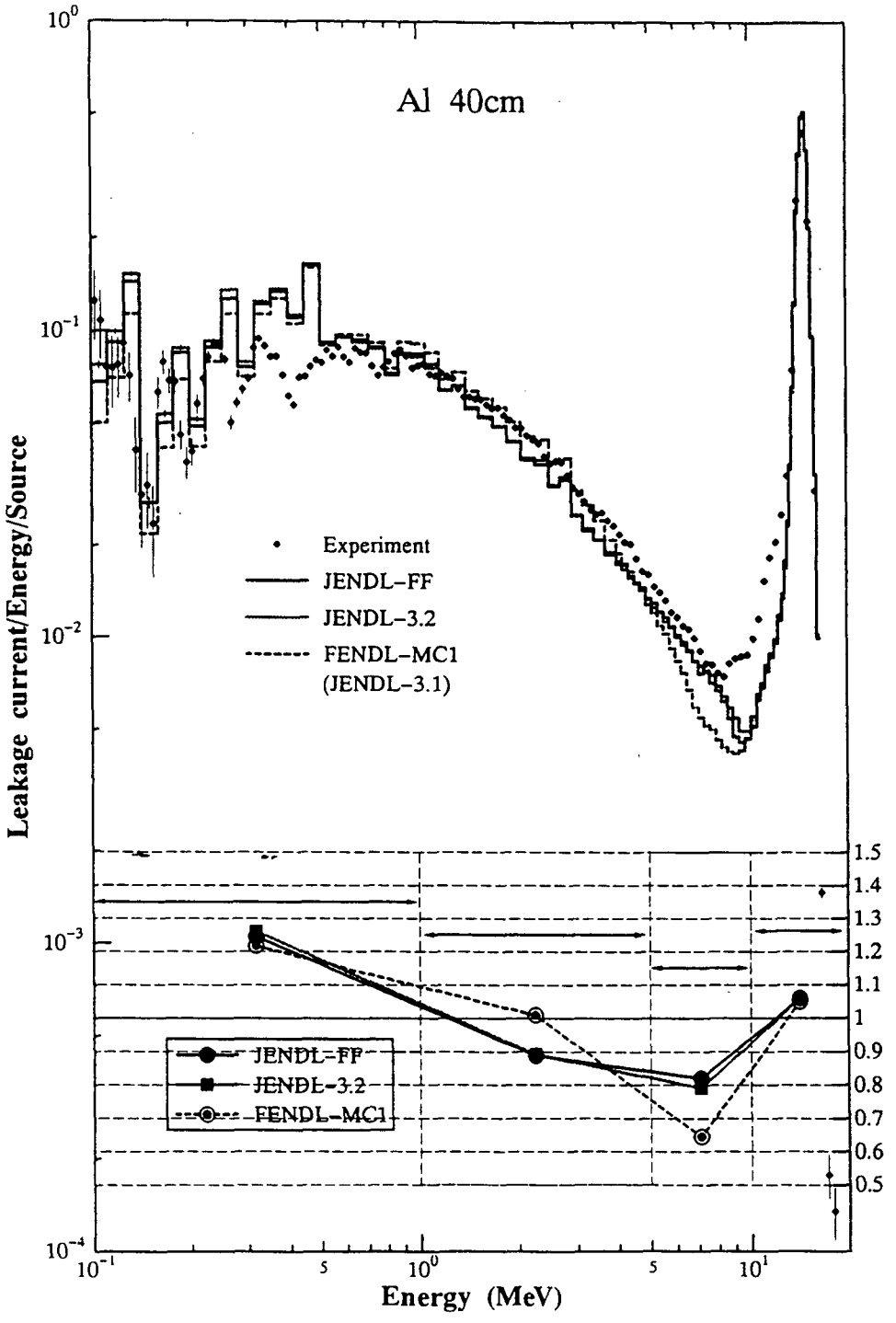

Fig. 27: MCNP -calculations with FENDL-1 and JENDL-3 data for OKTAVIAN aluminium spherical shell experiment - C. Ichihara, University of Kyoto

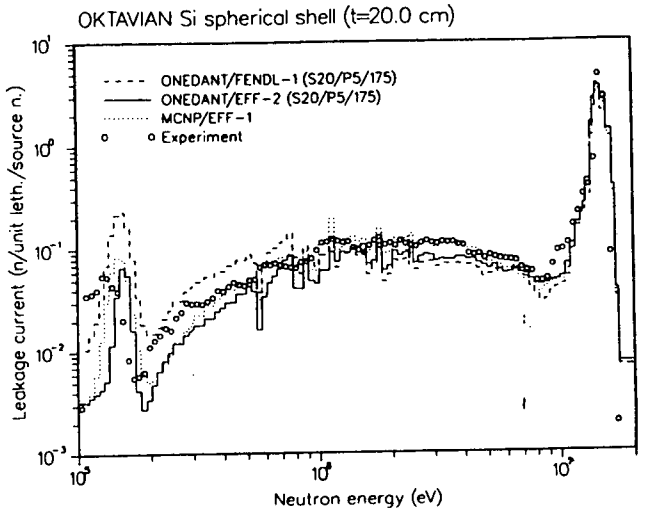

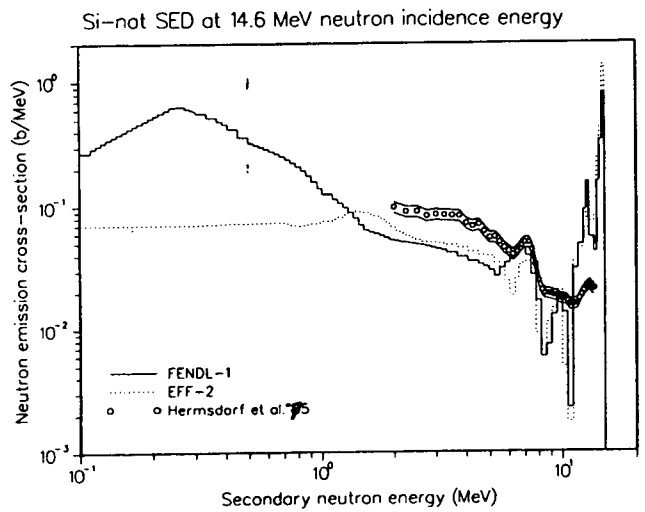

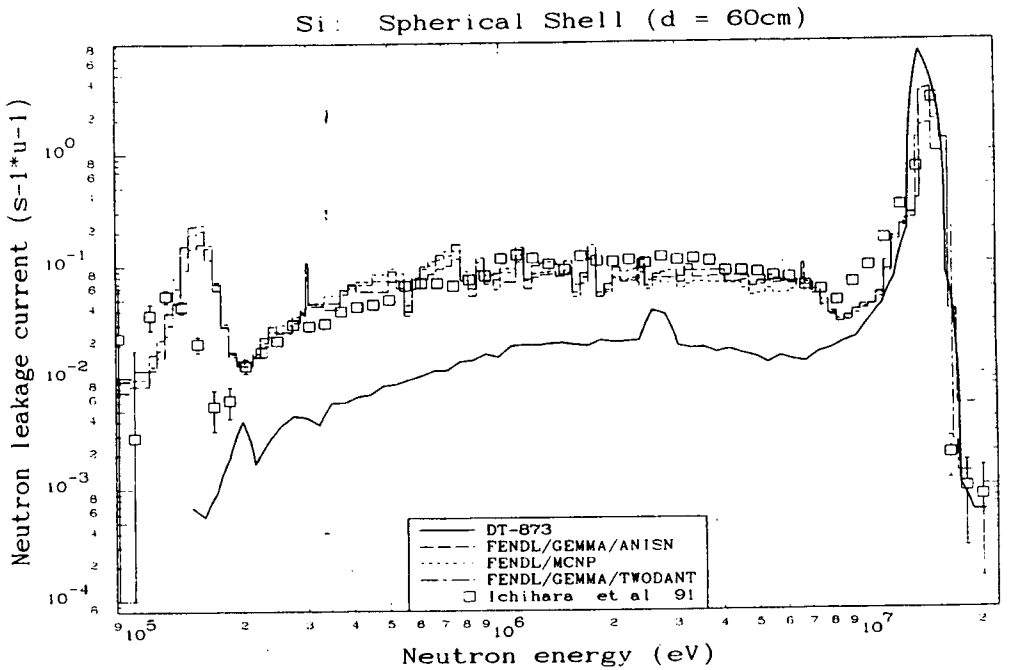

Fig. 28a, b: MCNP- and ONEDANT-calculations with FENDL-1 and EFF-data for silicon spherical shell experiments and Si secondary energy distributions - U. Fischer, E. Wiegner - FZK

Fig. 28 c: MCNP-, ONEDANT- and ANISN-calculations - A. Blokhin, IPPE Obninsk

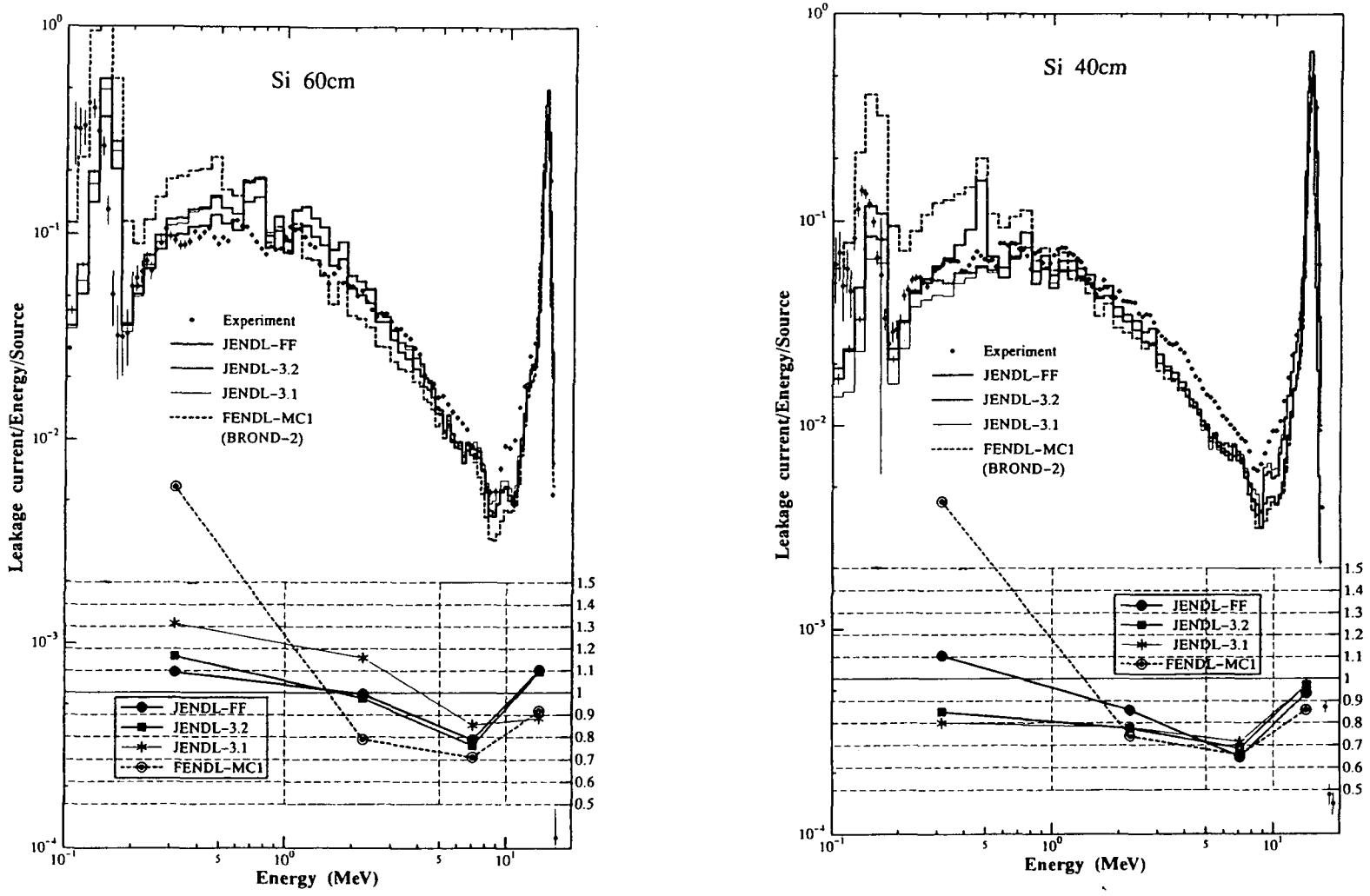

Fig. 29: MCNP-calculations with FENDL-1 and JENDL-3 data for Si spherical shells - C. Ichihara, University of Kyoto

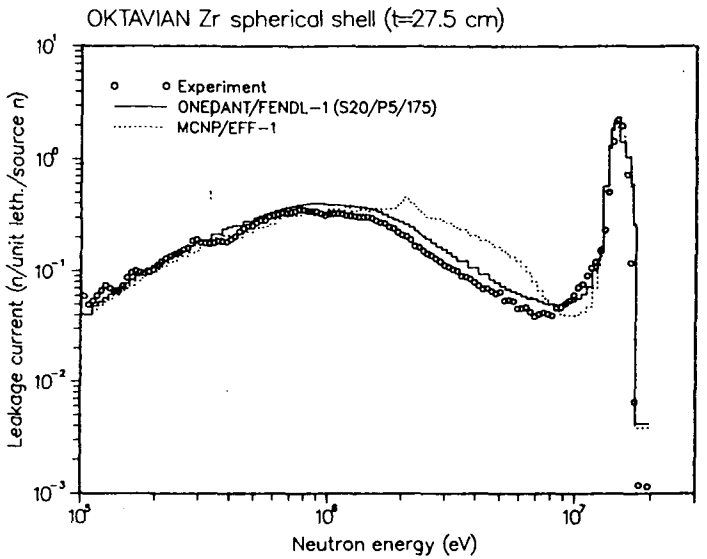

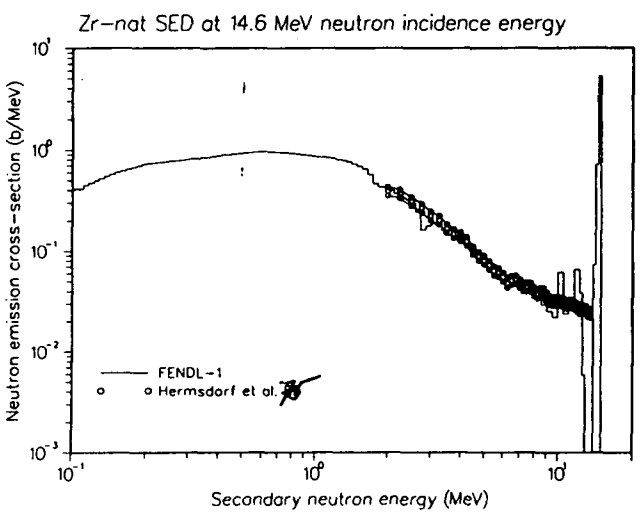

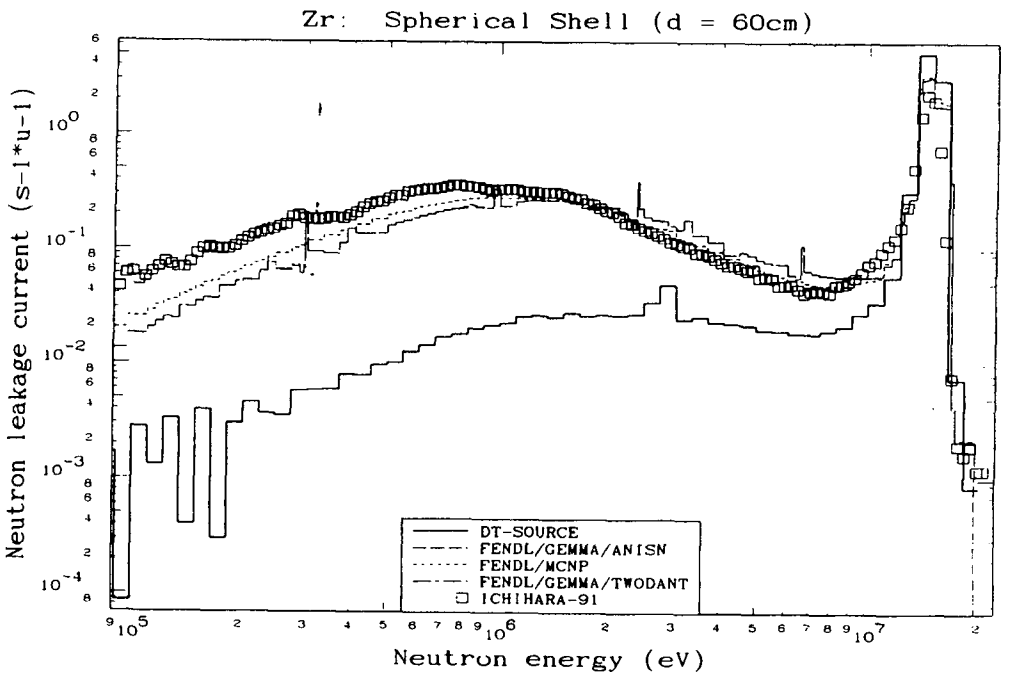

Fig. 30a, b: MCNP- and ONEDANT-calculations with FENDL-1 and EFF-data for zirconium spherical shell experiments and Zr secondary energy distributions - U. Fischer, E. Wiegner - FZK

Fig. 30c: MCNP-, ONEDANT- and ANISN-calculations - A. Blokhin, IPPE Obninsk

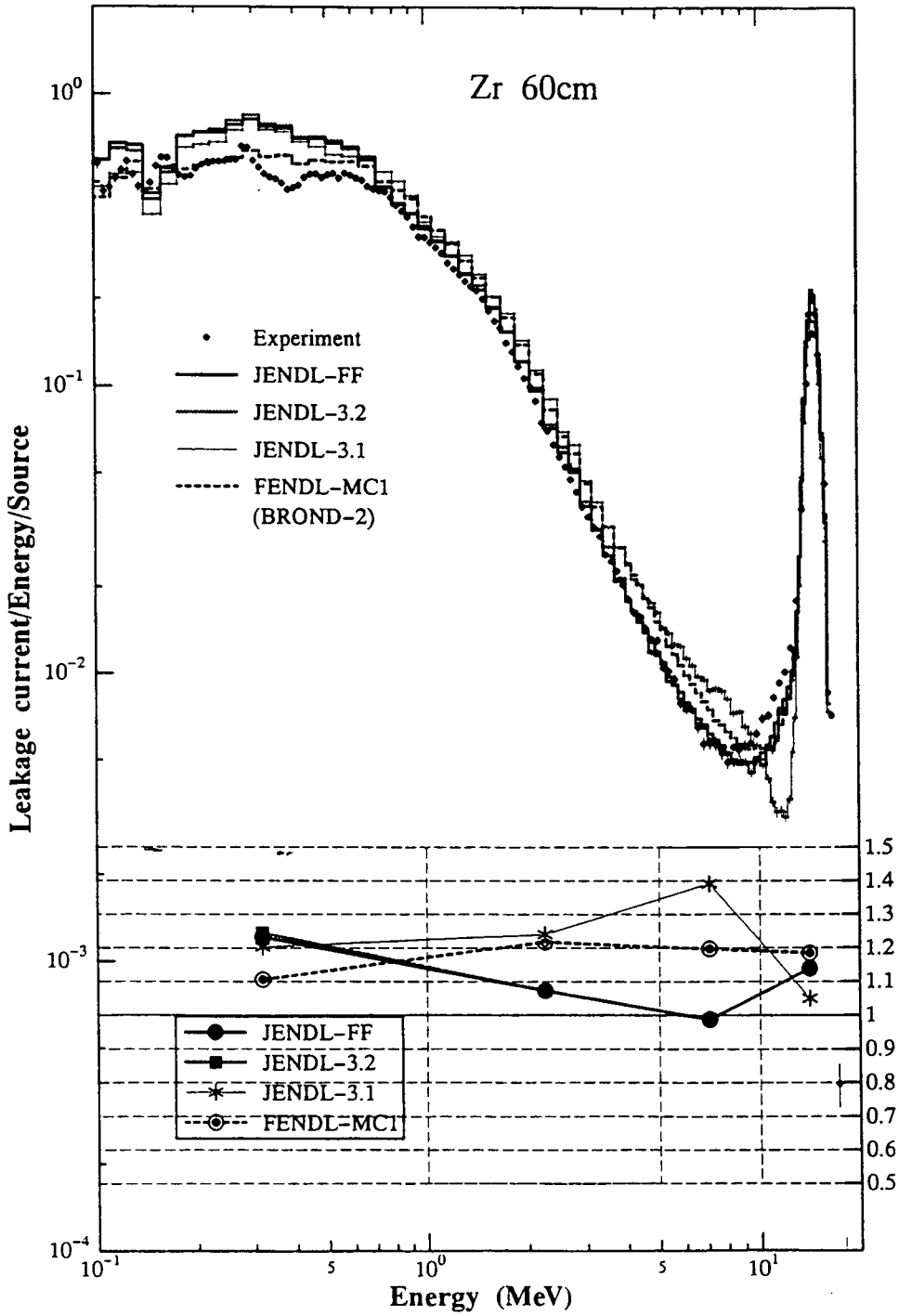

Fig. 31 : MCNP -calculations with FENDL-1 and JENDL-3 data for OKTAVIAN zirconium spherical shell experiment - C. Ichihara, University of Kyoto

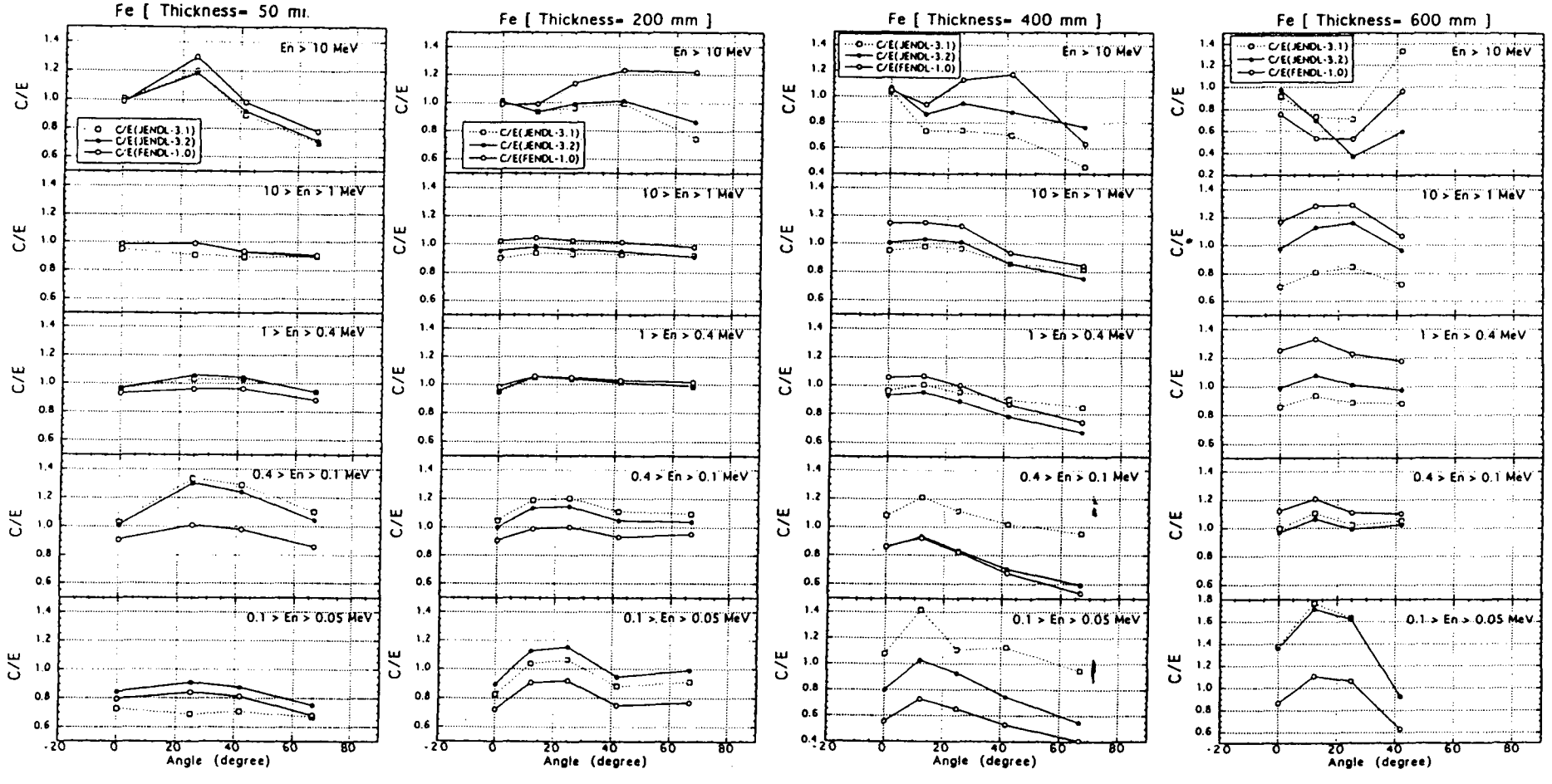

Fig. 32: MCNP-calculations with FENDL-1 and JENDL-3 data for FNS Fe cylindrical slabs - Y. Oyama, M. Wada -FNS/JAERI

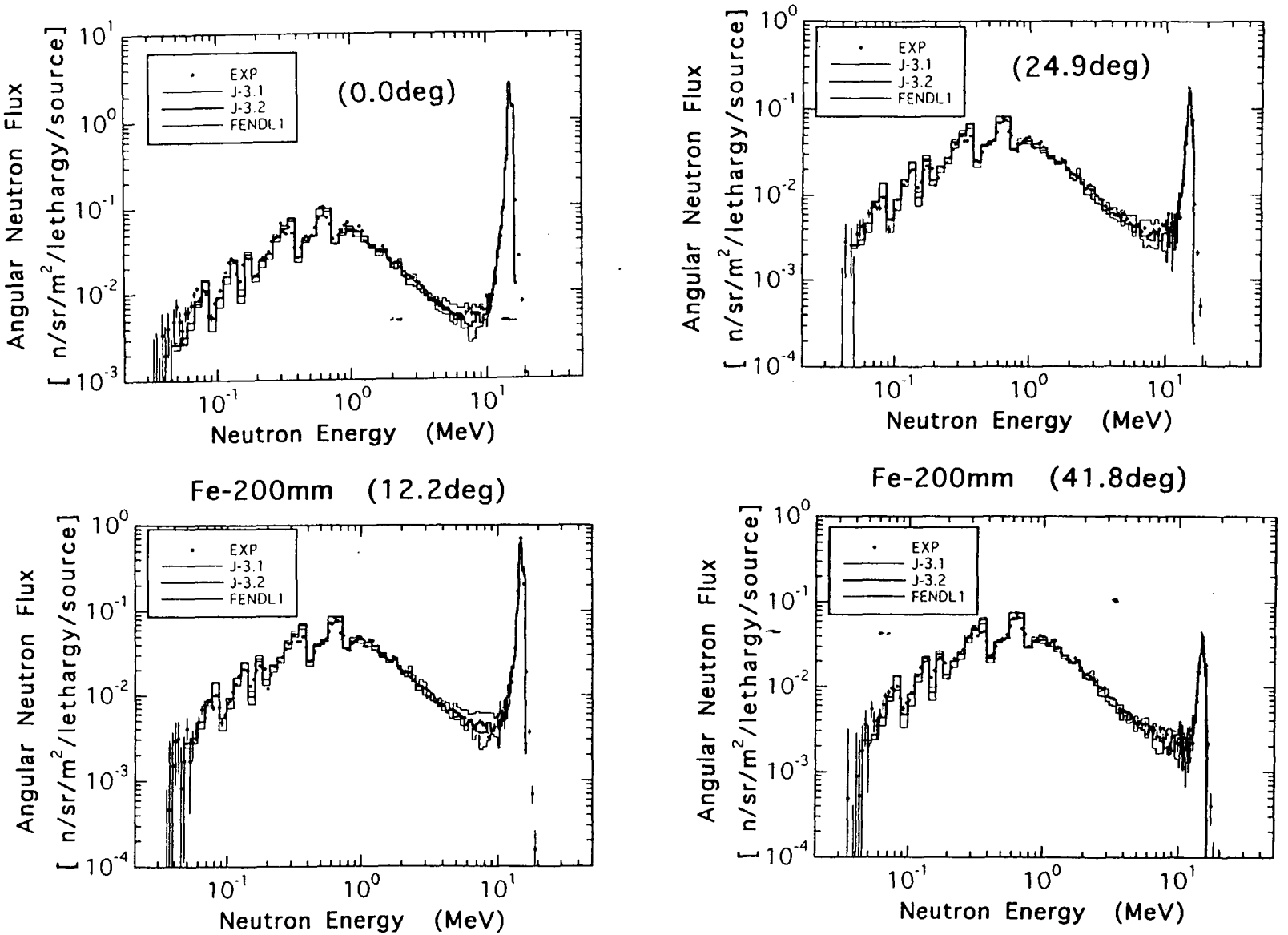

Fig. 33: MCNP-calculations with FENDL-1 and JENDL-3 data for FNS Fe cylindrical slabs - Y. Oyama, M. Wada -FNS/JAERI

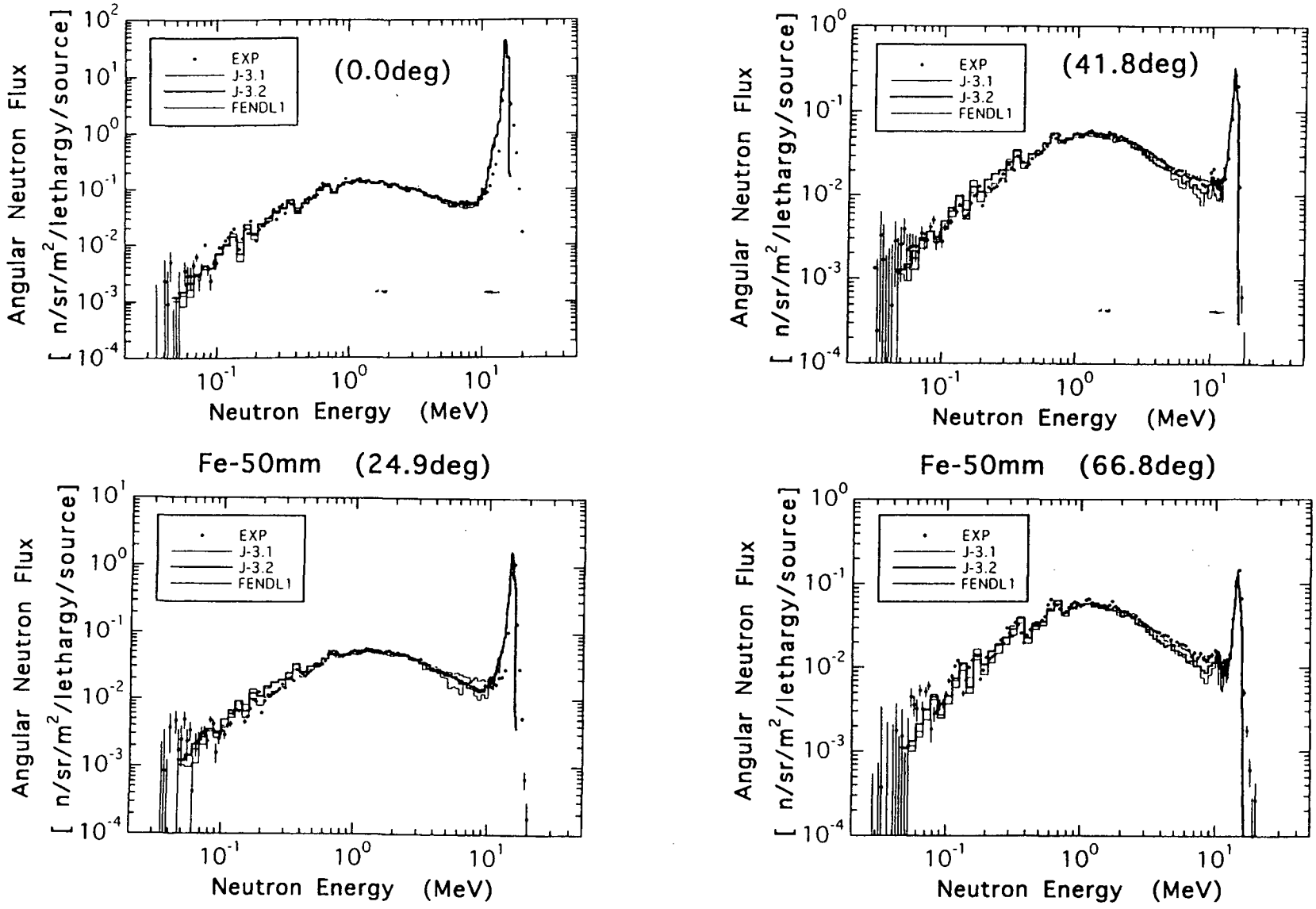

Fig. 34: MCNP-calculations with FENDL-1 and JENDL-3 data for FNS Fe cylindrical slabs - Y. Oyama, M. Wada -FNS/JAERI

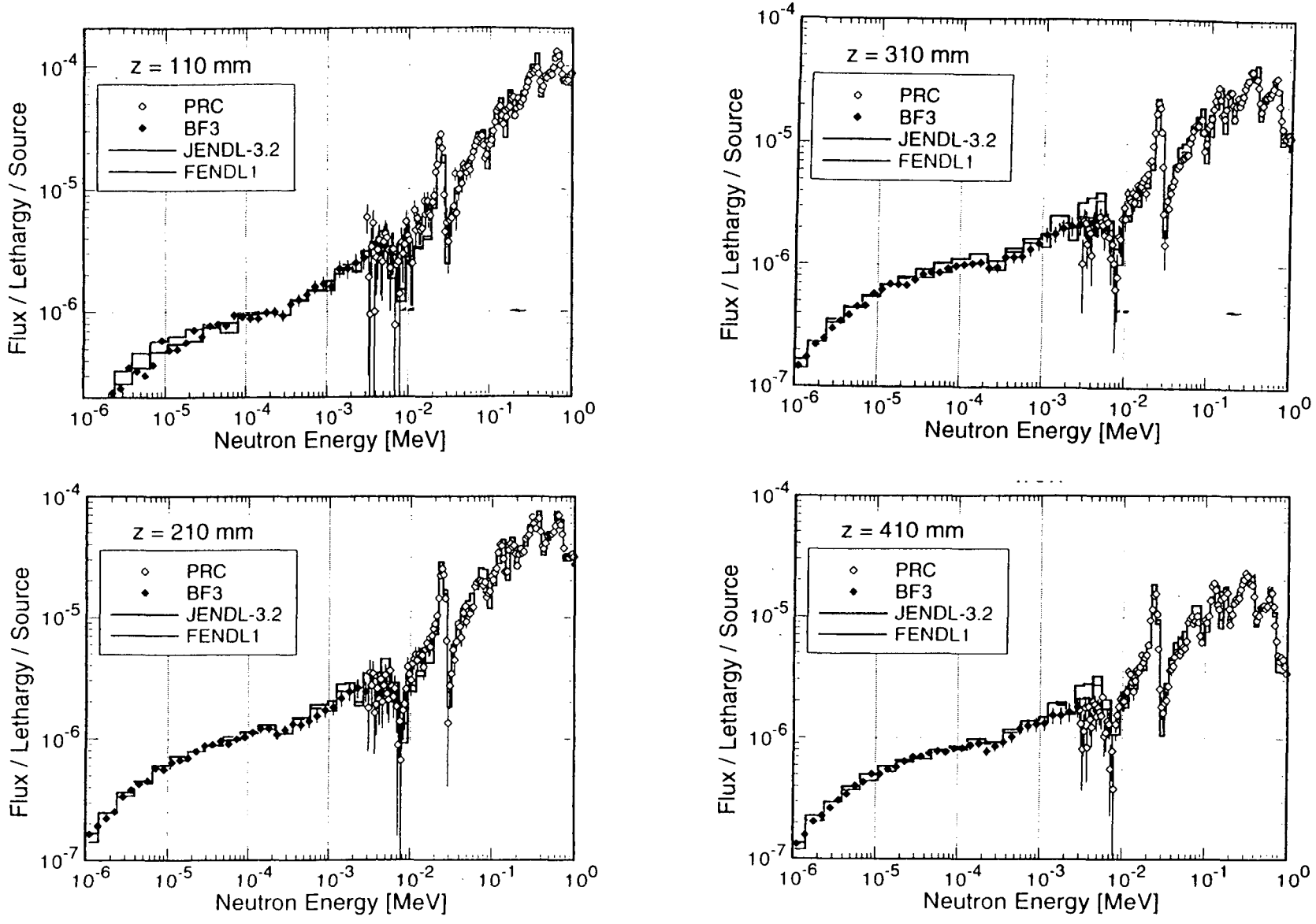

Fig. 35: MCNP-calculations with FENDL-1 and JENDL-3.2 data for neutron spectra inside FNS Fe cylindrical slabs
- F. Maekawa, Y. Oyama, M. Wada -FNS/JAERI

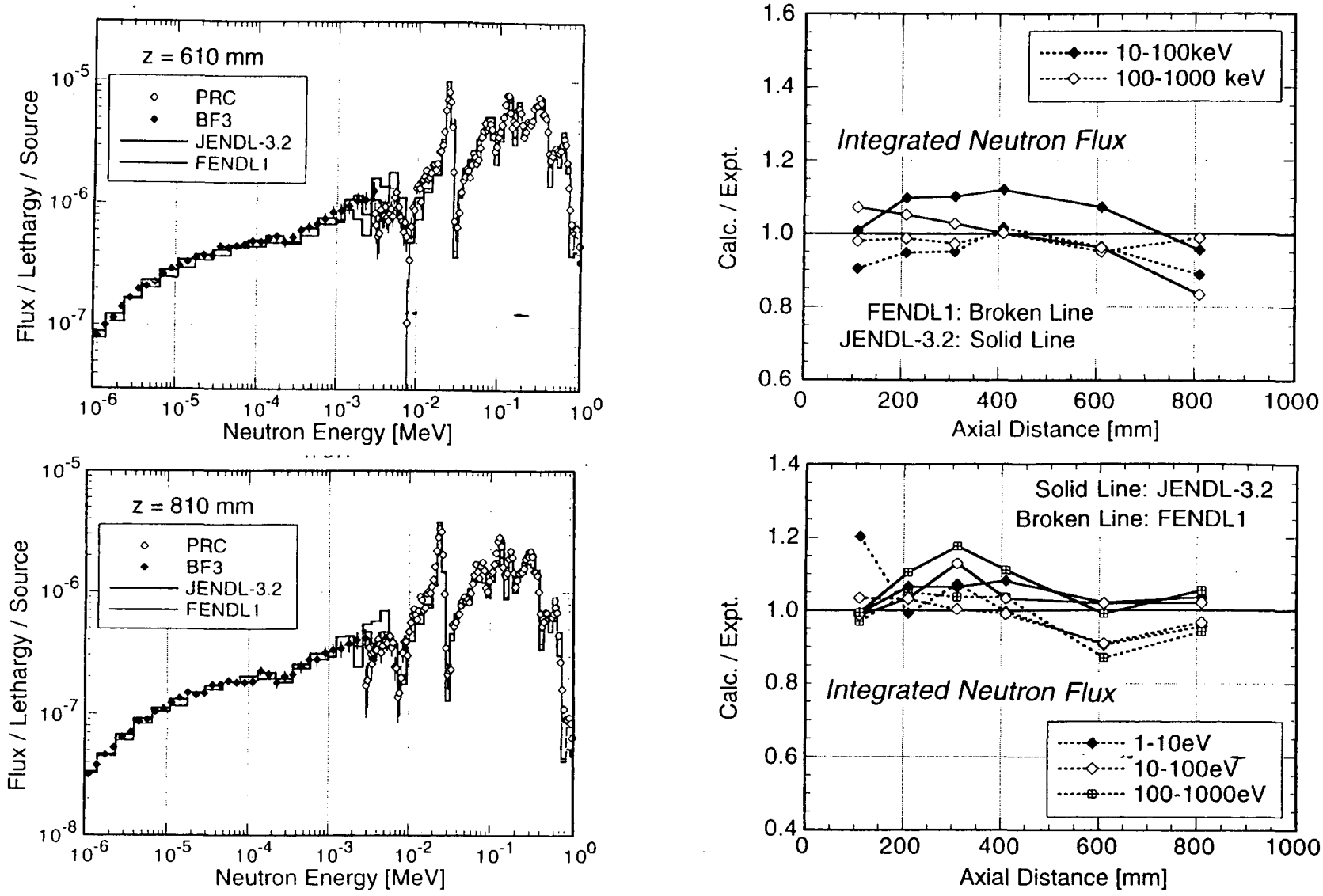

Fig. 36: MCNP-calculations with FENDL-1 and JENDL-3.2 data for neutron spectra inside FNS Fe cylindrical slabs
- F. Maekawa, Y. Oyama, M. Wada -FNS/JAERI

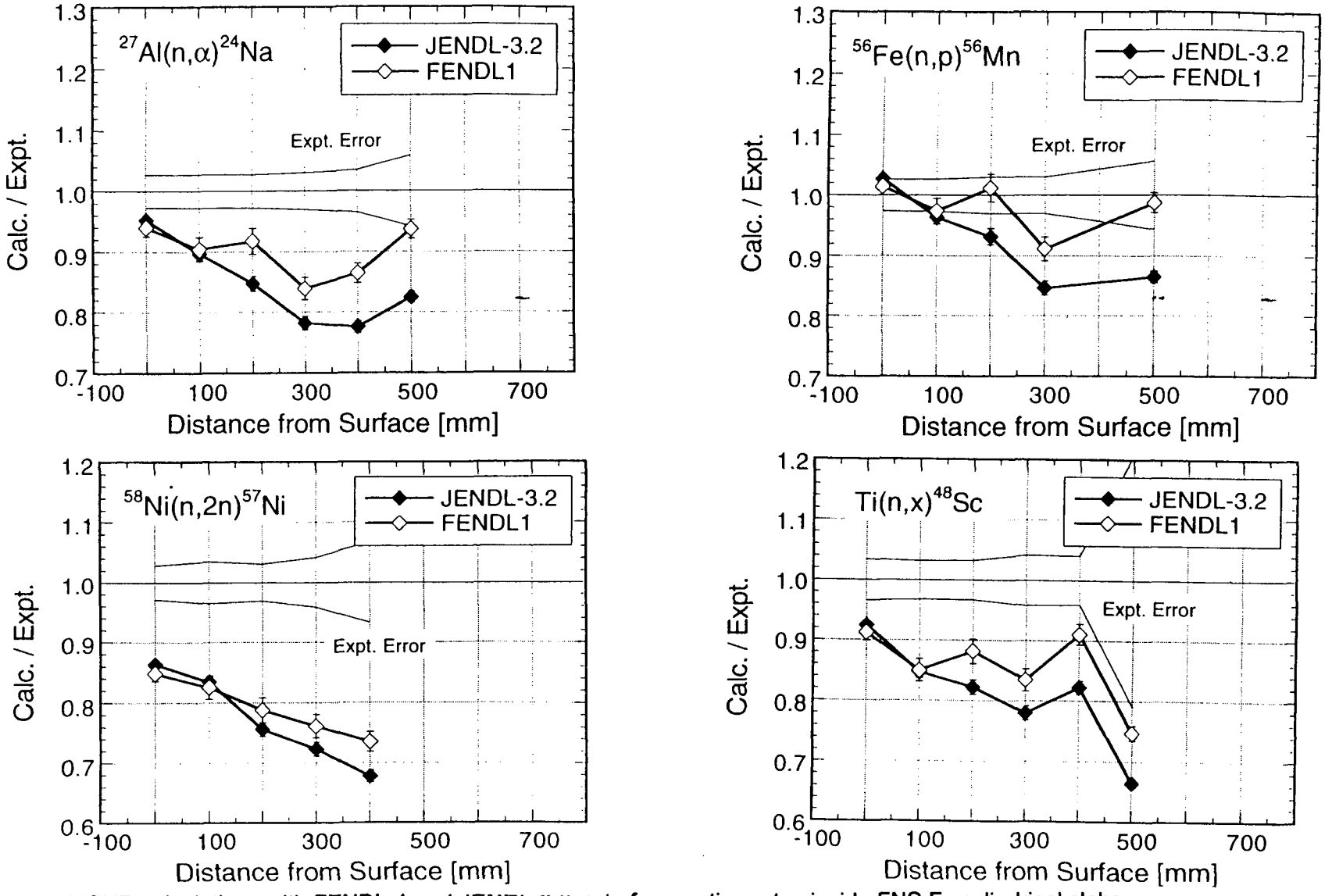

Fig. 37: MCNP-calculations with FENDL-1 and JENDL-3.2 data for reaction rates inside FNS Fe cylindrical slabs
- F. Maekawa, Y. Oyama, M. Wada -FNS/JAERI

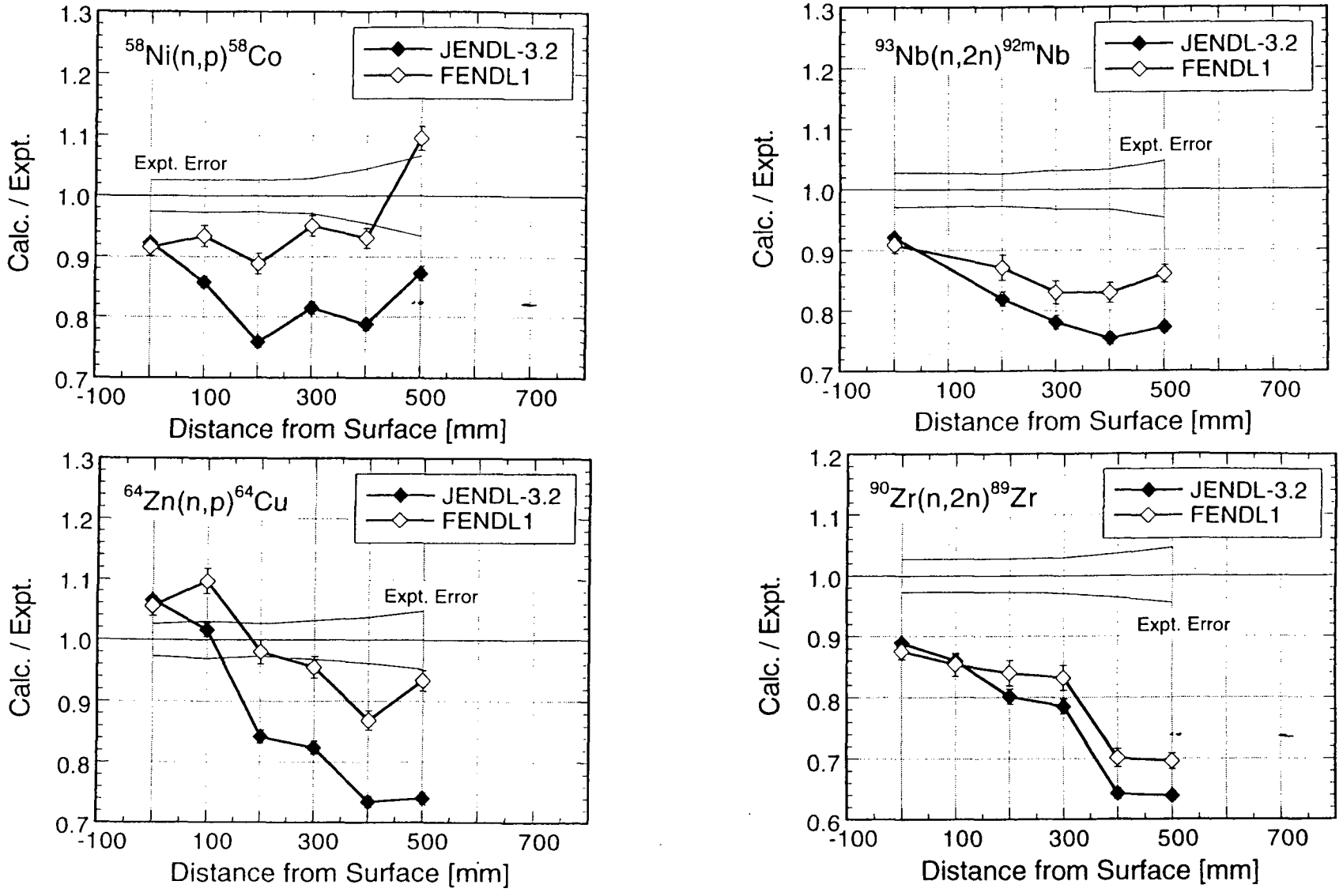

Fig. 38: MCNP-calculations with FENDL-1 and JENDL-3.2 data for reaction rates inside FNS Fe cylindrical slabs
- F. Maekawa, Y. Oyama, M. Wada -FNS/JAERI

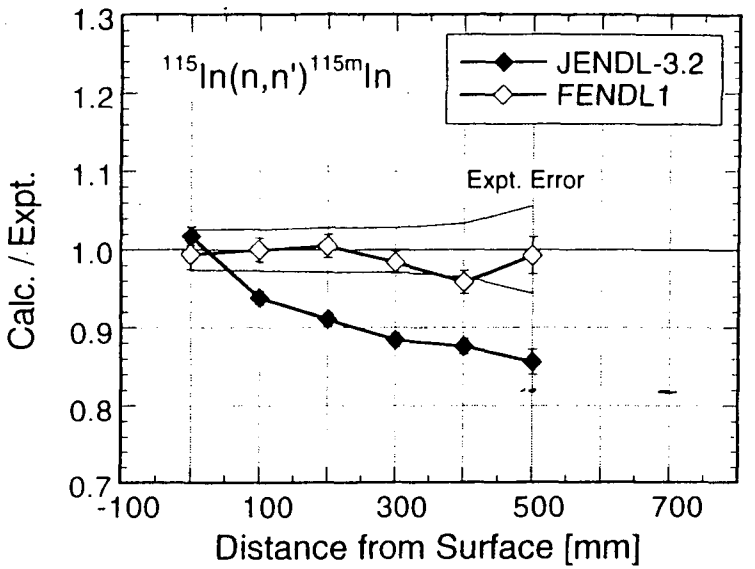

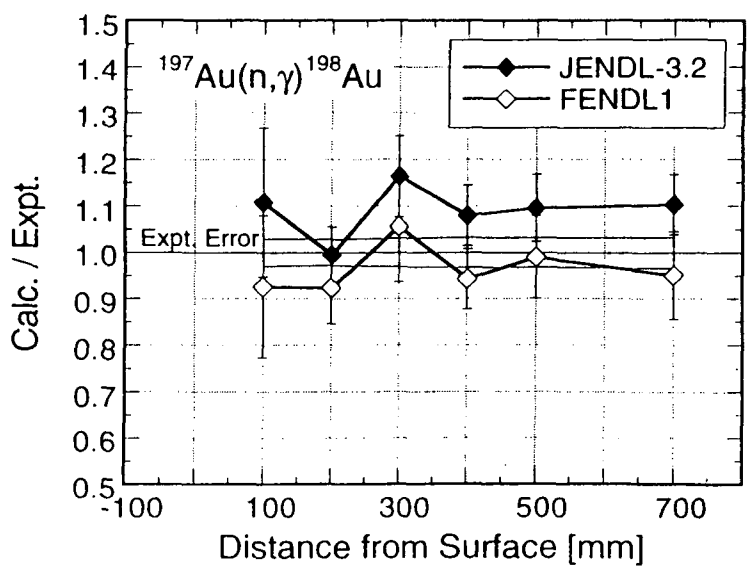

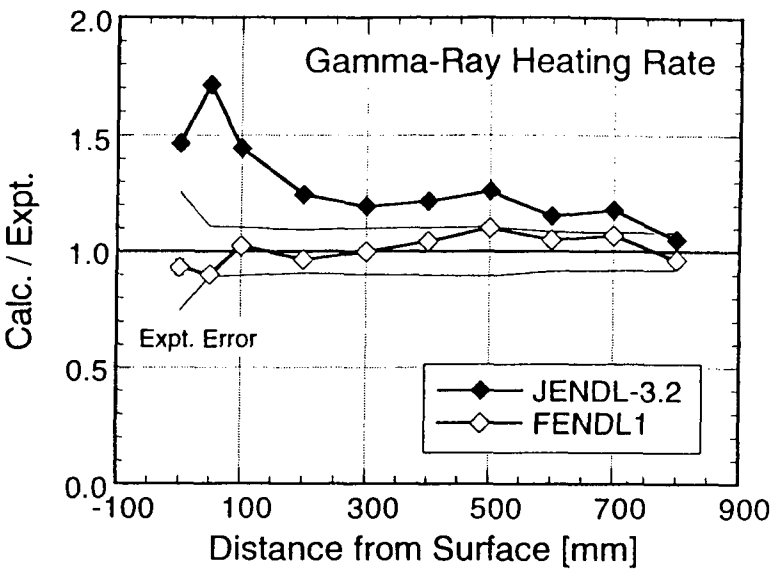

Fig. 39: MCNP-calculations with FENDL-1 and JENDL-3.2 data for reaction rates inside FNS Fe cylindrical slabs
- F. Maekawa, Y. Oyama, M. Wada -FNS/JAERI

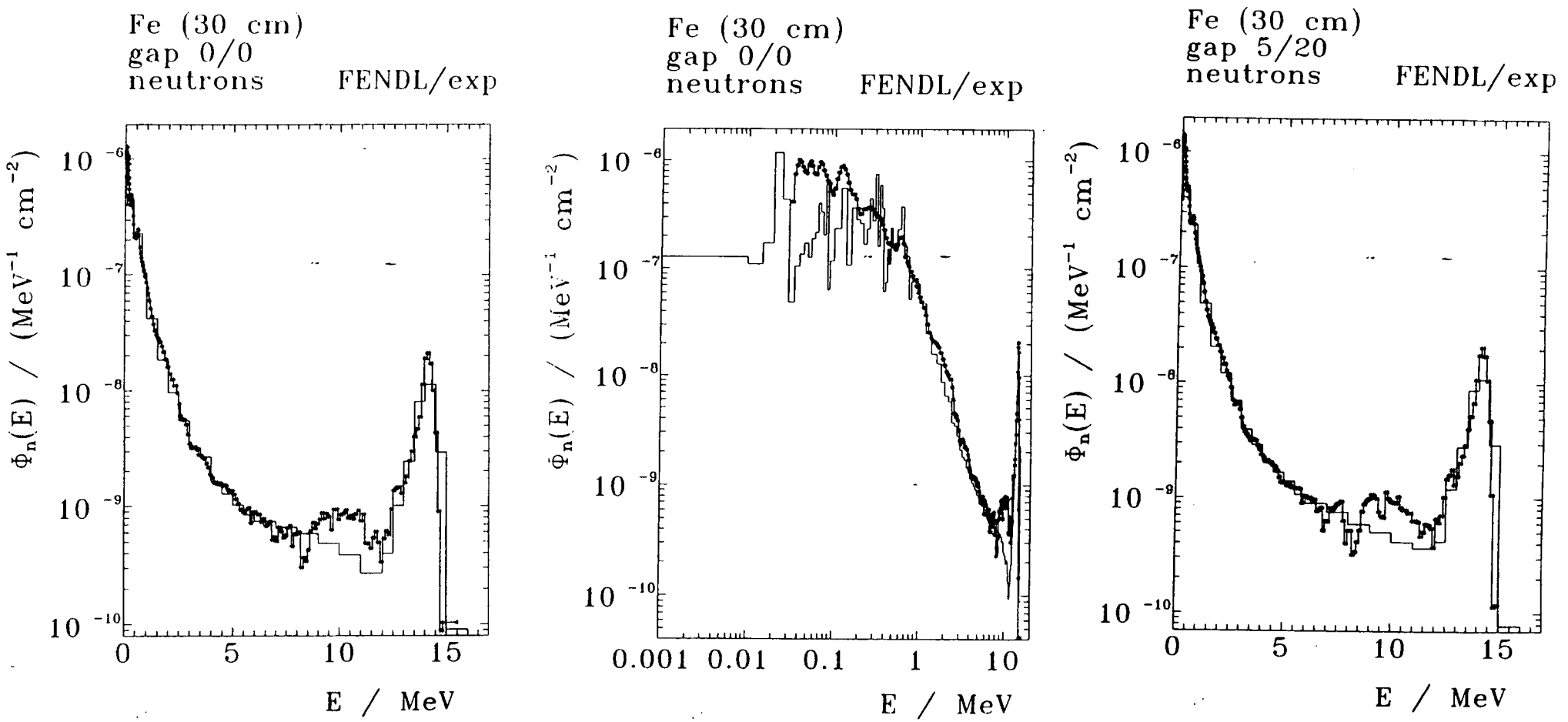

Fig. 40: MCNP-calculations with FENDL-1 data for TUD iron slab with and without gap - K. Seidel, TU Dresden

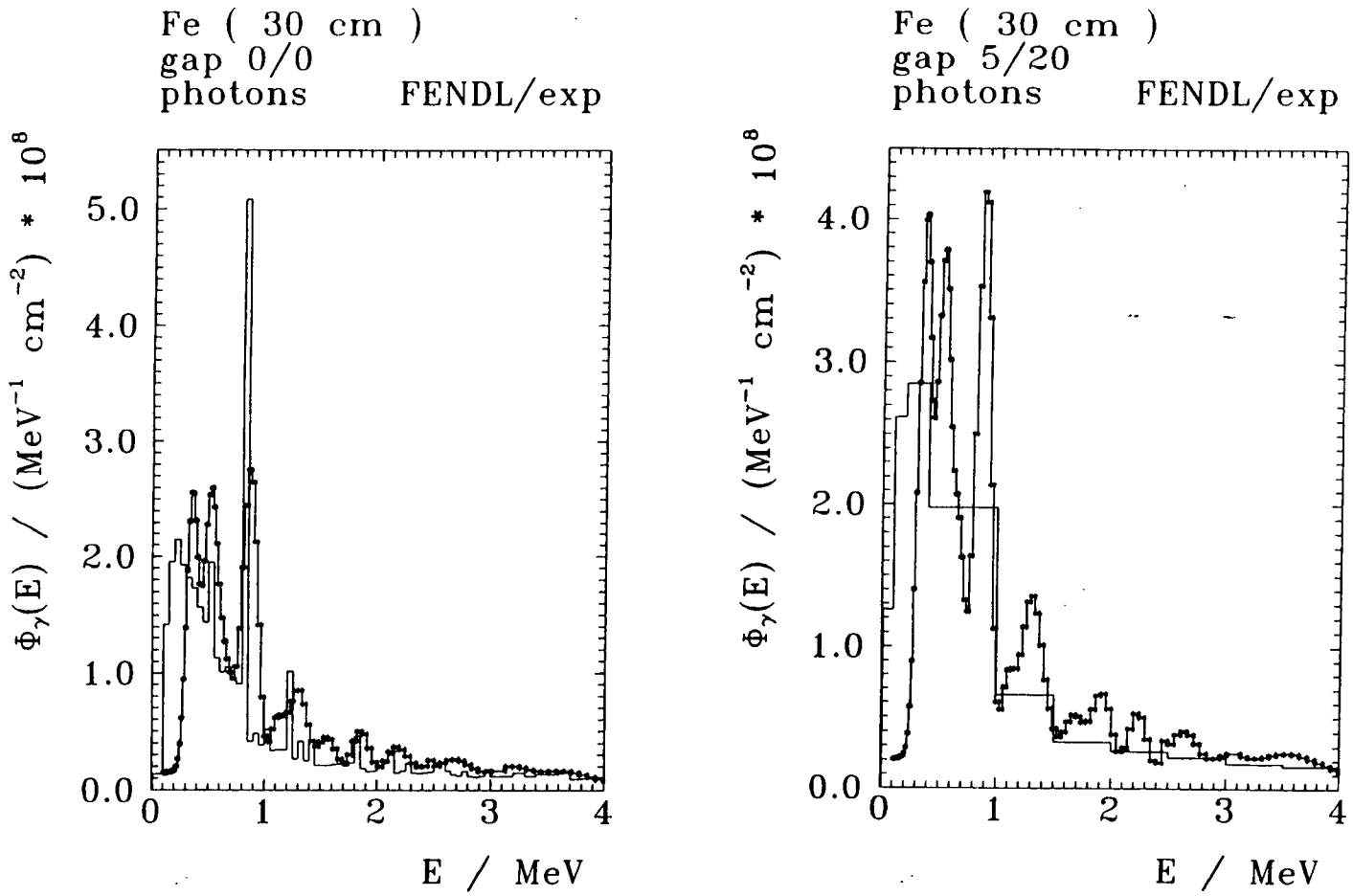

Fig. 41: MCNP-calculations with FENDL-1 data for TUD iron slab with and without gap - K. Seidel, TU Dresden

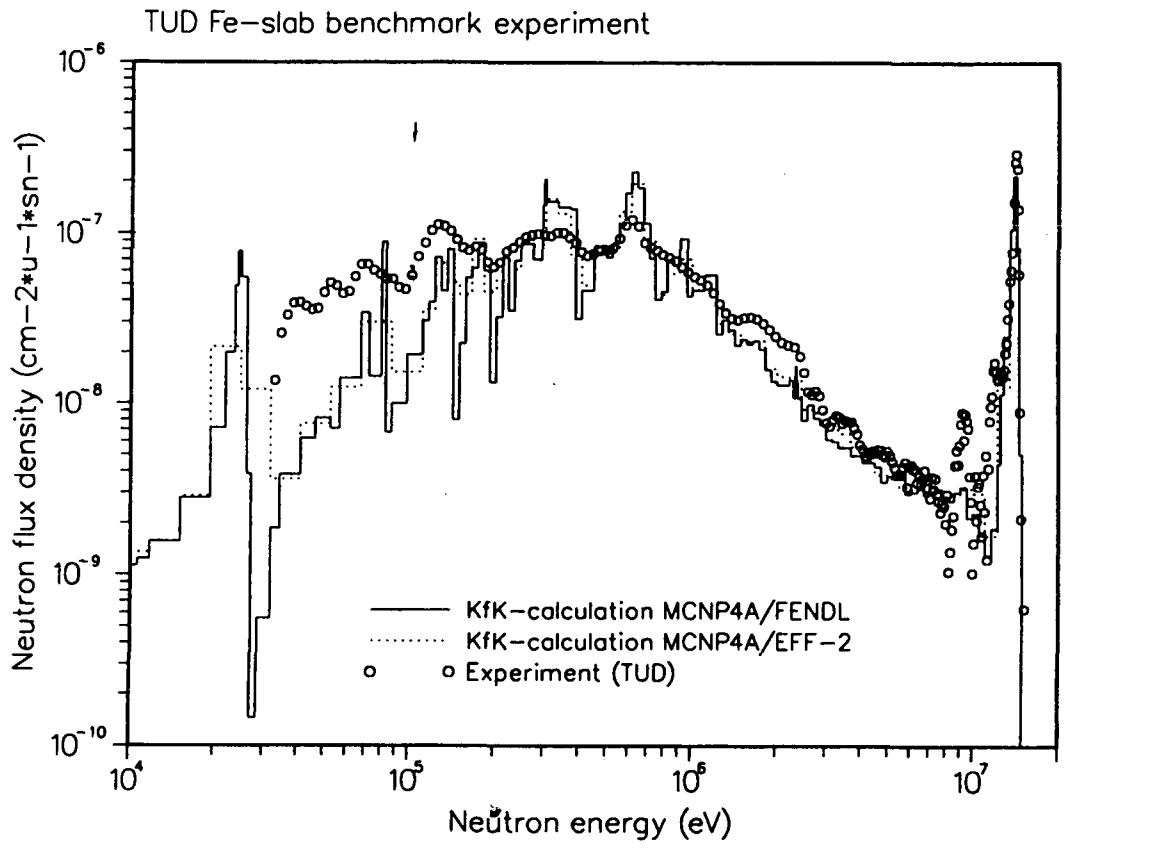

Fig. 42: MCNP-calculations with FENDL-1 and EFF-2 data for TUD iron slab without gap - U. Fischer, FZK, Karlsruhe

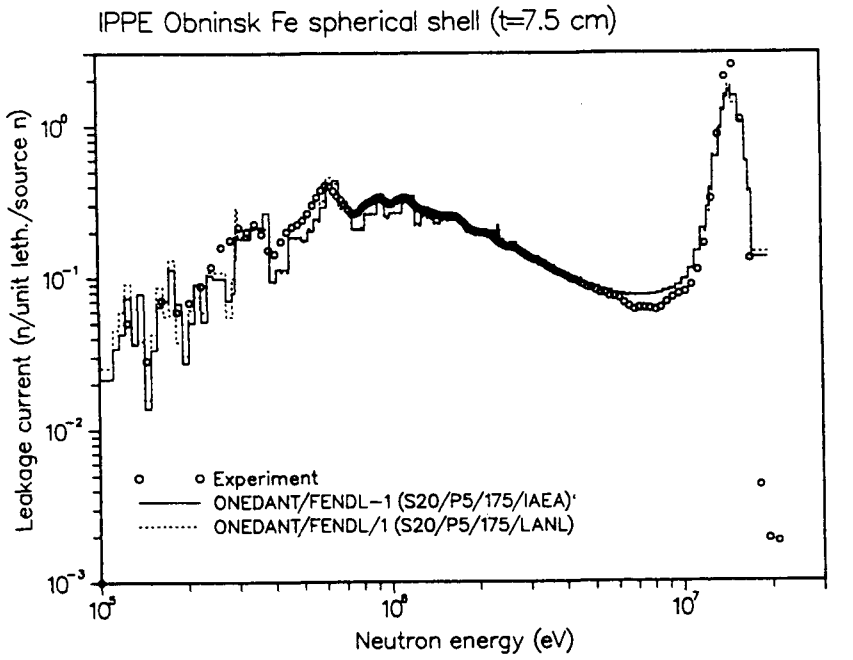

Figure 1 : Leakage spectrum from the Russian Fe sphere

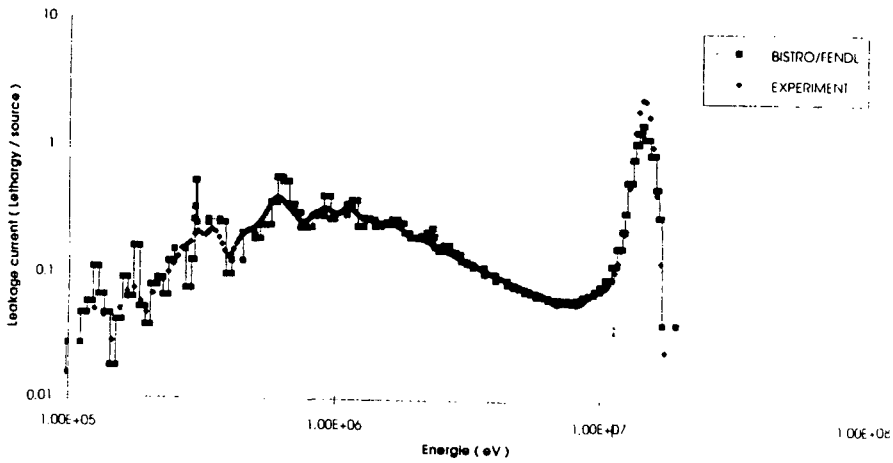

Fig. 43: ONEDANT and BISTRO-calculations with FENDL-1 data for IPPE iron shell experiment - U. Fischer, E. Wiegner - FZK ; L. Benmansour, A. Santamarina - CEA Cadarache

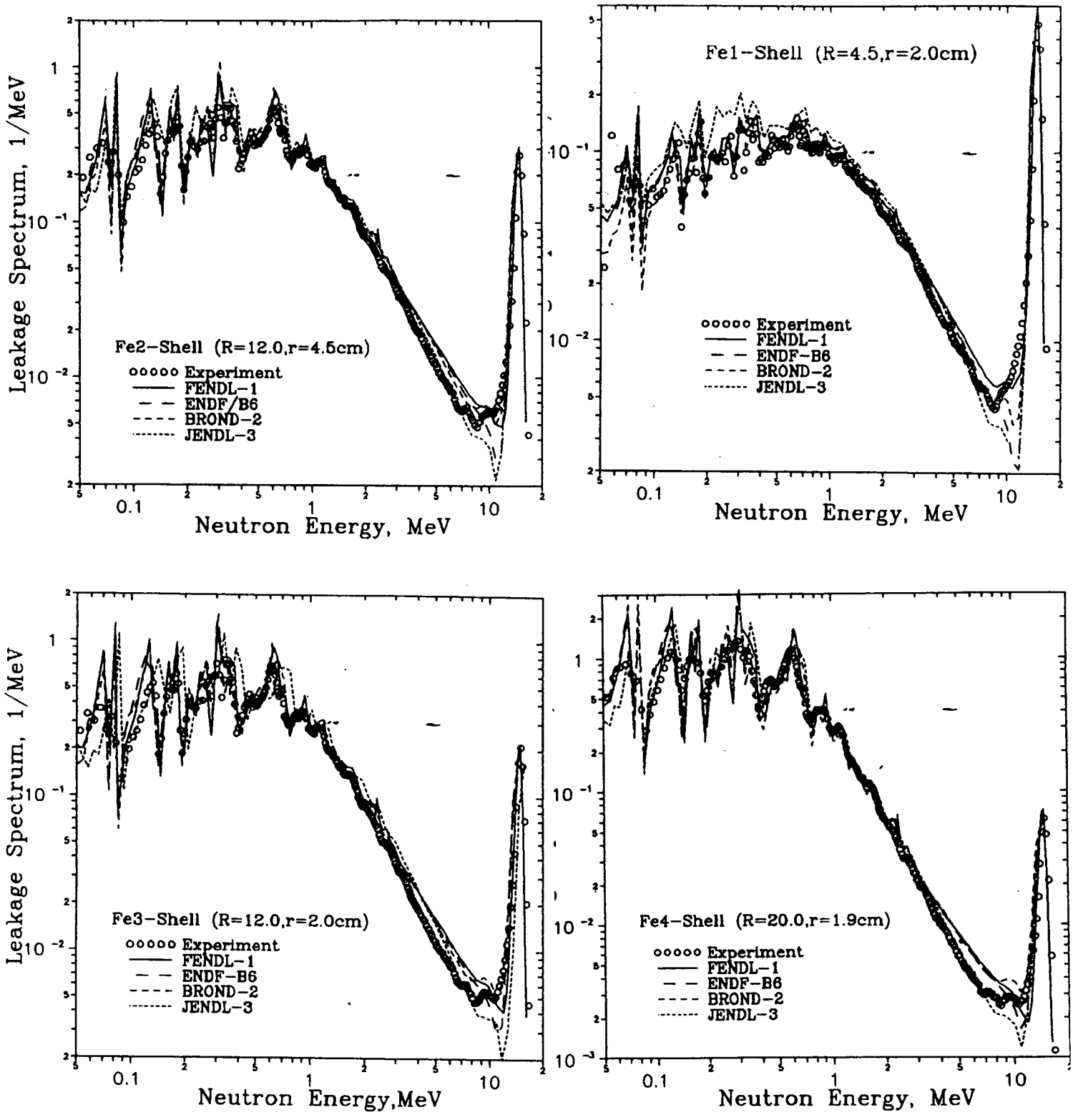

Fig. 44 : MCNP-, ANISN- and ONEDANT-calculations with FENDL-1, JENDL-3, BROND and ENDF/B-VI data for IPPE iron shell experiments - S. P. Simakov, IPPE Obninsk

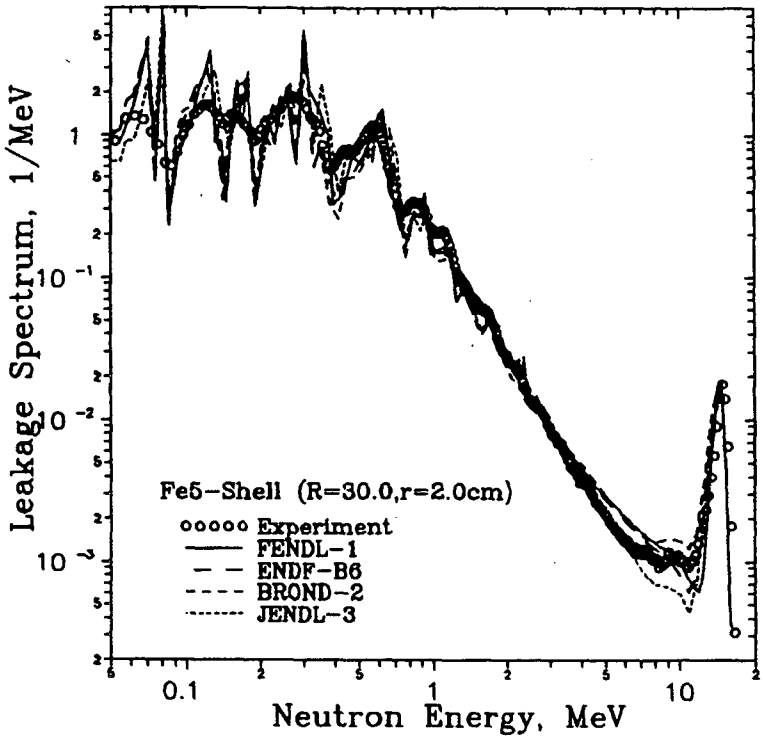

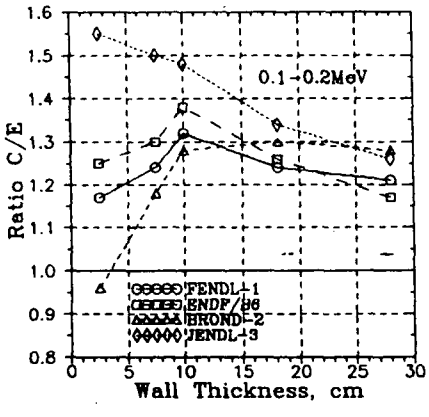

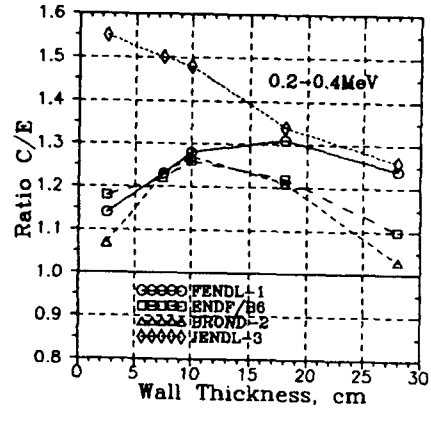

Fig. 45: MCNP-, ANISN- and ONEDANT-calculations with FENDL-1, JENDL-3, BROND and ENDF/B-VI data for IPPE iron shell experiments - S. P. Simakov, IPPE Obninsk

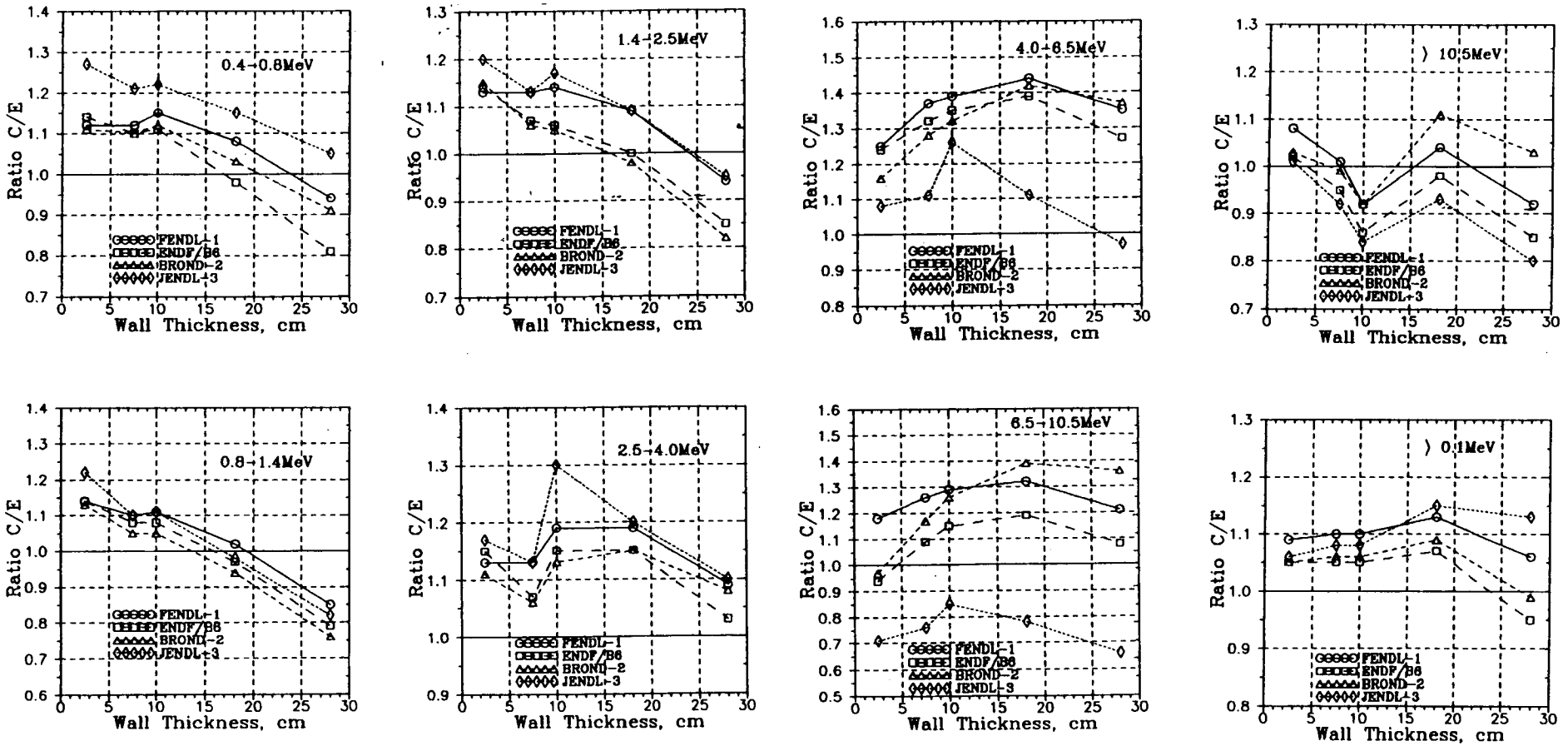

Fig. 46: MCNP-, ANISN- and ONEDANT-calculations with FENDL-1, JENDL-3, BROND and ENDF/B-VI data for IPPE iron shell experiments - S. P. Simakov, IPPE Obninsk

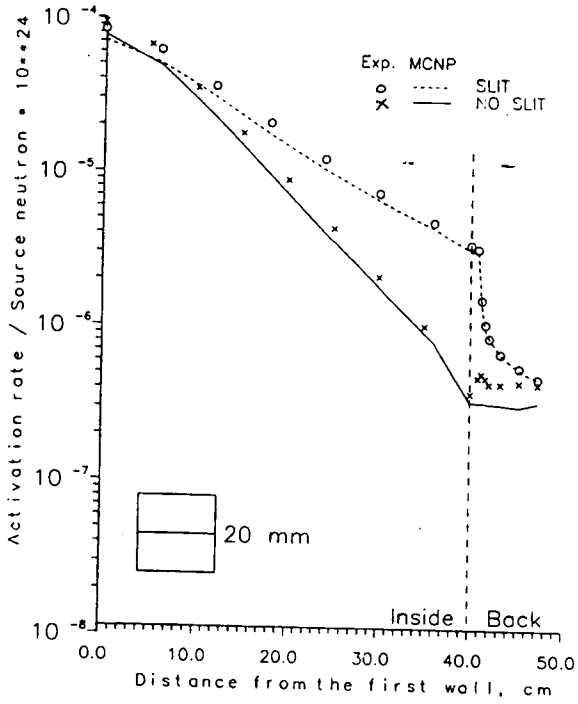

Fig. ^{115}In activation rate distribution for a straight slit 20 mm wide in iron shield 40 cm thick.

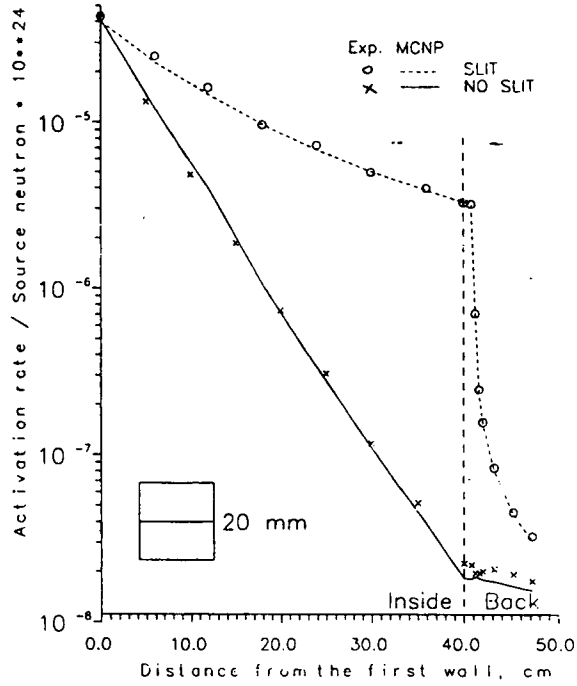

Fig. ^{56}Fe activation rate distribution for a straight slit 20 mm wide in iron shield 40 cm thick.

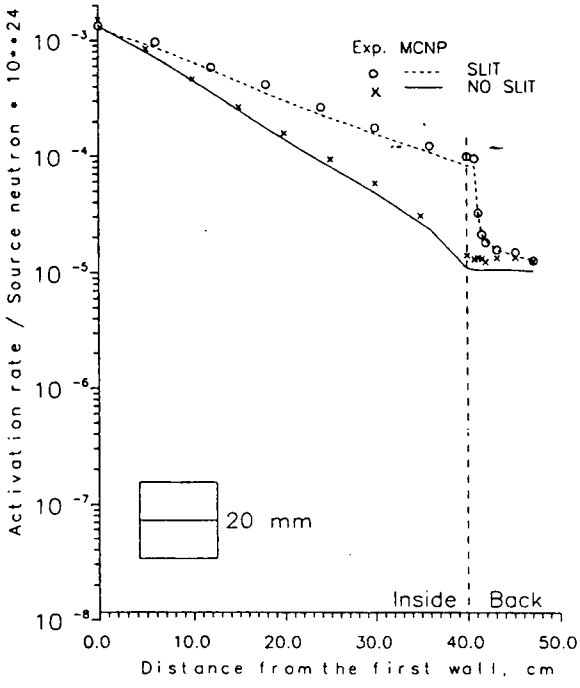

Fig. ^{237}Np activation rate distribution for a straight slit 20 mm wide in iron shield 40 cm thick.

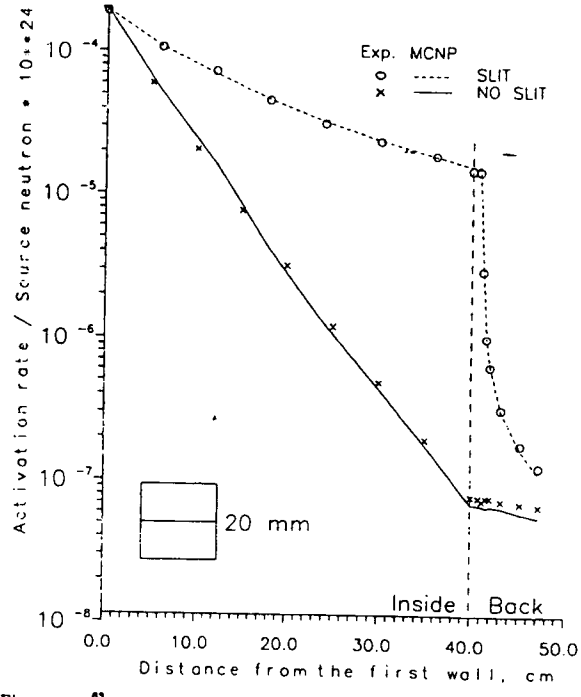

Fig. ^{63}Cu activation rate distribution for a straight slit 20 mm wide in iron shield 40 cm thick.

Fig. 47: MCNP -calculations with FENDL-1 data for KIAE iron shield experiment with and without straight gap - D. V. Markovskij, KIAE Moscow.

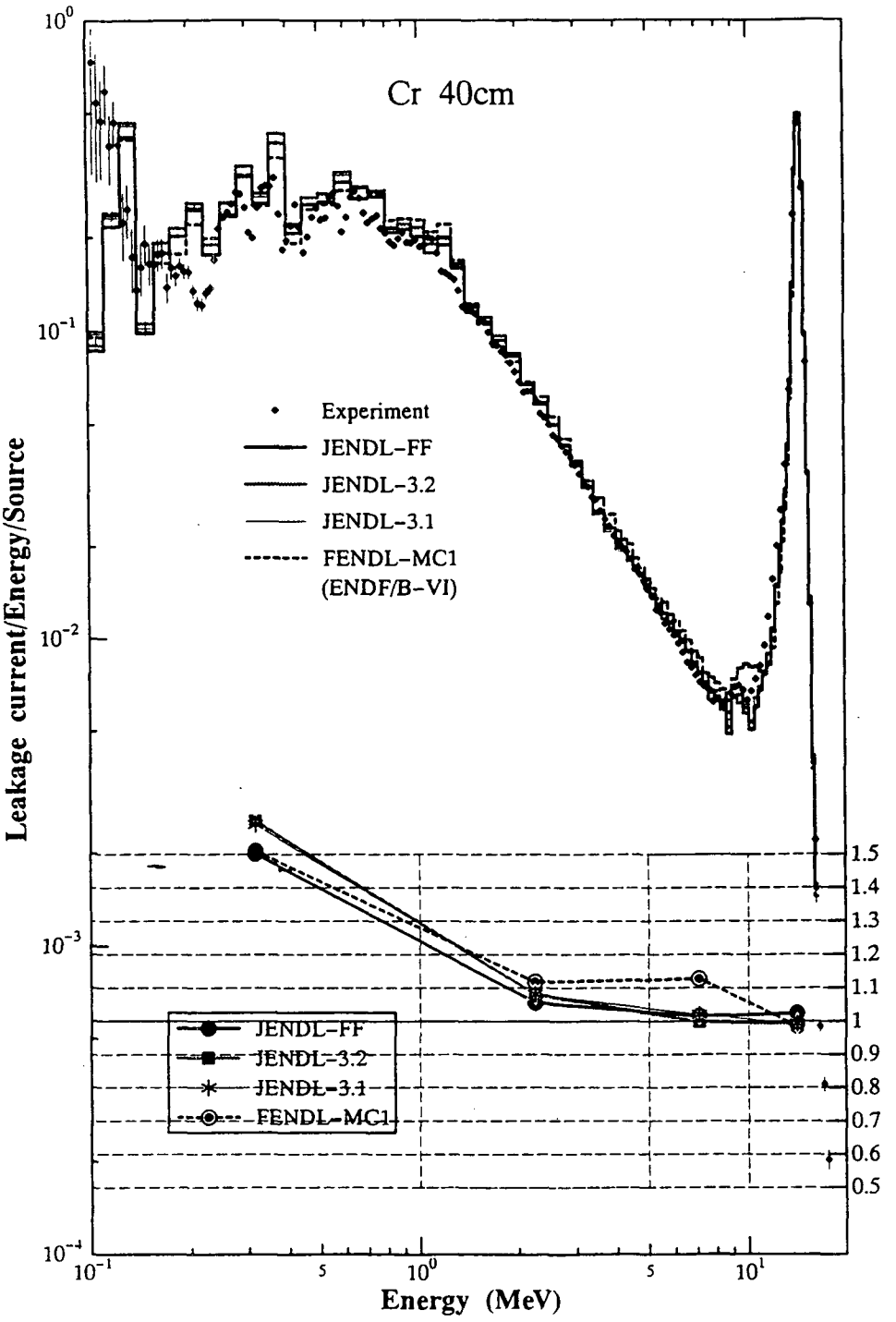

Fig. 48: MCNP -calculations with FENDL-1 and JENDL-3 data for OKTAVIAN chromium spherical shell experiment - C. Ichihara, University of Kyoto

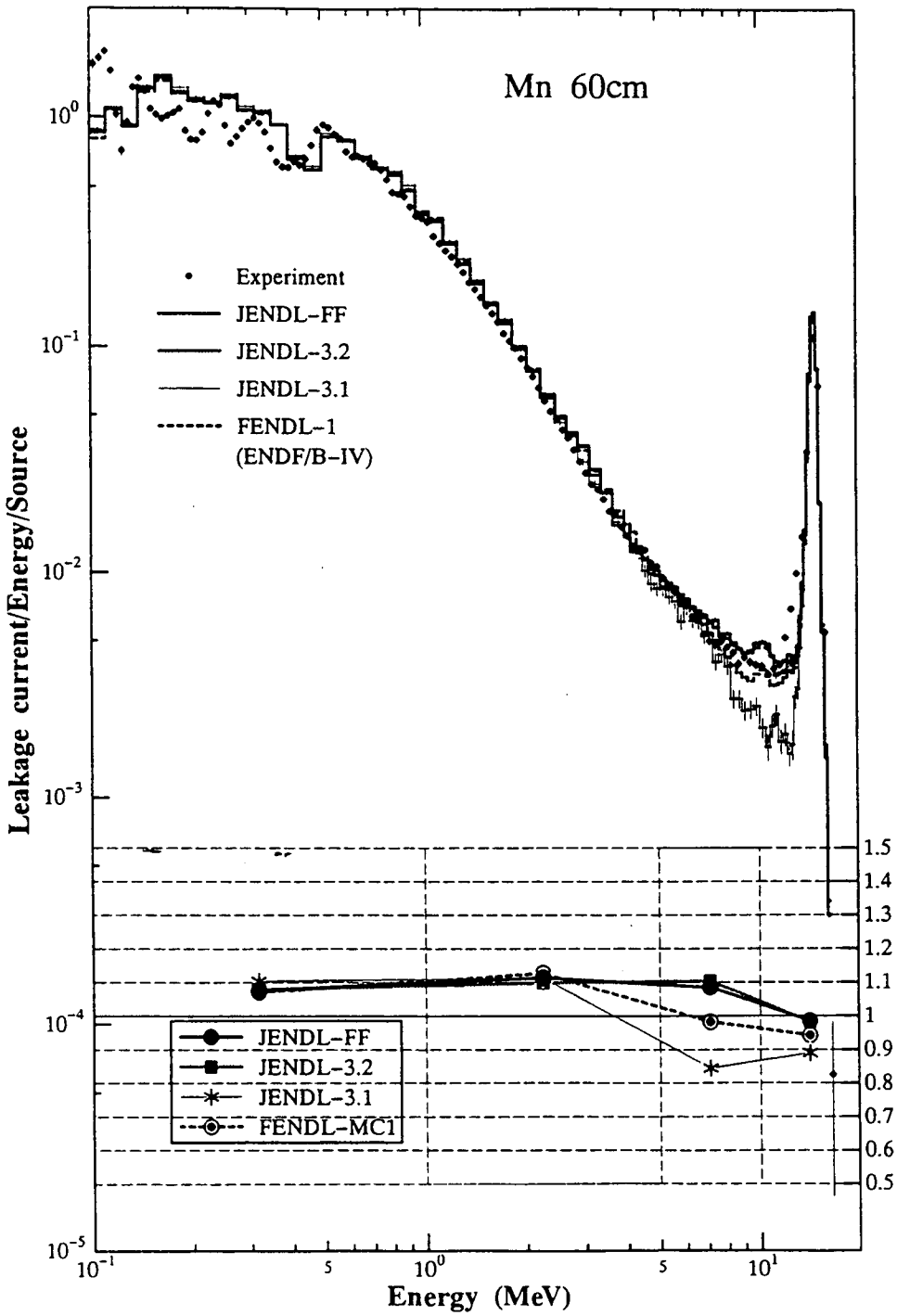

Fig. 49: MCNP -calculations with FENDL-1 and JENDL-3 data for OKTAVIAN manganese spherical shell experiment - C. Ichihara, University of Kyoto

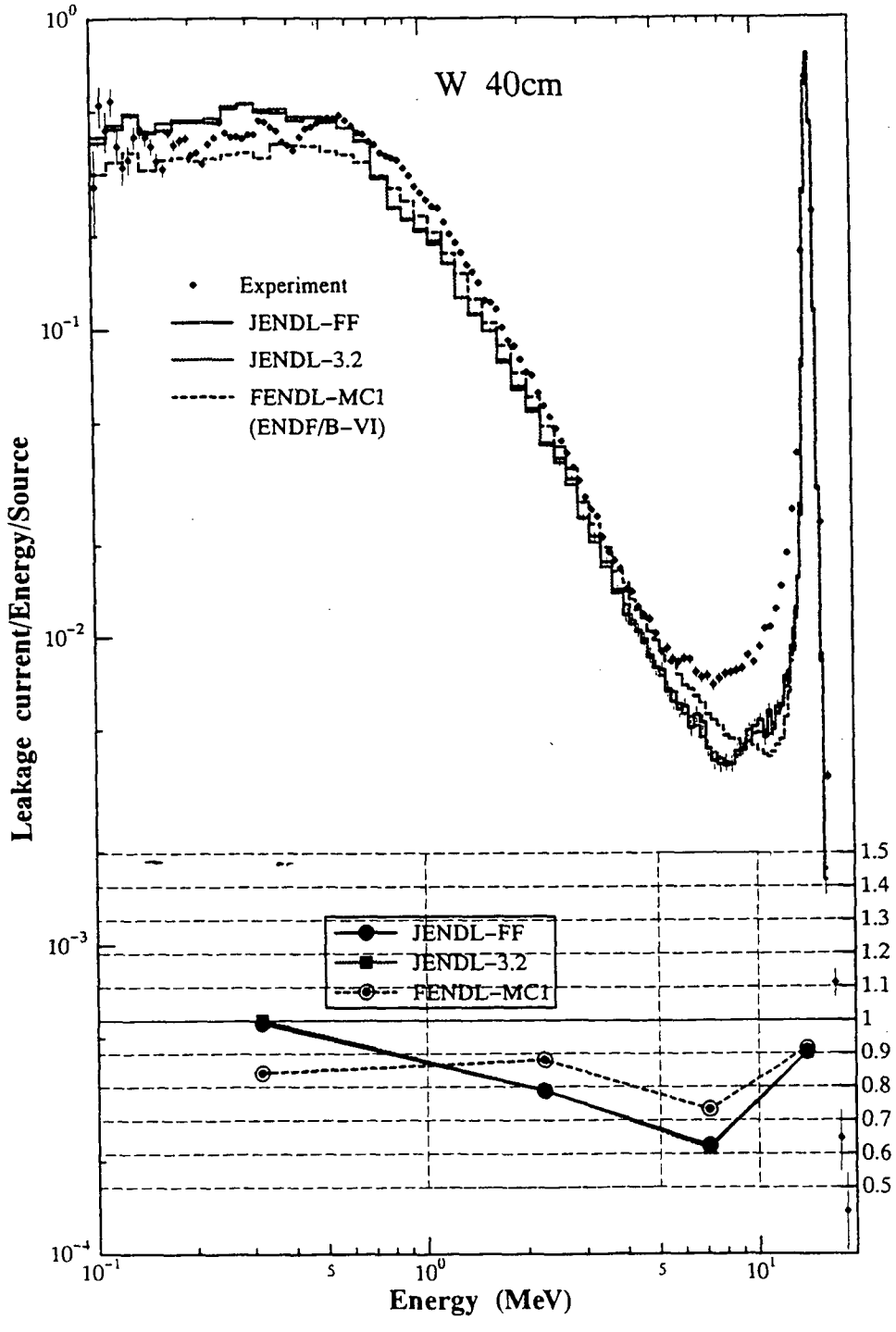

Fig. 50: MCNP -calculations with FENDL-1 and JENDL-3 data for OKTAVIAN tungsten spherical shell experiment - C. Ichihara, University of Kyoto

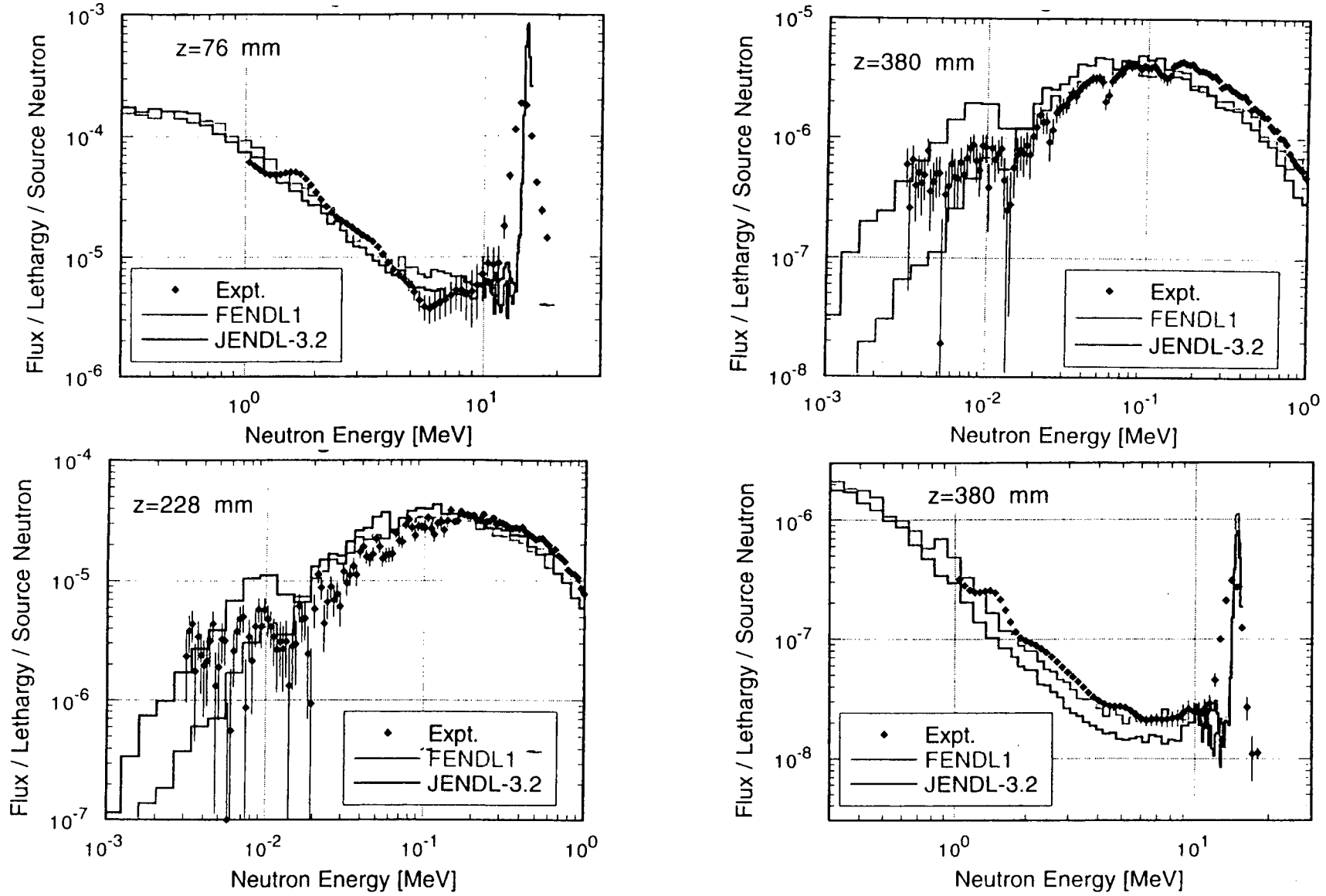

Fig. 51: MCNP-calculations with FENDL-1 and JENDL-3.2 data for neutron spectra inside FNS W cylindrical slabs
- F. Maekawa, Y. Oyama, M. Wada -FNS/JAERI

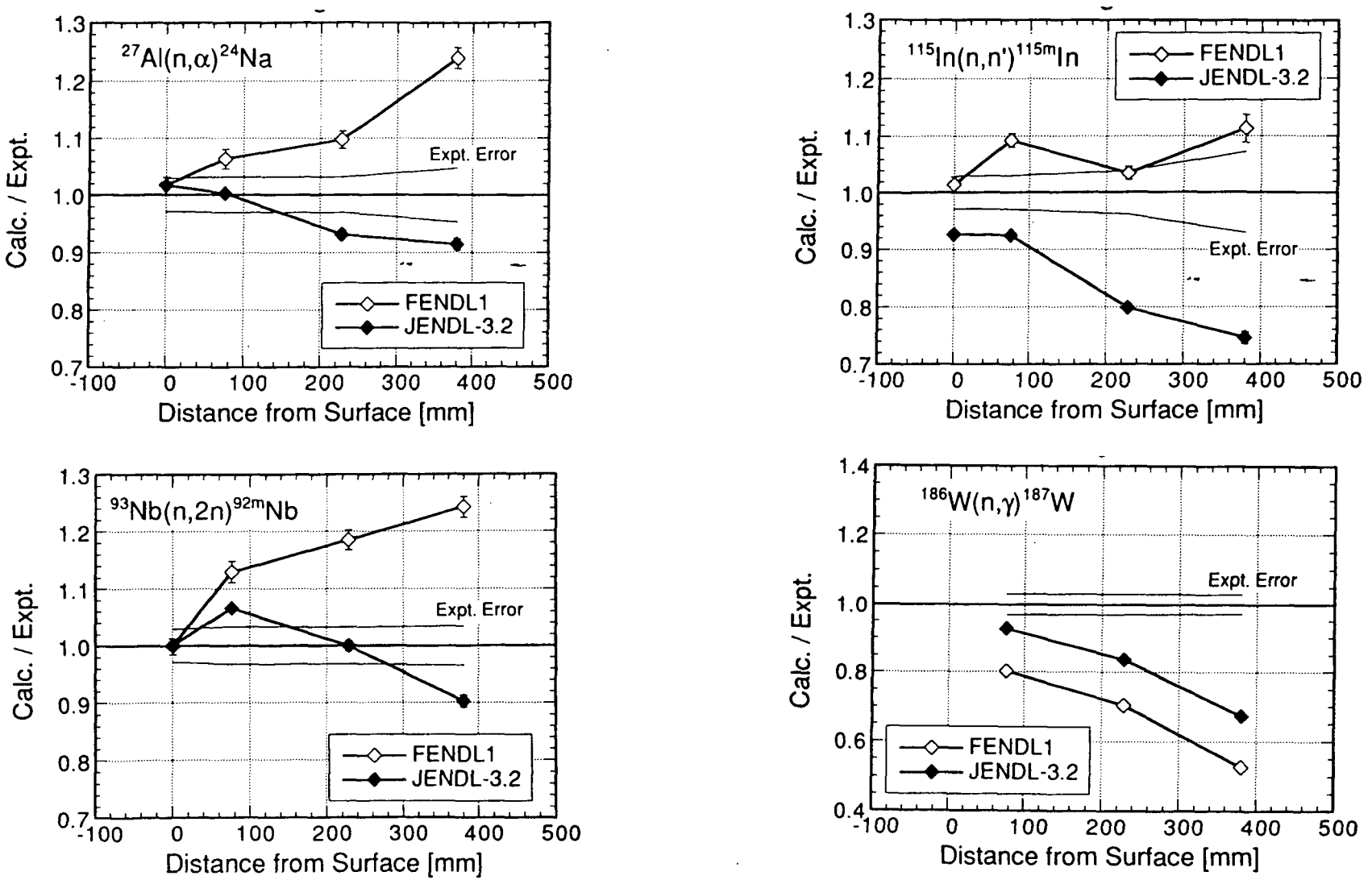

Fig. 52: MCNP-calculations with FENDL-1 and JENDL-3.2 data for reaction rates inside FNS W cylindrical slabs
- F. Maekawa, Y. Oyama, M. Wada -FNS/JAERI

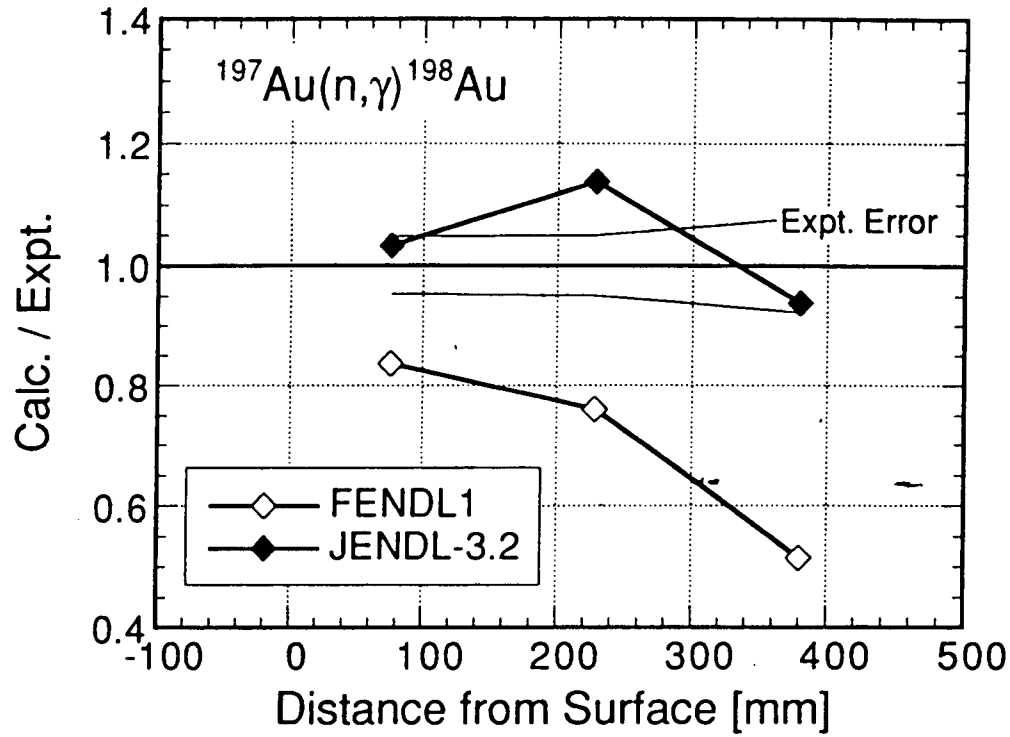

Fig. 53: MCNP-calculations with FENDL-1 and JENDL-3.2 data for reaction rates inside FNS W cylindrical slabs
- F. Maekawa, Y. Oyama, M. Wada -FNS/JAERI

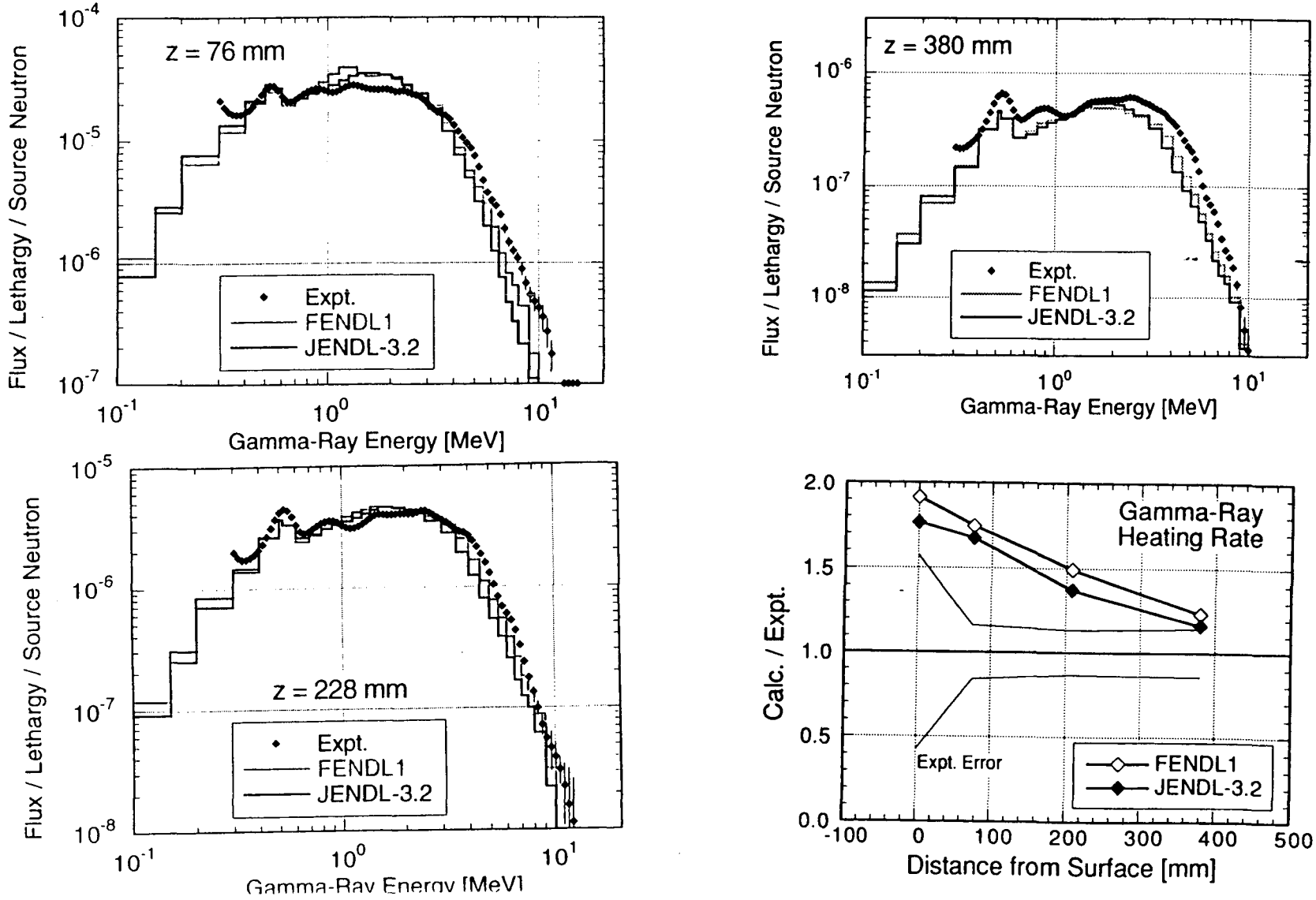

Fig. 54: MCNP-calculations with FENDL-1 and JENDL-3.2 data for gamma ray spectra and heating rates inside FNS W cylindrical slabs - F. Maekawa, Y. Oyama, M. Wada -FNS/JAERI

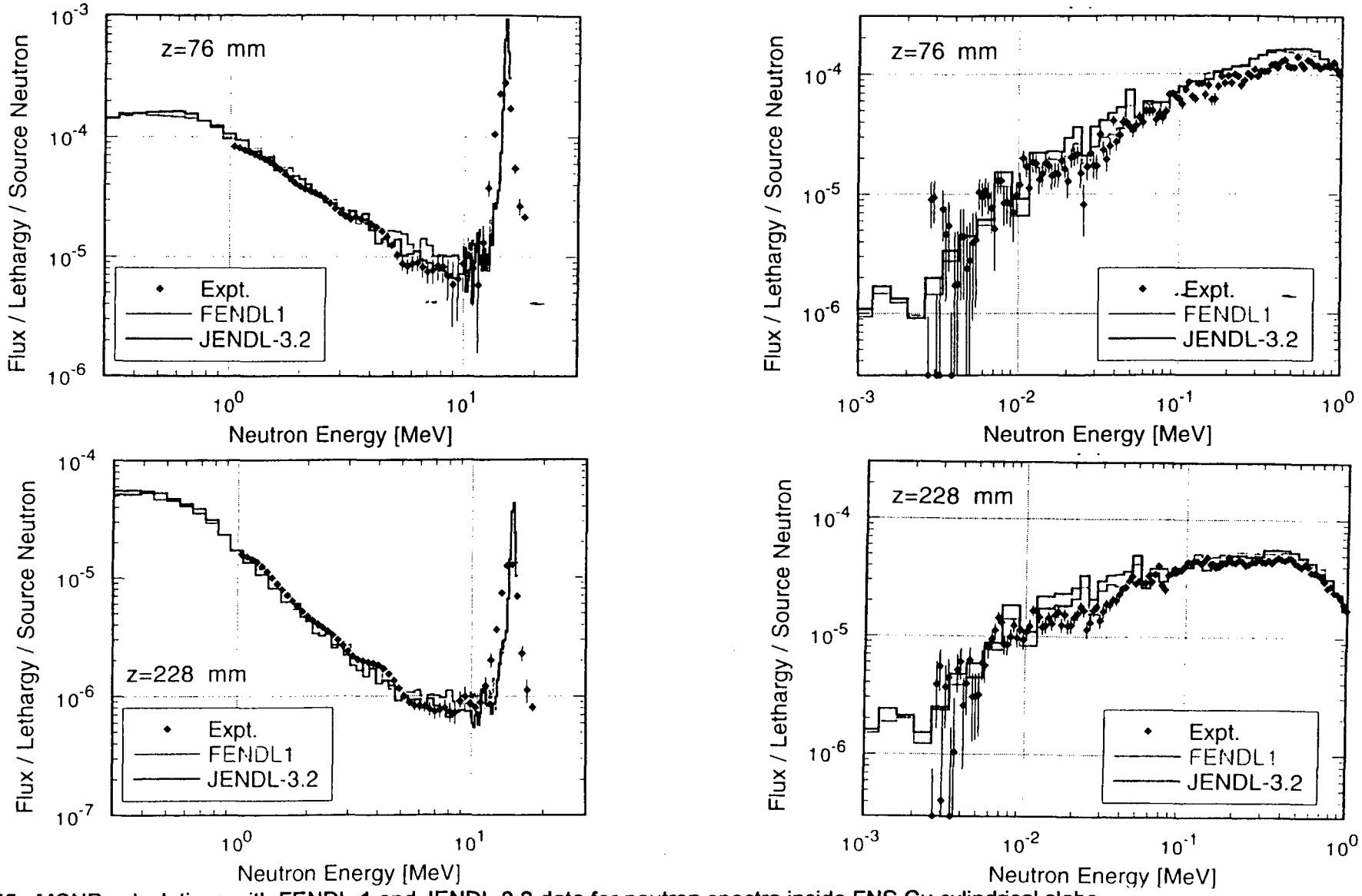

Fig. 55: MCNP-calculations with FENDL-1 and JENDL-3.2 data for neutron spectra inside FNS Cu cylindrical slabs
- F. Maekawa, Y. Oyama, M. Wada -FNS/JAERI

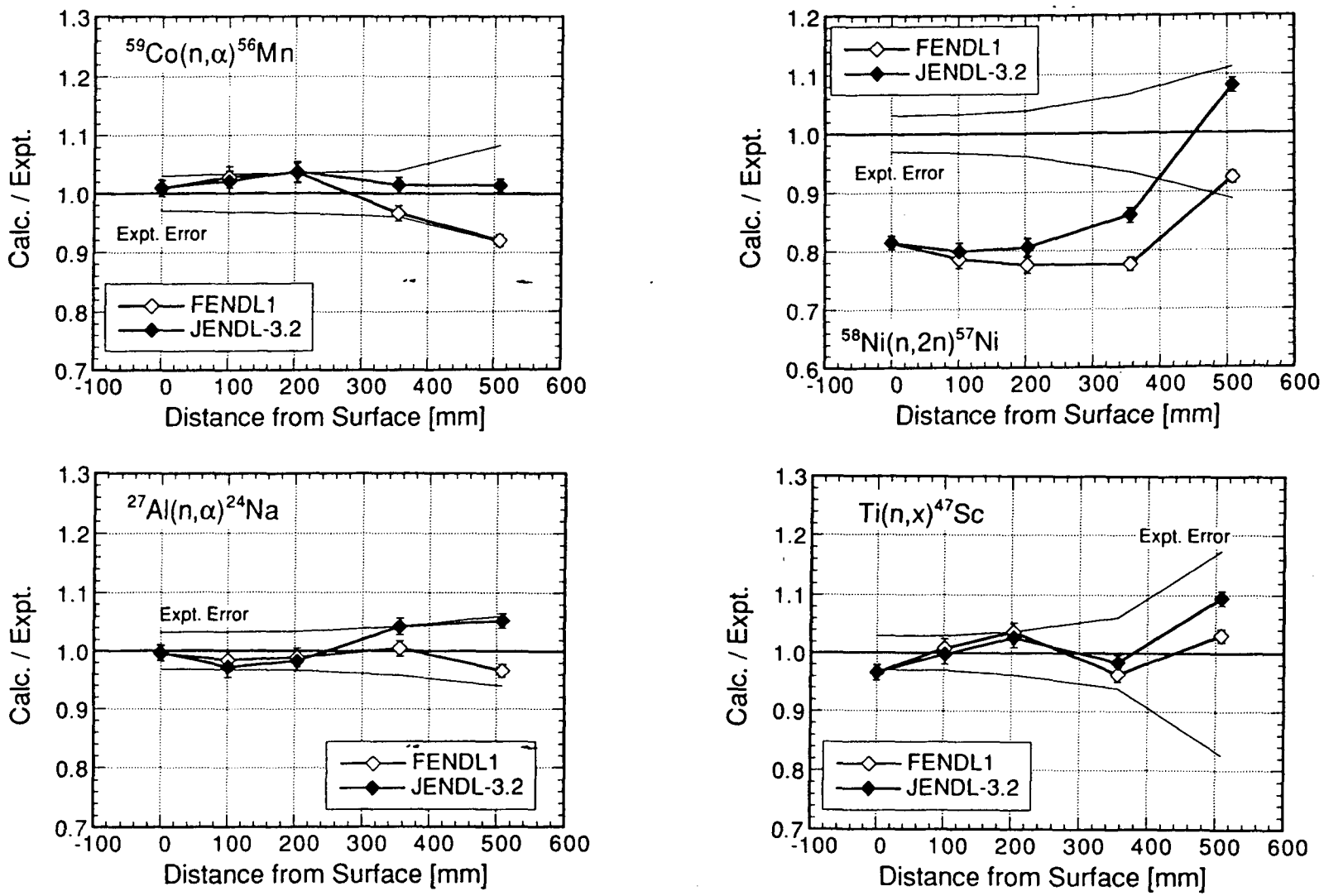

Fig. 56: MCNP-calculations with FENDL-1 and JENDL-3.2 data for reaction rates inside FNS Cu cylindrical slabs
- F. Maekawa, Y. Oyama, M. Wada -FNS/JAERI

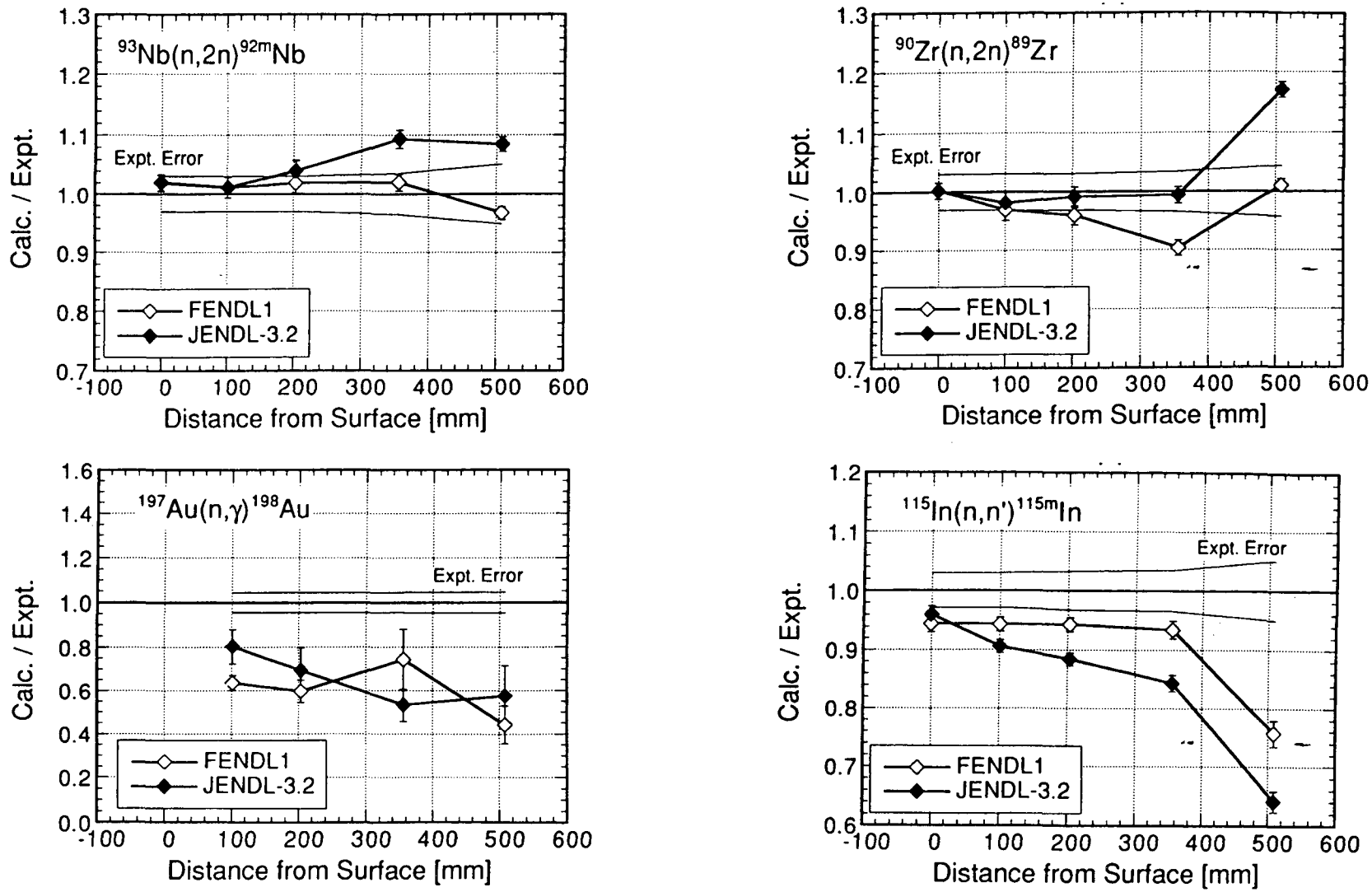

Fig. 57: MCNP-calculations with FENDL-1 and JENDL-3.2 data for reaction rates inside FNS Cu cylindrical slabs
- F. Maekawa, Y. Oyama, M. Wada -FNS/JAERI

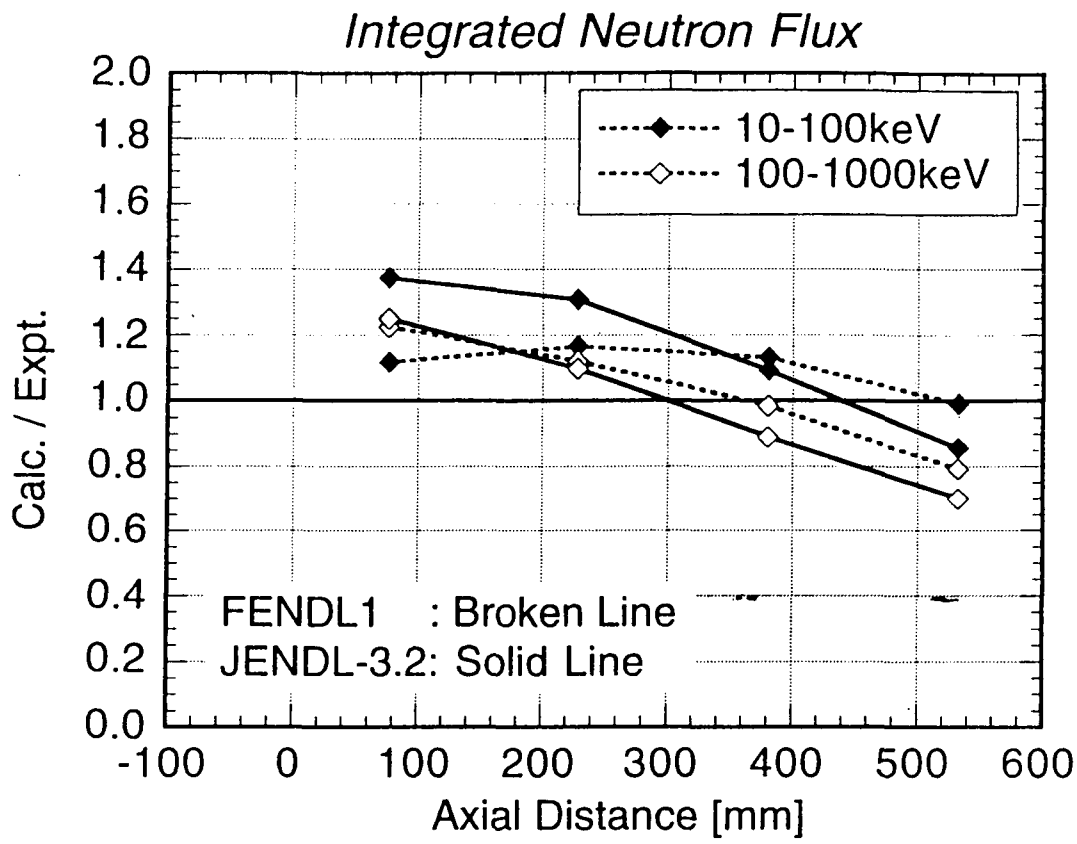

Fig. 58: MCNP-calculations with FENDL-1 and JENDL-3.2 data for neutron spectra inside FNS Cu cylindrical slabs
- F. Maekawa, Y. Oyama, M. Wada -FNS/JAERI

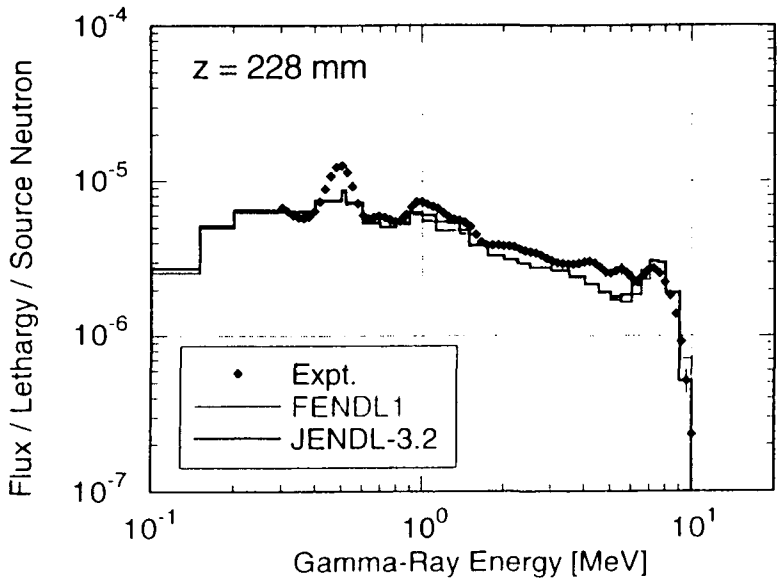

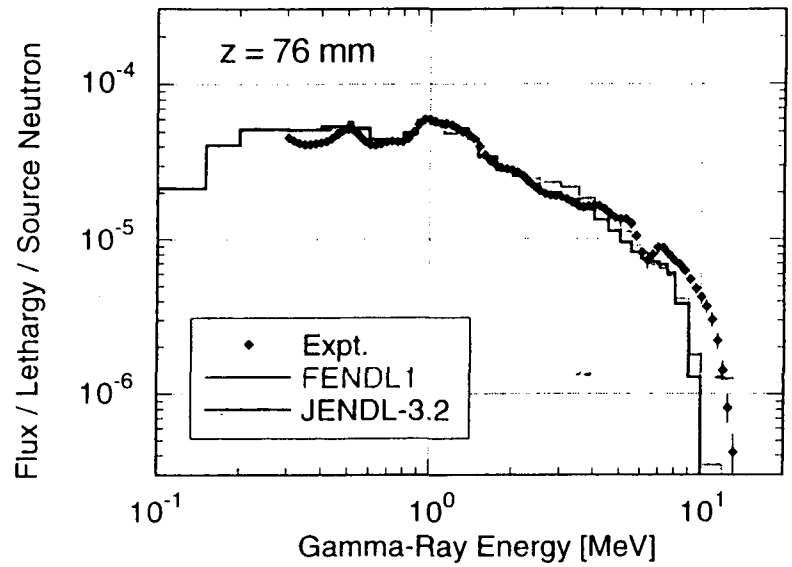

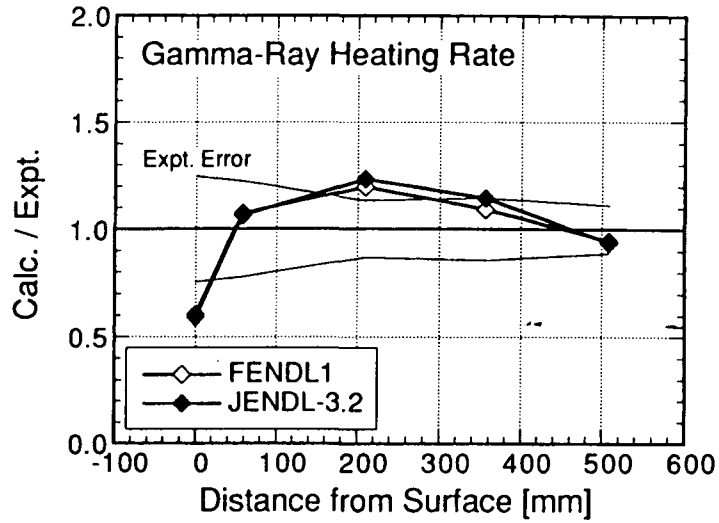

Fig. 59: MCNP-calculations with FENDL-1 and JENDL-3.2 data for gamma ray spectra and heating rates inside FNS Cu cylindrical slabs
- F. Maekawa, Y. Oyama, M. Wada, -FNS/JAERI

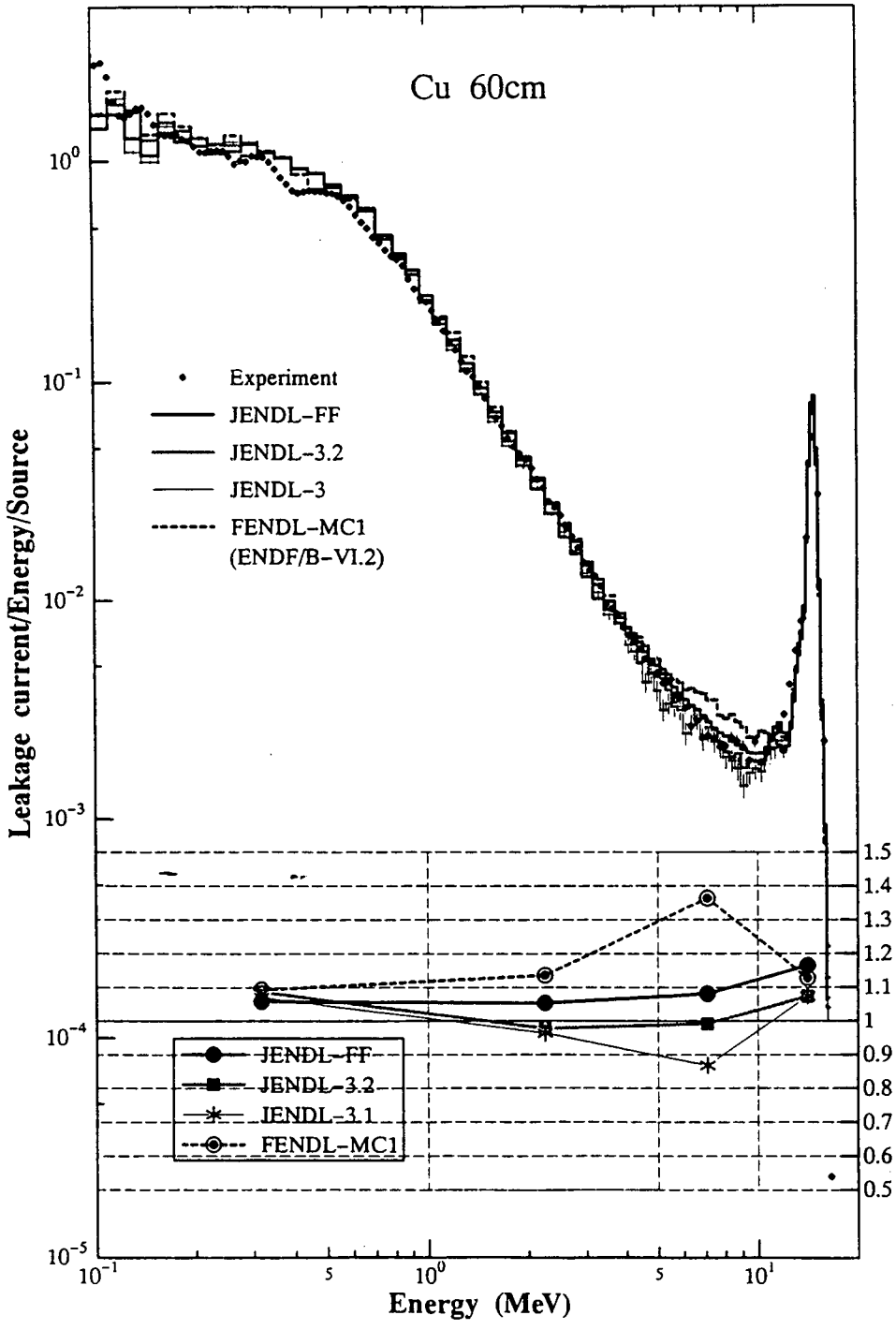

Fig. 60: MCNP -calculations with FENDL-1 and JENDL-3 data for OKTAVIAN copper spherical shell experiment - C. Ichihara, University of Kyoto

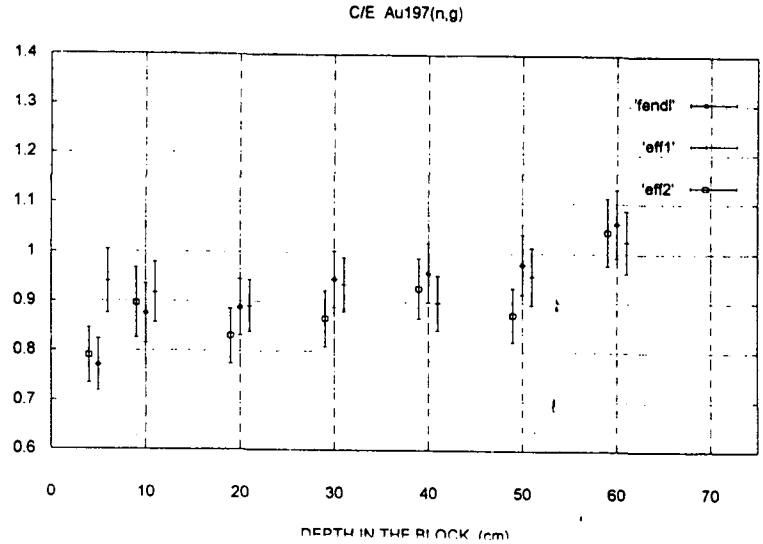

Fig. 61a: MCNP -calculations with FENDL-1, EFF-1 and -2 data for FNG SS-316 shield experiment - V. Rado, L. Petrizzi, P. Batistoni - ENEA Frascati

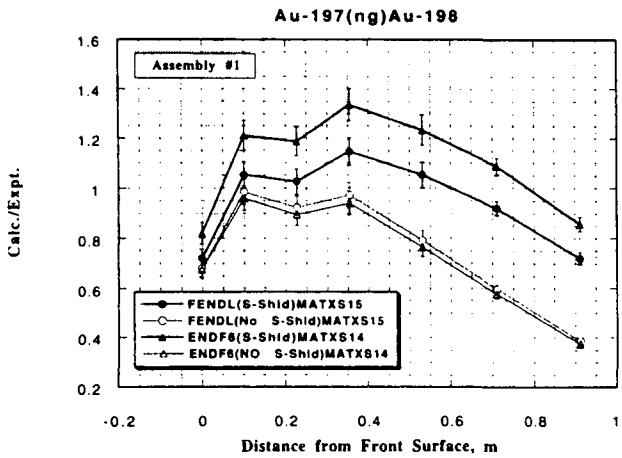

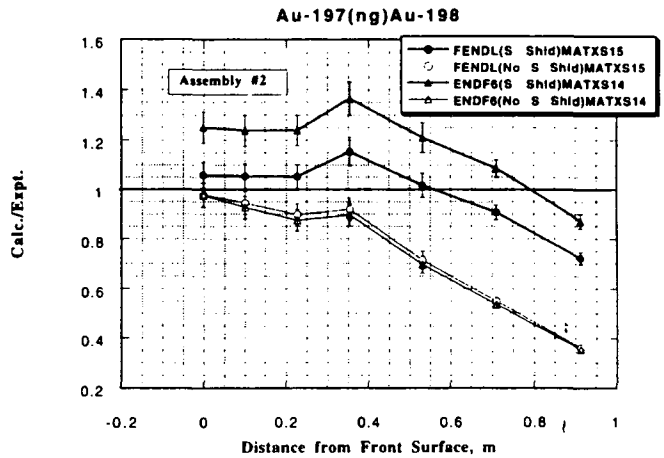

Fig. 61b, c: DORT -calculations with FENDL-1 and ENDF/B-VI data for FNS SS-316 shield experiments - M. Youssef, UCLA

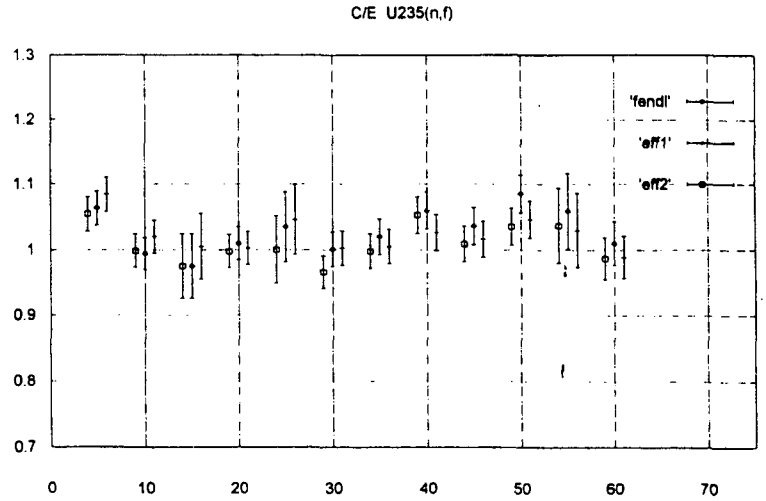

Fig. 62 a: MCNP -calculations with FENDL-1, EFF-1 and -2 data for FNG SS-316 shield experiment - V. Rado, L. Petrizzi, P. Batistoni - ENEA Frascati

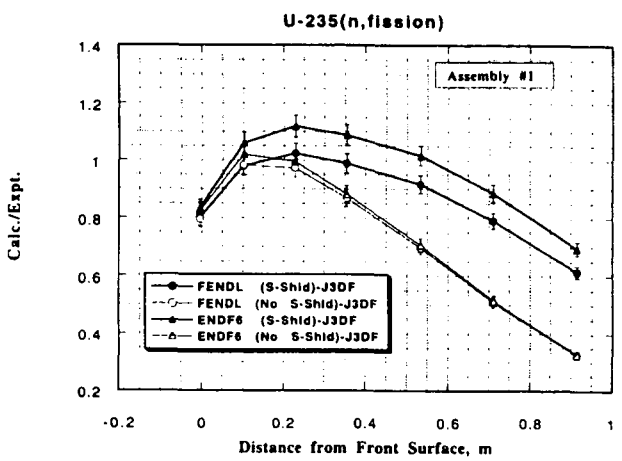

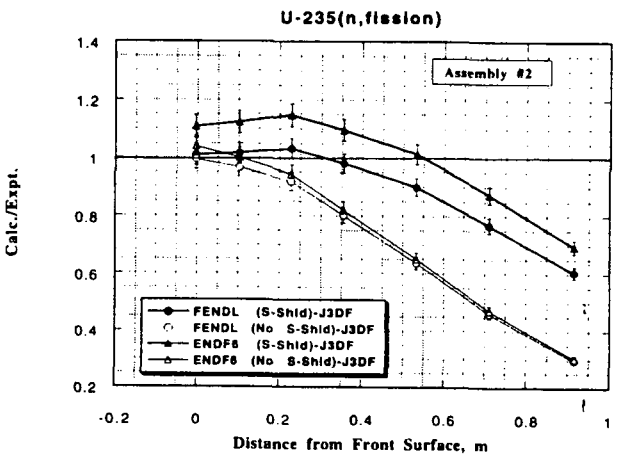

Fig. 62 b, c: DORT -calculations with FENDL-1 and ENDF/B-VI data for FNS SS-316 shield experiments - M. Youssef, UCLA

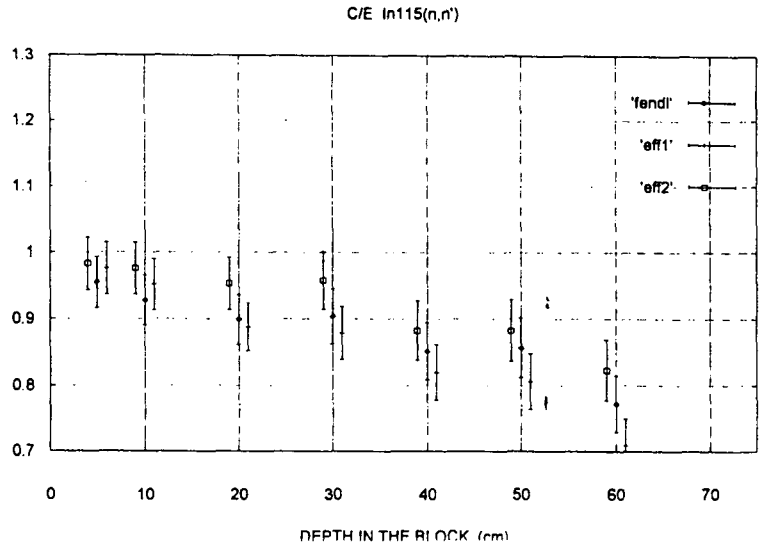

Fig. 63 a: MCNP -calculations with FENDL-1, EFF-1 and -2 data for FNG SS-316 shield experiment - V. Rado, L. Petrizzi, P. Batistoni - ENEA Frascati

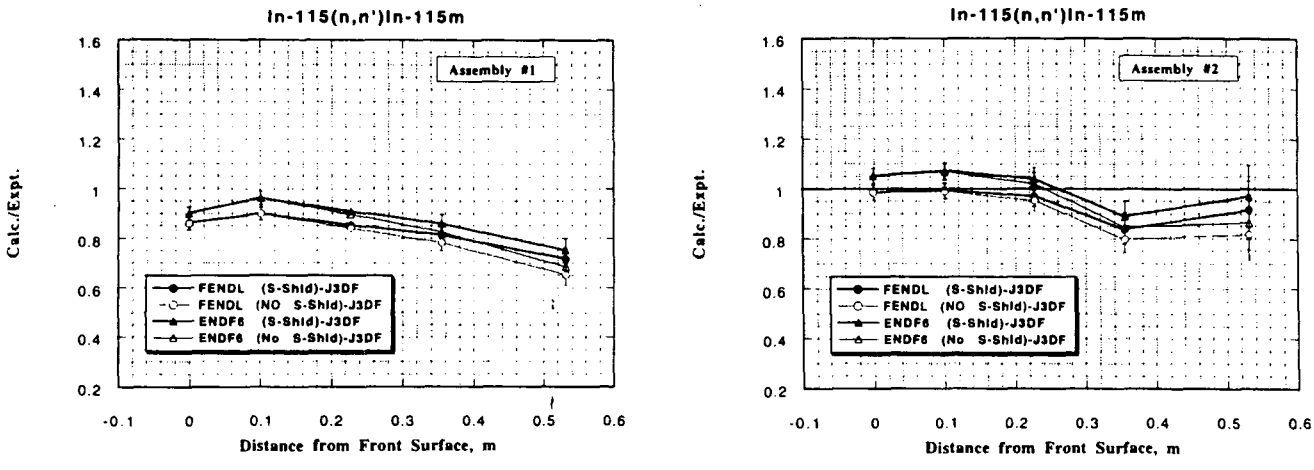

Fig. 63b, c: DORT -calculations with FENDL-1 and ENDF/B-VI data for FNS SS-316 shield experiments - M. Youssef, UCLA

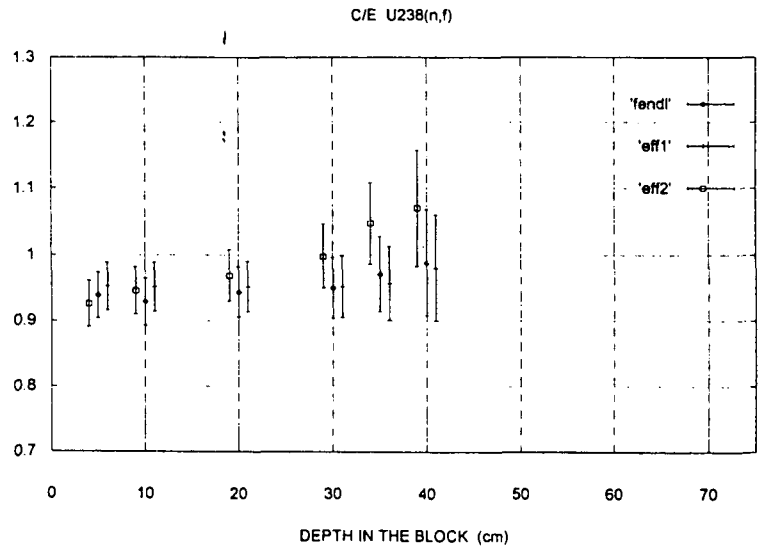

Fig. 64 a: MCNP -calculations with FENDL-1, EFF-1 and -2 data for FNG SS-316 shield experiment - V. Rado, L. Petrizzi, P. Batistoni - ENEA Frascati

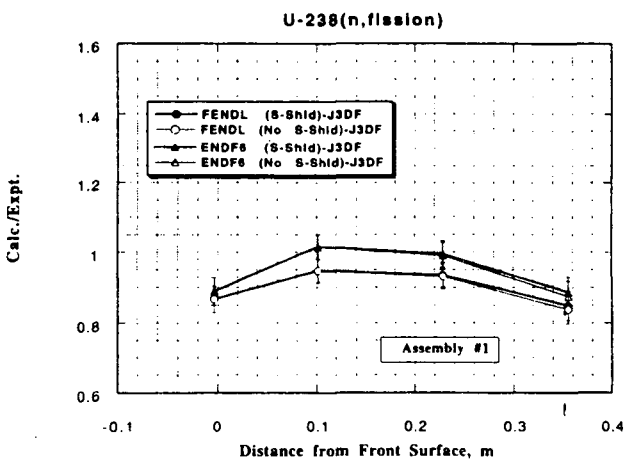

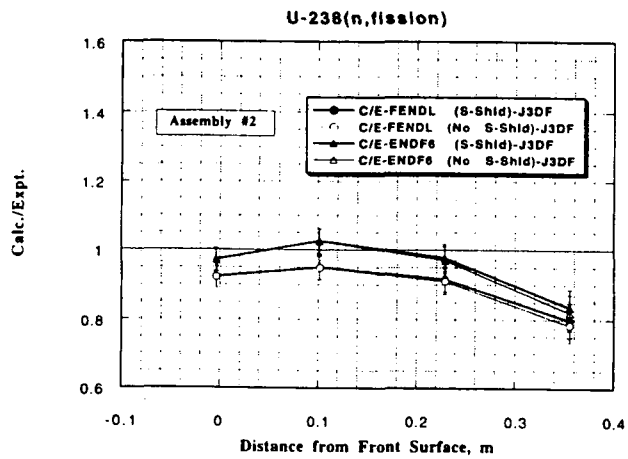

Fig. 64 b, c: DORT -calculations with FENDL-1 and ENDF/B-VI data for FNS SS-316 shield experiments - M. Youssef, UCLA

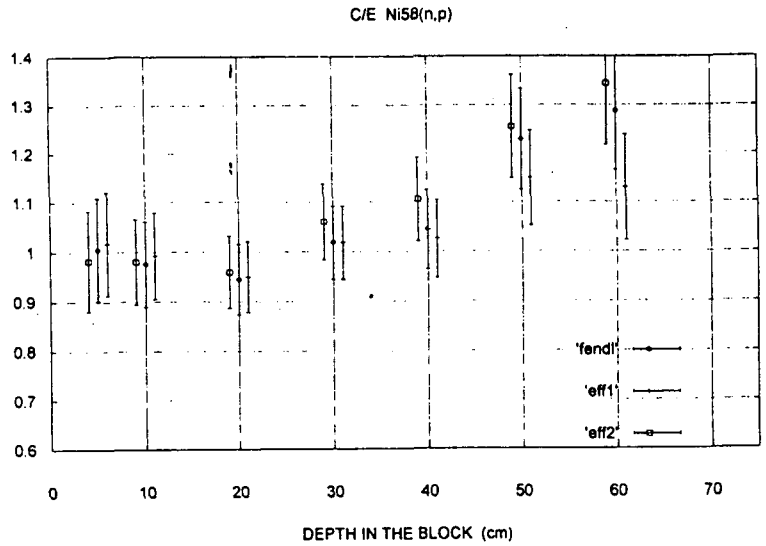

Fig. 65 a: MCNP -calculations with FENDL-1, EFF-1 and -2 data for FNG SS-316 shield experiment - V. Rado, L. Petrizzi, P. Batistoni - ENEA Frascati

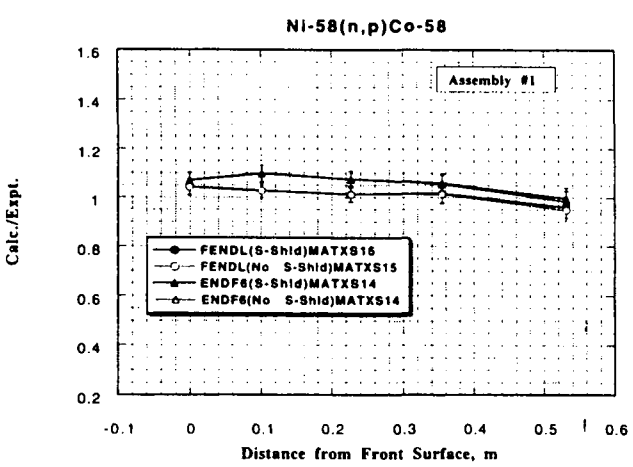

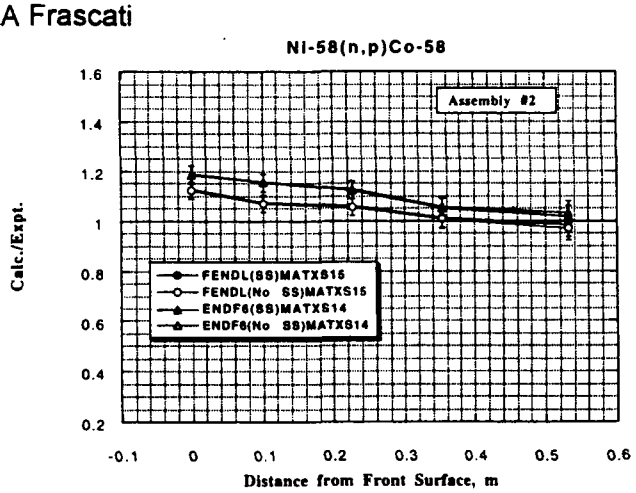

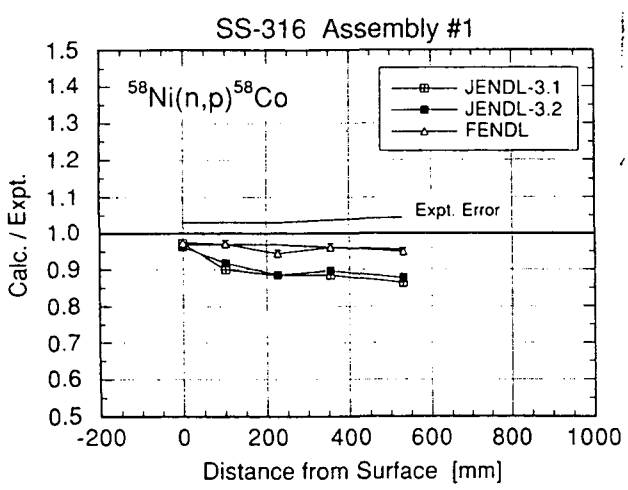

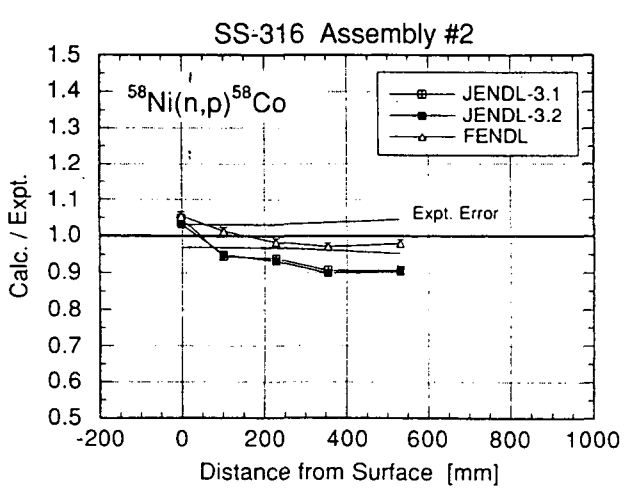

Fig. 65 b- e: DORT and MCNP-calculations with FENDL-1, ENDF/B-VI and JENDL-3 data for FNS SS-316 shield experiments - M. Youssef, UCLA; Y. Oyama, JAERI

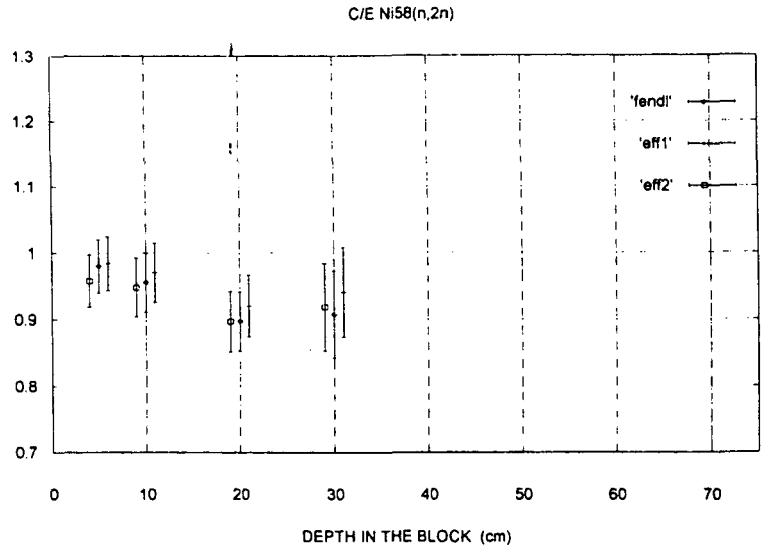

Fig. 66 a: MCNP -calculations with FENDL-1, EFF-1 and -2 data for FNG SS-316 shield experiment - V. Rado, L. Petrizzi, P. Batistoni - ENEA Frascati

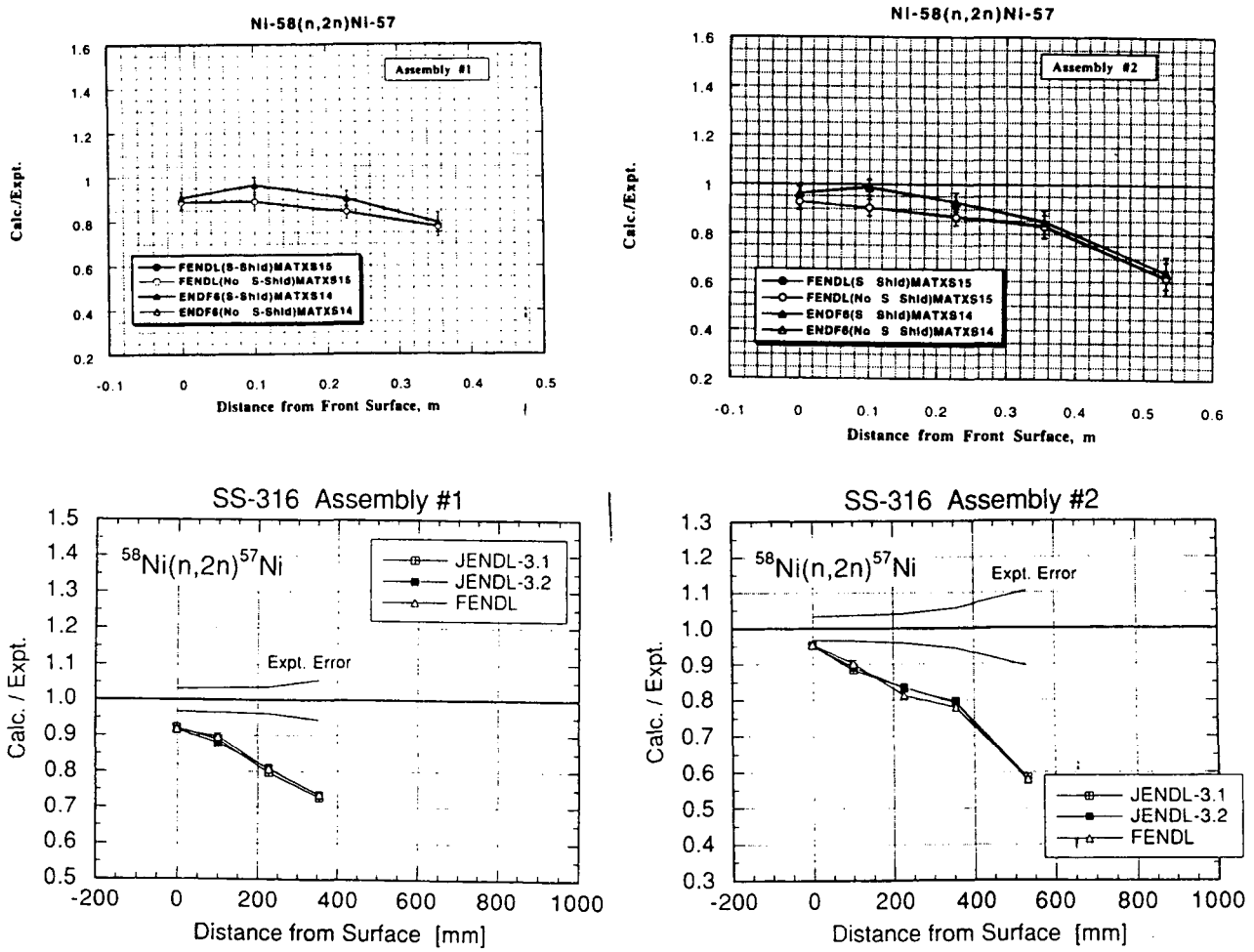

Fig. 66 b- e: DORT and MCNP-calculations with FENDL-1, ENDF/B-VI and JENDL-3 data for FNS SS-316 shield experiments - M. Youssef, UCLA; Y. Oyama, JAERI

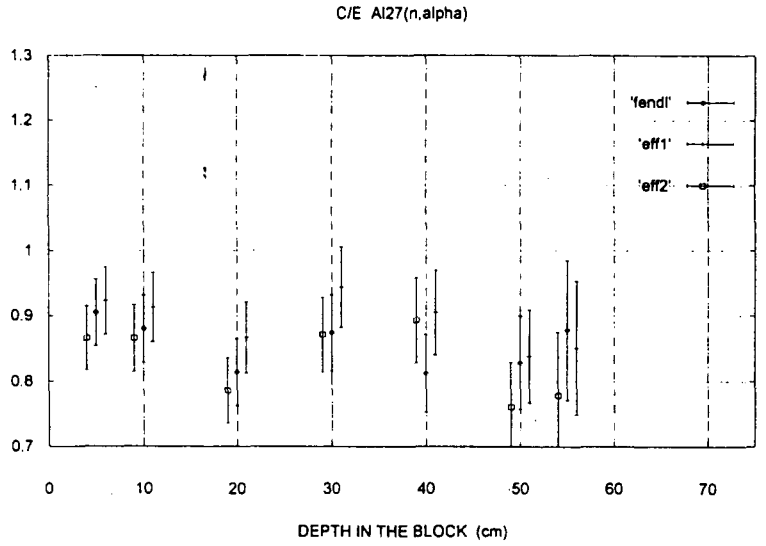

Fig. 67a: MCNP -calculations with FENDL-1, EFF-1 and -2 data for FNG SS-316 shield experiment - V. Rado, L. Petrizzi, P. Batistoni - ENEA Frascati

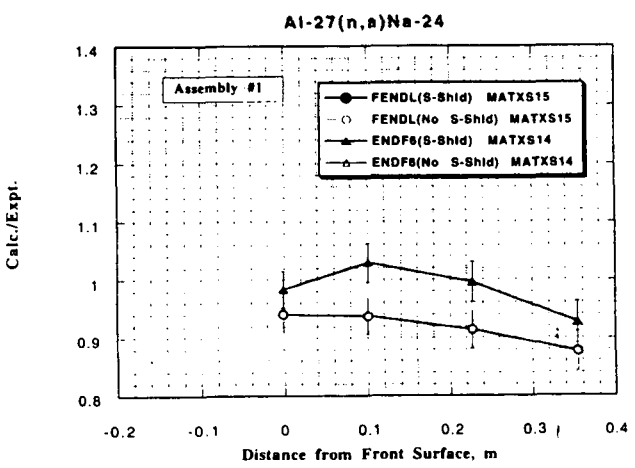

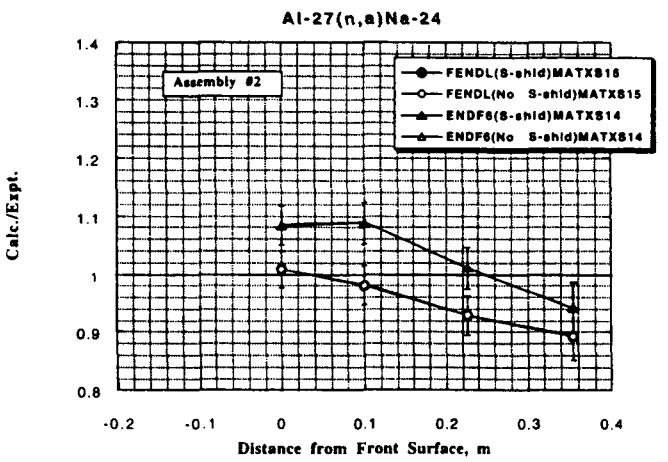

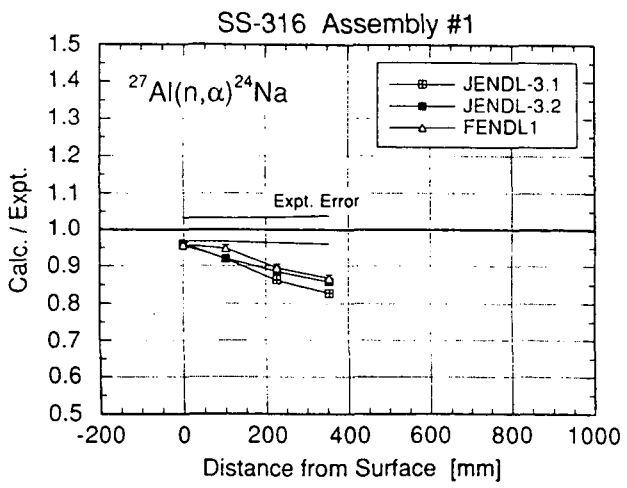

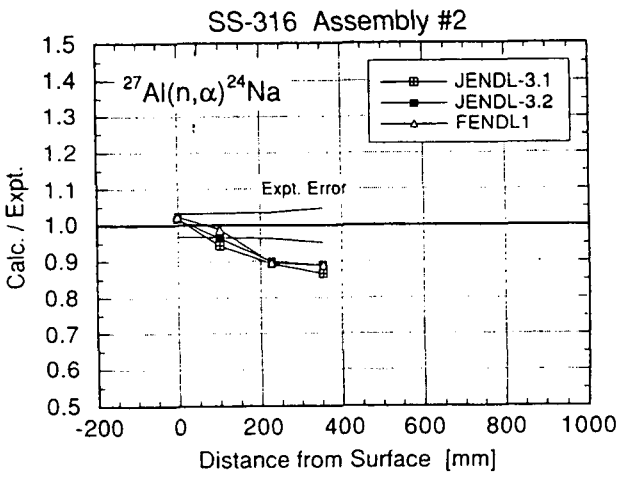

Fig. 67b - e: DORT and MCNP-calculations with FENDL-1, ENDF/B-VI and JENDL-3 data for FNS SS-316 shield experiments - M. Youssef, UCLA; Y. Oyama, JAERI

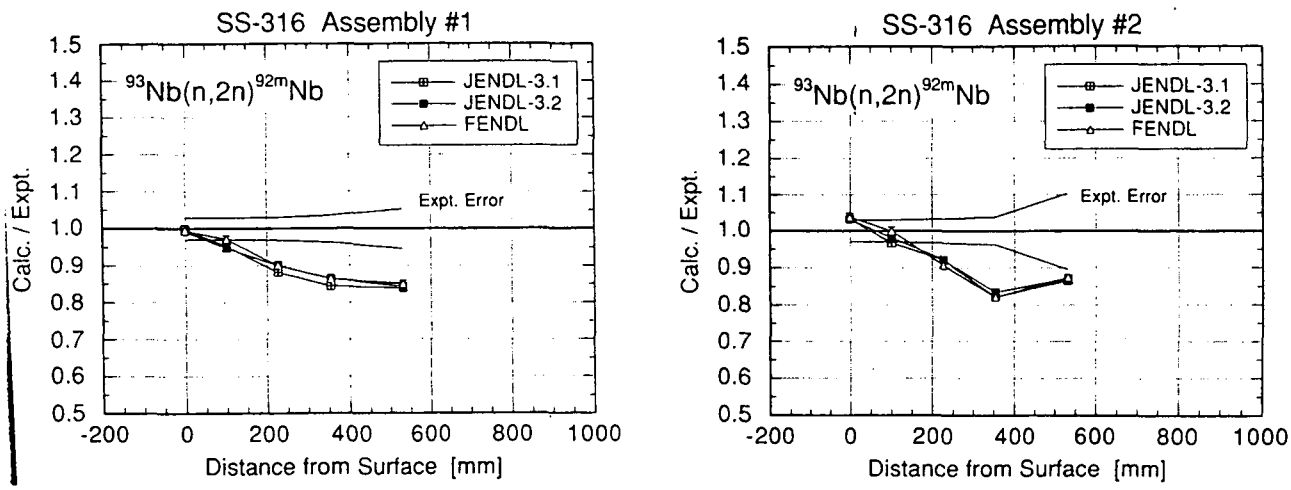

Fig. 68a, b: MCNP-calculations with FENDL-1 and JENDL-3 data for FNS SS-316 shield experiments - Y. Oyama, JAERI

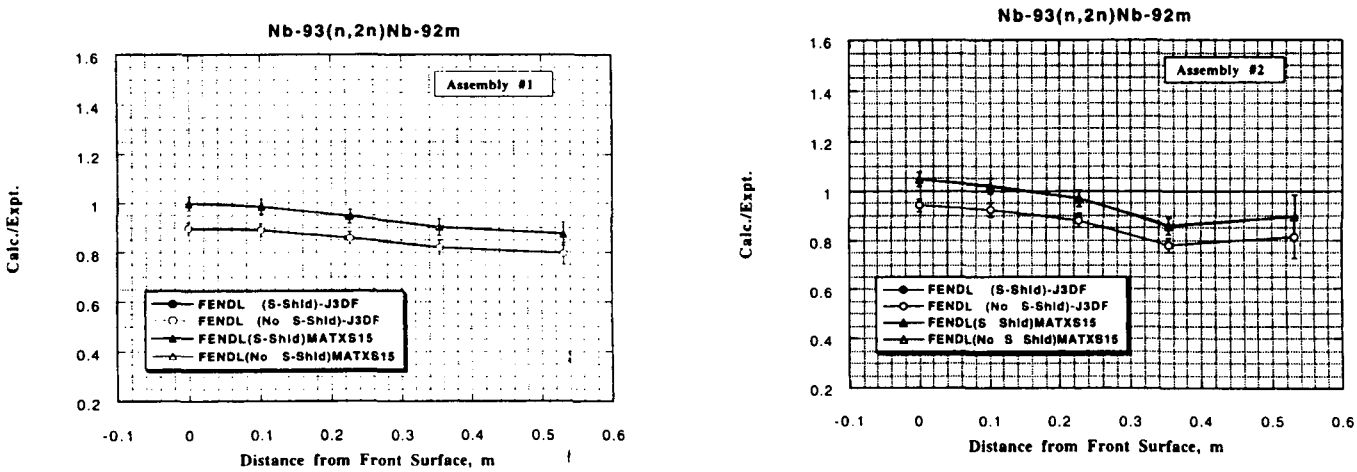

Fig. 68c, d: DORT-calculations with FENDL-1 and ENDF/B-VI data for FNS SS-316 shield experiments - M. Youssef, UCLA

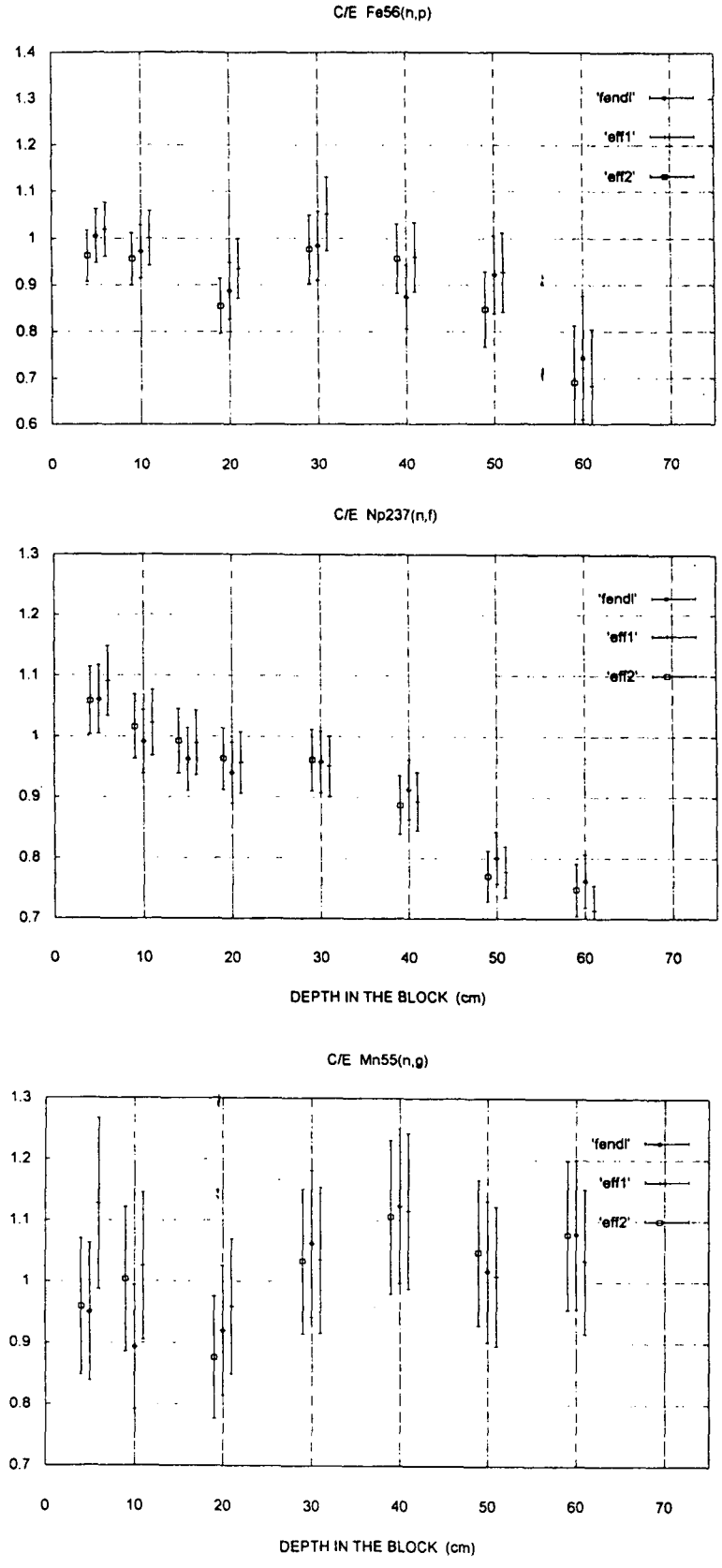

Fig. 69: MCNP-calculations with FENDL-1, EFF-1 and -2 data for FNG SS-316 shield experiment
- V. Rado, L. Petrizzi, P. Batistoni - ENEA Frascati

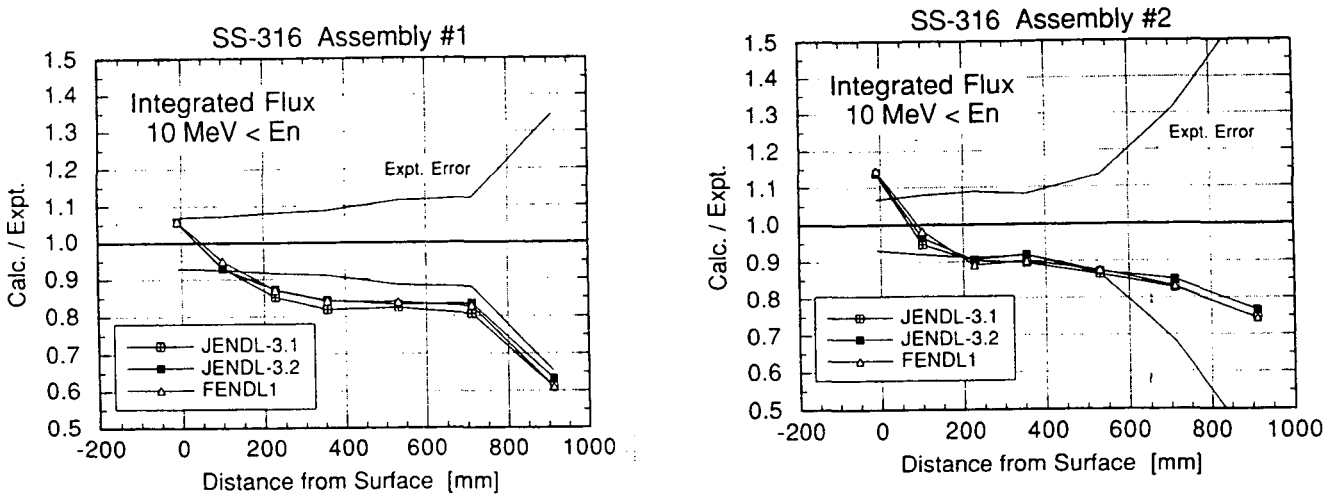

Fig. 70 a, b: MCNP-calculations with FENDL-1 and JENDL-3 data for FNS SS-316 shield experiments - Y. Oyama, JAERI

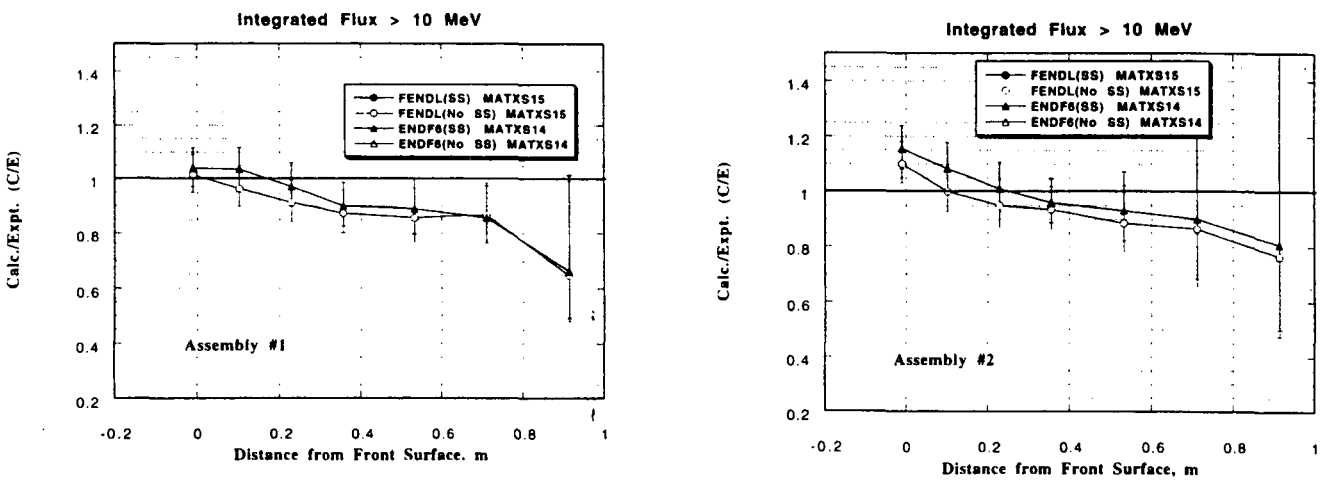

Fig. 70c, d: DORT-calculations with FENDL-1 and ENDF/B-VI data for FNS SS-316 shield experiments - M. Youssef, UCLA

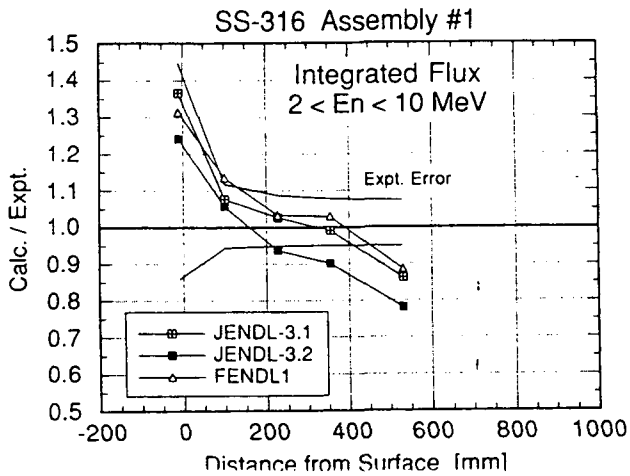

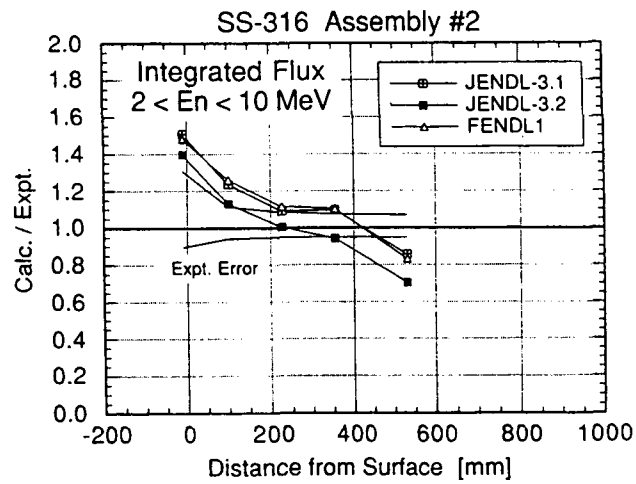

Fig. 71a, b: MCNP-calculations with FENDL-1 and JENDL-3 data for FNS SS-316 shield experiments - Y. Oyama, JAERI

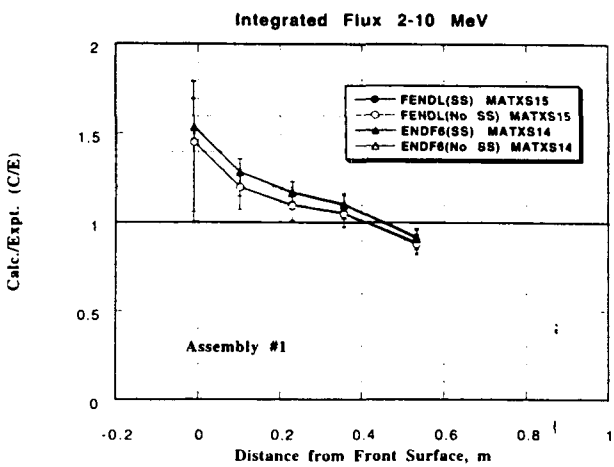

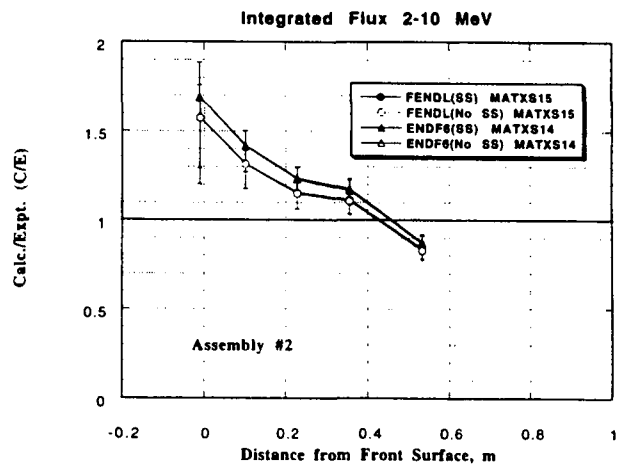

Fig. 71c, d: DORT-calculations with FENDL-1 and ENDF/B-VI data for FNS SS-316 shield experiments - M. Youssef, UCLA

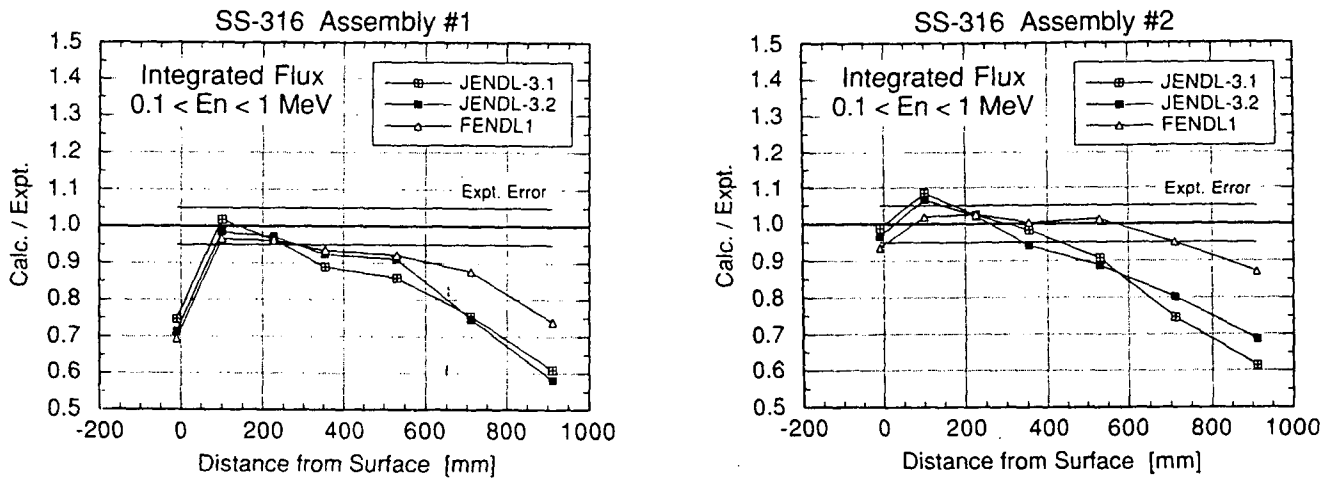

Fig. 72a, b: MCNP-calculations with FENDL-1 and JENDL-3 data for FNS SS-316 shield experiments - Y. Oyama, JAERI

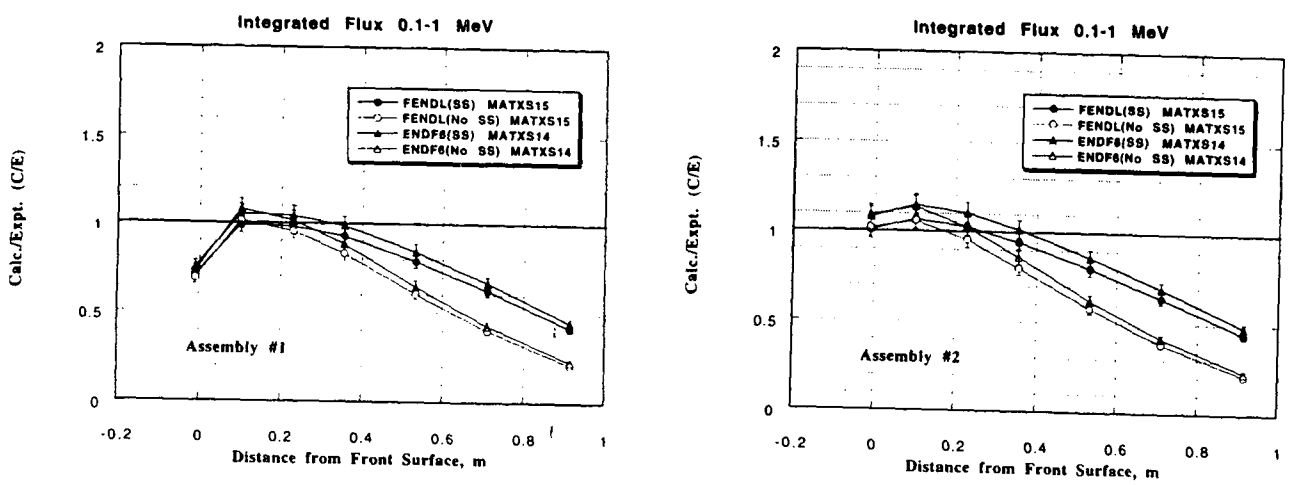

Fig. 72c, d: DORT-calculations with FENDL-1 and ENDF/B-VI data for FNS SS-316 shield experiments - M. Youssef, UCLA

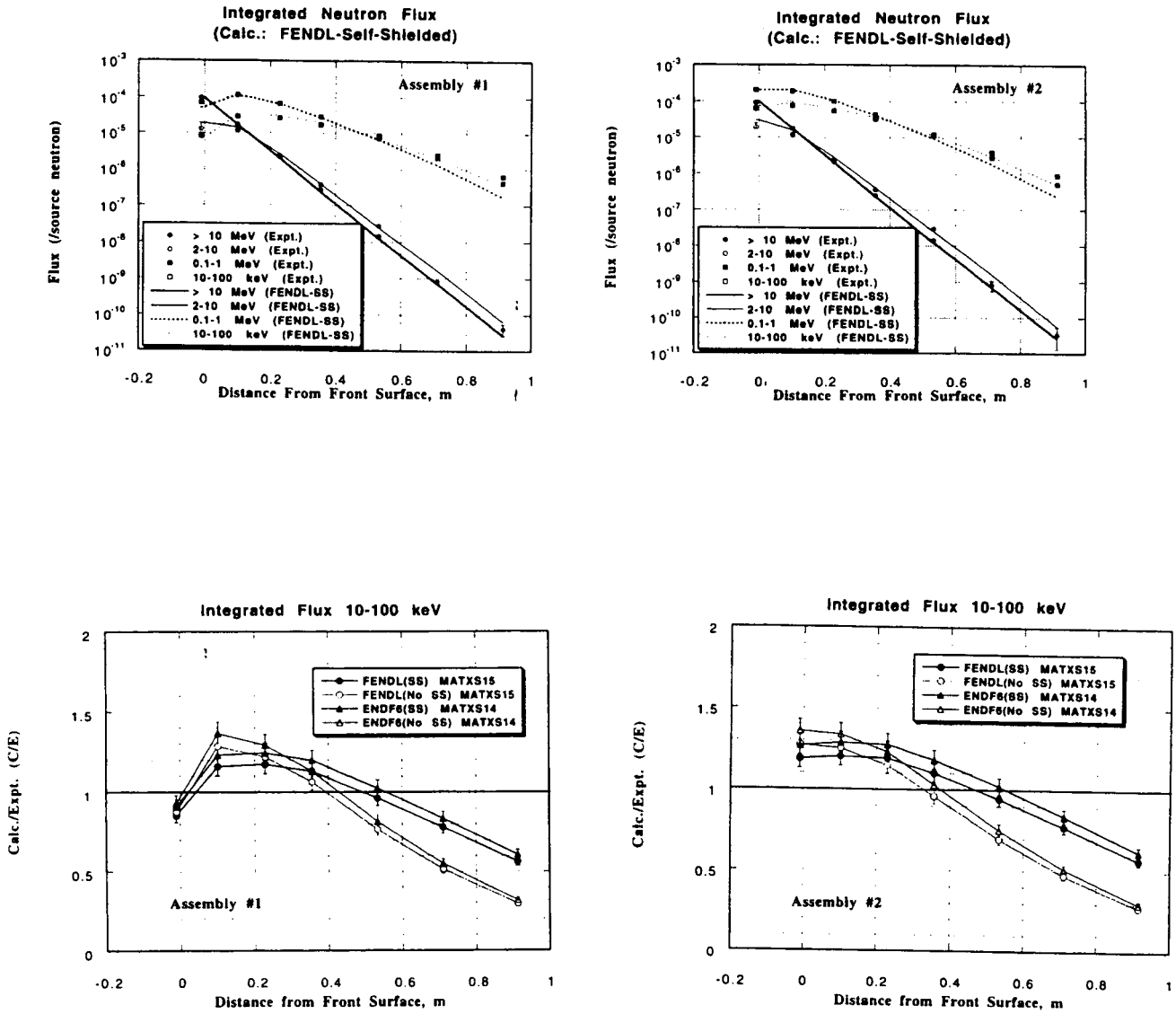

Fig. 73: DORT-calculations with FENDL-1 and ENDF/B-VI data for FNS SS-316 shield experiments - M. Youssef, UCLA

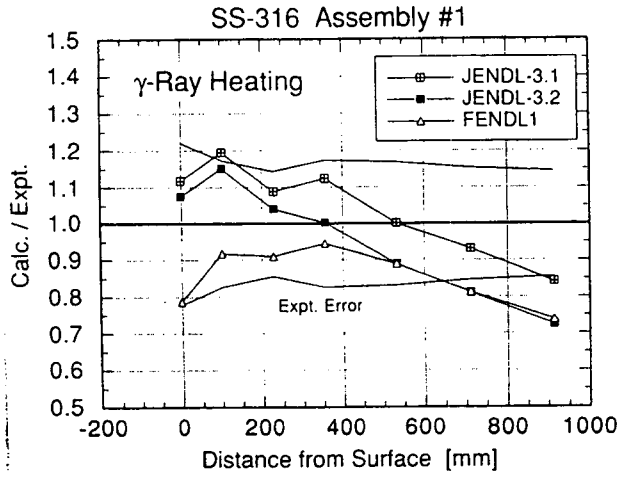

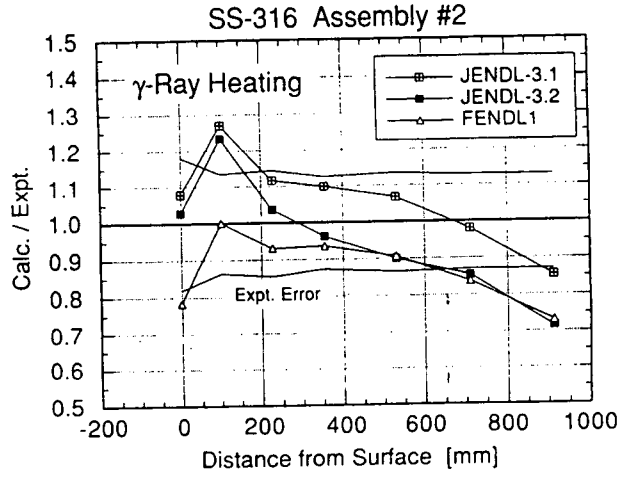

Fig. 74 a, b: MCNP-calculations with FENDL-1 and JENDL-3 data for FNS SS-316 shield experiments - Y. Oyama, JAERI

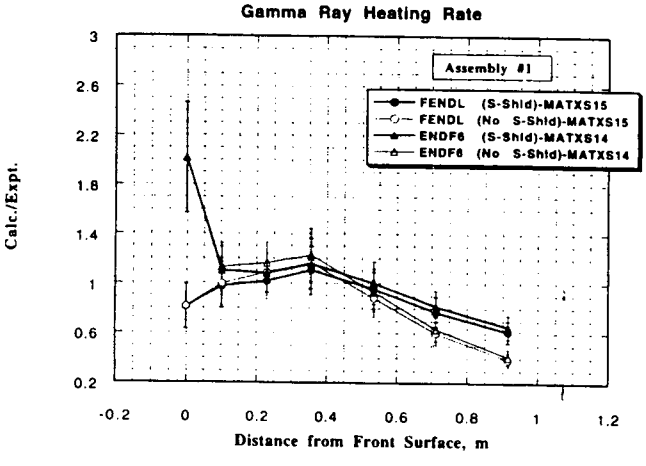

Figure 101: The C/E Values of Gamma Ray Heating in Assembly #1

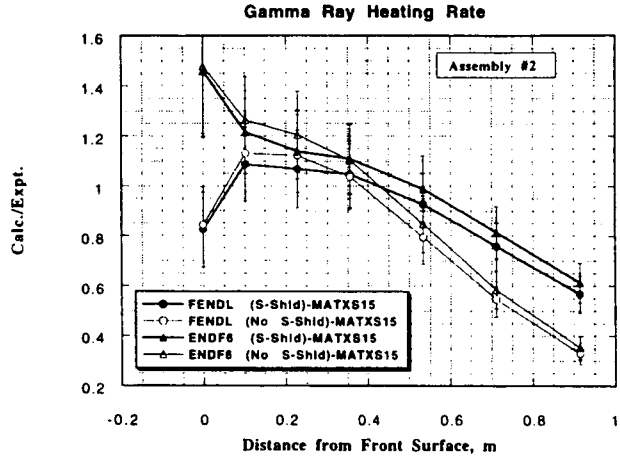

Figure 105: The C/E Values of Gamma Ray Heating in Assembly #2

Fig. 74c, d: DORT-calculations with FENDL-1 and ENDF/B-VI data for FNS SS-316 shield experiments - M. Youssef, UCLA

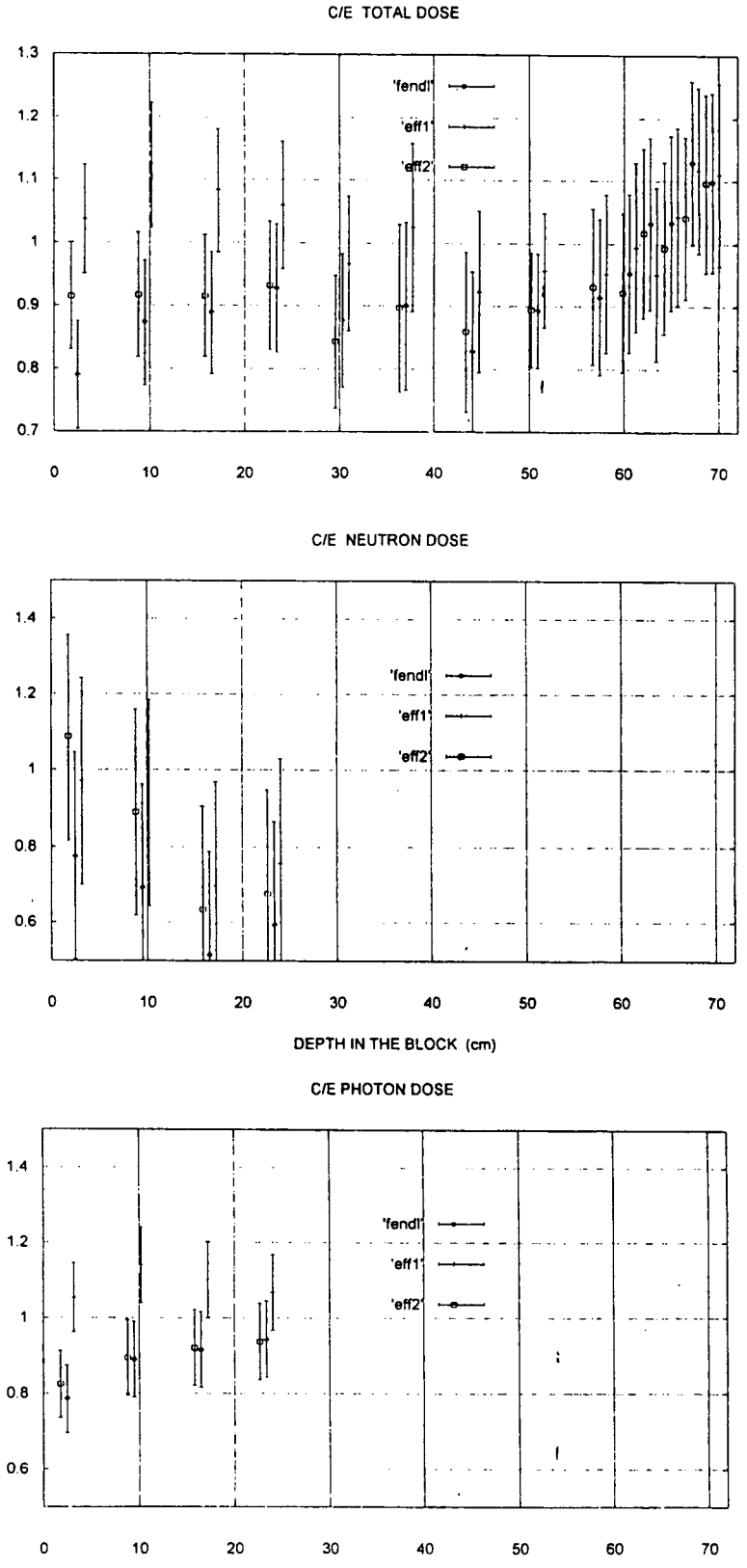

Fig. 75: MCNP-calculations with FENDL-1, EFF-1 and -2 data for FNG SS-316 nuclear heating experiment - V. Rado, L. Petrizzi, P. Batistoni - ENEA Frascati

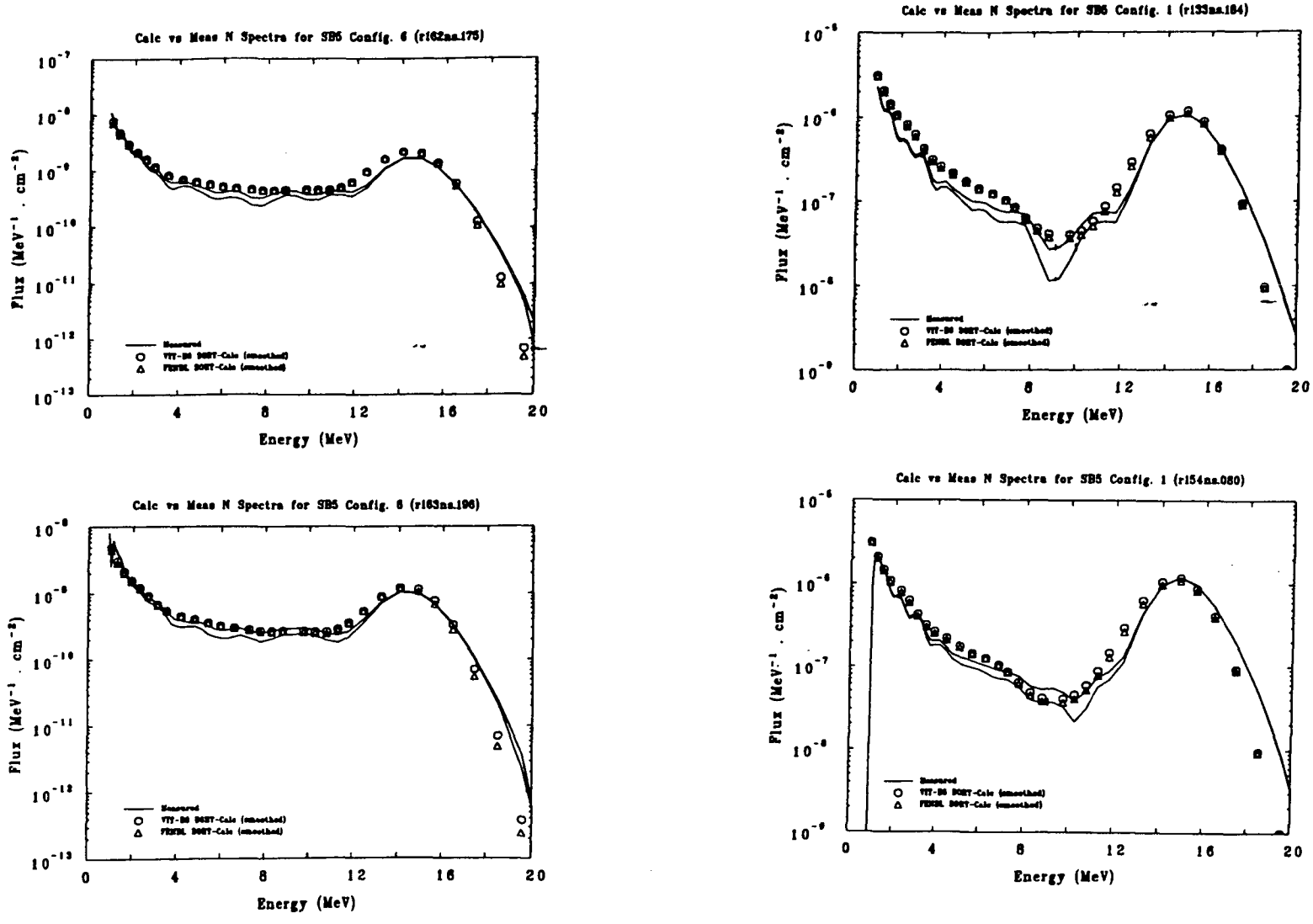

Fig. 76: DORT-calculations with FENDL-1 and ENDF/B-VI data for ORNL SS-316 bulk shield experiments - H. Hunter, C. Slater, ORNL

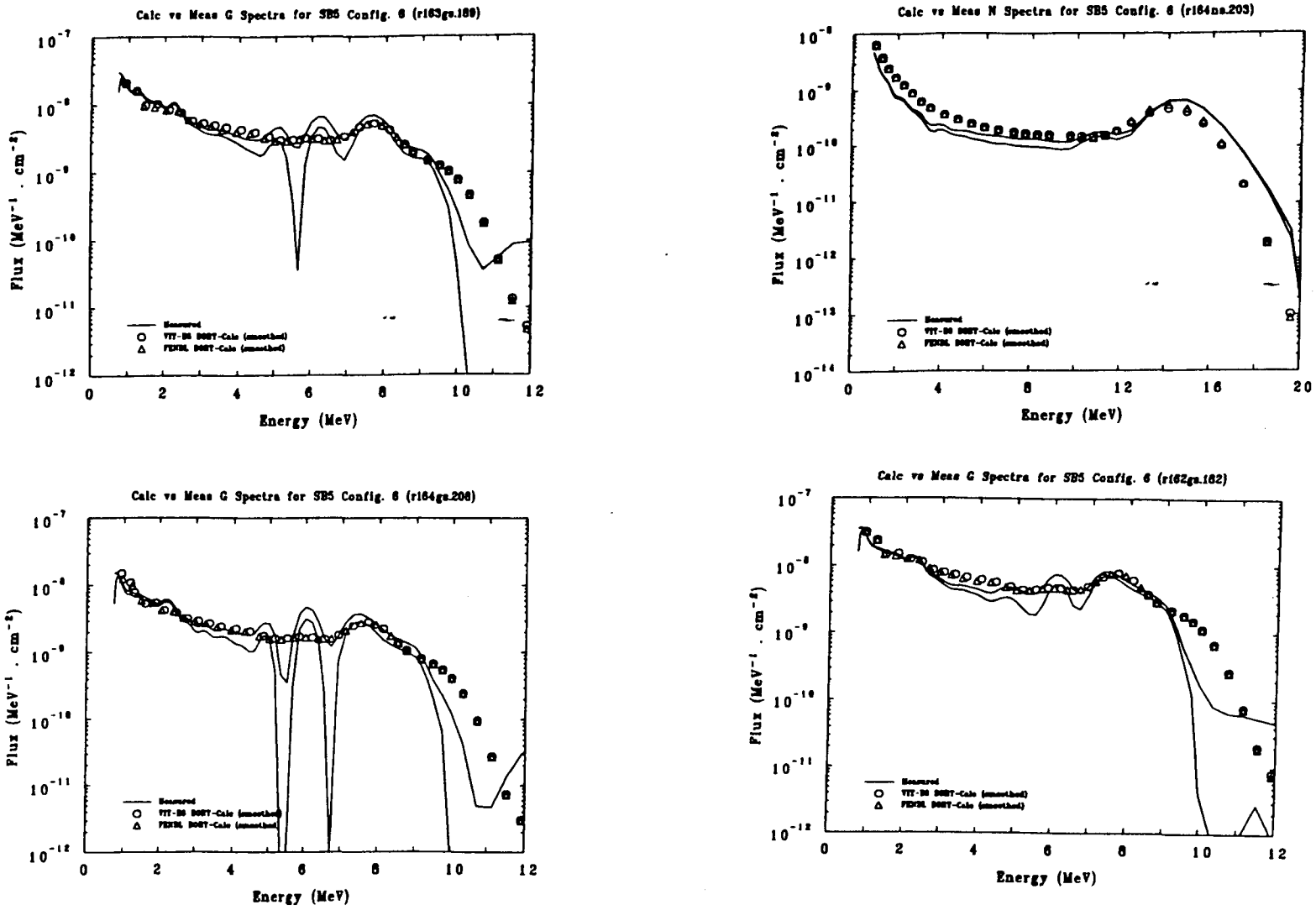

Fig. 77: DORT-calculations with FENDL-1 and ENDF/B-VI data for ORNL SS-316 bulk shield experiments - H. Hunter, C. Slater, ORNL

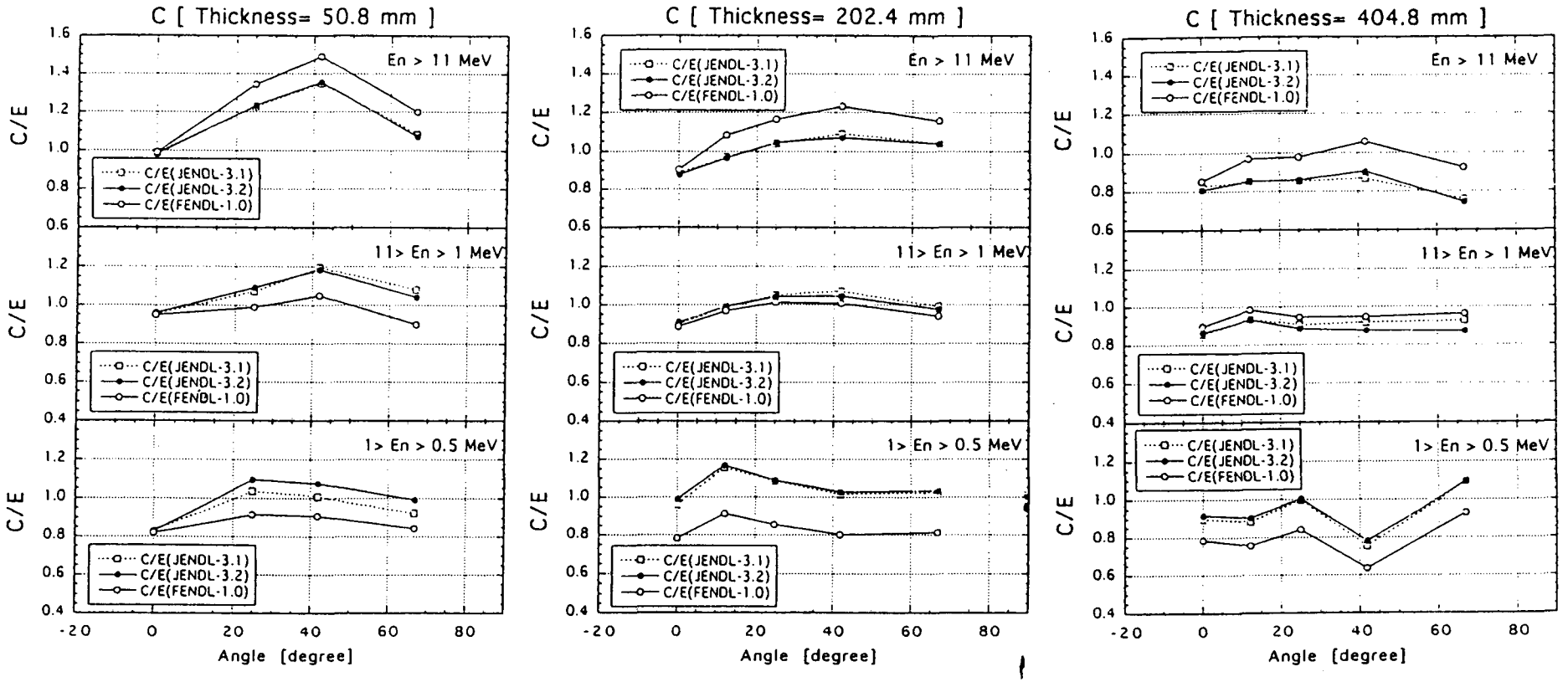

Fig. 78: MCNP-calculations with FENDL-1 and JENDL-3 data for FNS graphite cylindrical slabs - Y. Oyama, M. Wada -FNS/JAERI

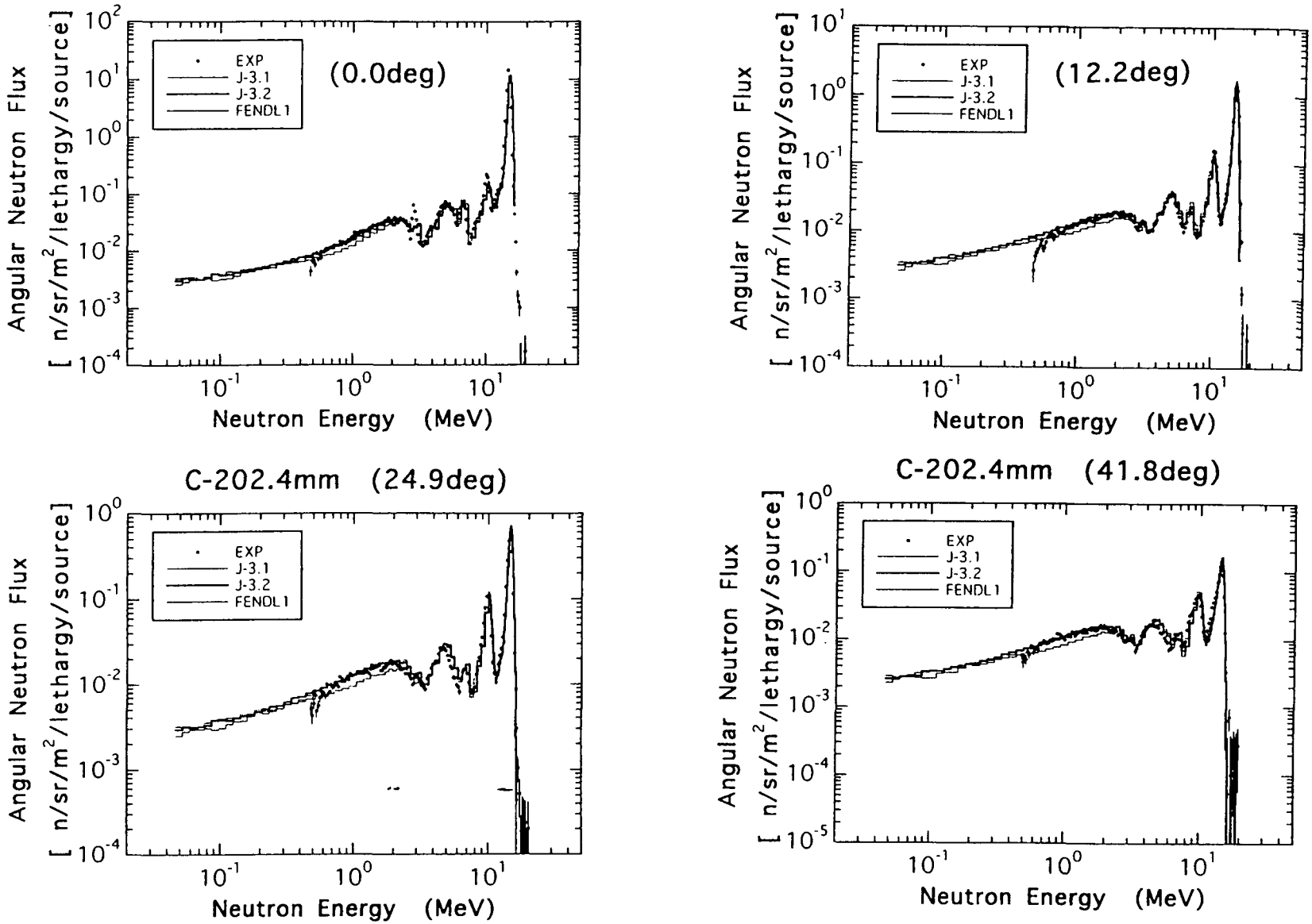

Fig. 79: MCNP-calculations with FENDL-1 and JENDL-3 data for FNS graphite cylindrical slabs - Y. Oyama, M. Wada -FNS/JAERI

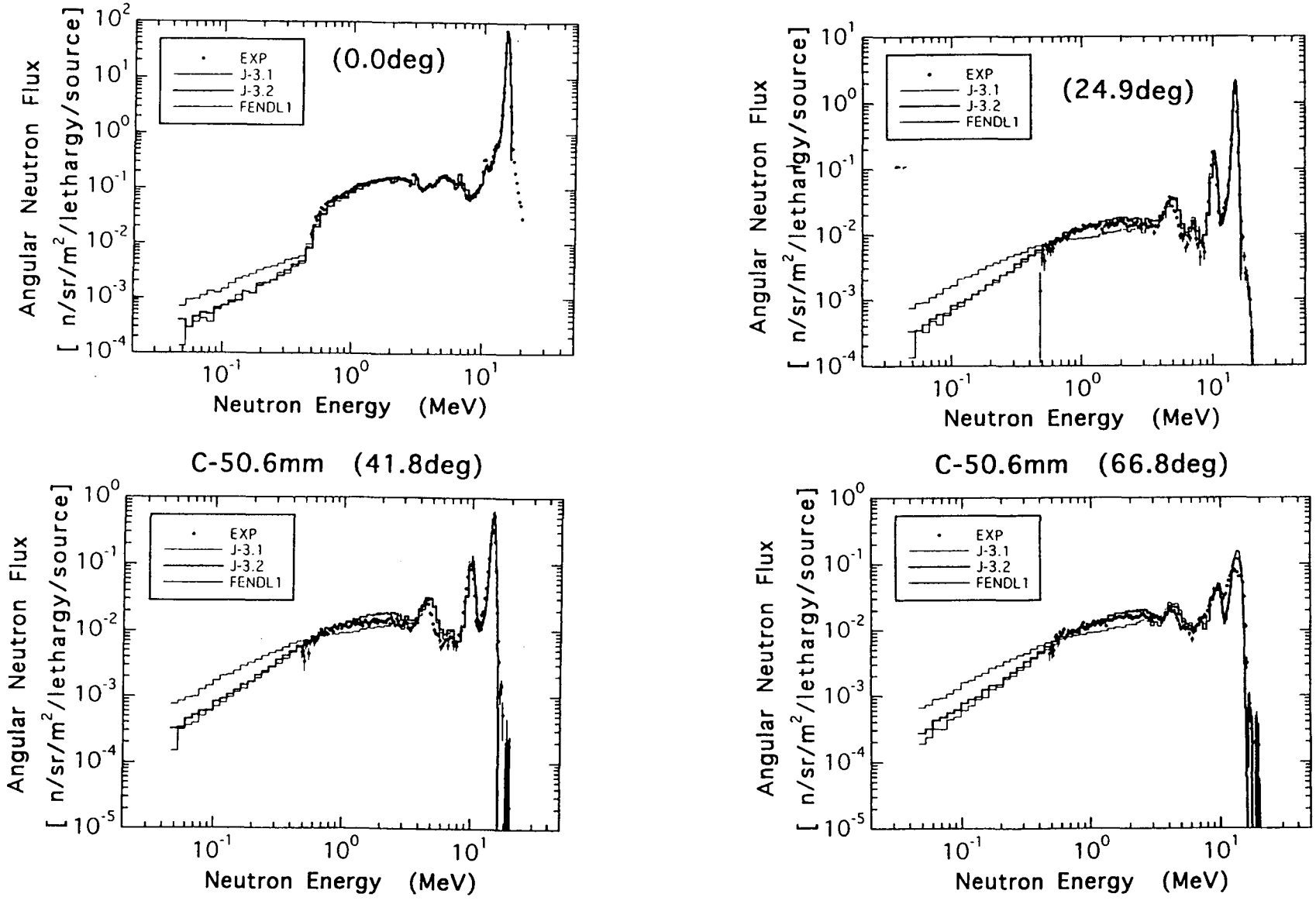

Fig. 80: MCNP-calculations with FENDL-1 and JENDL-3 data for FNS graphite cylindrical slabs - Y. Oyama, M. Wada -FNS/JAERI

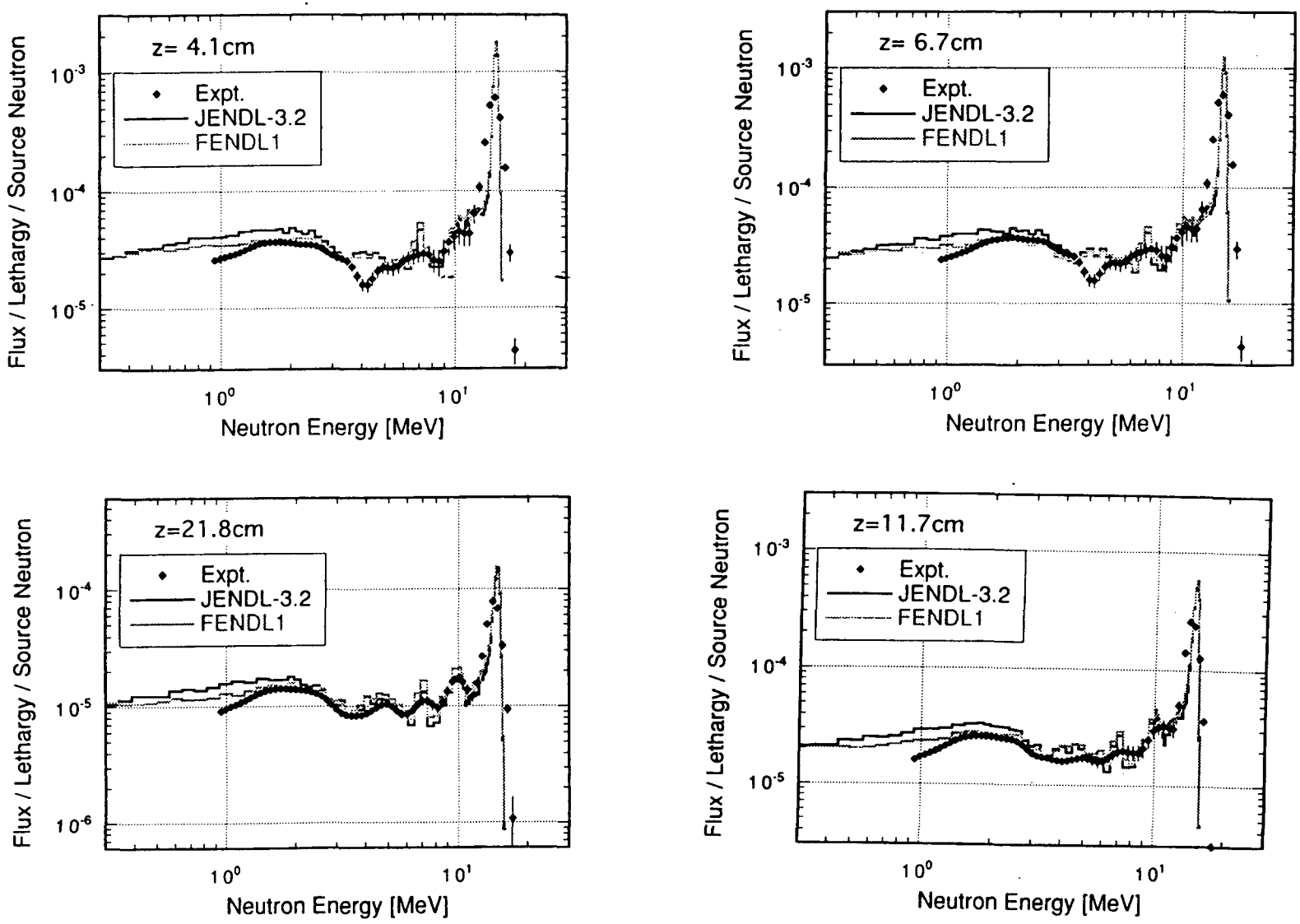

Fig. 81: MCNP-calculations with FENDL-1 and JENDL-3.2 data for neutron spectra inside FNS graphite cylindrical slabs
- F. Maekawa, Y. Oyama, M. Wada -FNS/JAERI

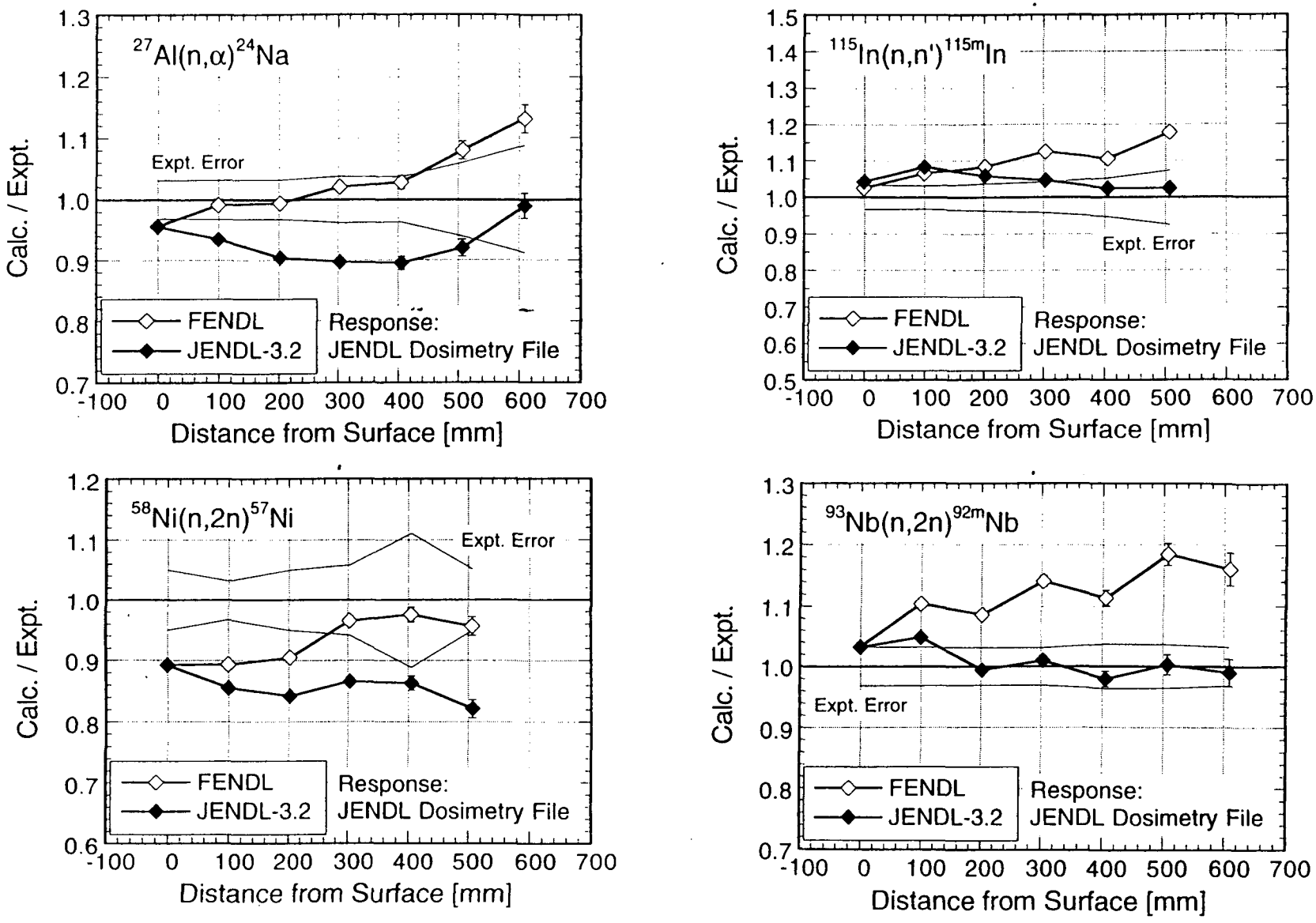

Fig. 82: MCNP-calculations with FENDL-1 and JENDL-3.2 data for reaction rates inside FNS graphite cylindrical slabs
- F. Maekawa, Y. Oyama, M. Wada -FNS/JAERI

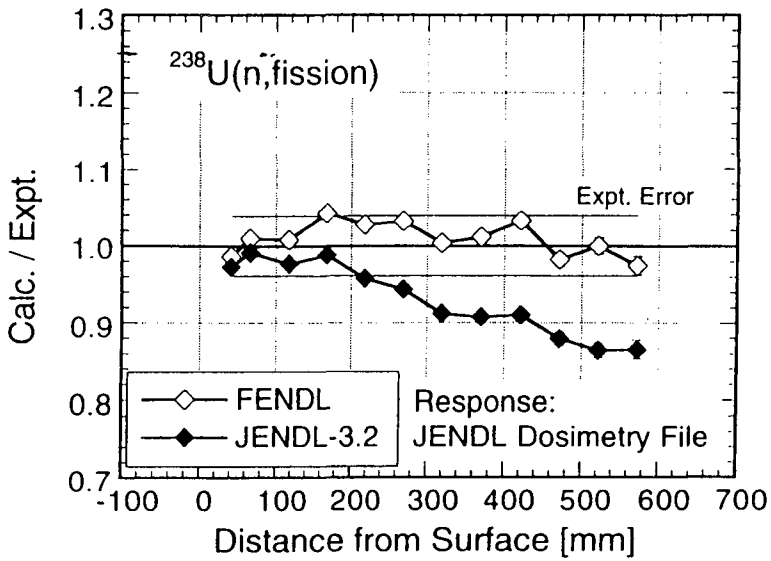

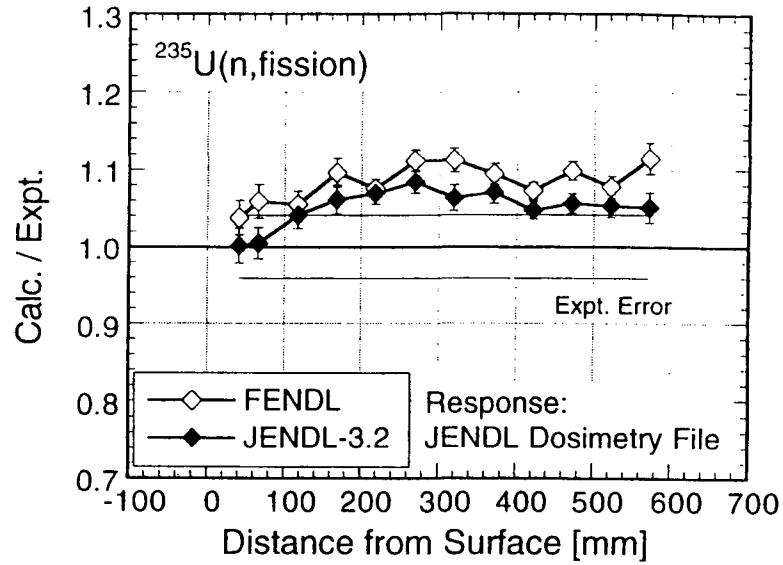

Fig. 83: MCNP-calculations with FENDL-1 and JENDL-3.2 data for reaction rates inside FNS graphite cylindrical slabs
- F. Maekawa, Y. Oyama, M. Wada -FNS/JAERI

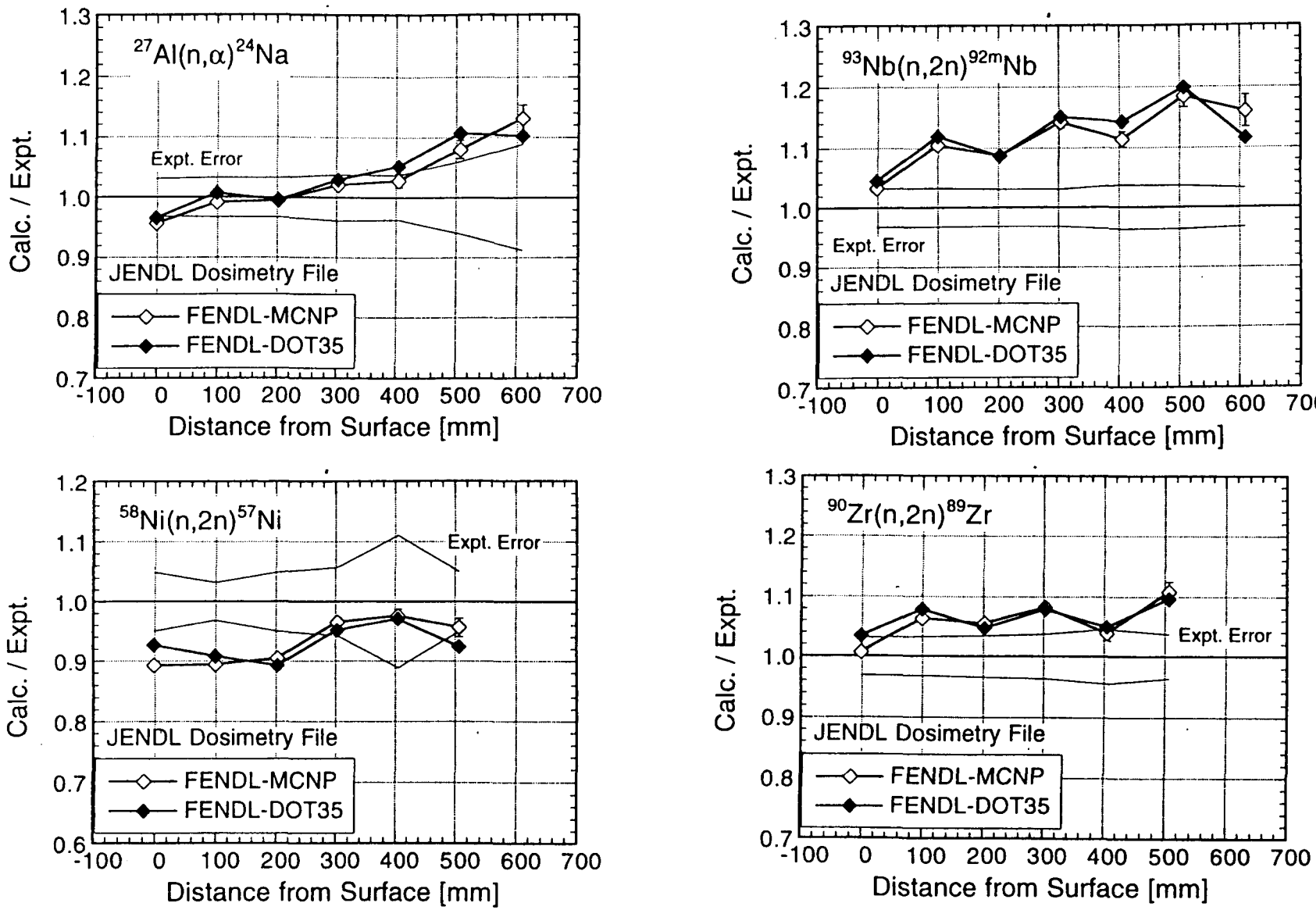

Fig. 84: MCNP- and DOT-calculations with FENDL-1 data for reaction rates inside graphite cylindrical slabs
- K. Hayashi, Hitachi Eng., Y. Oyama -FNS/JAERI

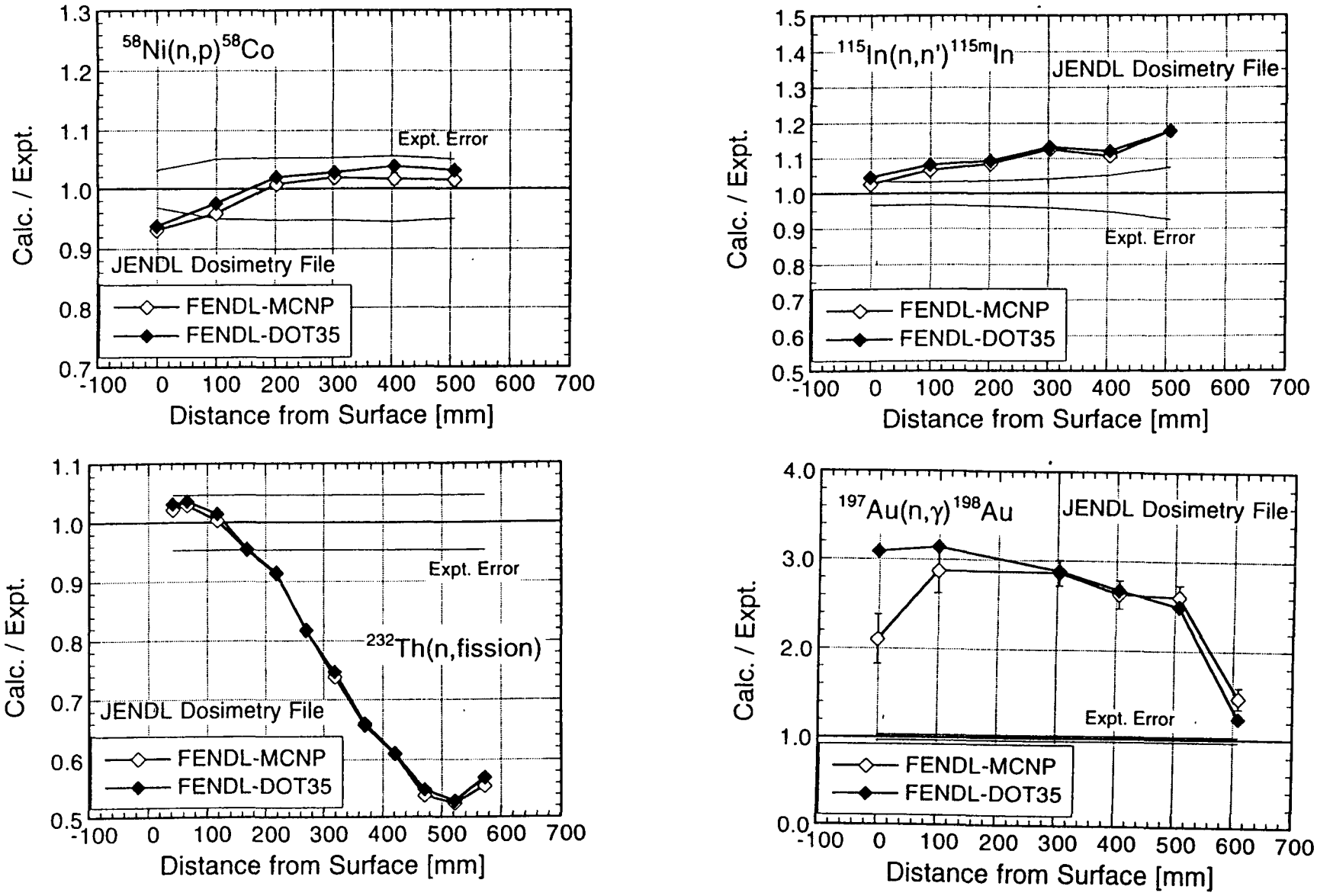

Fig. 85: MCNP- and DOT-calculations with FENDL-1 data for reaction rates inside graphite cylindrical slabs
- K. Hayashi, Hitachi Eng., Y. Oyama -FNS/JAERI

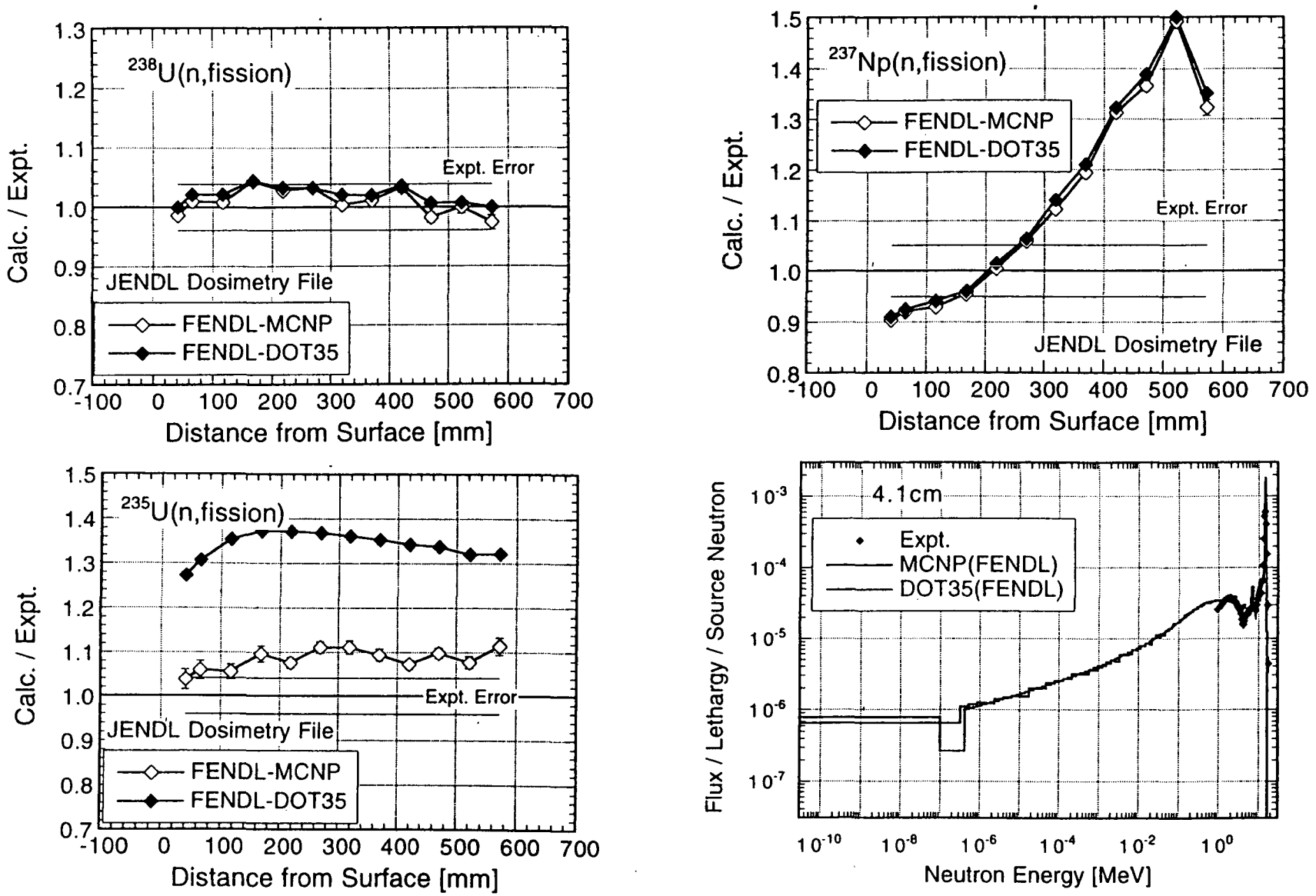

Fig. 86: MCNP- and DOT-calculations with FENDL-1 data for reaction rates and neutron spectra inside graphite cylindrical slabs - K. Hayashi, Hitachi Eng., Y. Oyama -FNS/JAERI

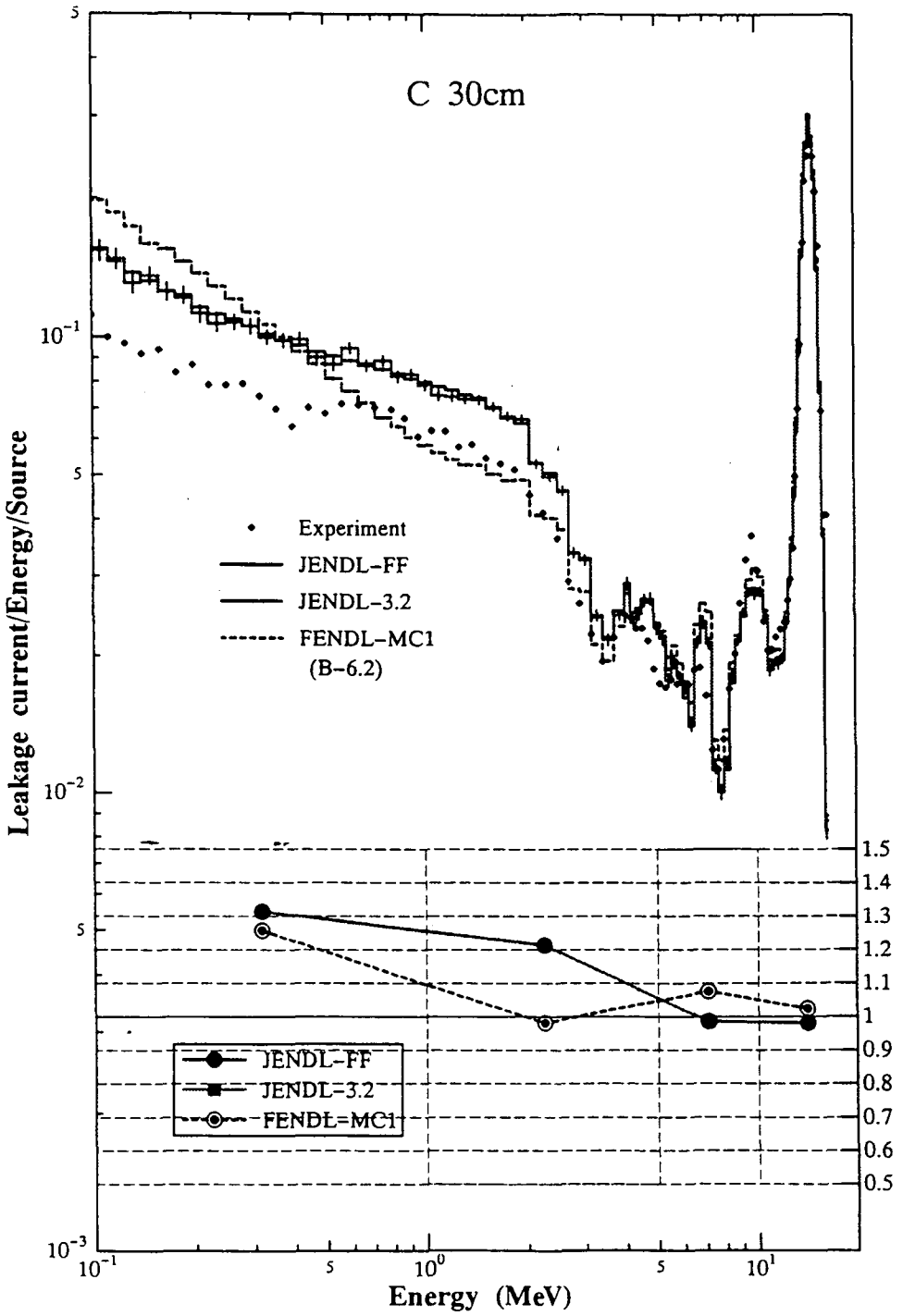

Fig. 87: MCNP -calculations with FENDL-1 and JENDL-3 data for OKTAVIAN graphite spherical shell experiment - C. Ichihara, University of Kyoto

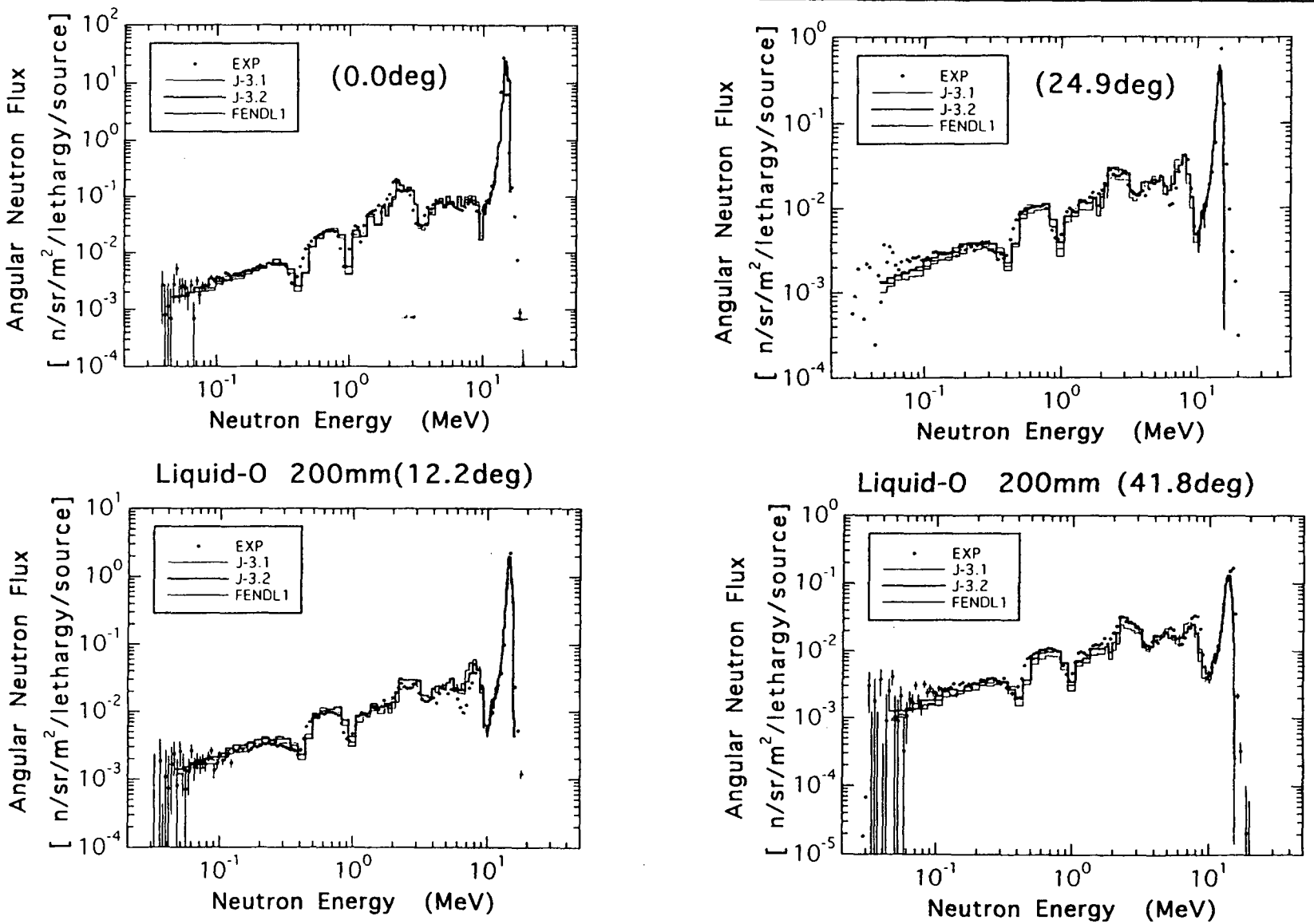

Fig. 88: MCNP-calculations with FENDL-1 and JENDL-3 data for FNS liquid oxygen cylindrical slabs - Y. Oyama, M. Wada -FNS/JAERI

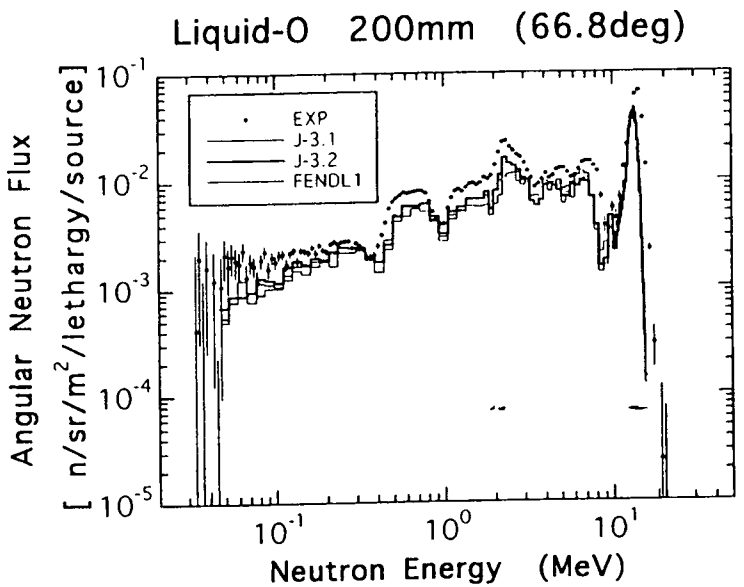

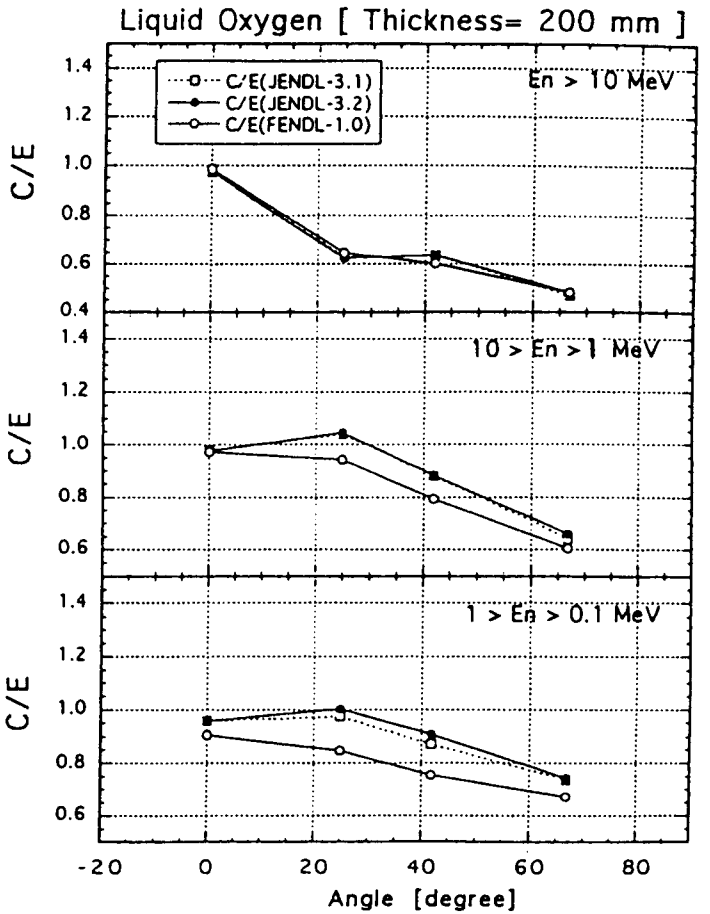

Fig. 89: MCNP-calculations with FENDL-1 and JENDL-3 data for FNS liquid oxygen cylindrical slabs - Y. Oyama, M. Wada -FNS/JAERI

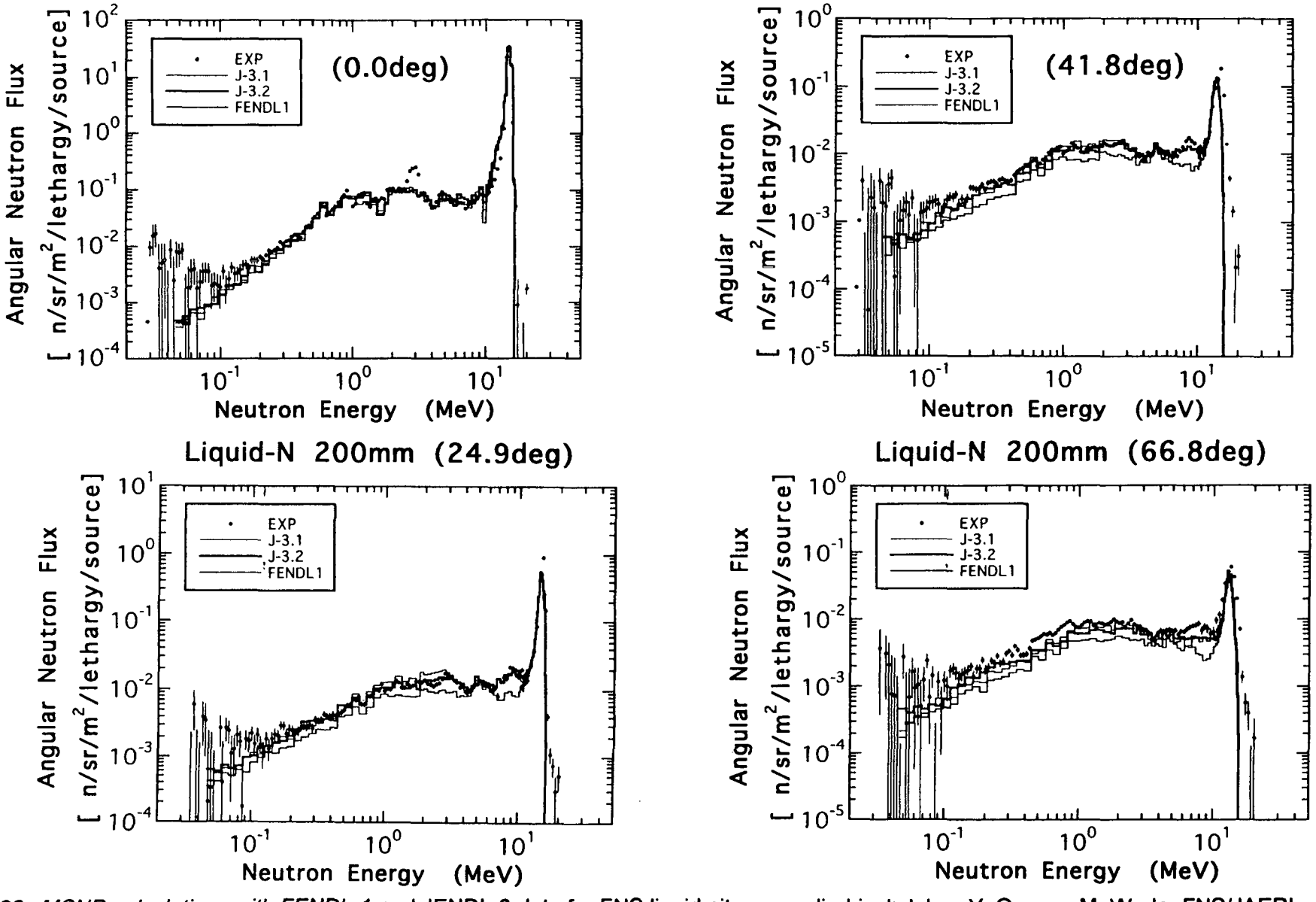

Fig. 90: MCNP-calculations with FENDL-1 and JENDL-3 data for FNS liquid nitrogen cylindrical slabs - Y. Oyama, M. Wada -FNS/JAERI

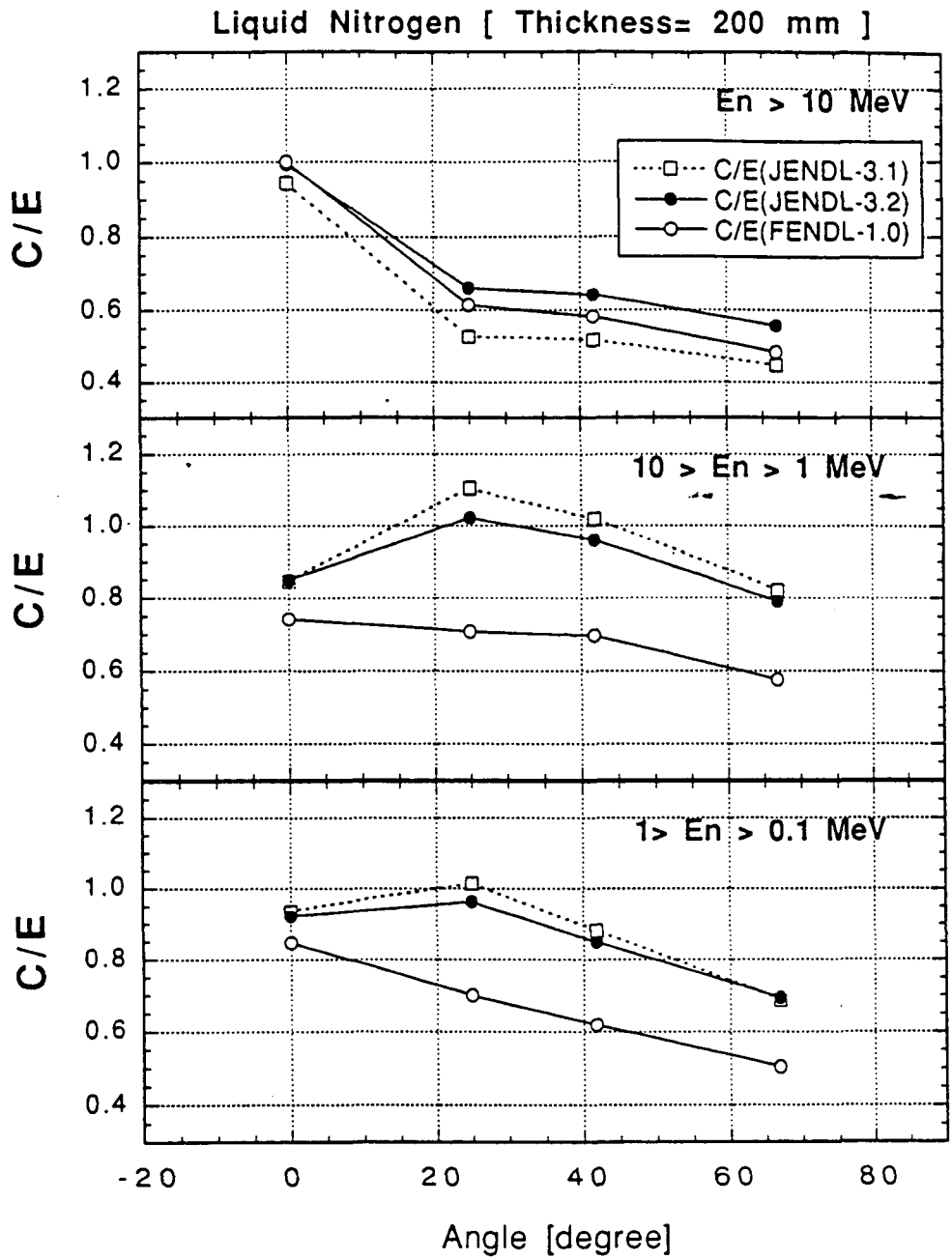

Fig. 91: MCNP-calculations with FENDL-1 and JENDL-3 data for FNS liquid nitrogen cylindrical slabs - Y. Oyama, M. Wada -FNS/JAERI

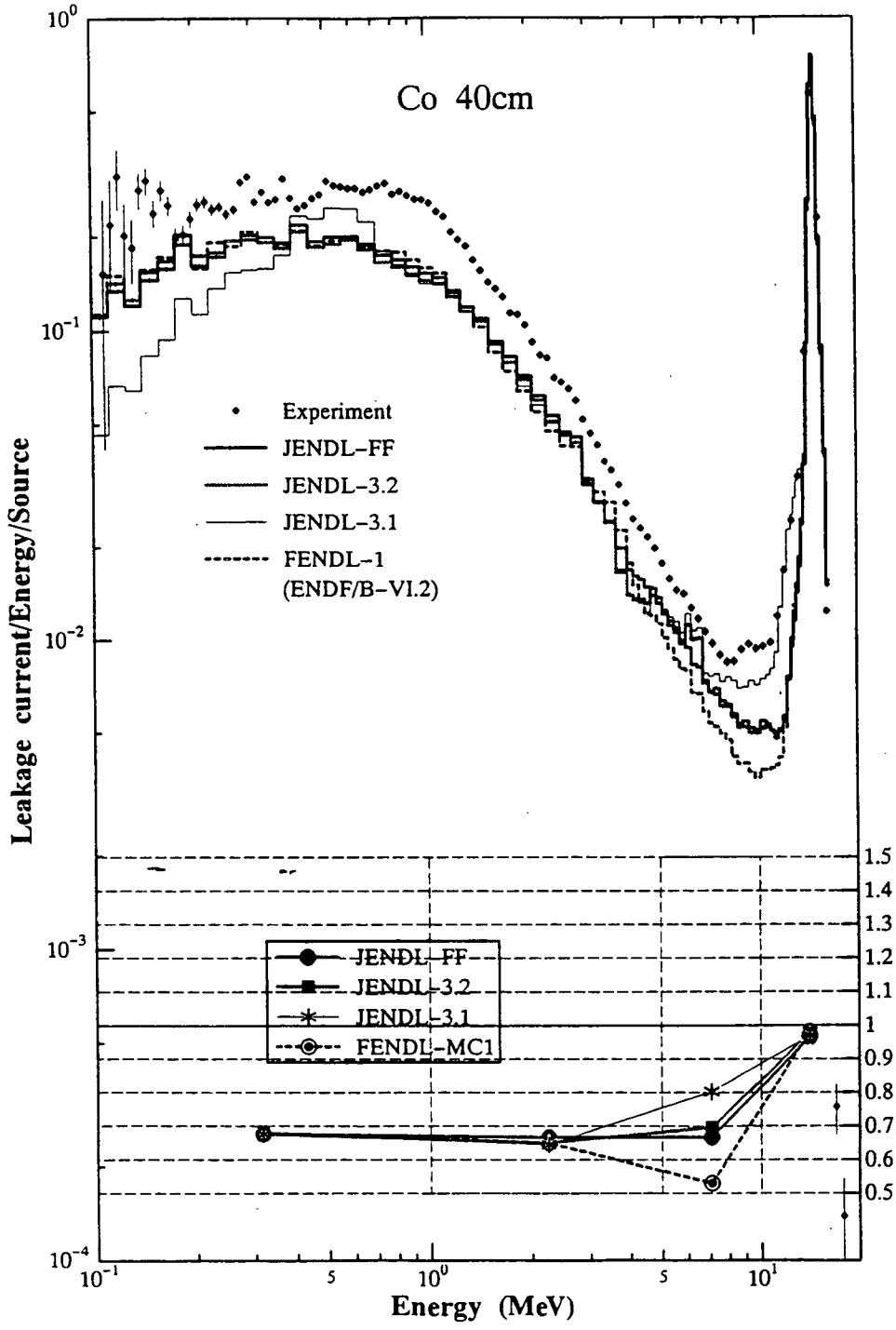

Fig. 92: MCNP -calculations with FENDL-1 and JENDL-3 data for OKTAVIAN cobalt spherical shell experiment - C. Ichihara, University of Kyoto

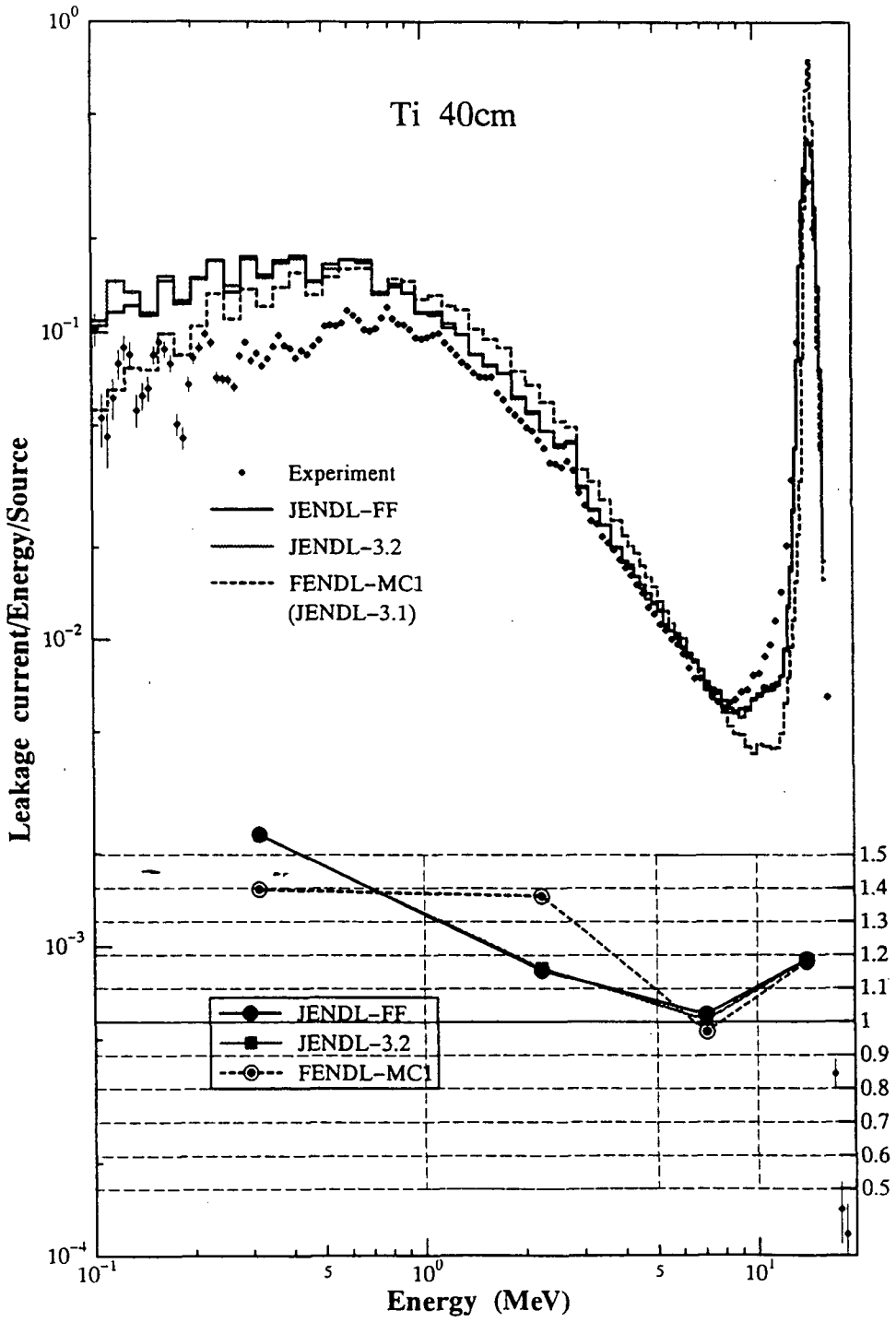

Fig. 93: MCNP -calculations with FENDL-1 and JENDL-3 data for OKTAVIAN titanium spherical shell experiment - C. Ichihara, University of Kyoto

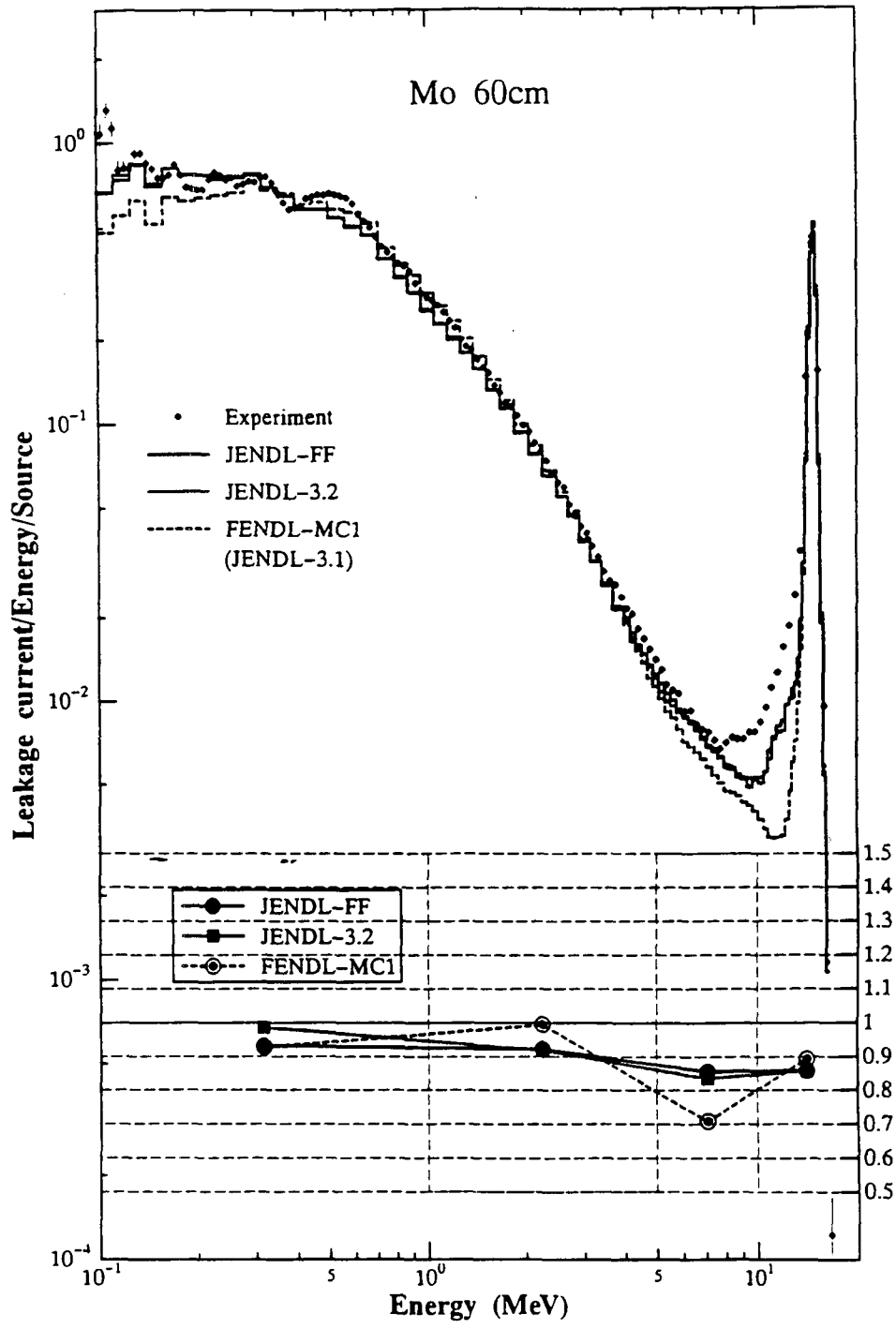

Fig. 94: MCNP -calculations with FENDL-1 and JENDL-3 data for OKTAVIAN molybdenum spherical shell experiment - C. Ichihara, University of Kyoto

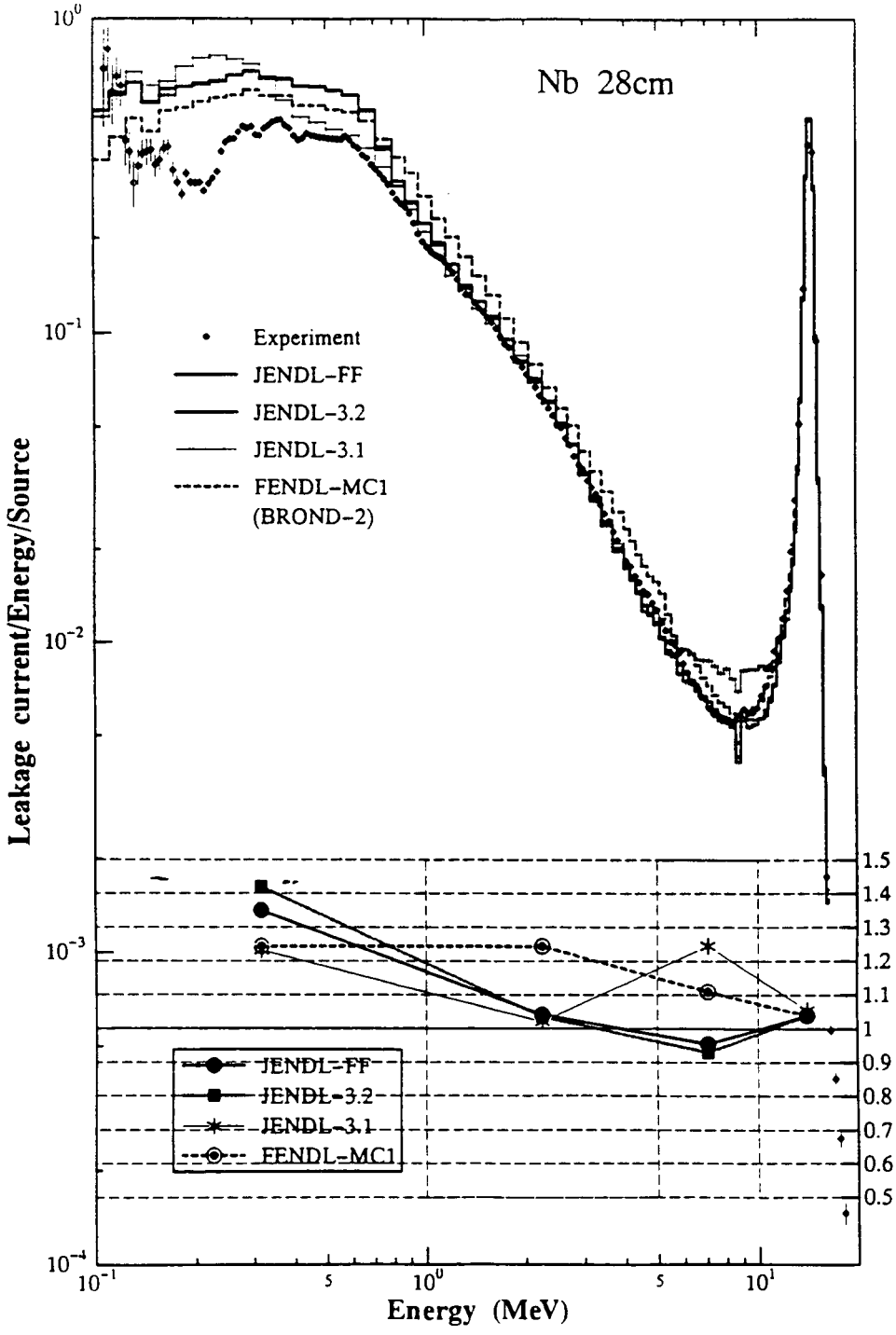

Fig. 95: MCNP -calculations with FENDL-1 and JENDL-3 data for OKTAVIAN niobium spherical shell experiment - C. Ichihara, University of Kyoto

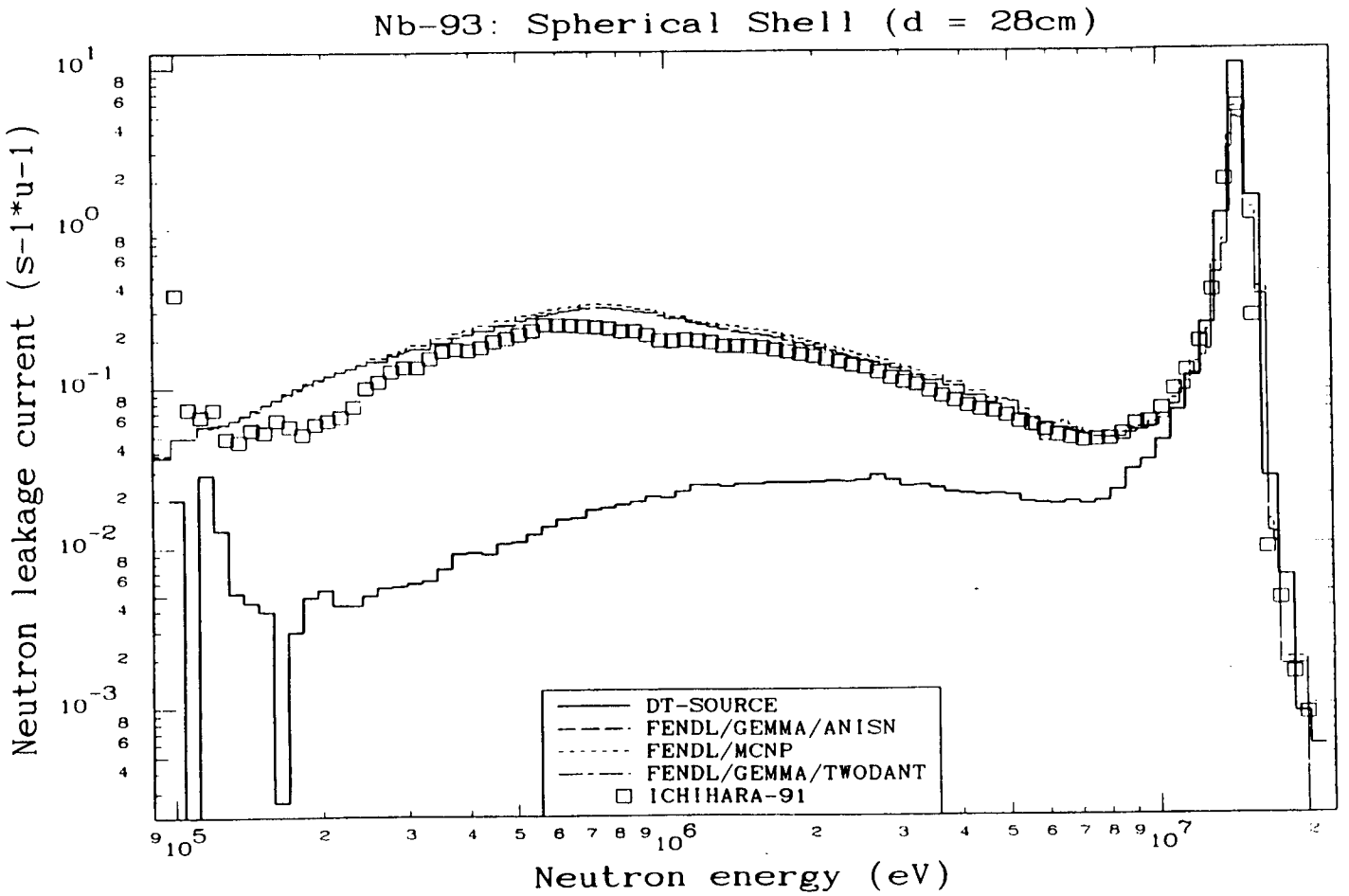

Fig. 96: ANISN-, MCNP and ONEDANT-calculations with FENDL-1 data for OKTAVIAN niobium spherical shell experiment
- A. Blokhin, IPPE Obninsk

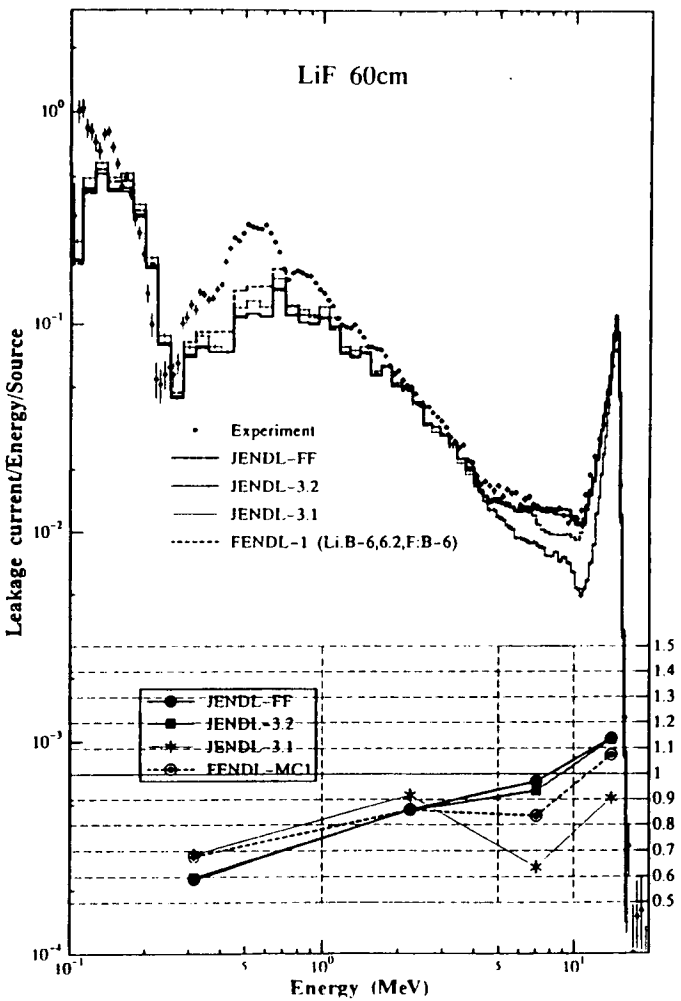

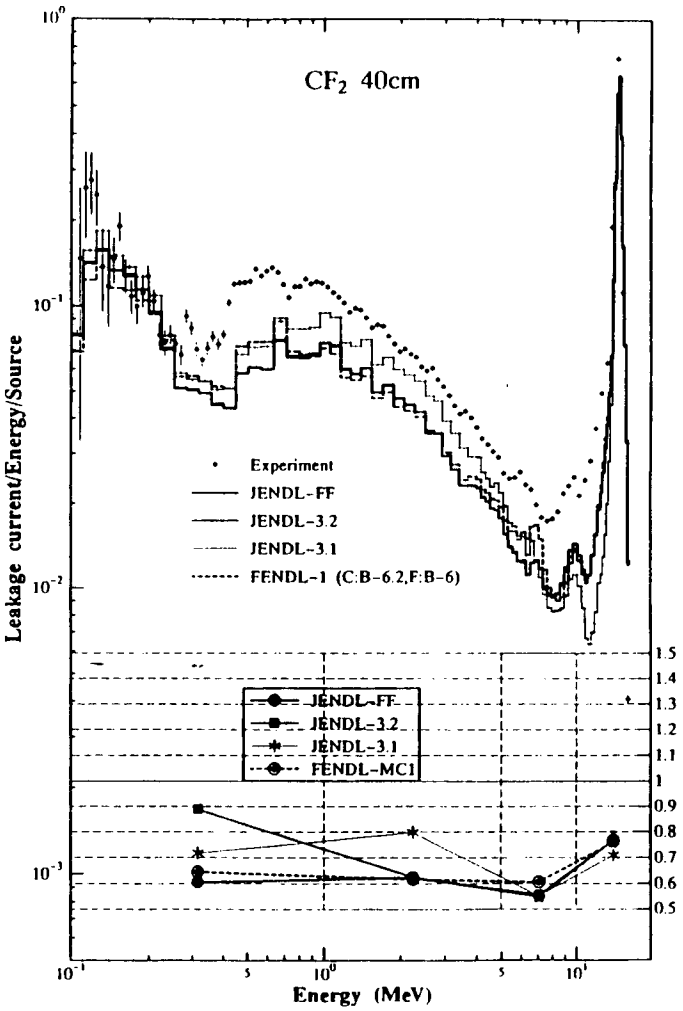

Fig. 97: MCNP -calculations with FENDL-1 and JENDL-3 data for OKTAVIAN LiF and CF_2 spherical shell experiments
- C. Ichihara, University of Kyoto

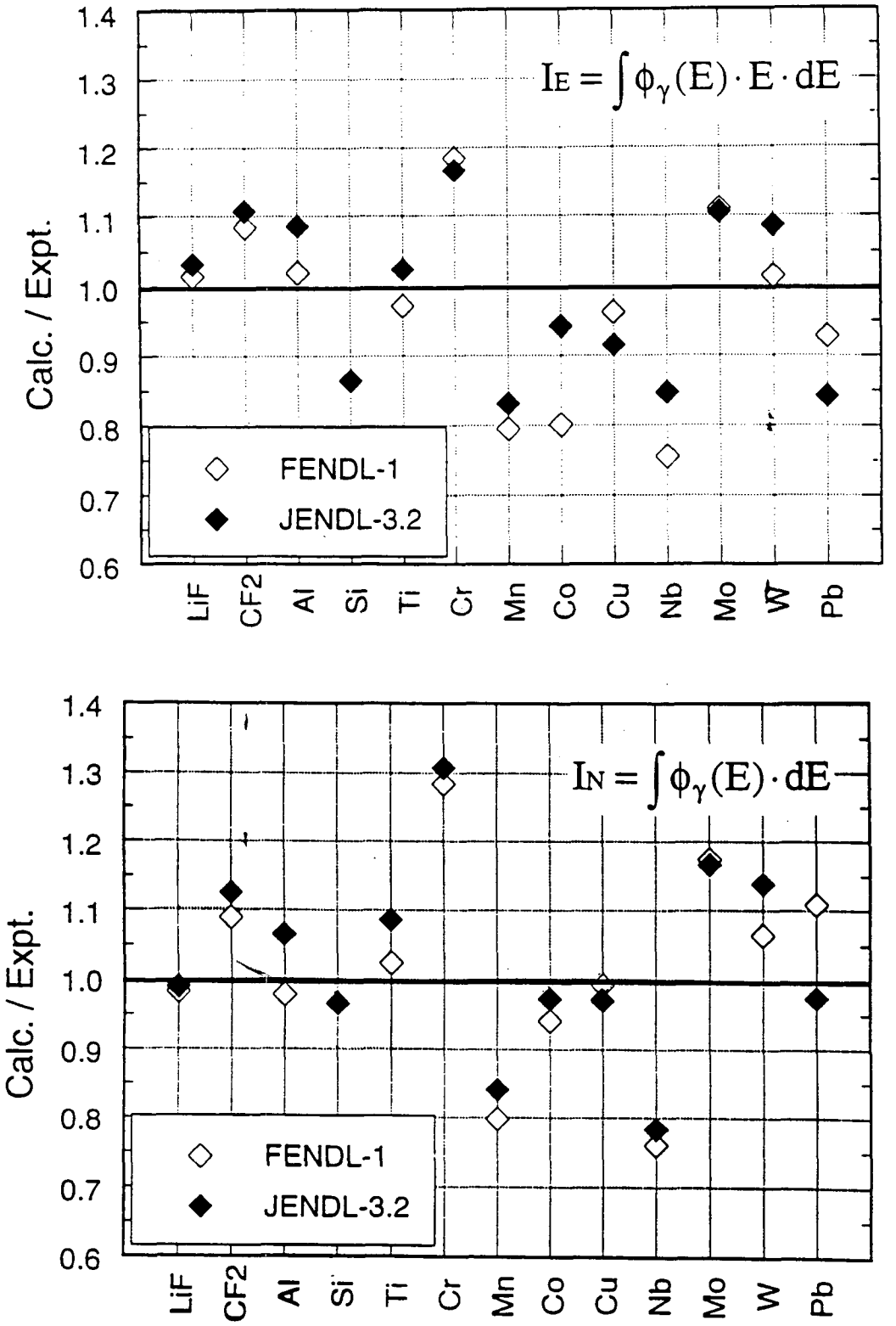

Fig. 98: MCNP -calculations with FENDL-1 and JENDL-3 data for OKTAVIAN spherical shell experiments - F. Maekawa, Y. Oyama, JAERI

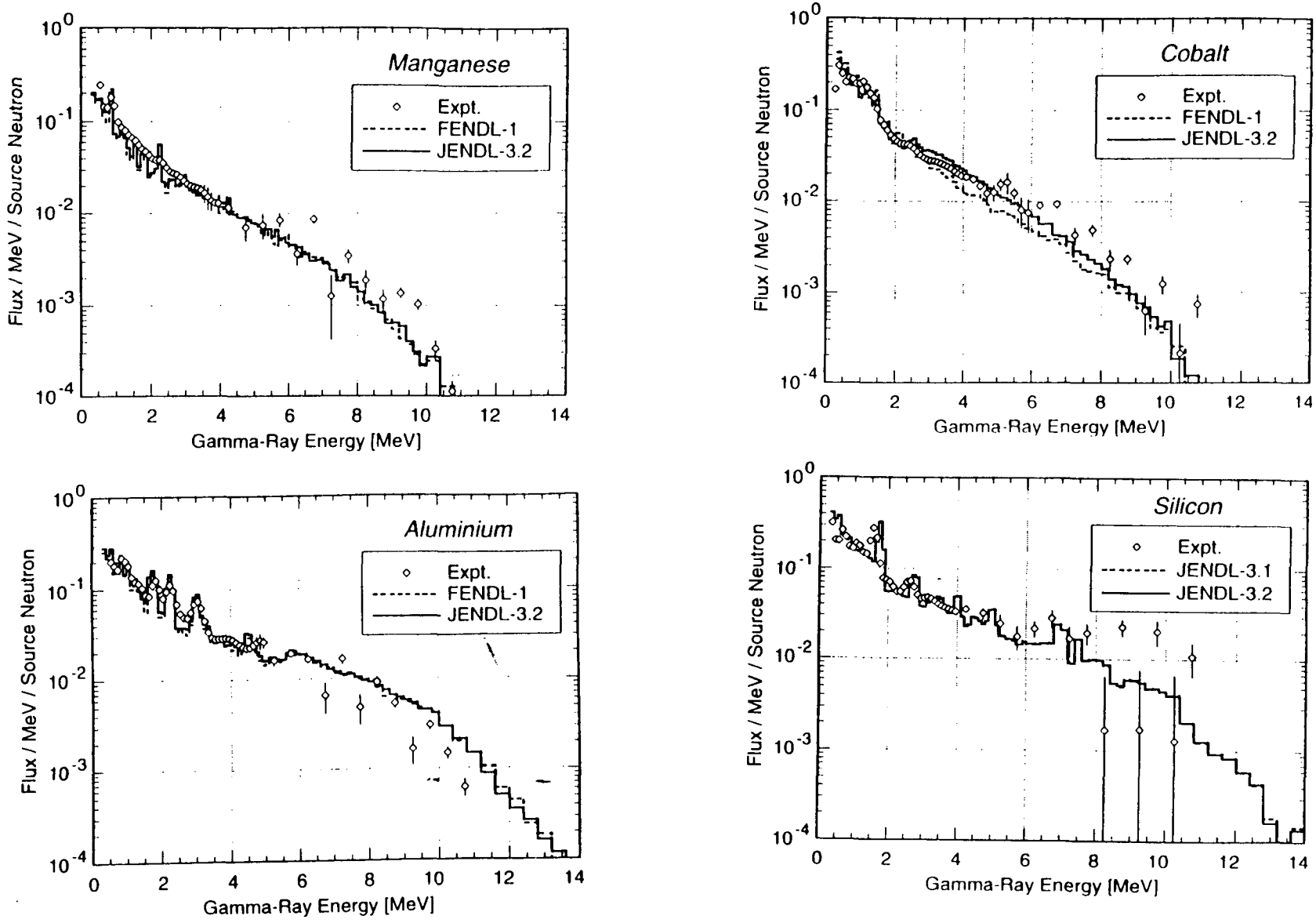

Fig. 99: MCNP -calculations with FENDL-1 and JENDL-3 data for OKTAVIAN spherical shell experiments - F. Maekawa, Y. Oyama, JAERI

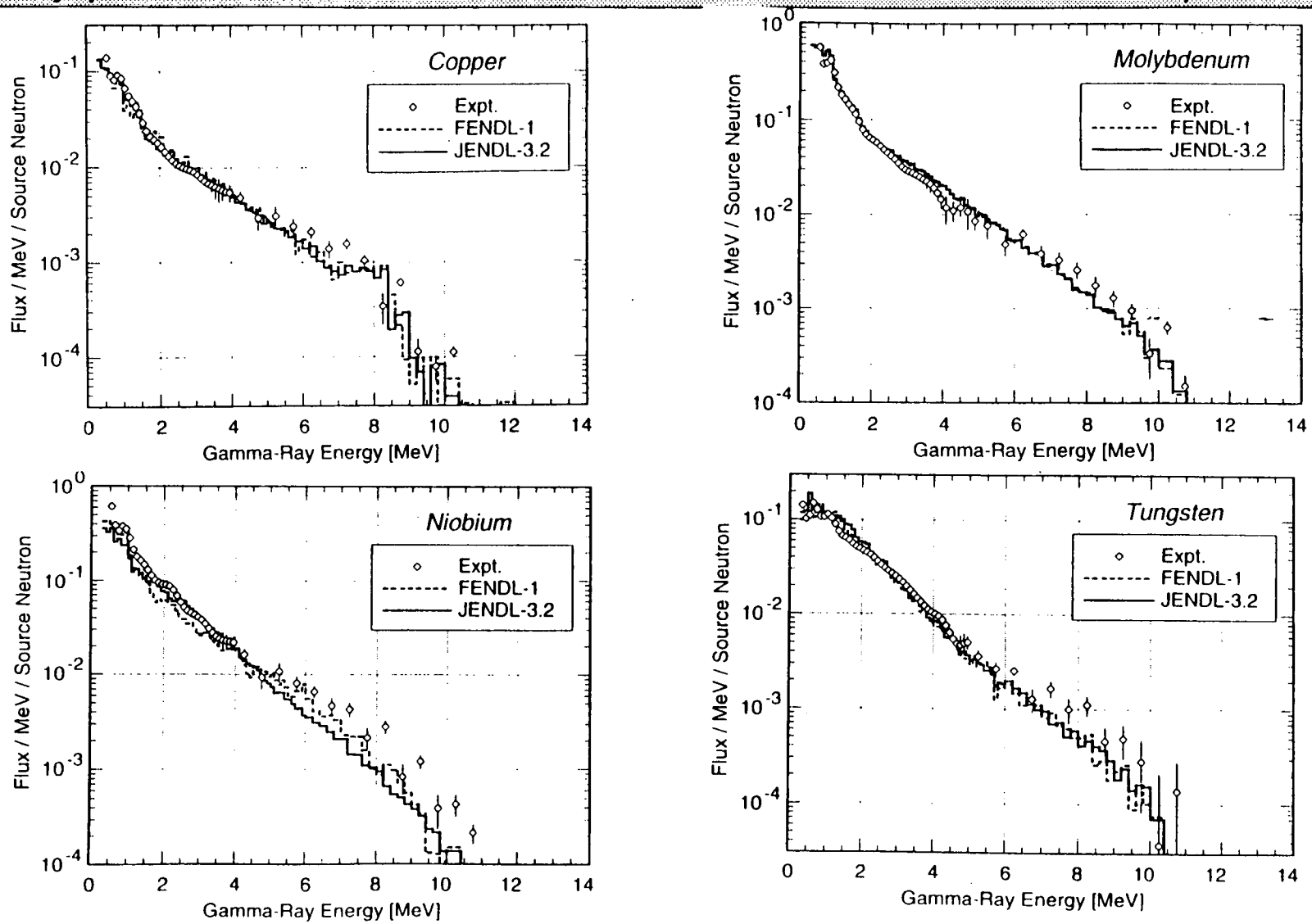

Fig. 100: MCNP -calculations with FENDL-1 and JENDL-3 data for OKTAVIAN spherical shell experiments - F. Maekawa, Y. Oyama, JAERI

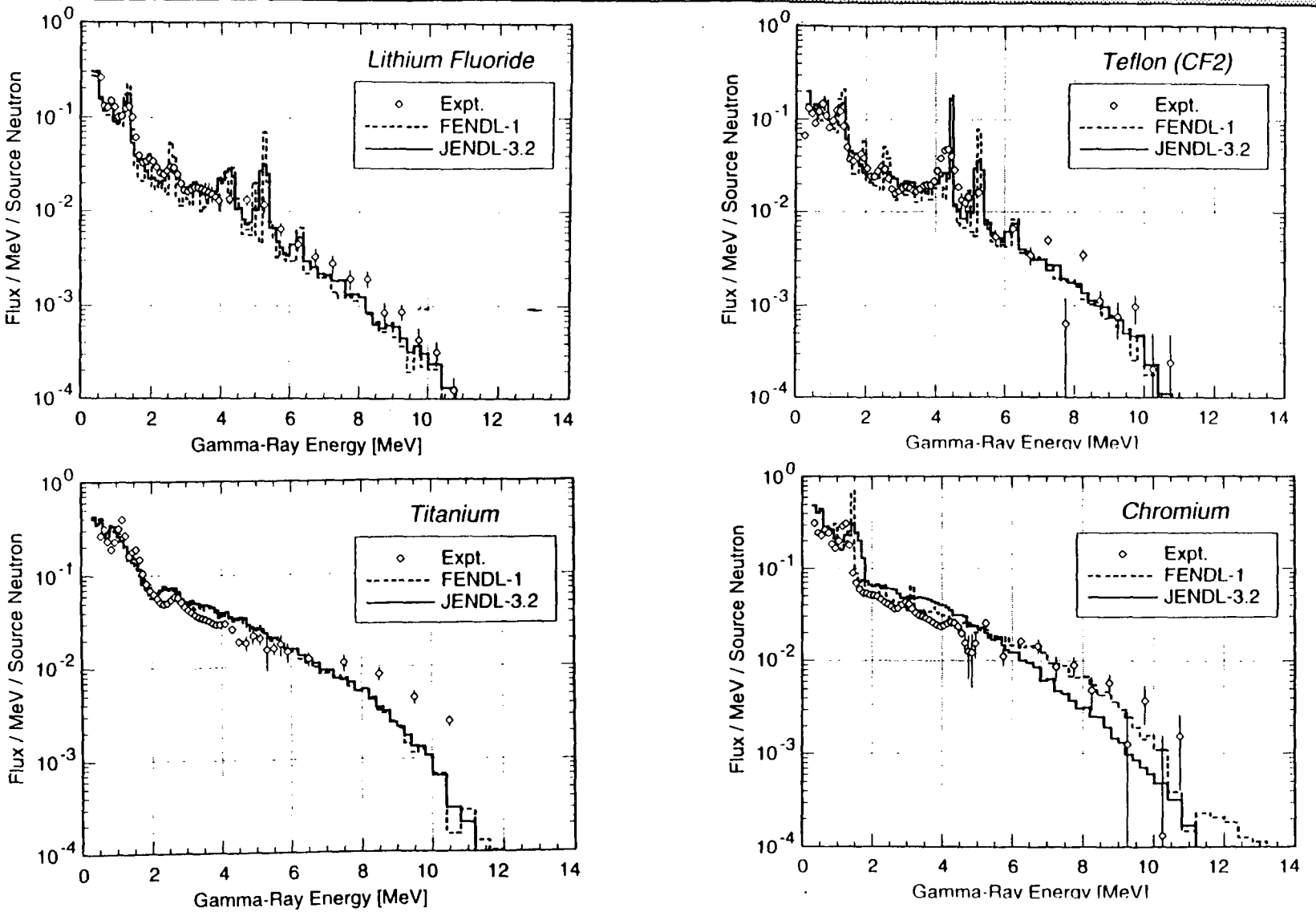

Fig. 101: MCNP -calculations with FENDL-1 and JENDL-3 data for OKTAVIAN spherical shell experiments - F. Maekawa, Y. Oyama, JAERI

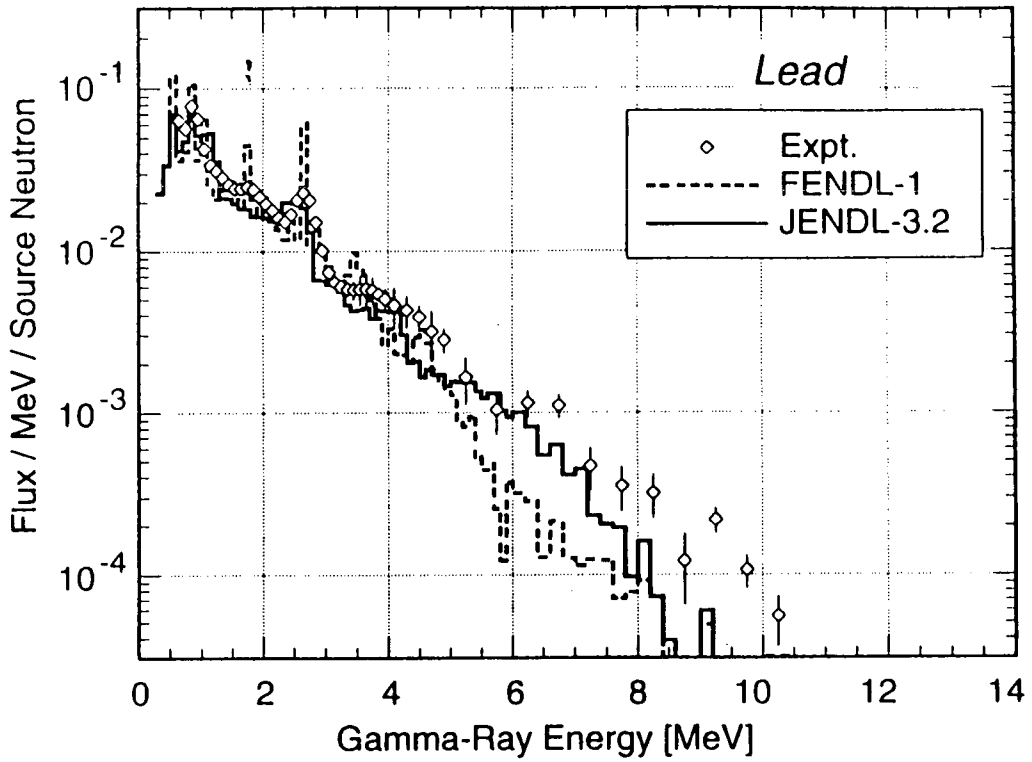

Fig. 102 : MCNP-calculations with FENDL-1 and JENDL-3 data for OKTAVIAN spherical shell experiments - F. Maekawa, Y. Oyama, JAERI